

MARINE GEOLOGY OF THE CONTINENTAL
MARGIN OFF SOUTHERN OREGON

Joseph John Spigai

Marine Geology of the Continental Margin
Off Southern Oregon

by

Joseph John Spigai

A THESIS

submitted to

Oregon State University

in partial fulfillment of
the requirements for the
degree of

Doctor of Philosophy

June 1971

APPROVED:

Associate Professor of Oceanography
in charge of major

Chairman of the Department of Oceanography

Dean of the Graduate School

Date thesis is presented _____

Typed by Gwendolyn Hansen for _____ Joseph John Spigai

ACKNOWLEDGMENTS

I would like to express sincere gratitude to Dr. LaVerne D. Kulm, my major professor, for his judicious advice and patient guidance during the entire course of this study. His generosity in giving so freely of his time and in critically reviewing this manuscript is greatly appreciated.

Discussions with many people stimulated my thinking and helped me to formulate many of the ideas presented here. In this regard, thanks are due William Bales, and Drs. Richard Couch, Gerald A. Fowler, Michael S. Longuet-Higgins, and Eli A. Silver. Many fellow graduate students unselfishly contributed their knowledge and assistance to this work; thanks go especially to Drs. David W. Allen, John R. Duncan, Jr., and Gary B. Griggs, and to David M. Chambers, Roger H. Neudeck, Robert E. Peterson, James B. Phipps, Robert C. Roush, and Kenneth F. Scheidegger.

I am indebted to Dr. Gerald A. Fowler for providing the identification and correlation of the rock fauna, and to Dr. G. Ross Heath for his assistance in the analysis and interpretation of the clay minerals. I am also grateful to Miss Anastasia Sotiropoulos for her excellent work in drafting many of the figures. Appreciation is extended to the staff and students of the Department of Oceanography, Oregon State University, and to the personnel of the R/V Yaquina for their invaluable

assistance in the collection of data at sea.

I am very grateful to my wife, Frances, for her enduring patience and for the unlimited help and encouragement she provided me during the course of the study. To my parents, whose sacrifices made my education possible, I am ever grateful.

The opportunity to undertake this graduate study was made possible by the United States Navy, under its Postgraduate Education Program; personal financial support was also provided by the Navy. The research pertaining to this study was made possible by grants from the United States Geological Survey made to Oregon State University (Contracts 14-08-0001-10766, -11941, and -1287). Initial support for the research and ship time was provided by the Office of Naval Research (Contract Nonr 1286 (10)).

TABLE OF CONTENTS

	Page
INTRODUCTION	1
SUBMARINE PHYSIOGRAPHY	5
General Physiographic Features	5
Physiographic Provinces of the Southern Oregon	
Continental Margin	9
Continental Shelf	12
Upper Continental Slope	13
Klamath Plateau	13
Cape Blanco Bench	15
Middle Bench	16
Lower Continental Slope	16
Rogue Submarine Canyon	17
REGIONAL GEOLOGY	22
General Geology of Southwestern Oregon and	
Northern California	22
Coastal Features and the History of Sea Level	
Fluctuations	31
SAMPLING AND ANALYTICAL PROCEDURES	33
Sample Collection and Processing	33
Laboratory Analyses	36
STRUCTURAL FEATURES OF THE SOUTHERN OREGON MARGIN	40
Regional Setting	40
Gravity	40
Magnetics	44
Heat Flow	47
Seismicity	48
Interpretation of the Tectonic Pattern	50
Continental Margin Structure	51
General Structural Trends	51
Continental Shelf	55
Upper Slope and Benches	58

	Page
Lower Slope	65
Rogue Submarine Canyon	67
Continental Margin Structure in Relation to the Regional Setting	70
STRATIGRAPHY	74
Unconsolidated Sediments	74
Planktonic Foraminifera-Radiolaria Abundance	74
Mazama Ash	78
Radiocarbon Dating	79
Faunal Stratigraphy of Consolidated Sediments	79
Rates of Sediment Accumulation	81
SEDIMENTOLOGY	85
Unconsolidated Sediments	85
Classification and Distribution of Sediment Types	85
Olive Gray Lutite	88
Gray Lutite	95
Sand-Silt Layers	96
Minor Sediment Types	97
The Present Sediment Pattern	99
Textural Relationships	100
Mineralogy	102
Light Minerals	106
Heavy Minerals	109
Clay Minerals	114
Organic Carbon	119
Consolidated Sediments	122
Classification and Distribution of Rock Types	122
PROCESSES OF SEDIMENTATION	128
A Proposed Model for Modern Sediment Transport on the Southern Oregon Continental Margin	128
The Initial Regime of Sedimentation	128
The Concept of Lutum Transport	133
The Oceanographic Regime	134
Turbid Layer Formation and Transport	
Across the Shelf	141
Transport Down the Slope	145
Deposition of Lutum on the Lower Slope	150
The Late Pleistocene and Holocene Sedimentation Patterns	153

	Page
SUMMARY AND CONCLUSIONS	157
Development of the Structural Framework	157
Pre-Tertiary History	157
Tertiary History	158
Quaternary History of Sedimentation	162
Pleistocene	162
Holocene and Modern	164
BIBLIOGRAPHY	168
APPENDICES	183
Legend for Appendices	183
Appendix 1. Piston core and rock dredge station locations	184
Appendix 2. Radiocarbon age determinations from selected cores	185
Appendix 3. Coarse-fraction composition of sediment samples	186
Appendix 4. Textural analyses of sediment samples	198
Appendix 5. Light mineral composition of the sand fraction in selected sediment samples	207
Appendix 6. Heavy mineral composition of the sand fraction in selected sediment samples	208
Appendix 7. Quantitative analyses of the major clay minerals from X-ray diffraction records of selected samples	211
Appendix 8. Mineralogy of the major rock types from dredge hauls	212

LIST OF FIGURES

Figure	Page
1. Oregon continental margin and adjacent deep-sea areas.	3
2. Bathymetry of the southern Oregon continental margin.	7
3. Precision Depth Recorder track lines in the area of investigation.	8
4. Physiographic provinces of the southern Oregon continental margin.	10
5. Selected bathymetric profiles of the continental margin.	11
6. Generalized bathymetry and selected profiles across the Rogue Submarine Canyon.	19
7. Geographic and drainage features of southwestern Oregon and northern California.	23
8. Geologic map of southwestern Oregon and northern California.	26
9. Location of piston core and dredge samples.	34
10. Flow chart for core processing and sample analysis.	35
11. Major tectonic features and earthquake epicenters in the northeast Pacific.	41
12. Free-air gravity anomaly map west of the southern Oregon-northern California coast.	43
13. Magnetic anomaly patterns off southern Oregon and northern California.	45
14. Fault-plane solutions of earthquakes and possible displacements from first motion studies in the northeast Pacific.	49
15. Track line map of continuous seismic profiles.	52

Figure	Page
16. Major structural features of the southern Oregon margin.	53
17. Sparker profiles across the southern Oregon shelf and upper slope.	57
18. EDO subbottom profiles across the southern Oregon shelf edge and base of slope.	59
19. Sparker profile across Cape Blanco Bench.	60
20. EDO subbottom profile across the upper continental slope.	62
21. Sparker profile across the entire southern Oregon slope.	63
22. Sparker profile across the upper continental slope illustrating slumping.	64
23. Reflection profiles of the southern Oregon and northern California continental margins.	66
24. North-south Sparker profile across the Upper Rogue Canyon.	68
25. Summary of lithologic and stratigraphic information from piston cores from the southern Oregon margin and adjacent Blanco Valley.	76
26. Textural classification of unconsolidated sediments.	87
27. Coarse-fraction constituents of unconsolidated sediments.	89
28. Lithology of piston cores from the southern Oregon continental shelf.	90
29. Lithology of piston cores from the upper continental slope and benches.	91
30. Lithology of piston cores from the lower slope.	92
31. Lithology of piston cores from the Rogue Submarine Canyon.	93

Figure	Page
32. Distribution of surface sediment types on the southern Oregon margin.	101
33. Phi Mean Diameter versus Phi Deviation.	103
34. Phi Mean Diameter versus Phi Skewness according to depositional environment.	104
35. Phi Mean Diameter versus Phi Skewness according to sediment type.	105
36. Light mineral composition of selected sediments and sedimentary rocks.	107
37. Major drainage basins of northwestern United States.	110
38. Clay mineral composition of selected sediments from the continental margin and major Oregon rivers.	115
39. Rock types from the southern Oregon margin.	123
40. Schematic model of modern sediment transport processes on the southern Oregon margin.	129
41. Schematic model of the oceanographic conditions over the southern Oregon margin in winter and summer.	135
42. Idealized cross-section of the late Pleistocene sediment distribution on the southern Oregon margin.	154
43. Idealized cross-section of the Holocene and modern sediment distribution on the southern Oregon margin.	156

LIST OF TABLES

Table	Page
1. Age, correlation and paleo-depth of Foraminifera from selected consolidated sediments on the southern Oregon continental margin.	80
2. Sedimentation rates from the southern Oregon continental margin.	82
3. A comparison of the light mineral composition of selected margin sediments with southwestern Oregon sandstones.	108
4. Comparison of the heavy mineral suites and pyroxene/amphibole ratios of southern Oregon margin environments with continental drainage basins.	112
5. Total carbon, organic carbon and calcium carbonate in selected margin sediments.	120

MARINE GEOLOGY OF THE CONTINENTAL MARGIN OFF SOUTHERN OREGON

INTRODUCTION

Investigations of the world's continental margins have expanded in recent years owing to increased political awareness, economic need, and a more sophisticated technology. More important, however, is the fact that both interest and understanding of continental margins have increased due to a deeper scientific insight into the basic processes of margin development and due to an awareness of the importance of continental margins in the evolution of both continents and ocean basins. Recent theories concerning sea-floor spreading and plate tectonics (e.g. Vine, 1966; Isacks, et al., 1968; Le Pichon, 1968) have had a major influence on the interpretation of both the geology of ocean basins and the geologic structure and evolution of the adjoining continents. Because of these theories, new attention has been focused on the continental margins as the critical zones of transition between interacting continental and oceanic plates. An understanding of the tectonic history of continental margins in the light of sea-floor spreading must now be an essential prerequisite to help explain the processes of growth and development of ocean basins and continental masses.

The continental margin off the state of Oregon has been the subject of detailed investigation since 1962. The early work on the geomorphology of the Oregon margin by Byrne (1962, 1963a, b) was

followed by more detailed studies (Kulm and Byrne, 1966; Byrne, et al., 1966) as well as a number of other works. Geophysical studies have also been carried out on, or adjacent to, the Oregon margin (Dehlinger, et al., 1967, 1968; Emilia, et al., 1968; McManus, 1965; Shor, et al., 1968; Silver, 1969a, b).

The Department of Oceanography, Oregon State University, in a joint effort with the United States Geological Survey (USGS), has sought to gain further and more detailed information about the Oregon continental margin since 1967. Under this program an intensive and systematic study of the sediments and structure of this area is being carried out in an effort to better understand its geologic history, the dynamics of sediment movement in the water column and on the sea floor, and its possible economic mineral potential. Several published and unpublished reports describe preliminary findings of this program (Kulm, et al., 1968a, b; Clifton, 1968; Chambers, 1968; Mackay, 1969; Bales and Kulm, 1969; Kulm and Bales, 1969; Spigai and Kulm, 1969; Roush, 1970; Neudeck, 1970).

The present study of the continental margin off southern Oregon (Figure 1) is part of the overall USGS-sponsored program. Emphasis in this study has been placed on the sediments and structure of the continental slope. Data concerning the continental shelf, derived from unpublished research, will be used as supplementary information to provide a more comprehensive picture of the margin as a whole.

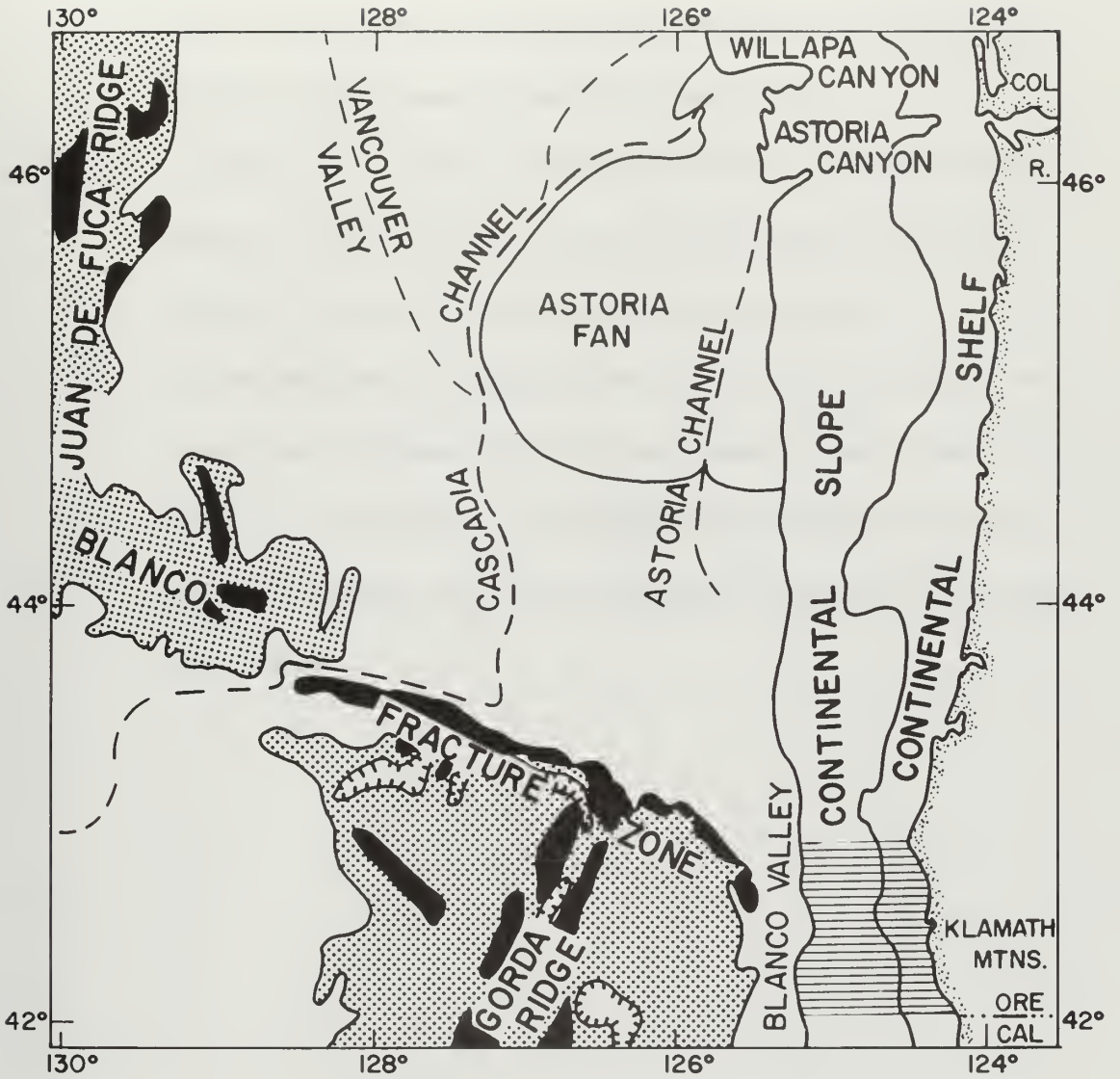


Figure 1. Oregon continental margin and adjacent deep-sea areas. Area of investigation is indicated by the horizontal rulings.

The objectives of this study are:

1. to determine the structure of the continental slope, its relation to the structure of the entire margin, and its influence on the present geomorphology of the slope;
2. to delineate the major bathymetric features of the slope and determine their influence on the sedimentary processes acting on the slope, both past and present; and
3. to develop a three-dimensional picture of the surface and subsurface sediment distribution pattern, and relate this pattern to the dynamic sedimentary processes operating in the water column over the continental slope and on the sea floor below.

SUBMARINE PHYSIOGRAPHY

General Physiographic Features

The geomorphology of the Oregon continental margin was first described in detail by Byrne (1962, 1963a, b). The continental margin off Oregon was called a continental terrace by Byrne and includes only the continental shelf and slope. The Oregon shelf is narrower, steeper and has its outer edge (the shelf break) in deeper water than the world's "average" shelf as given by Shepard (1963). It is also considerably wider in the north than it is in the south. The continental slope extends from the shelf break to a depth of approximately 3000 m, and is also wider, and has a gentler gradient, in the north than in the south.

In general terms, the northern Oregon margin is marked by the appearance of the Astoria Canyon and Fan system, a ridge-trough complex below 800 m, and a prominent bench below 500 m, while the central margin is characterized by submarine banks such as Heceta, Stonewall, and Coquille (Maloney, 1965). The southern margin is noted for the numerous slope benches at various depths, the Rogue Canyon, and numerous small submarine valleys.

In describing the southern Oregon margin, Byrne (1963b) noted the appearance of "terraces" at various depths as well as the numerous

submarine valleys, including the Rogue Canyon. He also noted the apparent antecedent nature of the "terraces" in relation to the submarine valleys, implying that the valleys have subsequently dissected the pre-existing "terraces." Byrne (1963b) compiled a bathymetric map in fathoms of the southern Oregon margin utilizing United States Coast and Geodetic Survey (USC&GS) smooth sheets of surveys done mostly in the mid- and late-1920's. More recently (1968), the USC&GS issued a bathymetric chart of the same region (USC&GS Chart 1308N-17). This chart was reconstructed from the data of the 1920 surveys and recontoured in meters. It gives a somewhat more detailed picture of the submarine physiography. The southern half of this chart, which includes only the area of this study from Cape Blanco to the Oregon-California border ($42^{\circ}00'N$ to $42^{\circ}50'N$) is used as the bathymetric base map (Figure 2).

Twenty-five hundred kilometers of bathymetric profiles were made on four Yaquina cruises (6706, 6708, 6711 and 6802) conducted during the course of this study, utilizing a Precision Depth Recorder. They have been used to supplement the existing bathymetric information (Figure 3). Navigational control was obtained using dual Loran A receivers and standard radar and navigational procedures which gave a maximum positioning error of ± 2 km.

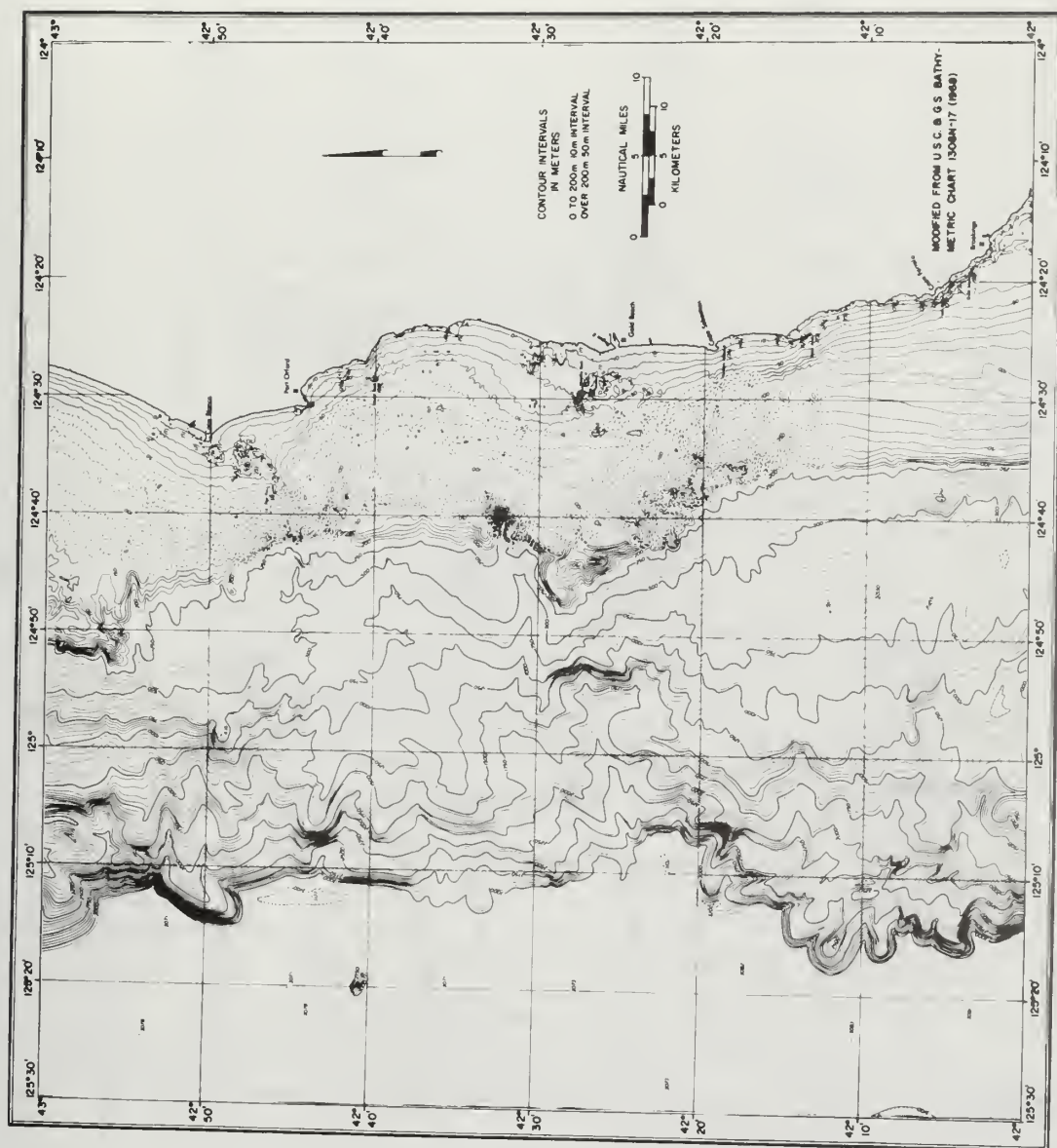


Figure 2. Bathymetry of the southern Oregon continental margin.

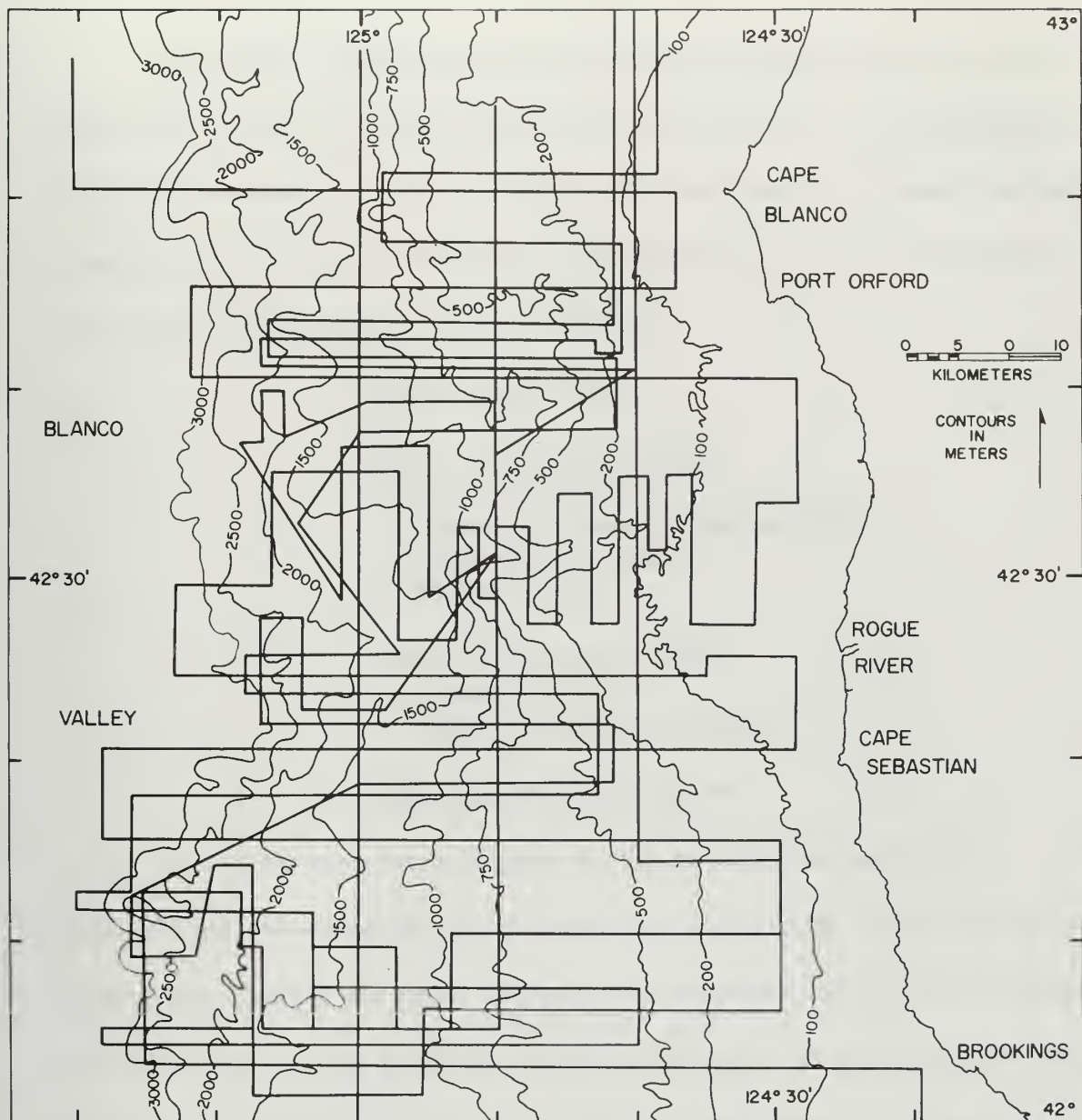


Figure 3. Precision Depth Recorder track lines in the area of investigation.

Physiographic Provinces of the Southern Oregon
Continental Margin

An analysis and comparison of previous work with the newer bathymetric data described above and combined with sub-bottom profiles has enabled the writer to subdivide the southern Oregon continental margin into a number of discrete physiographic provinces (Figure 4).

The provinces can be grouped as follows:

Continental Shelf

Upper Continental Slope

Klamath Plateau

Upper and Lower Plateau Slope

Cape Blanco Bench

Middle Bench

Lower Continental Slope

Lower Bench

Minor Submarine Valleys

Rogue Submarine Canyon

As can be seen from Figure 4, the boundaries have been generalized somewhat to approximate the underlying structural limits rather than follow the exact bathymetric contours, which only indicate the boundaries of the present dissected surface. A number of selected bathymetric profiles across the margin, which show the relation of the various physiographic provinces with depth, are shown in Figure 5.

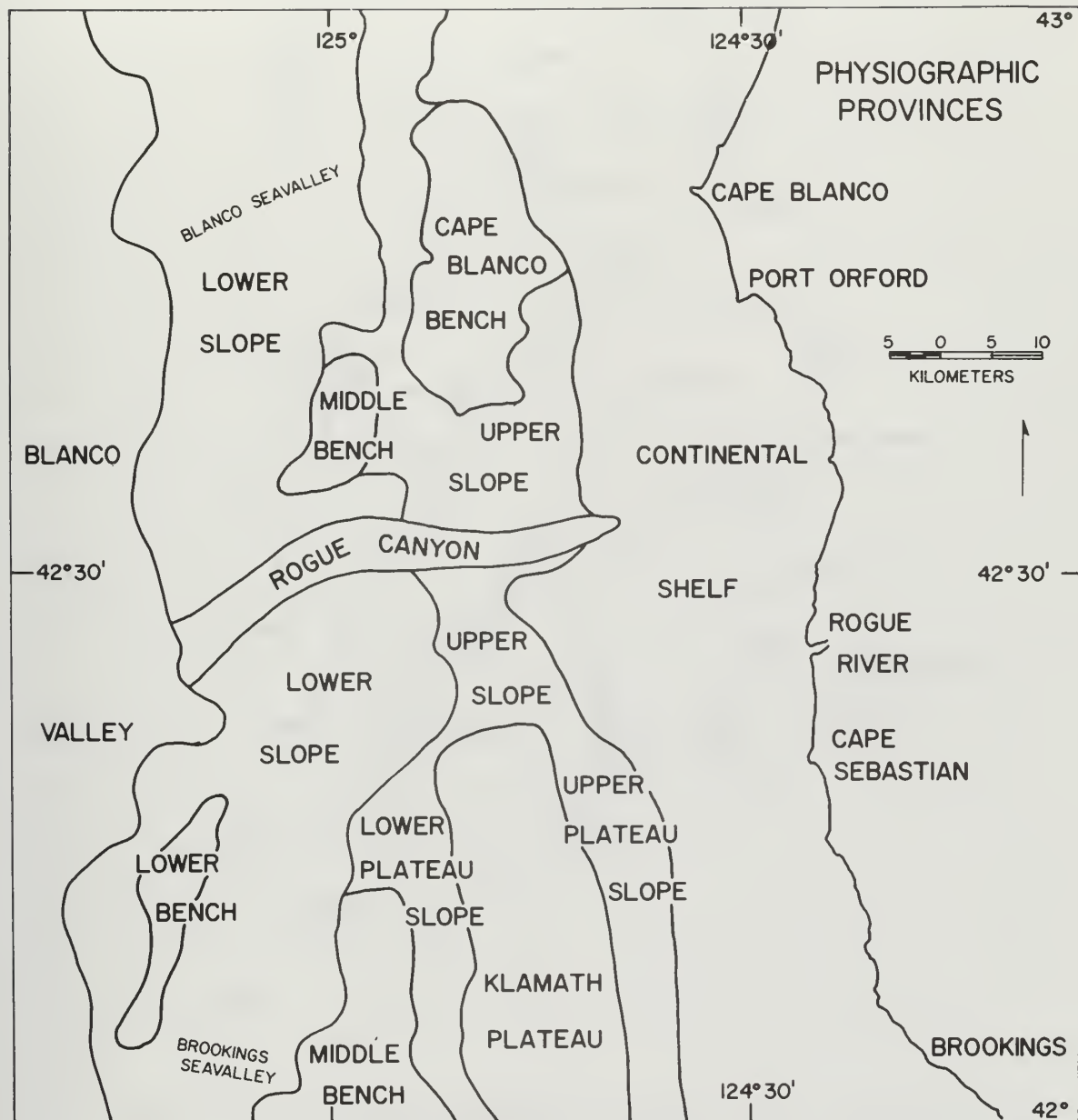


Figure 4. Physiographic provinces of the southern Oregon continental margin.

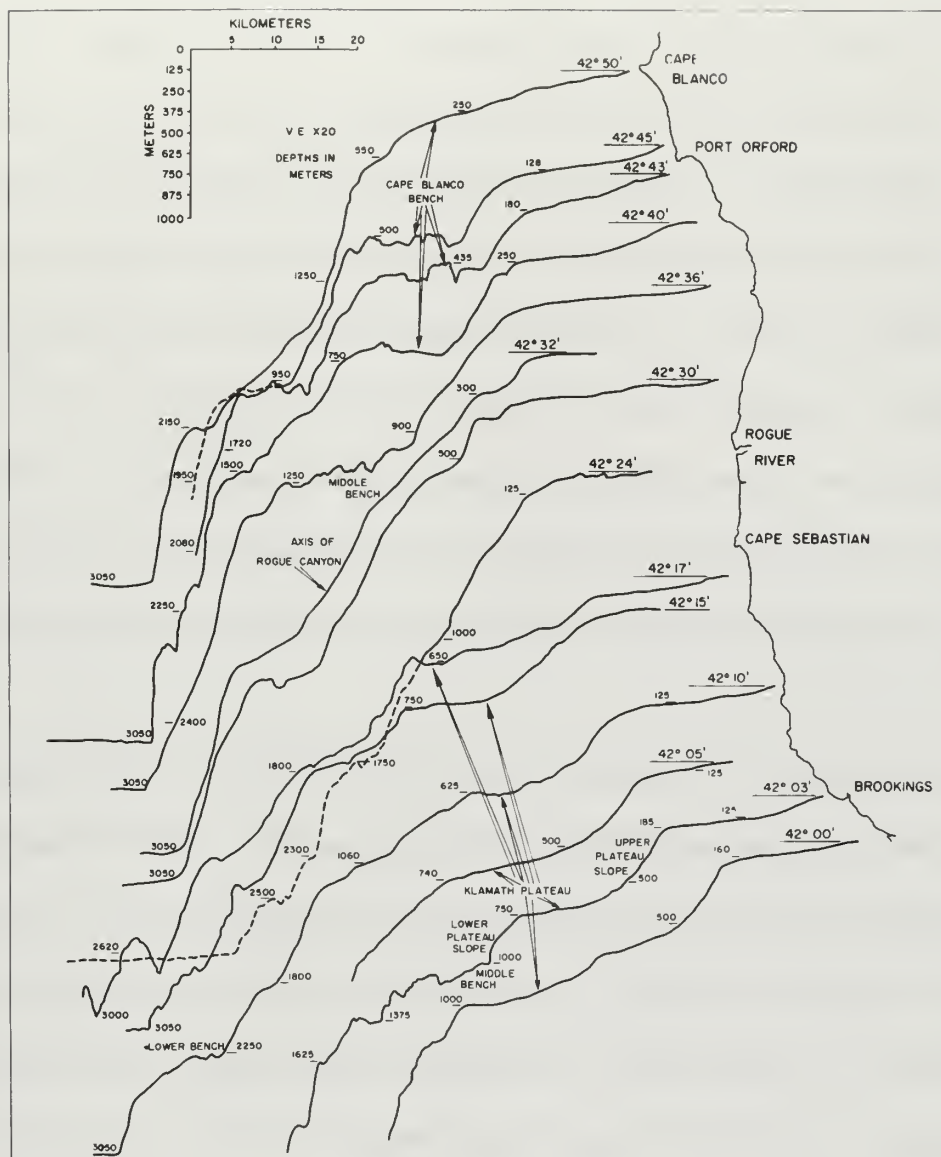


Figure 5. Selected bathymetric profiles of the continental margin.

Continental Shelf

The continental shelf off southern Oregon extends to depths varying between 120 m off the Rogue River to 200 m off Port Orford. Directly off Cape Blanco the shelf break is difficult to determine because the Cape Blanco Bench abuts the shelf edge and results in a gradually decreasing gradient of approximately 1° down to a depth of nearly 500 m before the first sharp break in slope (Figure 5, profile at $42^\circ 50'N$). In the area of investigation the slope width varies from 15 to 30 km; it is narrowest off Port Orford and Cape Sebastian and widest near the California border and just north of the Rogue River mouth.

Chambers (1968) has described the southern Oregon shelf between $42^\circ 20'N$ and $42^\circ 40'N$. He particularly noted the meandering contours in this area, which indicates a thin sediment cover, and the exposure of bedrock such as the Rogue River Reefs. Similar outcrops or shoals, such as the Blanco Reef, occur southwest of Cape Blanco. Chambers also noted the occurrence of submerged terraces which are especially well defined at latitude $42^\circ 21'N$. Here terraces occur at 35, 60, 70, 85, 100, 120 and 145 meters (± 5 m) and were most likely formed during stillstands of sea level which interrupted the last major transgression of the sea.

Upper Continental Slope

With the exception of the continental shelf, all of the physiographic provinces recognized in this study lie within the boundaries of the southern Oregon continental slope between $42^{\circ}00'N$ and $42^{\circ}50'N$. The slope is widest just off Cape Blanco and also south of Cape Sebastian (Figure 5). The steepness of the slope ranges from an average of 2° on the upper slope (above 1000 m) to an average of 5° on the lower slope (below 1000 m) because of the presence of benches.

The upper slope is characterized by the presence of benches, plateau slopes, and the Upper Rogue Canyon. It extends from the shelf break to depths varying from 750 to 1250 m. The lower boundary is the lowest extent of the gently inclined benches and/or the beginning of the steeper lower slope. The benches are distinctive not only because they occupy the greatest area of the upper slope, but also because their gentler gradient suggests a different structural origin from the steep escarpments above and below (Figure 5).

Klamath Plateau

The largest bench on the southern Oregon margin lies between 500 and 750 m within the southern part of the upper slope between Cape Sebastian and the California border (Figure 5, profiles at $42^{\circ}00'N$ to $42^{\circ}17'N$). This feature is the continuation of a large marginal plateau

which extends unto the upper slope off northern California as far south as $41^{\circ}10'N$. It has been named the Klamath Plateau by Silver (1969a) and this name is used here. The profiles of Figure 5 illustrate the moderate steepness ($1^{\circ}30'$) and relief of the Klamath Plateau and show how its width narrows from 25 km at $42^{\circ}00'N$ to 10 km west of Cape Sebastian. Silver (1969a, p. 11) noted a maximum width of 30 km for the Plateau on the northern California margin and also found that the Plateau slopes gently to the south.

The relatively flat topography and bench-like appearance of the Plateau terminates abruptly with the appearance of a topographic high, or a series of highs, which mark its western edge (Figure 5, profiles at $42^{\circ}03'N$, $42^{\circ}10'N$, and $42^{\circ}17'N$). Silver (1969a) and Kulm and Bales (1969) suggest that such topographic highs on the Klamath Plateau represent anticlinal folds. These folds have dammed, or ponded, the sediments behind them and have tended to smooth any underlying topographic irregularities. Other benches on the upper slope probably have a similar origin; this underlying structural control may in fact be more extensive and continuous than the boundaries of the Klamath Plateau (Figure 4) would indicate. The Klamath Plateau, the Cape Blanco Bench (Figure 4; Figure 5, profile at $42^{\circ}50'N$) and the large bench areas on the upper slope north of Coquille Bank (Byrne, 1963b) may actually represent a single bench controlled by a single anticlinal fold system. The folds may even be contemporaneous in origin. The

ponded sediments have formed a single bench which has since been partially obscured by slumping and dissected by submarine valleys.

Immediately above and below the Klamath Plateau are the Upper and Lower Plateau Slope respectively (Figure 5, profile at $42^{\circ}03'N$). The Upper Plateau Slope forms a transitional zone between the continental shelf and the Klamath Plateau, while the Lower Plateau Slope forms a transition between the Plateau and Middle Bench.

Cape Blanco Bench

The Cape Blanco Bench is named after Cape Blanco on the Oregon coast (Figures 2, 4, and 5). Although there is an almost continuous slope of about 1° from the shoreline at Cape Blanco down to a depth of about 500 m, the Cape Blanco Bench extends from about 250 to 500 m. As was previously noted, the Cape Blanco Bench and the Klamath Plateau may have formed as parts of a single bench system, the connecting segment between the two having since been obscured by the Upper Rogue Canyon and by slumping on the upper slope.

The extremely dissected nature of the Cape Blanco Bench differentiates it from the Klamath Plateau. This can readily be seen in the profiles at $42^{\circ}45'N$ and $42^{\circ}43'N$ (Figure 5). The dissected nature of the Bench appears to be the result of a number of small north-south trending channels which are restricted to this portion of the Bench and may be structurally controlled.

Middle Bench

The Middle Bench is so named because of its occurrence midway down the continental slope. It is exposed in the southern part of the slope below $42^{\circ}05'N$ at depths between 1000 and 1250 m and occurs again at approximately the same depth at $42^{\circ}36'N$ (Figure 5). It is apparent that the two exposures of the Middle Bench are part of a continuous system, representing the second in a series of at least three bench systems which extend the length of the southern Oregon margin and probably beyond. From physiographic data alone, however, it is not possible to determine whether these three systems also represent three different structural episodes. The southerly exposure of the Middle Bench marks the transition of the upper to the lower slope on the southernmost Oregon margin.

Lower Continental Slope

The lower continental slope extends from a depth of 1000 to 1250 m down to 3000 to 3050 m where it meets the abyssal plain. However, south of Cape Blanco Bench the lower slope may begin at depths as shallow as 750 m. Between Cape Blanco and the Oregon-California border the lower slope has an inclination from $4^{\circ}20'$ to $8^{\circ}10'$.

In general the lower slope is marked by the existence of a number of small submarine valleys which extend from the upper reaches

of the lower slope down to the abyssal plain. There are approximately eleven such submarine valley systems, excluding the Rogue Submarine Canyon. The two most prominent valley systems are called the Blanco Seavalley at $42^{\circ}45'N$, and the Brookings Seavalley at $42^{\circ}05'N$ (Figures 2 and 4). Most of the valley systems drain only the lower slope, extending from a depth of about 1000 to 1250 m. They terminate on the sea floor at a depth of about 3000 m. Their average gradient is about 4° .

The Lower Bench is also exposed on the lower slope between $42^{\circ}05'N$ and $42^{\circ}15'N$ at a depth between 2250 and 2500 m (Figure 5). The topography shown in Figure 5 suggests that this bench may also be part of a continuous system at this level, the third such system identified on the southern Oregon slope. Exposures of this bench further to the north on the lower slope may be absent due to sedimentation. Byrne (1963b) cites other exposures of benches, or in his terminology "terraces," at various depths, such as those occurring at 1600 to 1700 m at $42^{\circ}50'N$.

Rogue Submarine Canyon

Byrne (1963b) recognized the Rogue Submarine Valley and placed its terminus at a depth of approximately 1100 to 1200 m. However, the present study shows that this depth only marks what is now termed the Upper Rogue Canyon, and that this valley system is continuous to

the base of the slope to a depth of 3050 m. The Upper Rogue Canyon heads on the continental shelf at a depth of 145 meters and is located some 12 miles northwest of the mouth of the Rogue River. From here it continues to a depth of about 1500 m in a generally east-west direction. The Lower Rogue Canyon extends from this depth down to 3050 m at the base of the slope (Figure 2), and has a general northeast-southwest trend. As can be seen from Figure 2, the Lower Rogue Canyon is actually a continuation of a northeast-southwest-trending swale which lies to the north of the Canyon and enters it at approximately 1500 m.

The writer believes that the Canyon system is continuous, and although it may not be structurally continuous in its entirety, it is a single valley system from shelf break to base of slope. Figure 6 shows the major contours of the Rogue Canyon system together with a series of north-south profiles across the axis and a longitudinal profile down-axis. Structural control on the Upper Rogue Canyon is suggested in the profiles C-C', F-F', G-G', and I-I', which show a notch or bench-like feature; this characteristic is not apparent on the profiles of the Lower Canyon. The north side of the Upper Canyon slopes 8° , the south side 15° ; the steepness of both the northwest and southeast walls of the Lower Canyon averages 12° . The entrance of the swale, which marks the beginning of the Lower Rogue Canyon, is a gradual one. It occurs between 1500 and 1750 m (profiles J-J' and K-K', Figure 6),

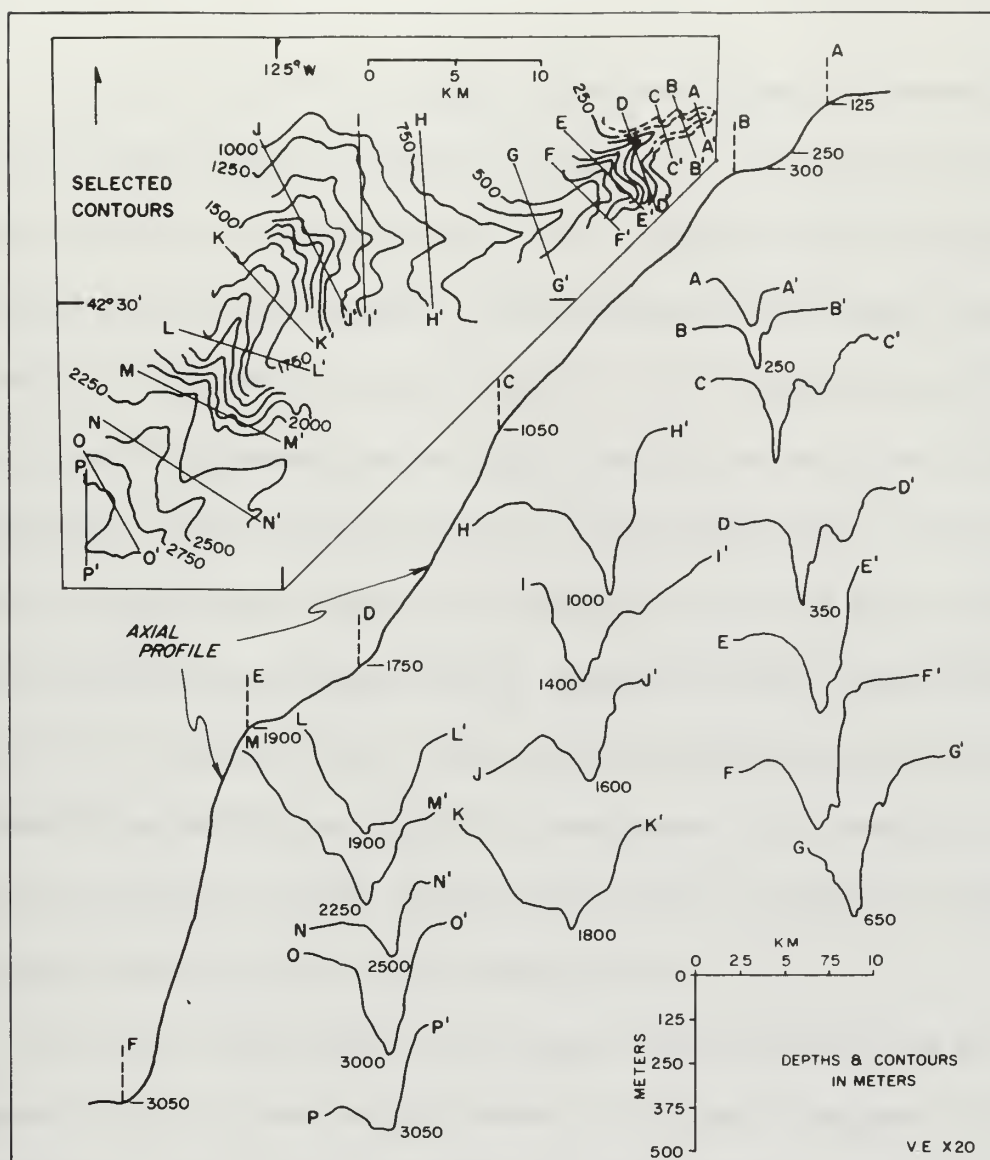


Figure 6. Generalized bathymetry and selected profiles across the Rogue Submarine Canyon.

but a noticeable change in the axial profile is evident in profiles K-K' and L-L'.

The axial slope of the Rogue Canyon varies over its extent, with the axis divided into five segments (Figure 6). The steepness of the axis varies down canyon from only $1^{\circ}50'$ at segment AB to a very steep 14° at EF, the lowest segment. The steepness of the Upper Canyon is similar to that for the upper slope (2° , or 5° if the benches are ignored) which indicates that the Upper Canyon may be more or less in equilibrium, or at grade with the surrounding upper slope. This would tend to indicate either that the lower slope is accreting or up-building faster than the Lower Rogue Canyon, or that the Lower Rogue Canyon may in fact be down-cutting. These generalizations do not take into account the added effects of uplift or subsidence. For example, during a period of uplift the Lower Canyon would down-cut faster and thus have a steeper gradient than the surrounding slope.

The axis configuration of the Rogue Canyon may also be an important factor in determining whether a particular segment is eroding or accreting. The axis is distinctly V-shaped in the upper reaches of the Canyon, particularly between segments AB and BC. This suggests an erosional character, but this is not particularly borne out by the axial slope of these segments. The Upper Rogue Canyon may then owe its V-shape to a structural origin. The Lower Rogue Canyon has a generally more rounded shape. This indicates that sediment may be

accumulating in the axis of the Lower Canyon, although the steepness seemingly contradicts this. In short, physiographic evidence alone may not be sufficient to determine the character of the Rogue Canyon; however, sedimentological and structural evidence to be presented later indicates that the Upper Rogue is stable or slightly erosional, while the Lower Rogue Canyon appears to be accumulating sediment.

REGIONAL GEOLOGY

General Geology of Southwestern Oregon and Northern California

The geologic history of the continental margin off southern Oregon is directly or indirectly related to the adjacent geologic provinces of the continent which lies landward of the margin. It is pertinent, therefore, to review the geology not only of the possible sediment source areas, but also of those areas whose geology and structural history may be related to that of the margin. All or part of the southern Oregon Coast Ranges, the Klamath Mountains, the Cascade Mountains, and the northern California Coast Ranges lie within southwestern Oregon and northern California (Figure 7).

Oregon's Coast Ranges are a series of coastal hills composed of thick sequences of Tertiary volcanic and sedimentary rocks. They are divided into northern and southern ranges which together stretch for about 250 miles along western Oregon. The southern Coast Ranges consist mainly of Eocene sedimentary and volcanic rocks, with younger Mio-Pliocene and Quaternary formations present only near Coos Bay and Cape Blanco. The Siuslaw, Umpqua, Coos, and Coquille are the main rivers which drain this portion of the Coast Ranges. The middle fork of the Coquille River is considered to be the province's southern boundary (Figure 7). Structurally, the southern Coast Ranges consist

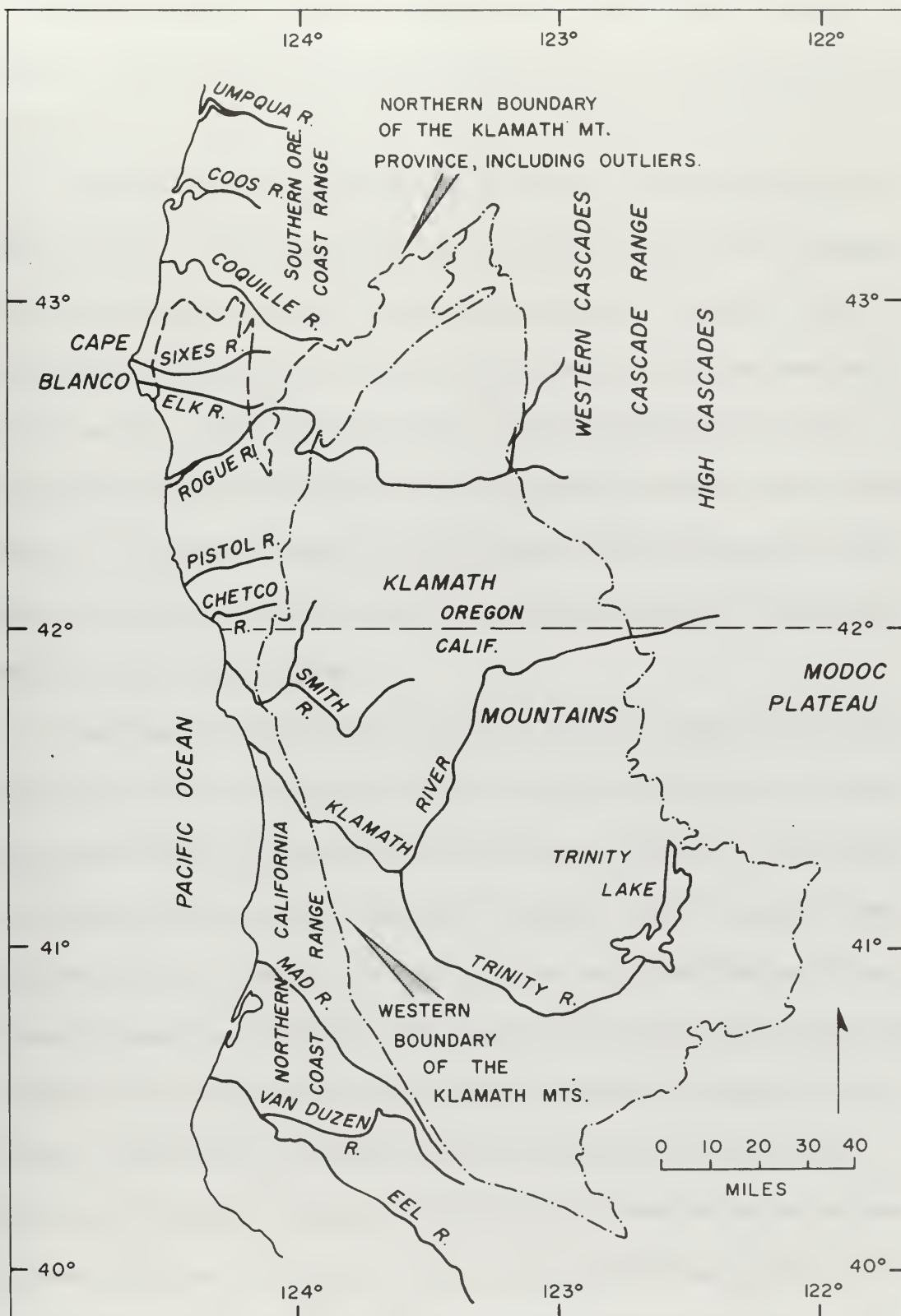


Figure 7. Geographic and drainage features of southwestern Oregon and northern California.

of folded and faulted sediments and volcanics which were uplifted during the mid-Tertiary to form a series of low hills with an average elevation of 1500 feet.

Two formations within the southern Oregon Coast Ranges are worthy of note. The oldest formation in this province is the Umpqua Formation (Early to Middle Eocene) which consists mainly of interbedded basalt and sandstones, with minor amounts of siltstones and conglomerates. The Tyee Formation unconformably overlies the Umpqua Formation and is the most widespread formation in the Coast Ranges. It consists mainly of rhythmically-bedded micaceous sandstones and siltstones which grade upward into siltstones (rhythmites) and are locally argillaceous.

The Klamath Mountains occupy the extreme southwestern corner of Oregon south of the southern Coast Ranges and west of the Cascade Range and extend into northwestern California (Figure 7). In Oregon, the Klamath Mountains are drained by the Sixes, Elk, Rogue, Pistol and Chetco Rivers, and in California by the Smith and Klamath Rivers. These drainages are comprised of rugged hills and mountains with 2000 to 5000 feet of relief, and consist mostly of folded and faulted pre-Tertiary strata which in places have been intruded by granitic and serpentized ultrabasic rocks. The Klamath Mountains are much older than any other part of western Oregon and probably contain the oldest formations in the state. Both Paleozoic and Mesozoic volcanic and

sedimentary rocks are present, which have been altered locally to schist, phyllite and marble. Irwin (1966) has applied the term "subjacent" to denote the entire sequence of eugeosynclinal and plutonic rocks within the Klamath Mountains which were folded and thrust-faulted during the Late Jurassic Nevadan orogeny. They are distinguished from the sequence of younger rocks which unconformably overlie them, to which he has applied the term "superjacent."

The subjacent eugeosynclinal rocks range in age from Ordovician to Late Jurassic (Kimmeridgean) and consist mainly of graywacke sandstones, mudstones, greenstones, radiolarian cherts, minor amounts of limestone, as well as metamorphic equivalents of the foregoing and abundant granitic and ultramafic intrusives. Irwin (1966) describes the pattern of distribution of the rocks in the Klamath Mountains as one of concentric, rudely arcuate belts, which he divides from east to west into the eastern Klamath, central metamorphic, western Paleozoic and Triassic, and western Jurassic (Figure 8). All belts, except the eastern Klamath, contain outliers of adjacent belts and contain somewhat linear ultramafic and granitic bodies which generally conform to the arcuate pattern. The Western Jurassic belt in Oregon consists of the Dothan, Rogue, and Galice Formations; the last, the youngest known subjacent formation, is made up of slaty detrital rocks and a schist which forms the western boundary of this belt and of the entire Klamath Mountain province. The Dothan Formation is predominantly

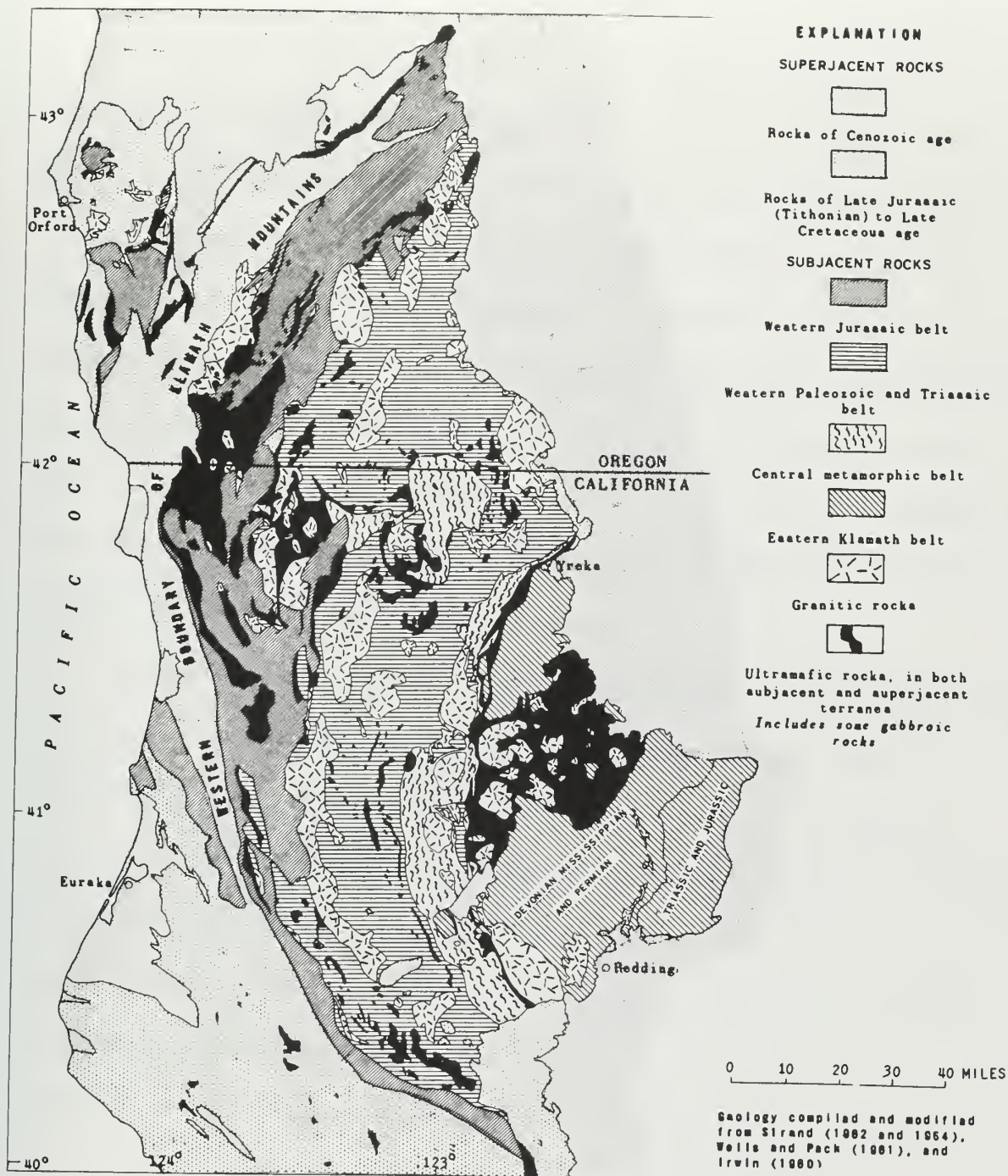


Figure 8. Geologic map of southwestern Oregon and northern California.

a medium-grained, indurated sandstone with interbeds of dark-gray or black mudstone, shale, siltstone, chert, and volcanics. These formations, all Late Jurassic in age, were folded and thrust-faulted during the Nevadan orogeny and were intruded by ultramafic, chiefly peridotite, and granitic bodies mostly of quartz diorite composition. The superjacent rocks are uppermost Late Jurassic or Early Cretaceous in age and in Oregon consist of a pair of formations known as the Myrtle Group. Middle and Late Cretaceous formations, the latter at Cape Sebastian, cap the Mesozoic sequence of the Klamath Mountains in Oregon, with later Cenozoic marine and river formations forming the youngest overlying deposits.

The arcuate, concentric distribution of the lithic belts of the subjacent rocks is the most obvious large-scale structural feature of the Klamath Mountains (Irwin, 1966; Wells and Peck, 1961). The lithic belts are separated by faults or by linear ultramafic and granitic bodies. These faults are thrusts which commonly dip eastward and separate eastward-dipping strata. They probably resulted from compressional forces normal to the arcuate trend, accompanied by westward over-riding of low angle thrust plates which occurred in pulses during the Late Jurassic Nevadan orogeny and also in Late Cretaceous time. Dott (1965) has noted that the predominant north-northeast thrust pattern of the Klamath Mountains has been superimposed by a predominantly north-northeast pattern of intense shears in northern

California and southwestern Oregon. These shears occurred during the late Cenozoic Cascadan orogeny (Dott, 1965).

The sediments and structure of the continental margin off southern Oregon may reflect the complexity of southwestern Oregon, particularly the varied geology and structural history of the Klamath Mountains. The dominance of the Klamath Mountain rock types, and the fact that they are drained by the major streams in the area, indicate that the Klamath Mountains are the most likely source of sediment found on the southern Oregon continental margin. Structurally, what is now the margin has probably also been affected by the major orogenies from the Nevadan to the Cascadan, and may still be actively involved in geologically recent movements.

The Cascade Mountains, the dividing line between eastern and western Oregon, are a line of high volcanic peaks running north-south the length of the state. In southern Oregon they are bounded on the east by the Basin and Range Province and on the west by the Klamath Mountains and are divided into two physiographic sub-provinces, the Western Cascades and the High Cascades.

The rocks of the Western Cascades, which range in age from Eocene to Pliocene (Peck, et al., 1964), include lava flows of pyroxene andesite and beds of pyroclastic debris, both interbedded in places with non-marine and shallow marine sediments. High Cascade Range rocks are also predominantly pyroxene andesite and range in age from

Pliocene to Recent. The Klamath and Rogue Rivers have their headwaters in these rocks, and flow westward from this source across the Klamath Mountains of southwestern Oregon and northern California (Figure 7).

Volcanic rocks in the Western Cascades differ from those in most of the High Cascades; the former have a greater variety of petrographic types and a larger proportion of pyroclastic rocks. A characteristic greenish hue is also noted in most of the Western Cascade rocks due to widespread chloritic alteration which resulted from late Miocene uplift and erosion.

The northern California Coast Ranges, like most of the Coast Range province in California, is a region of many separate ranges, coalescing mountain masses and major structural valleys. It consists of two different core complexes, one being the Franciscan rocks which are a complex Jurassic-Cretaceous eugeosynclinal assemblage, and the other consisting of Early Cretaceous granitic intrusions and older metamorphic rocks (Page, 1966). The two core complexes lie adjacent to one another separated by large-scale faults. Covering the core material are thick sequences of Late Cretaceous and Cenozoic clastic sediments which tend to conceal much of the complexity of the underlying "basement" core. The entire province is marked by continuing crustal disturbances represented by folds, thrust faults, steep reverse faults and strike-slip faults. These complex geology and structural

relationships have been studied by Reed (1933) and by Bailey, et al. (1964). Extensive Mesozoic rocks peripheral to the Coast Range core represent continuous thick sequences from the Upper Jurassic to the Upper Cretaceous. Overlying these are the Cenozoic shelf and slope deposits where marine sedimentary formations of nearly every epoch and stage from early Paleocene to Pleistocene are represented in thick accumulations (Taliaferro, 1943; Ogle, 1953; Christensen, 1966).

Page (1966) has recognized four major structural boundaries in the California Coast Range; three of which, the Nacimiento Fault Zone, the San Andreas Fault and the Sierran-Franciscan boundary, separate the granitic-metamorphic core complex from the Franciscan core. The fourth structural boundary is represented by the continental-oceanic boundary at the base of the present continental slope, and abruptly truncates the continental rocks and structures and separates them from the ocean basin (Hanna, 1952; Uchupi and Emery, 1963; Rusnak, 1966; Curray, 1966). The Sierran-Franciscan boundary is represented by the South Fork Mountain Fault, a 300-mile long eastward-dipping thrust that separates the Klamath terrane from the Franciscan complex of the Coast Ranges (Figure 7). The San Andreas is presently active (Meade and Small, 1966), but the Nacimiento Fault is not (Page, 1966).

Coastal Features and the History of Sea Level Fluctuations

In addition to the resistant headlands of the southern Oregon coast, such as Cape Blanco, Humbug Mountain and Cape Sebastian, the most prominent coastal features of southern Oregon are the numerous elevated marine terraces. These terraces were first studied by Diller (1902) and later by Griggs (1945) and Baldwin (1945), and most recently by Janda (1969). There are at least four prominent terraces in the vicinity of Cape Blanco. The lowest, the Elk River Terrace, which correlates with the Whiskey Run Terrace of Griggs, ranges in elevation from 65 m above sea level near Cape Blanco to a point below sea level south of Cape Blanco. Above this terrace, in ascending order, are the Pioneer, Seven Devils, Bills Peak, and Blue Ridge terraces. The last terrace is elevated more than 1500 feet above sea level in southern Oregon. Pleistocene sea level fluctuations are most probably recorded by these terraces, as is evidence of regional differential uplift and warping.

Faunal studies by Addicott (1964) and Richards and Thurber (1966) on mollusk shells from the Elk River Terrace indicate a minimum age for this level of 33,000 years. Janda (1969) reports a 45,000 year minimum age for this same level. This evidence indicates the Elk River Terrace to be late Pleistocene in age. Comparison of this data with the sea level rise curves of Curray (1964) and Milliman and Emery

(1968) suggest uplift of this terrace at the rate of 2 m/1000 years.

Since the Elk River Terrace dips near, or below sea level south of Cape Blanco, uplift is minimal in this area. The highest marine terrace, the "unnamed" terrace of Janda (1969), which may correlate with the Bills Peak or Blue Ridge Terrace of Baldwin and Griggs, is most probably Early Pleistocene or even Late Pliocene in age. The rate of uplift on this level remains indeterminate, until it can be precisely dated.

The rise of sea level which followed the last glacial advance and which marked both the end of the Pleistocene and the beginning of the Holocene is assumed to have begun about 18,000 years B.P. (Before the Present) (Curry, 1965). This Holocene transgression of the sea from about 125 m below present sea level to the present sea level may have been interrupted by several minor regressions (Curry, 1965). Assuming that these regressions did occur, they would have resulted in stillstands of the sea at 18, 40, 65, 87, and 125 m below sea level, according to Curry. These stillstands may be recorded as the submerged terraces which are to be found at 35, 60, 70, 85, 100, 120, and 145 m (± 5 m) on the southern Oregon shelf (Chambers, 1968). The effects of uplift or subsidence along the southern Oregon coast preclude precise correlation of these latter depths with the former; however, possible placer accumulations found by Kulm et al. (1968a) at similar depths suggest that these may be ancient shorelines.

SAMPLING AND ANALYTICAL PROCEDURES

Sample Collection and Processing

A total of 23 piston cores and ten dredge hauls was collected on the continental margin off southern Oregon. All of the piston cores and dredge samples were collected on cruises of the R/V Yaquina in 1967 and 1968 (Figure 9). The sample details are given in Appendix 1. A modified Ewing piston corer, utilizing a multiple corer (Fowler and Kulm, 1966) as a trip weight, was employed for coring. The cores were collected in plastic liners and cut into 3-meter sections aboard ship. Each section was sealed, placed in a galvanized downspout and kept at a temperature of 4°C until processed. Representative sedimentary rocks were selected from each dredge haul, thin-sectioned and described petrographically. A number of surface samples were taken on the southern Oregon shelf and slope at selected stations with a Shipek bucket-type sampler and a box corer. The shelf sediment samples have been analyzed and described by Chambers (1968). The core processing procedure is outlined in the flow chart in Figure 10. Cores were sampled at various intervals for the different lithologies and sediment textures, and at least every 50 centimeters.

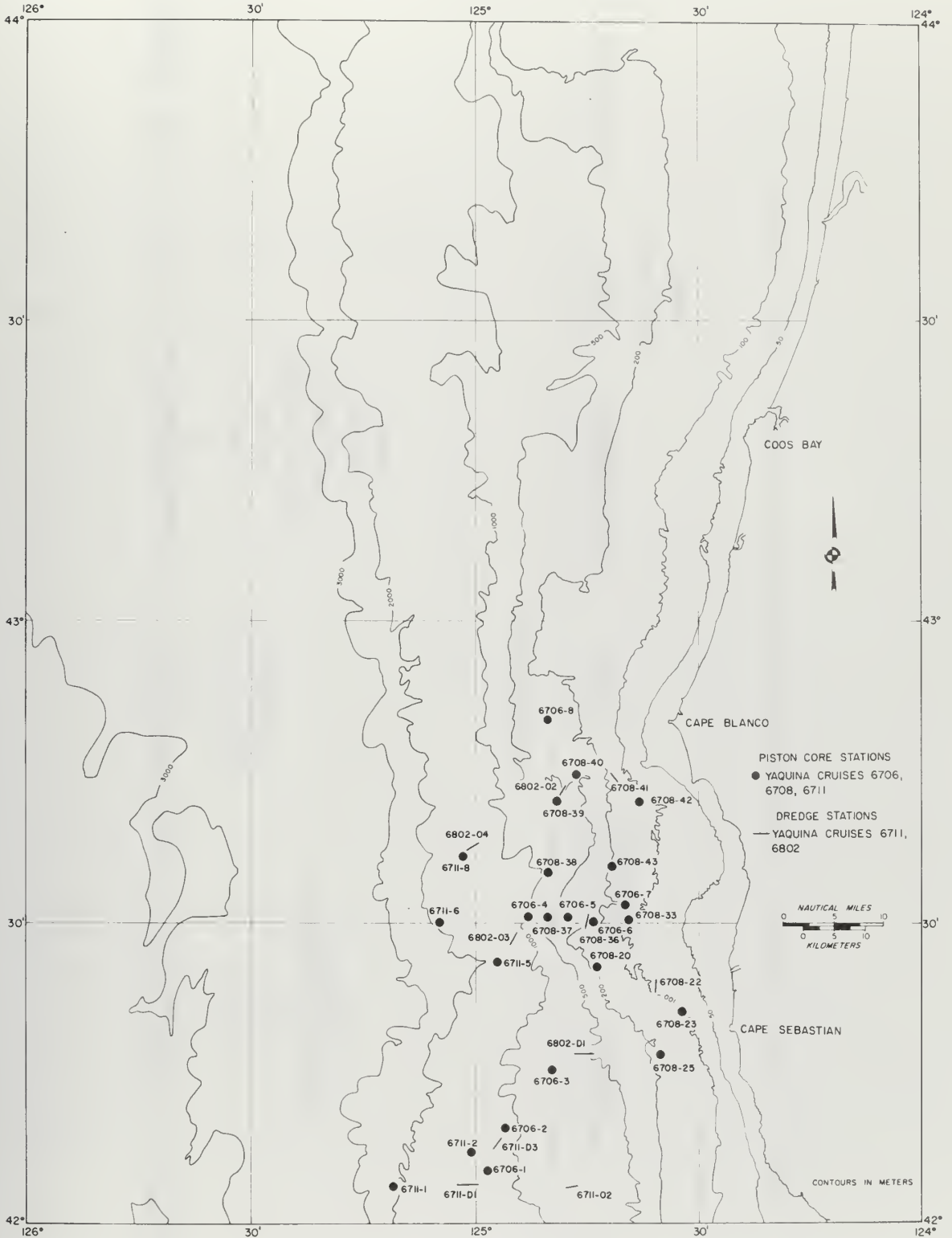


Figure 9. Location of piston core and dredge samples.

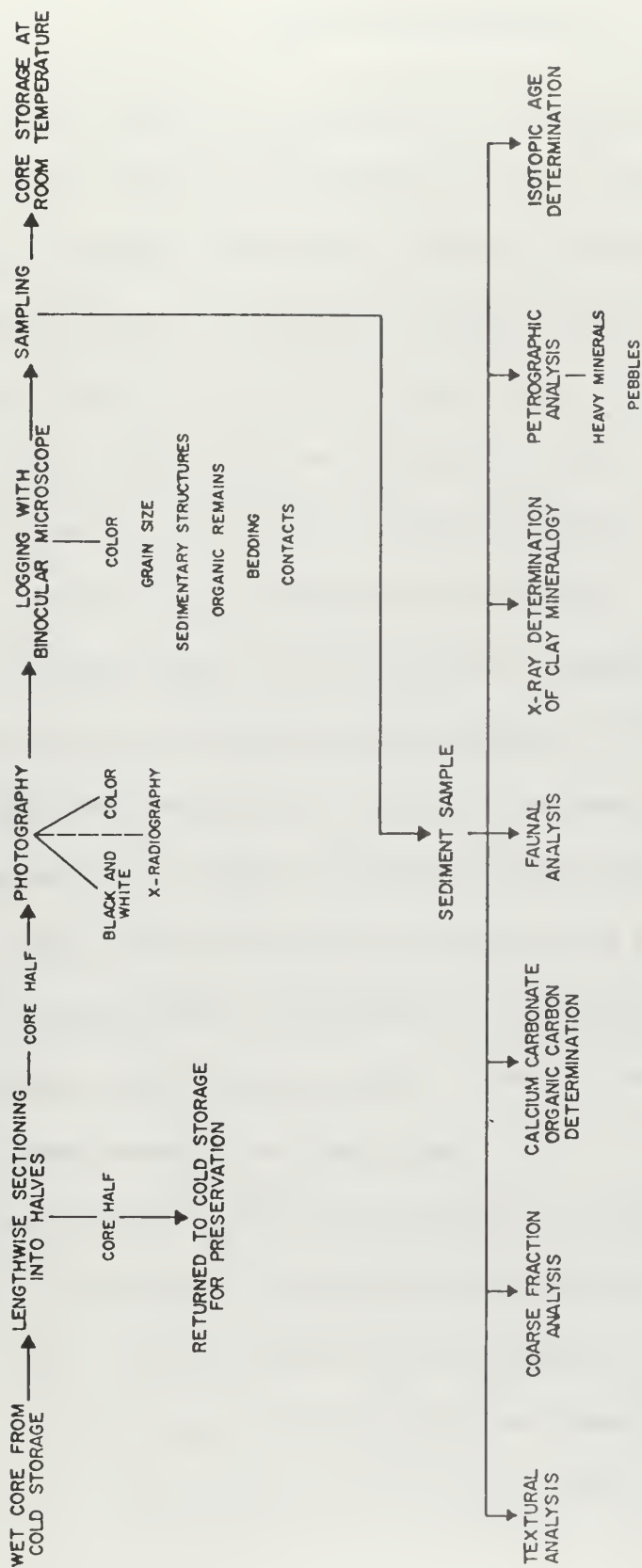


Figure 10. Flow chart for core processing and sample analysis. After Griggs (1969).

Laboratory Analyses

Textural analyses were made on 305 samples to determine the grain size distributions and variations for each of the sediment types. A fine-grain analysis was made by utilizing a vacuum-operated pipette and following standard techniques (Krumbein and Pettijohn, 1938). Sand textural analysis ($> 62 \mu$) was made with a standard Emery settling tube (Emery, 1938) as modified by Poole (1957). The percentages of sand, silt and clay were determined for each sample; in addition, standard grain size parameters (Inman, 1952) were computed for each sample using a CDC 3300 computer (Appendix 4). Coarse-fraction analyses were made on approximately 350 samples to determine the compositional variations of the major sediment types within each core (Appendix 3). A split of at least 300 grains were identified and counted using a binocular microscope following a grid pattern. A count of the Radiolarian and planktonic Foraminiferan faunas was made on all samples where it was possible to obtain a combined count of at least 100 specimens for the two groups.

Heavy mineral analyses were made on 33 selected samples. The heavy minerals were concentrated using tetrabromethane (specific gravity 2.96). The concentrate was mounted on a glass slide in Aroclor (R.I. 1.66) and at least 200-300 grains were identified and counted (Appendix 6). The majority of the mineral grains had a median

diameter between 62 and 125 μ , but no attempt was made to determine the exact size variations within mineral groups or among various samples. The light mineralogy of twelve selected samples was analyzed using the feldspar staining techniques of Bailey and Stevens (1960); the tabulated results are given in Appendix 5.

Organic carbon and calcium carbonate determinations were made on 16 selected samples representing the various sedimentary environments using a LECO Automatic Carbon Analyzer. The method outlined by Peterson (1969, p. 44) was followed in preparing the samples; the formulas used in computing the percent total carbon, organic carbon and calcium carbonate were also taken from Peterson (1969). These values are recorded in Table 5 (see Sedimentology), together with those samples taken from cores 6711-2 and 6706-5, which were analyzed by Peterson (1969).

The clay mineralogy of 22 samples was determined using X-ray diffraction techniques; the samples were treated and prepared for examination according to the methods outlined by Heath (1968) except for the use of the silver plug sample holder and the sample spinner described below. The treated suspensate from the $< 62 \mu$ fraction of each sample was allowed to settle until only the $< 2 \mu$ fraction remained in suspension. Only this fraction was collected and used in subsequent analyses. In order to minimize differential segregation of the clay mineral particles, approximately 1-1.5 milliliter of the clay suspension

was applied by means of a replicating pipette to the surface of a porous silver plug which served as the sample holder. This procedure produced a thin highly-oriented aggregate. A solution of 60% glycerol and 40% 0.3 molar magnesium chloride was sprayed on the oriented sample, then dried for at least one-half hour and analyzed. This latter procedure enhanced detection of the montmorillonite clays by expanding their lattices.

All the clay mineral samples were analyzed on a Phillips-Norelco diffractometer with a Geiger-Muller counting tube. Samples were scanned from 2° to $14^{\circ} 2\theta$ at a goniometer speed of $1/2^{\circ} 2\theta/\text{minute}$, and from 24° to $26^{\circ} 2\theta$ at a goniometer speed of $1/8^{\circ} 2\theta/\text{minute}$. The resulting diffractograms were produced on a linear scale strip chart recorder running at $1/2$ inch/minute. A sample spinner was employed which spun samples in the plane of reflection.

The presence of montmorillonite, illite and chlorite was determined from the diffractograms by identifying the peaks at 16.8 \AA , 9.95 \AA , and 7.05 \AA , respectively. Using the criteria of Biscaye (1964), and comparing the 3.54 \AA chlorite peak with the 3.58 \AA kaolinite peak, it was concluded that no kaolinite was present in any of the samples and that this latter peak represented only chlorite. The semi-quantitative method of Biscaye (1965) for determining the relative proportions of montmorillonite, illite and chlorite by means of weighting factors was employed to interpret the diffractograms. The resulting percentages

for each of the three major clay minerals in each sample are provided in Appendix 7. Persistent minor peaks on several of the diffractograms were identified as amphiboles.

STRUCTURAL FEATURES OF THE SOUTHERN OREGON MARGIN

Regional Setting

The structural and tectonic pattern in the northeast Pacific adjacent to Oregon and California has been examined and interpreted by McManus (1965), Wilson (1965a, b), Vine and Wilson (1965), and most recently by Tobin and Sykes (1968), Menard and Atwater (1968, 1969), McKenzie and Morgan (1969), Silver (1969a, b), and Atwater and Menard (1970). The two fracture zones which lie directly west of southern Oregon and northern California are the Blanco Fracture Zone (Figures 1 and 11A) and the Mendocino Fracture Zone (Figure 11A), respectively. The former is a transform fault (Wilson, 1965b) which separates the Juan de Fuca Ridge and the Cascadia Basin on the northwest from the Gorda Ridge to the southeast (Figure 1). The ocean area immediately north of the Mendocino Fracture Zone is one of active sea-floor spreading at present (Vine, 1966) and this undoubtedly has had an effect on the continental margin off northern California and southern Oregon.

Gravity

Gravity data for the southern Oregon margin and the adjacent ocean basin has been analyzed by Dehlinger (1969) and Dehlinger,



Figure 11. Major tectonic features (A) and earthquake epicenters (B) in the northeast Pacific.
After Tobin and Sykes (1968).

et al. (1967, 1968, 1970). The area west of southern Oregon has near-zero average free-air anomalies (Figure 12) which indicates that the area is essentially in isostatic equilibrium (Dehlinger, et al., 1970). In addition, the Blanco Fracture Zone does not appear to affect the bathymetry of the southern Oregon margin (McManus, 1965) nor the pattern of gravity anomalies (Figure 12).

On the other hand, the southern Oregon margin does exhibit a pattern of three distinct gravity anomalies (Couch, 1970). A high negative anomaly (-80 to -100 mgal) is located over the base of the southern Oregon continental slope (Figure 12). This anomaly may be due to the dip of the Moho beneath the continent and the overlying wedge of sediments at the base of the slope which appear to thicken northward of $42^{\circ}00'N$ (Couch, 1970). A positive anomaly of +1 to +10 mgal is situated near the edge of the continental shelf and suggests the presence of a structural high. Another negative anomaly (-40 to -60 mgal) is situated over the continental shelf south of $42^{\circ}30'N$ and is especially well developed over the northern California shelf at about $41^{\circ}00'N$ (Figure 12). Couch (1970) suggests that this anomaly could represent a large depression such as a basin or down-faulted structure which may be filled with sediment. A small positive anomaly of +20 mgal is present immediately southwest of Cape Blanco over the shelf and upper slope and may be related to a structural high.

A distinct break in the gravity anomaly pattern is present on

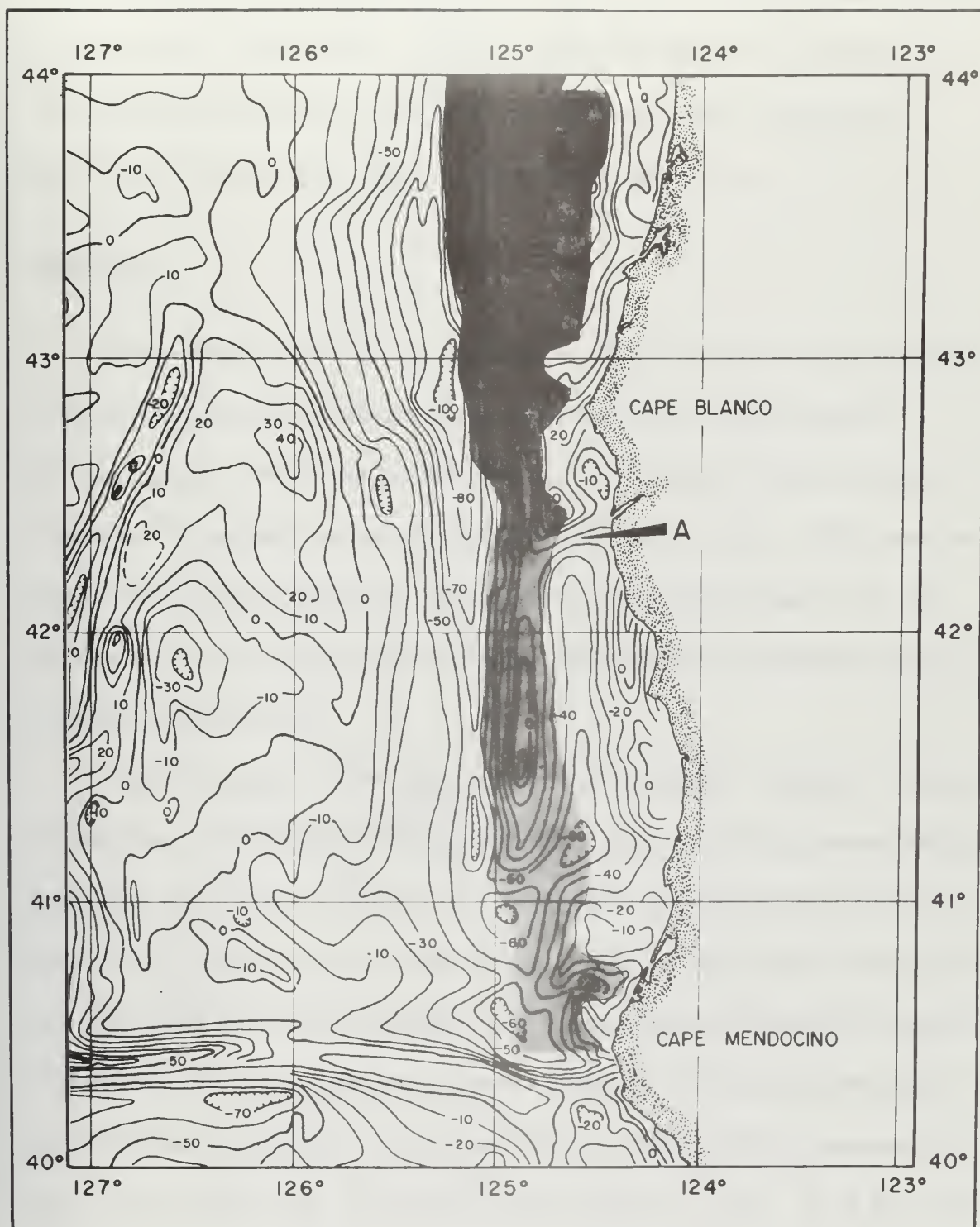


Figure 12. Free-air gravity anomaly map west of the southern Oregon-northern California coast. After Dehlinger, *et al.*, (1970). Shaded pattern denotes continental slope. Arrow (A) indicates the position of the surface trace of the west-southwest unconformity on the shelf.

the southern Oregon shelf (Figure 12, arrow A). The location and trend of this break corresponds to that of a west-southwest unconformity which Bales and Kulm (1969) have recognized as the dividing line between two regions of differing structural character.

Magnetics

The pattern of magnetic anomalies off the southern Oregon and northern California continental margins has been interpreted by Emilia, et al. (1968) and Silver (1969a, b). Silver (1969a) notes the presence of magnetic anomaly 3 (5 million years, Vine, 1966) near the base of the continental slope off northern California (Figure 13, D). He cites this as evidence for underthrusting of the continental margin in late Cenozoic time.

Emilia, et al. (1968) have noted the anomalous magnetic character of the crust off northern Oregon and the presence of high susceptibility material which dips in toward the continent near the Mendocino Fracture Zone (Figure 13, A). Only minor negative and positive anomalies are observed over the continental shelf and slope off southern Oregon. The small 100 to 150 gamma negative anomaly is the only distinctive negative feature (Figure 13, A), while only small positive anomalies are seen at the base of the continental slope (Figure 13, B). It is not clear whether these small positive anomalies are a continuation of anomaly 2 (Emilia, et al. 1968; Figure 13, B and C) or whether they represent

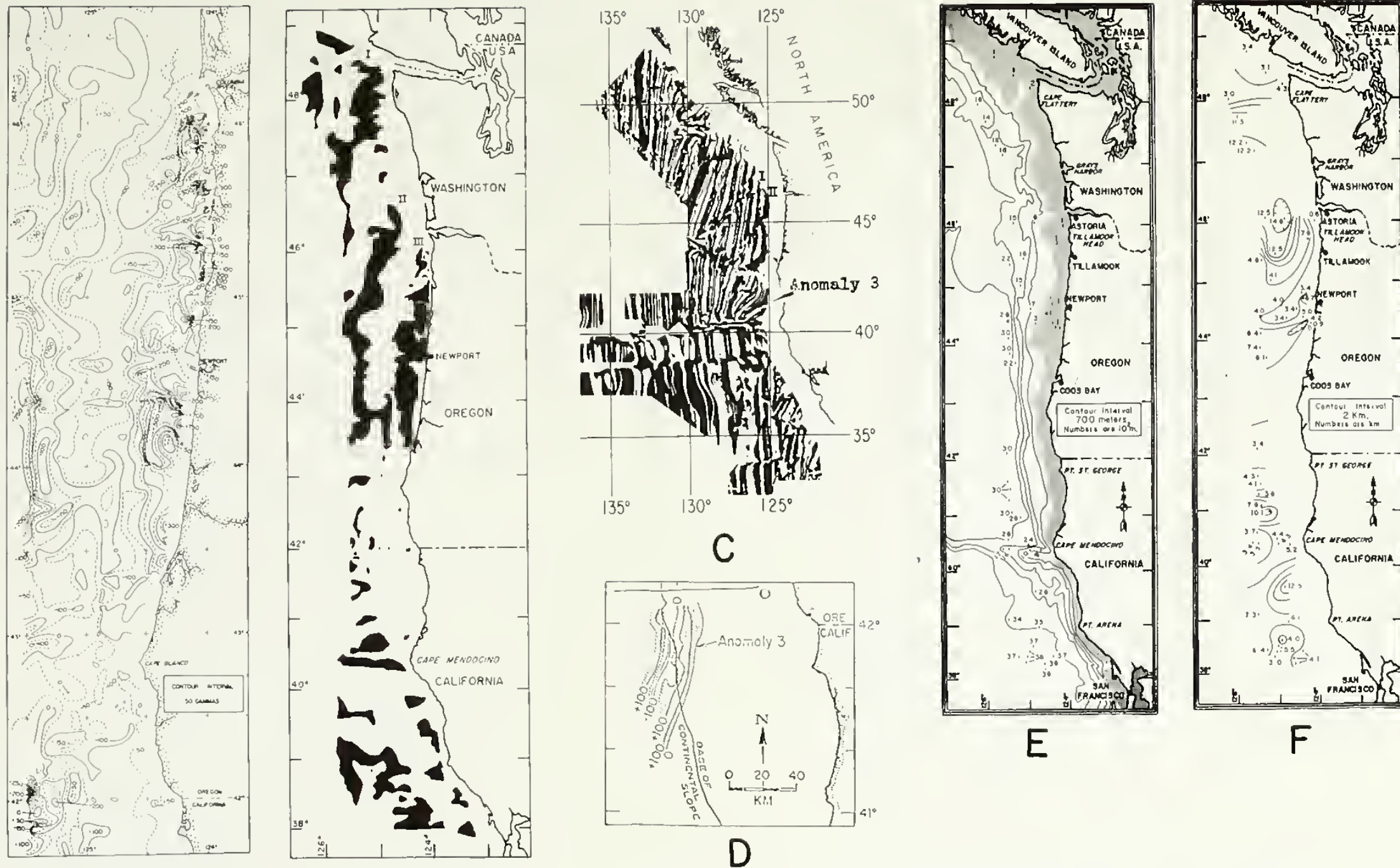


Figure 13.

Magnetic anomaly patterns off southern Oregon and northern California. A. Total magnetic field. B. Positive magnetic anomalies. C. Magnetic anomalies in the northeast Pacific. Anomaly 3 (arrow) is the westernmost positive anomaly adjacent to the continental margin. D. Anomaly 3 as mapped on the continental slope. E. Water-depth contour map off Oregon (700 m contour interval). Shaded portion indicates shelf. Numbers indicate stations where source depths were calculated. F. Source depths to magnetic anomalies. Contours in 2 km intervals; source depths to nearest hundred m. A, B, E, and F after Emilia *et al.* (1968); (modified after Raff, 1966); D after Silver (1969b).

anomaly 3 noted by Silver (Figure 13, C and D). It is also not clear whether anomaly 2 of Emilia, et al. (1968), and anomaly 3 noted by Silver are the same.

The source depth of the magnetic anomalies (Figure 13, E and F) on the southern Oregon and northern California continental slope vary between 3.4 and 4.5 km (Emilia, et al., 1968), which agrees with similar calculations made by Silver (1969a) for anomaly 3. This would place the anomalies, depending upon water depth, within the second layer (consolidated sediments and basalts). According to Vine and Wilson (1965), the bulk of the magnetization rests in this thin (1 to 2 km) layer of basalts (layer 2) which overlies the main oceanic crust. Deeper anomalies have been noted by Emilia, et al. at the base of the slope off the Eel River in northern California (10.1 km), and on the northern Oregon margin (12.5 and 14.6 km). The sources for these latter anomalies are deeper within the oceanic crustal layer.

Figure 13, B indicates the distinct difference between the magnetic character of the northern and southern Oregon continental shelf. Large positive anomalies are observed over the northern Oregon shelf, probably due to the presence of coastal volcanics which extend beneath the shelf of this area (Emilia, et al., 1968). In contrast, the southern Oregon shelf is nearly barren of such anomalies which may reflect the low magnetic susceptibility of the probable metamorphic rocks beneath the southern shelf. Kulm, et al. (1968a) have analyzed magnetic data

of a more detailed nature for the continental shelf adjacent to the Rogue River and have interpreted the anomalies as possible evidence for placer deposits.

Heat Flow

Dehlinger, et al. (1970) report the heat flow values from 76 stations measured in the northeast Pacific. Those stations north of the Mendocino escarpment have an average heat flow value of $2.4 \mu\text{cal}/\text{cm}^2 \text{ sec.}$, which is one-third greater than the average for ocean ridges and nearly double the value for ocean basins. Mesecar (1968) and Korgen (1969) have studied the sediment temperature gradients and heat flow values over the Oregon continental slope. Mesecar measured heat flow values at eight stations down the continental slope and on the adjacent abyssal plain and noted a linear increase in the value of both the sediment temperature gradient and the heat flow with depth. He found the mean heat flow values on the slope to be $2.0 \mu\text{cal}/\text{cm}^2 \text{ sec.}$ and that on the abyssal plain to be $3.2 \mu\text{cal}/\text{cm}^2 \text{ sec.}$ Thus the continental slope, and the deep sea environment adjacent to it are areas where the heat flow is higher than normal, reflecting the presence of high heat sources, which in turn may suggest the presence of a low density convecting mantle.

Seismicity

The seismicity of the areas adjacent to the southern Oregon margin has been examined by Tobin and Sykes (1968) and Bolt, et al. (1968). Earthquake epicenters concentrate along the Gorda Ridge, the Mendocino Fracture Zone east of Gorda Ridge, and the Blanco Fracture Zone between Juan de Fuca and Gorda Ridges (Figure 11, B). According to Dehlinger (1969), fault-plane solutions (Figure 14) indicate that all but one of the relative motions in this area are consistent with tension in an east-west direction. Hamilton (1969) also postulates that crustal extension has been the dominant tectonic movement during most of Cenozoic time along the western United States. Bolt, et al. (1968) postulate that the fault-plane solutions on the shelf north of Cape Mendocino and in Gorda Basin are consistent with a right-lateral strike-slip which trends about N40°W. They suggest that distortion of the oceanic crust within Gorda Basin, as well as some degree of underthrusting along the continental margin may account for the eastward component of strike-slip.

Dehlinger's interpretation (1969) of tension in an east-west direction negates the existence of regional compression and casts doubt on the possibility of underthrusting along the southern Oregon-northern California margin. However, Byrne, et al. (1966) and Silver (1969a, b) have cited evidence of compressional features on the margin off central

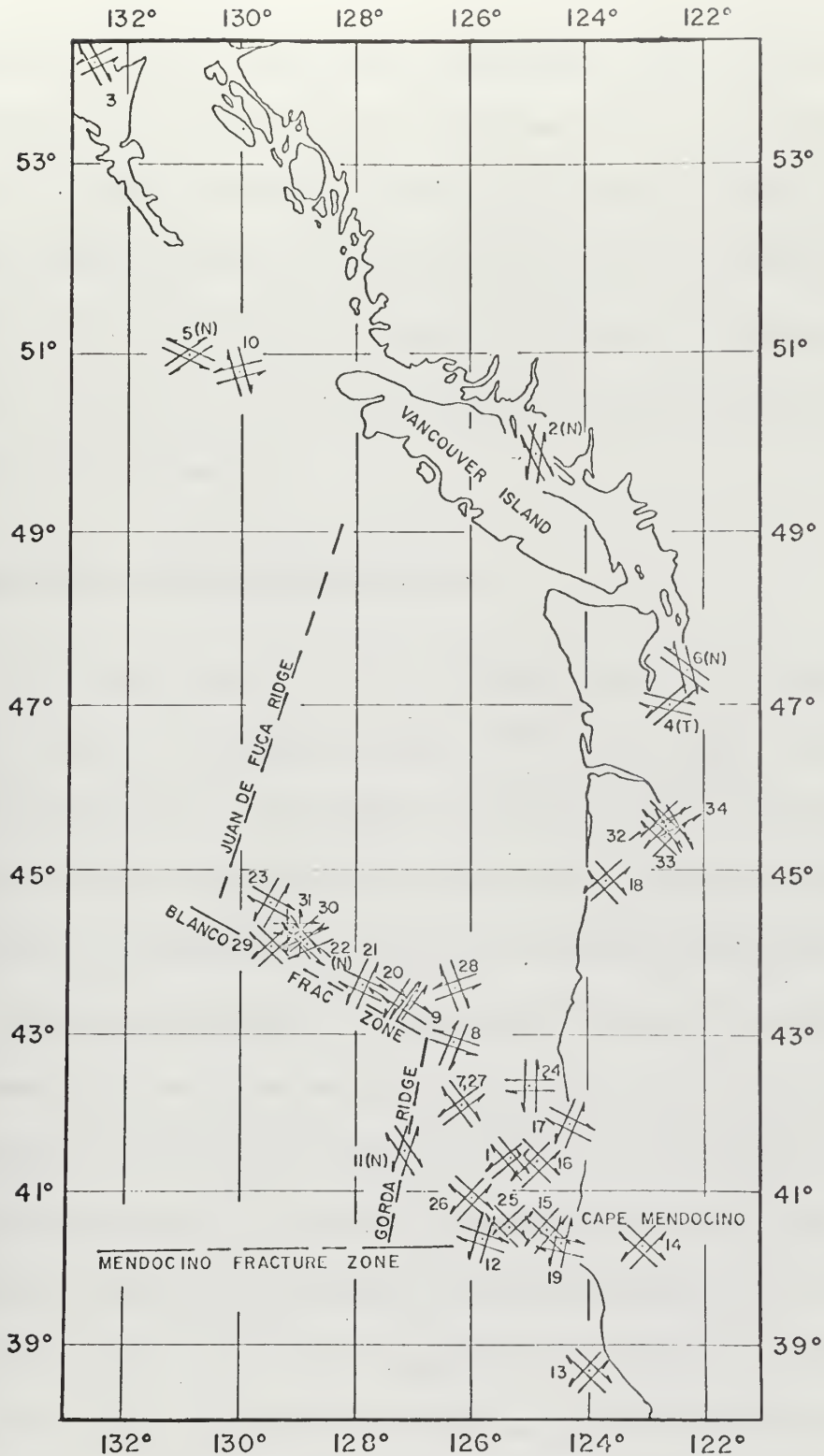


Figure 14. Fault-plane solutions of earthquakes (numbers 1-23) and possible displacements from first motion studies (numbers 24-34) in the northeast Pacific. Arrows indicate horizontal component of displacement; N indicates normal faulting. After Dehlinger, *et al.*, (1970).

Oregon and northern California, respectively. Silver (1969a) notes that the presence of anticlinal and synclinal folds on the northern California margin corroborates his view of underthrusting in that area. Compressional features on the margin may also be attributable to local vertical forces rather than to large-scale underthrusting; hence, the origin of these features is an open question at present and one which requires further analysis.

Interpretation of the Tectonic Pattern

The tectonic pattern of the northeast Pacific is a complex one. Silver (1969a, b), Dehlinger, et al. (1970), Bolt, et al. (1968), Menard and Atwater (1968, 1969), Atwater and Menard (1970), and others have developed various theories for the large-scale tectonic movements involving the interaction of oceanic and continental lithospheric plates.

A general consensus of these workers indicates a predominantly east-west direction of movement of these plates prior to Miocene time. From Miocene time to the present, however, the movement of oceanic and continental plates (i. e. the Pacific and North American plates, respectively) with respect to one another has shifted direction to a northwest-southeast trend. This major component of movement is a right lateral strike-slip motion along the San Andreas-Queen Charlotte Fault systems (Figure 11, A) accompanied by a smaller component of eastward underthrusting of the oceanic plate against the continent.

Continental Margin Structure

The structure of the continental margin off southern Oregon has been investigated with the aid of detailed continuous seismic-profiling surveys conducted during 1967, 1968, and 1969. Approximately 2000 km of track lines have been made off the southern Oregon shelf and slope between Cape Blanco and the Oregon-California border (Figure 15). The profiling equipment used included an EG&G Sparker with both 5,000 and 10,000 joule capacity, a 20 cu. in. Bolt air gun and a 3.5 KHz Edo transducer. Based on an analysis of these continuous seismic profiles, a map has been compiled (Figure 16) which illustrates the major structural features of the southern Oregon margin. The structure of the continental shelf illustrated in Figure 16 has been derived from the interpretation of Bales and Kulm (1969).

General Structural Trends

The trend of both the major fault and fold systems on the margin is generally north-south, parallel or sub-parallel to the margin (Bales and Kulm, 1969). The major exceptions to this trend are the east-west faults running through the Upper Rogue Canyon and the several east-west folds on the continental shelf south of Cape Sebastian. It appears from Figure 16 that the continental shelf and upper slope are characterized by folds, whereas the lower slope topography may owe its origin

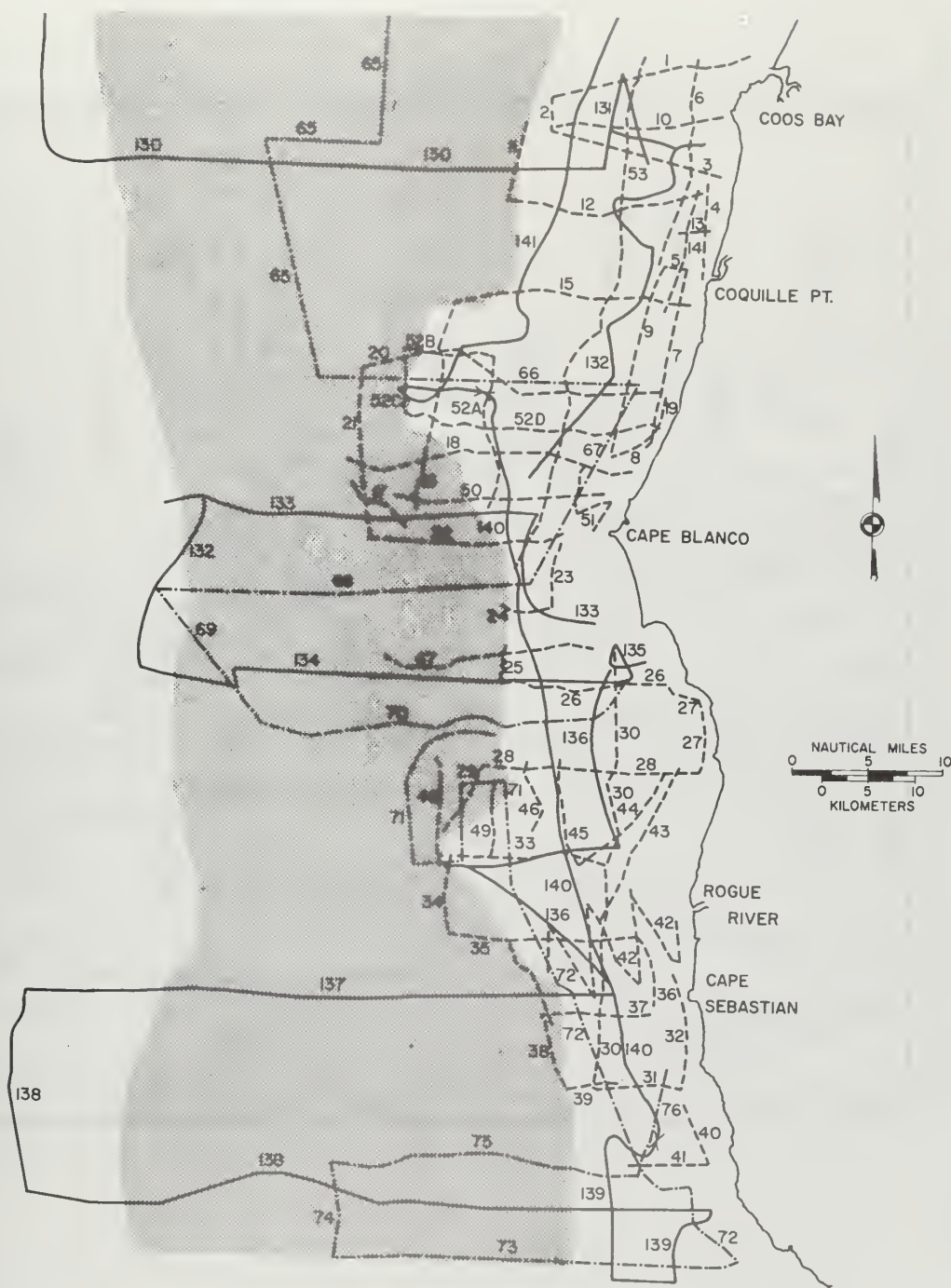


Figure 15. Track line map of continuous seismic profiles. Shaded area denotes the continental slope. After Kulm and Fowler (1970).

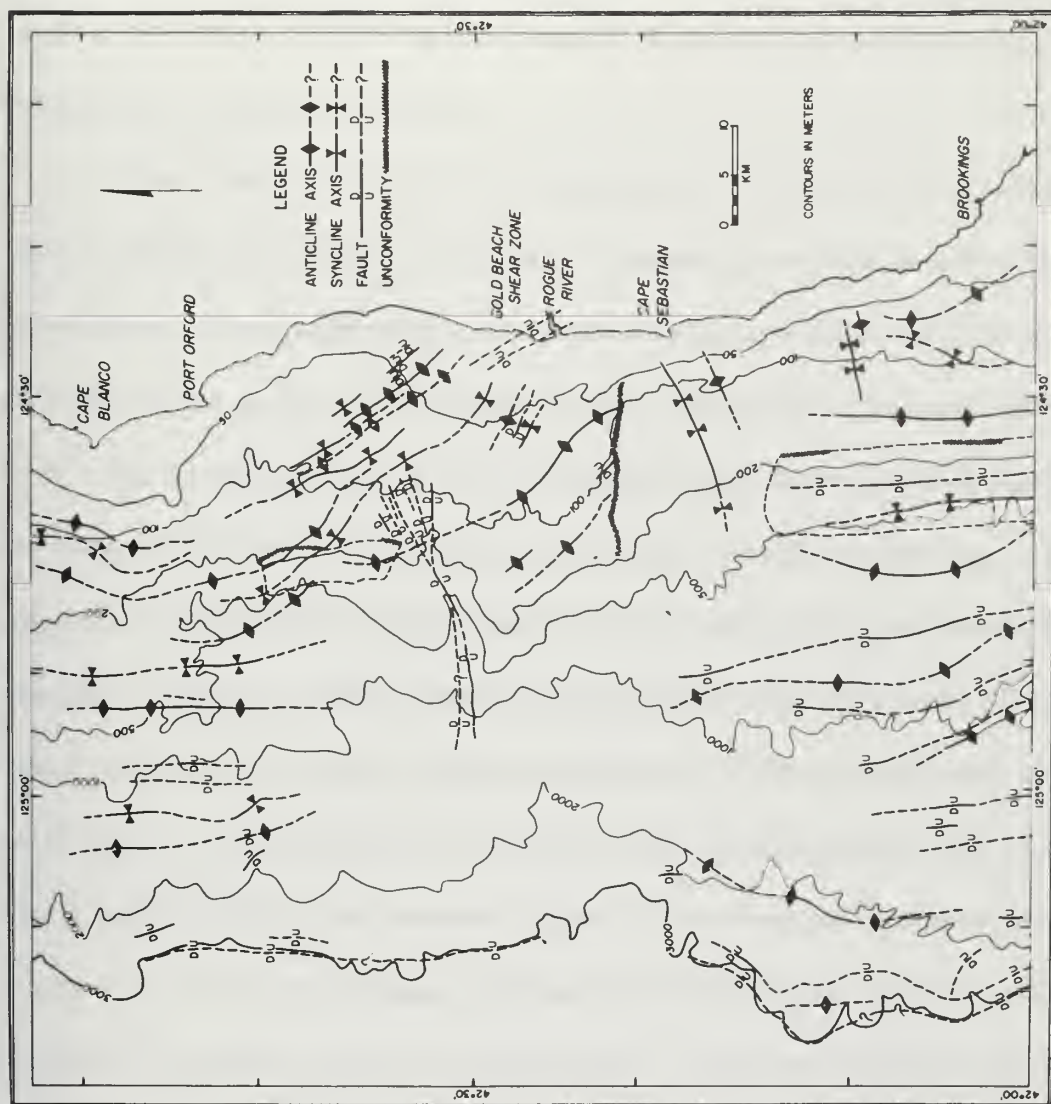


Figure 16. Major structural features of the southern Oregon margin. Continental shelf structure modified after the interpretation of Bales and Kulm (1969).

to large-scale faulting. A number of small-scale anticlinal folds appear on the reflection profiles on the lower slope which have not been plotted in Figure 16. These folds are smaller in amplitude and wavelength than those of the upper slope and do not appear to detract from the general trend noted above.

Nearly all of the faults determined, or inferred, from the reflection profiles and shown on Figure 16 appear to strike in a north-south direction. They apparently are high-angle or nearly vertical and down-thrown to the west. This has also been observed by Silver (1969a, p. 24). These faults appear to be normal faults; although data sufficient to determine their true dip directions and attitude is lacking. The fault pattern on the lower slope appears to be one of a typical block-faulted region. Maloney (1965) classified similar faults off central Oregon as step faults and the intervening benches and hills as step fault blocks, although he was unable to determine if any displacement had occurred. Step faults differ from normal faults in that they are compressional in nature and both the hanging wall and foot wall move up, the foot wall moving up farther than the hanging wall. The net displacement is similar to that of a normal fault.

The faults on the southern Oregon margin appear to be normal faults which are tensional in origin. If this is correct, then it must be reconciled with the apparently compressional origin of the folds which exist on the same margin (Figure 16). Even if both faults and

folds result from compressional forces, then the interpretation of east-west tension noted earlier from fault-plane solutions (Dehlinger, 1969) would still have to be explained.

A solution to this problem might be found by assuming a mechanism where both tension and compression are possible. Such a mechanism has been postulated by Malahoff (1970) to account for simultaneous underthrusting of oceanic crust under island arcs and the formation of gravity faults in trenches; he suggests that a transformed thrust mechanism may exist under trenches, whereby a gravity fault located at the trench surface would become a thrust fault at depths of 30 to 40 km beneath the island arc. Assuming that the southern Oregon continental margin at its interface with the adjacent ocean basin presents an analogous situation, then the existence of normal gravity faults in an area of active underthrusting can be explained.

Continental Shelf

The southern Oregon continental shelf can be divided into two regions which do not appear to be structurally related (Bales and Kulm, 1969). The dividing line of the two regions is the surface trace of a west-southwest trending angular unconformity within the late Cenozoic sedimentary sequence between the Rogue River and Cape Sebastian (Figure 16). This division can also be noted on the gravity map (Figure 12, arrow A). A series of parallel and subparallel

northwest-southeast trending folds characterize the northern region, with folds becoming gentler on the outer shelf and increasing in number towards the coastline. The Gold Beach shear zone may extend offshore in a similar northwest-southeast trend. This latter feature reflects the northwest-southeast trend of shears found in northwestern California which were formed during the late Cenozoic Cascadan orogeny.

A north-south trending angular unconformity between the late Cenozoic sedimentary sequence and the later Quaternary deposits is present along the shelf break southwest of Port Orford (Figure 17, A, at 26 km). The wedge of sediment above the unconformity suggests that the shelf may be prograding in this area. The unconformity apparently terminates north of the head of the Upper Rogue Canyon and is not observed south of the Canyon.

The southern part of the shelf is characterized by a southwest-trending basin off Cape Sebastian which extends westward across the entire shelf (Figure 17, B) and southward to the southernmost portion of the shelf (Figure 16). It appears to be only slightly deformed by local folding and warping near the coastline (Bales and Kulm, 1969; Figure 16). West of this basin, an anticlinal fold underlies the shelf edge (Figures 16 and 17, B). A north-south unconformity, similar to the one in the northern region, lies between this anticline and the upper slope (Figure 16).

Several prominent reflectors observed on the seismic records at

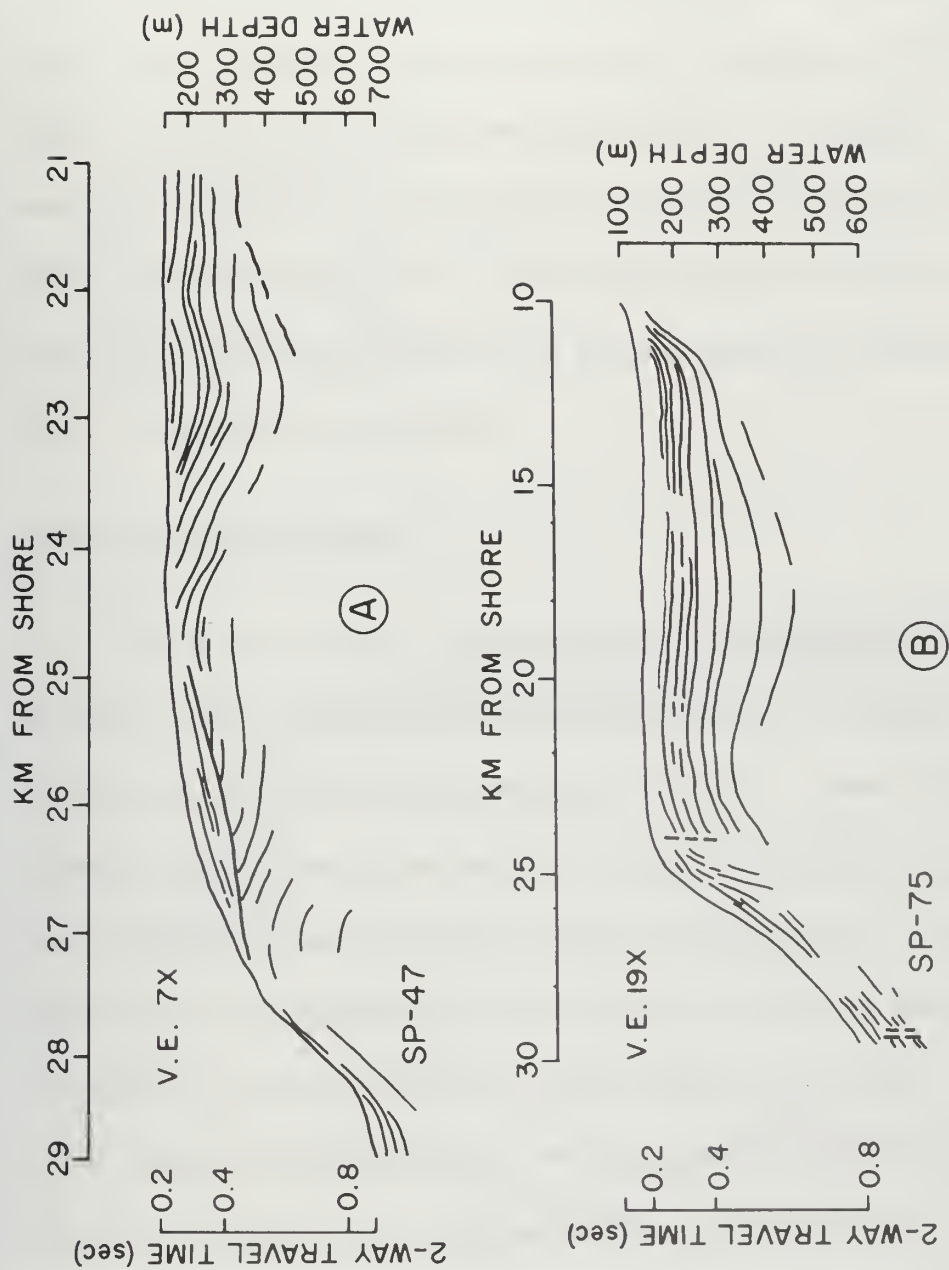


Figure 17. Sparker profiles across the southern Oregon shelf and upper slope. A. SP-47 ($42^{\circ}42'N$). B. SP-75 ($42^{\circ}08'N$). After Kulm and Fowler (1970).

the shelf break (Figure 18, A and C) suggest that the shelf is prograding. The truncated surface (Figure 17, A) suggests that erosion of the shelf has also occurred in some places off southern Oregon. The erosion was caused by the numerous transgressions and regressions resulting from Pleistocene glaciation. In addition, these sea-level fluctuations were superimposed on a tectonically active area, which could account for the complex structure of the shelf. Since the last regression of the sea and the subsequent Holocene transgression, the shelf has prograded.

Upper Slope and Benches

The upper slope is characterized by bench-like features such as the Cape Blanco Bench and the Klamath Plateau. In general these benches are formed by the ponding of sediment, some of which is slumped, behind anticlinal folds. The structure underlying Cape Blanco Bench appears to fit this pattern (Figure 19). A synclinal basin underlies the main part of the bench, while the anticline observed at a depth of 350 m marks the western edge of the bench. The origin of the small submarine valleys running north-south along the bench surface is unclear. They appear to have originated from small faults or between small folds within the synclinal basin which do not appear at the surface. However, their present surface topographic expression appears to be mainly the result of erosion and small amounts of

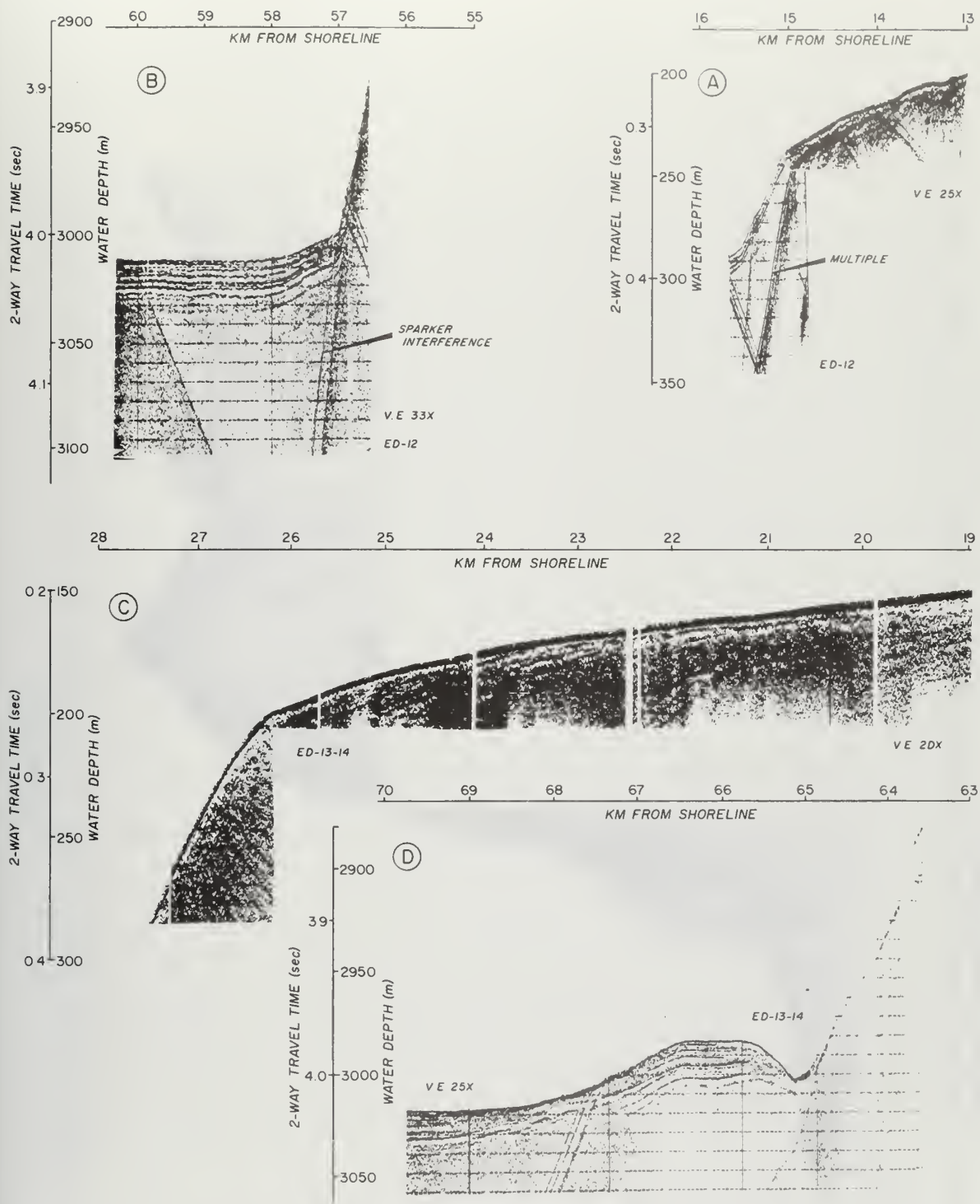


Figure 18. EDO subbottom profiles across the southern Oregon shelf and base of slope. A. Shelf edge (42°46'N). B. Base of slope (42°46'N). C. Shelf edge (42°40'N). D. Base of slope (42°37'N).

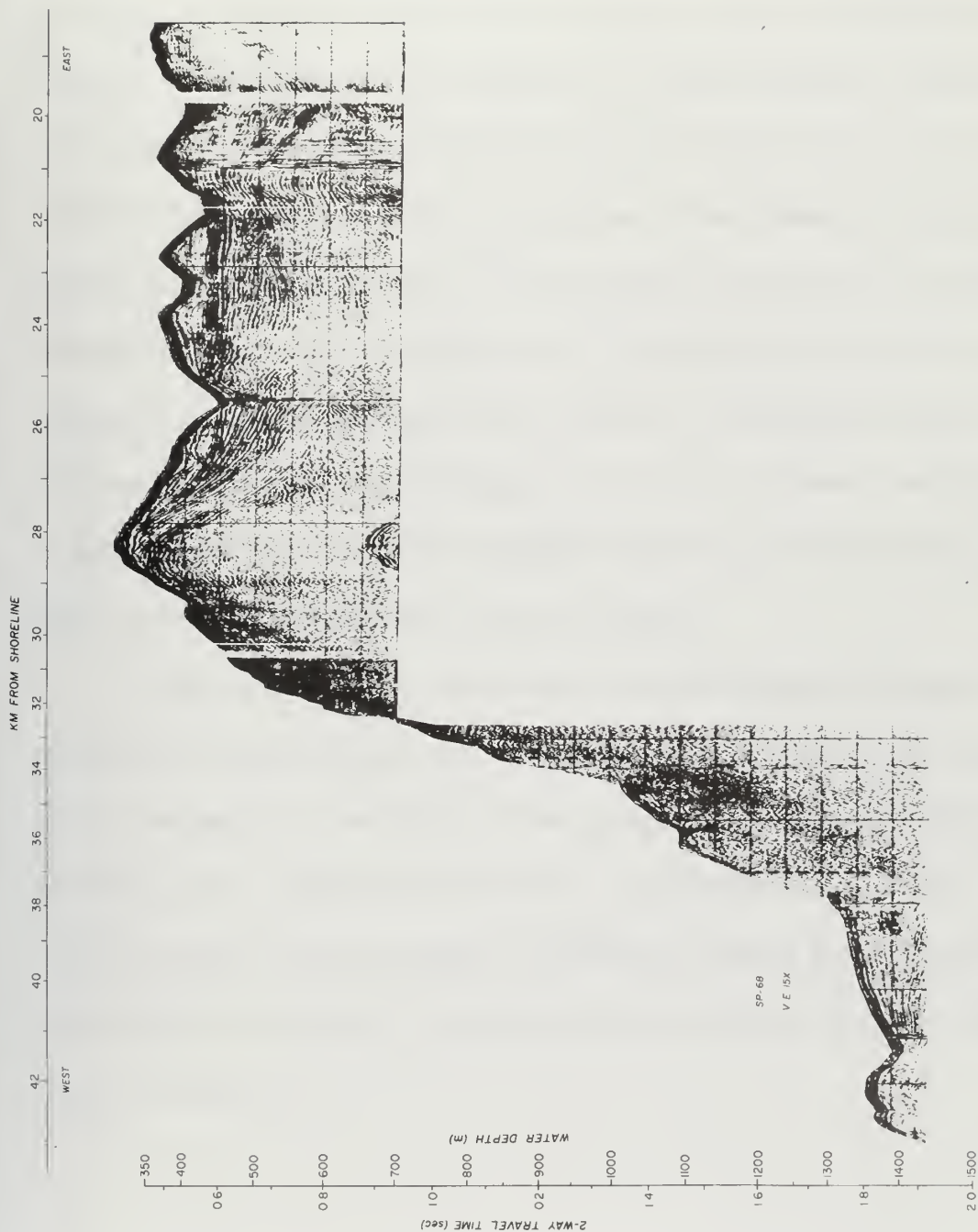


Figure 19. Sparker profile across Cape Blanco Bench (SP-68, 42°46'N). Vertical dashed lines indicate normal faults.

erosion and small amounts of valley filling.

The Klamath Plateau is the largest bench-like structure on the southern Oregon margin (Figures 5, 20 and 21). Starting at latitude $42^{\circ}10'N$, it continues south on the margin to about $41^{\circ}00'N$ (Silver, 1969a). Its western edge is marked by a large anticline, behind which a substantial amount of sediment has ponded (Figure 21, at 36-37 km). The flat-lying sediments which give rise to the Plateau are approximately 100 to 150 m thick, and thin to only a few meters immediately behind the anticline. In comparison, approximately 150 to 200 m of sediment are found on Cape Blanco Bench. The western flank of the Plateau is a normal fault (Figure 21 at 41 km). Another normal fault is inferred at the base of the Upper Plateau Slope at the extreme eastern edge of the Klamath Plateau (Figure 17, B).

Slumping of sediment from the outer shelf down the upper slope and Upper Plateau Slope may account for a number of small-scale, but thick, sediment accumulations found along the upper slope (Figure 21 at 42 to 45 km; Figure 22 at 30 km). The Middle Bench (1000 to 1250 m) is a smaller-scale example of sediment ponding behind anticlinal folds (Figures 20 and 21); normal faults also occur within the Middle Bench (Figure 16).

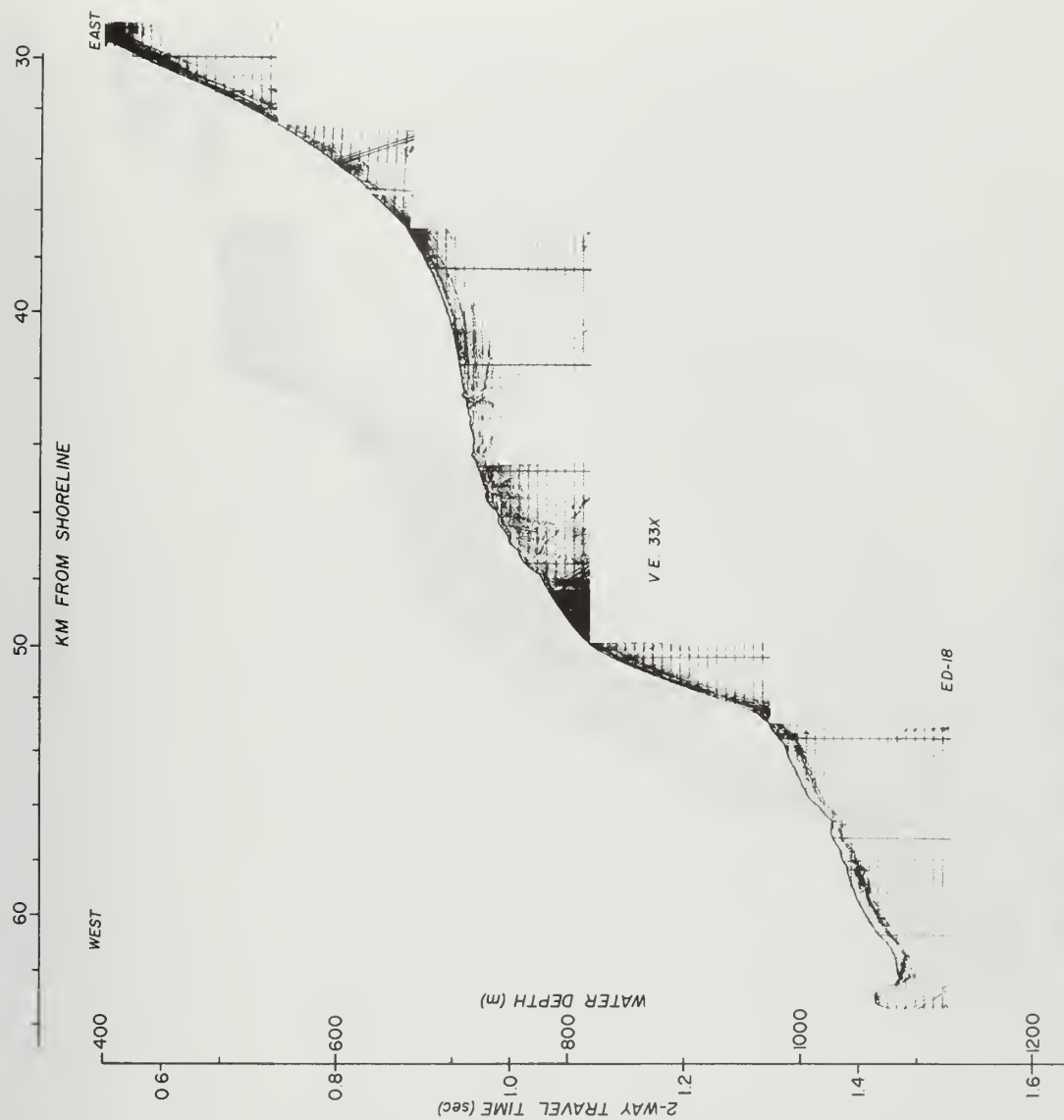


Figure 20. EDO subbottom profile across the upper continental slope. (ED-18, 42°01'N).

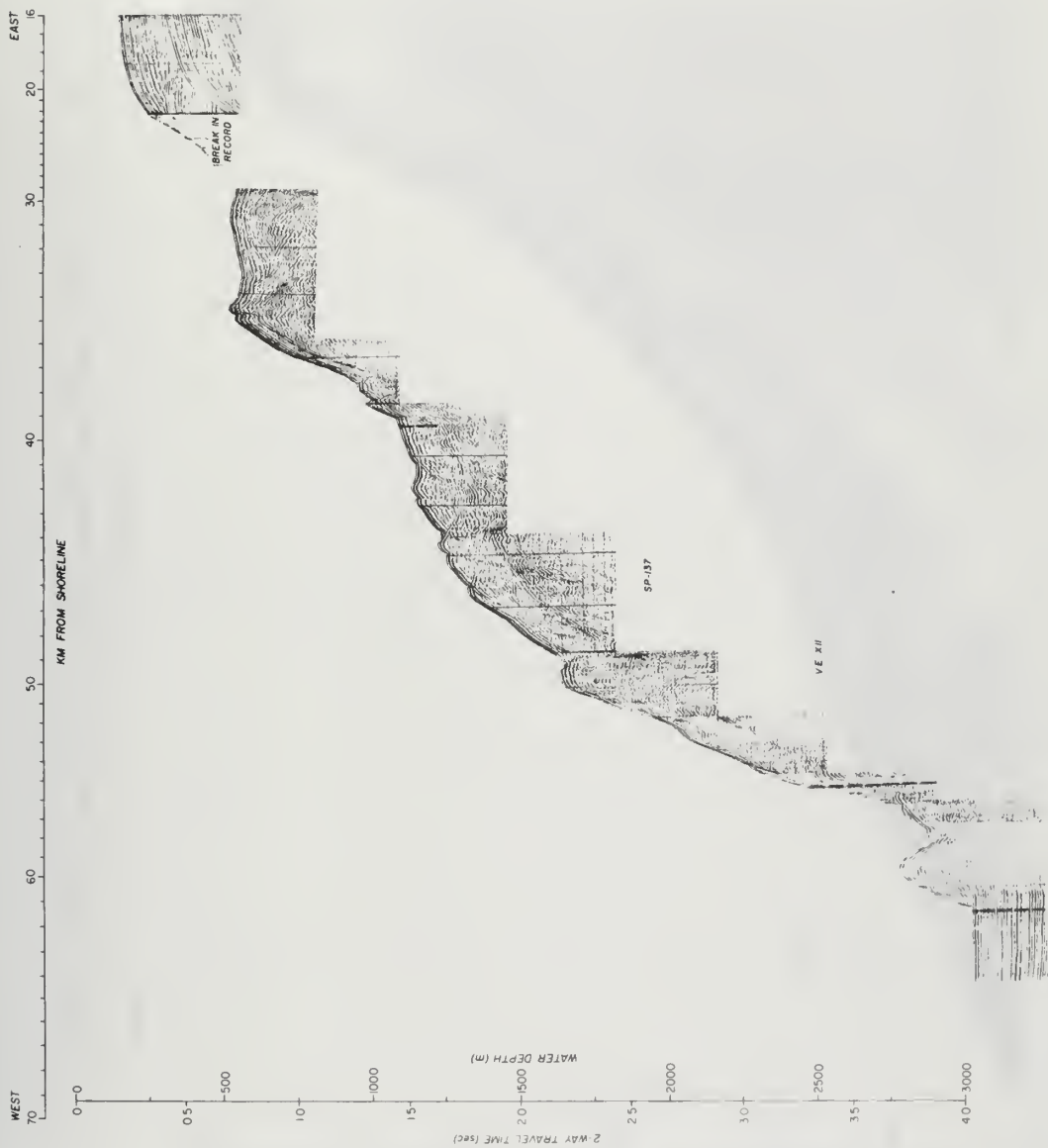


Figure 21. Sparker profile across the entire southern Oregon slope (SP-137, 42°19'N). Vertical dashed lines indicate normal faults.

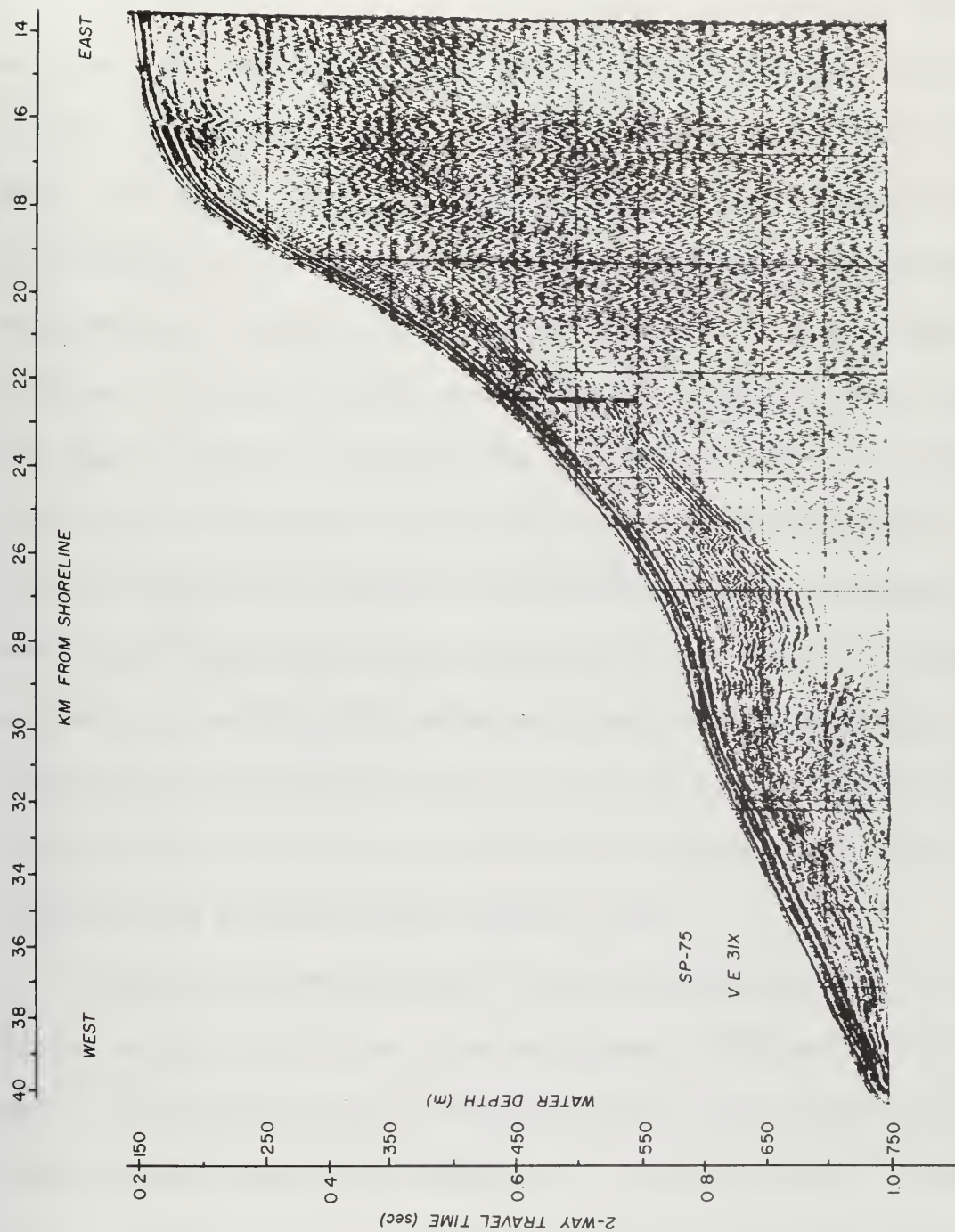


Figure 22. Sparker profile across the upper continental slope illustrating slumping (SP-75, 42°08'N). Vertical dashed lines indicate normal faults.

Lower Slope

The lower slope consists of small-scale, north-south trending anticlinal folds and normal faults down-dropped to the west. They form a series of sediment traps and step fault blocks down to the base of the slope. The Lower Bench (2250 to 2500 m) is the most prominent bench-like structure on the lower slope. The most prominent normal fault is that forming a marginal escarpment at the base of the slope (Figure 21 at 64 km). Silver (1969a) also postulated the existence of such a fault and others similar to it on the northern California margin. He finds structural trends similar to those off southern Oregon (Figure 23). He has recognized the Klamath Plateau and other ponded sediment basins and benches and has described the northern California margin as a series of north-south trending anticlinal folds and high-angle normal faults down-dropped to the west (Figure 23). He believes his interpretation of the structure is consistent with compression and underthrusting directed broadly from the west.

In general the sediment cover drapes conformably over the underlying structures on the lower slope and appears to thicken near its base. The thickest section is found at the base of the lower slope and on the adjacent abyssal floor (Figures 18, A and D and 21). This thick section (Figure 23, line O) consists of flat-lying, relatively undeformed strata which conformably overlie the irregular basement topography;

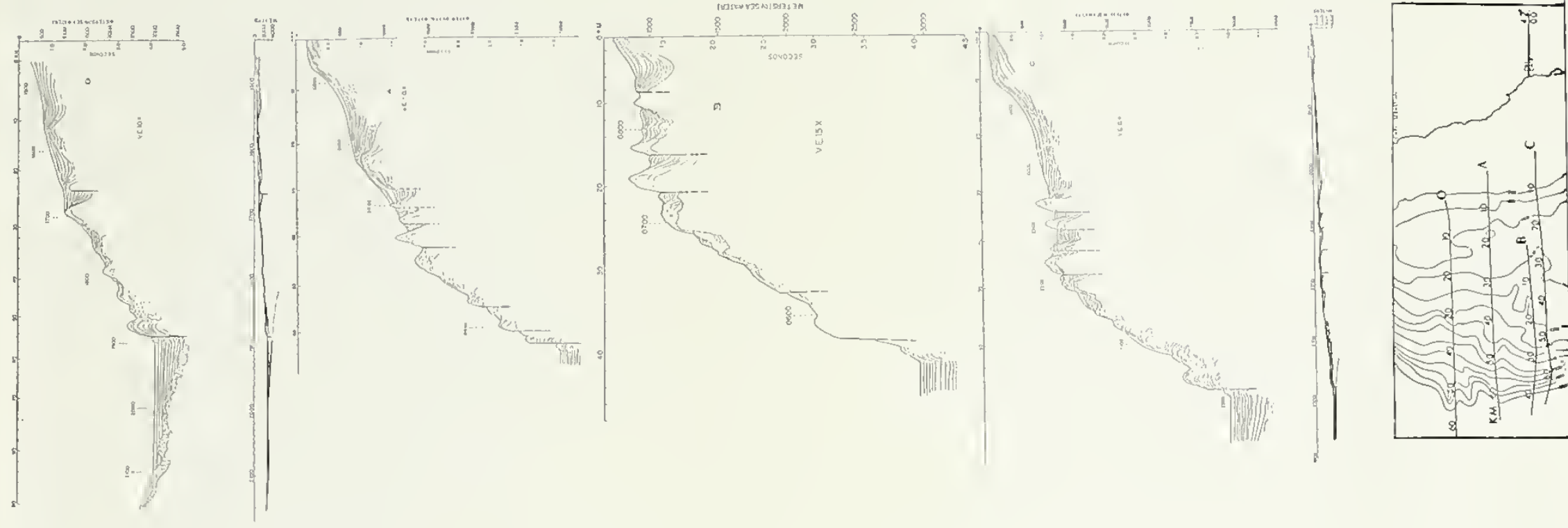


Figure 23. Reflection profiles of the southern Oregon and northern California continental margins. Map at bottom indicates the location of each profile: line 0, 42°13'N; line A, 42°09'N; line B, 42°00'N; line C, 41°58'N. Modified after Silver (1969a).

however, deformation of the sediments appears to increase with depth.

A continental rise is not well developed off southern Oregon and probably reflects the lower sediment supply from the Rogue, Klamath and other rivers which feed the area. In contrast, the continental rise off the east coast of the United States results from the much larger influx of sediment supplied by the numerous large coastal rivers.

Rogue Submarine Canyon

The Upper Rogue Canyon, situated from 150 to approximately 1500 m, is an east-west trending submarine canyon that is predominantly structurally controlled but exhibits erosional features (Figure 24). The Upper Canyon has about 400 m of relief and a distinctly sharp V-shape. An east-west fault can be inferred from the rapidly-steepening dips observed on either side of the Canyon which suggest down-dragged strata, in addition to what appears to be a fault sliver on the south wall (Figure 24). Other seismic reflection profiles across the Upper Canyon show similar fault features. The fault is possibly split into two branches: one strikes along the axis of the Canyon and the other along the steeper south wall which has been down-dropped to the north forming a small bench along part of the channelway (Figure 24). The fault terminates eastward on the shelf against a series of small-scale en echelon faults at the head of the Canyon (Figure 16). Little, if any, sediment accumulation exists in the Upper Rogue Canyon,

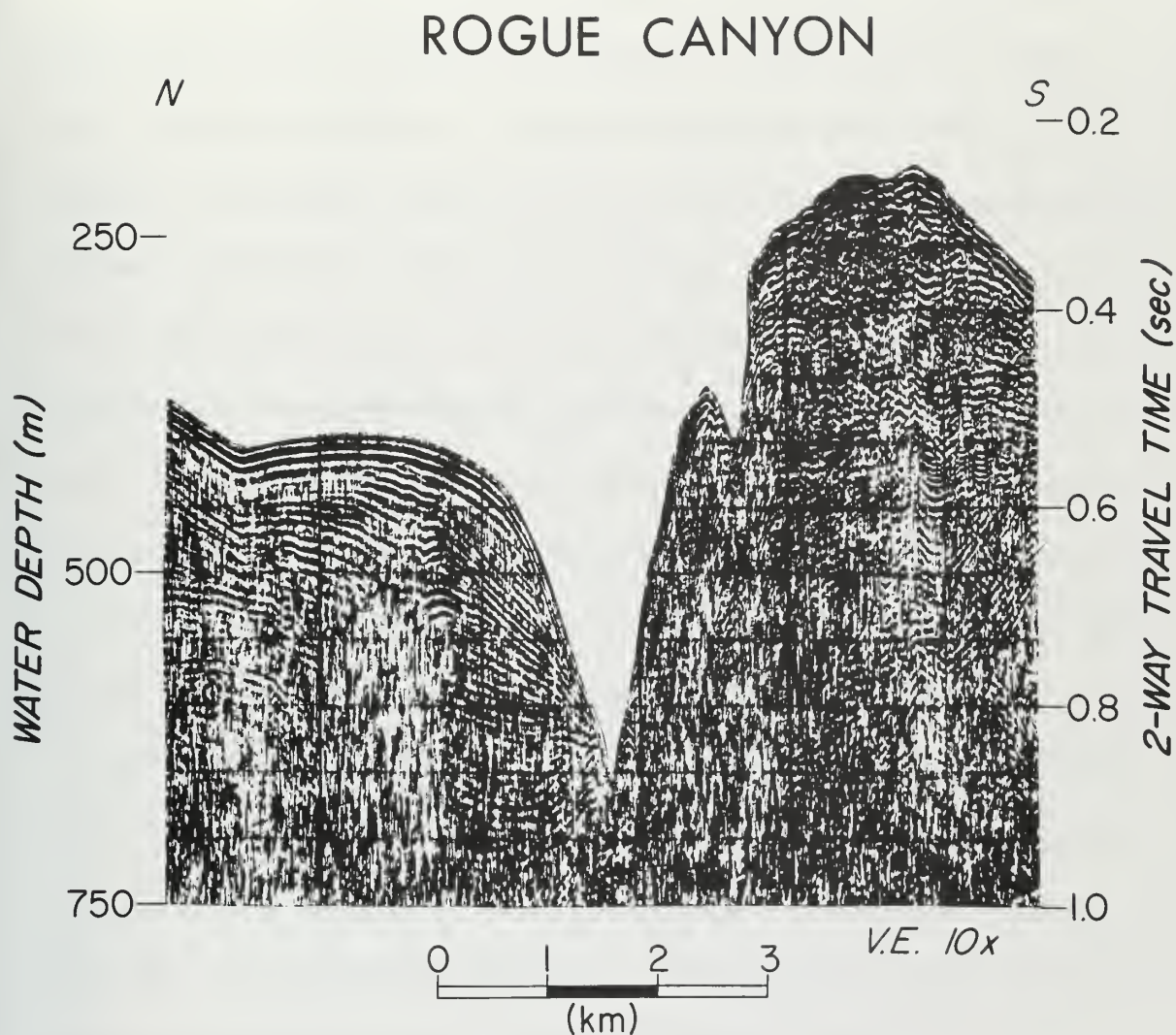


Figure 24. North-south Sparker profile across the Upper Rogue Canyon (SP-71, 124°50'W).

suggesting that it may still be erosional in nature.

The Lower Rogue Canyon, trends in a northwest-southwest direction and extends from 1500 to 3000 m. It has a much broader cross-sectional profile (e.g., Figure 6, profiles K-K' and L-L') in contrast to the Upper Canyon. It is at least in part an extension of the northeast-southwest trending swale (Figure 2) which is located to the north of the Rogue Canyon. The two valleys join at about 1500 m and continue down to the base of the slope as one system. Good seismic reflection profiles from the Lower Canyon are lacking, but it appears from cores taken in the axis of the Lower Canyon that this portion may be filling. The Lower Canyon does not appear to be offset by the Upper Canyon fault and hence may be younger than the Upper Canyon.

The writer concurs with Bales (1969) in the belief that the fault in the Upper Canyon may be of late Tertiary age, as is the S-shaped anticline west of the Rogue River mouth (Figure 16). Erosion of the Rogue Canyon was probably due to the influx of coarse clastic sediment during the late Pleistocene, when sea level was only slightly above 150 m. Other evidence (See Sedimentology) indicates that the late Pleistocene coarse sediment may have poured into the incipient faulted channelway during this time, initiating the development of the Upper Rogue Canyon.

No buried channels have been found on the continental shelf to indicate a possible connection between the Rogue River mouth and the

head of the Rogue Canyon (Kulm, et al., 1968a). However, the eastern flank of the S-shaped anticline to the west of the Rogue River could have acted as a pathway for sediment transport, during a lowered sea level. In a similar manner, other shelf structures, such as those now observed southeast of Port Orford, could have acted as pathways for sediment transport north along the shelf by-passing the Upper Rogue Canyon. If such a flow were diverted southwestward across the slope by banks or rock reefs, a feature similar to the swale on the could easily have formed.

Continental Margin Structure in Relation to the Regional Setting

Various theories can be developed to explain the evolution of the southern Oregon margin, each of which is dependent upon a different interpretation of the regional tectonics in the northeast Pacific. One interpretation of the magnetic data suggests that ocean-floor spreading is occurring eastward from the Juan de Fuca and Gorda Ridges and that this new crust is underthrusting beneath the southern Oregon and northern California continental margin (Silver, 1969b). However, based on fault plane solutions Dehlinger, (1969) and Dehlinger, et al. (1970) believe that the region is presently experiencing tension in an east-west direction.

The structure of the southern Oregon margin does not resolve this dilemma. The north-south fold system indicates compression

directed from the west, while the north-south faults are ambiguous in that they appear to be normal tensional faults down-dropped to the west. They may also be compressional step faults (i. e. vertical faults where the movement is mainly in the horizontal plane) or simply slump features produced by sediment loading. If underthrusting is occurring along the southern Oregon margin, the leading edge of the descending oceanic lithospheric plate could produce components of both tension and compression. Tension would result in subsidence and down-dragging at the base of the slope, giving rise to normal gravity faults. Compression would produce uplift directed to the east forming compressional north-south trending folds. If such a mechanism operated along a structural hinge line along the present shelf break or upper slope, the resultant structural pattern would be similar to that mapped in Figure 16. In an analogous situation that was described previously, Malahoff (1970) was able to reconcile both tension and compression existing in an area of active underthrusting. It would appear then that the complex of structures on the southern margin are compatible with underthrusting.

Several additional points need to be considered in attempting to explain the margin structural pattern. First, the margin off southern Oregon and northern California may have been more affected by compression than the margin off central and northern Oregon. Second, the warped coastal marine terraces near Cape Blanco indicate

differential uplift in the vicinity of Cape Blanco. Third, faunal studies (See Stratigraphy) indicate that both uplift and subsidence has occurred on the southern Oregon margin. These facts indicate a complex structural history for the southern Oregon margin; one that has varied with time.

Several current interpretations of the regional tectonics do take into account changing structural trends with both direction and time, and may serve to explain many of the complex structures on the southern Oregon margin. Dehlinger (1969) has postulated that much of the movement of crustal plates, especially between the Gorda and North American plates, may be due to differential slippage caused by the varying effects of tidal friction on the low velocity layer between the plates. He also notes that the interaction of two plates at the continental margin need not be resolved by underthrusting alone, but can also be accounted for by local vertical uplifts. These uplifts may express themselves as fold-like diapiric structures which are not compressional in nature, and probably not unlike the small-scale folds observed on the margin in Figures 20 and 21. Silver (1969b) has postulated a general eastward movement of the Gorda Plate, but with a larger component of right lateral slip of the plate along the continental margin which moves the plate mostly in a north-northwest direction. Wilson (1965a) first theorized that sea-floor spreading and the resulting direction of plate motion has changed to its present northwest-southeast sense due to

rapid outbuilding of the margin sometime in the mid-Tertiary, perhaps since Miocene time. Atwater and Menard (1970) have shown that this change in direction of sea-floor spreading may have begun as early as 55 million years ago (Eocene time).

These theories suggest that some degree of spreading and underthrusting occurred on the margin prior to mid-Tertiary time. Subsequent to mid-Tertiary time the direction of movement of continental and oceanic plates shifted to the northwest-southeast. Late Pliocene or early Pleistocene may have been a time of renewed underthrusting (Silver, 1969a); if so evidence for this episode should be found in the structure and unconformities on the northern California and southern Oregon margin. The current effects of underthrusting are considered by Silver (1969b), Dehlinger (1969), and others to involve only the southern portion of the Gorda Plate, affecting only that part of the margin lying between Cape Sebastian (Oregon) and Cape Mendocino. The northern part of the Gorda Plate above Cape Sebastian may not be actively underthrusting at present, as is suggested by the fact that sediments have begun to accumulate at the base of the northern Oregon-southern Washington slope in the form of submarine fans, which may eventually coalesce to form an incipient continental rise. Localized uplift and subsidence may also play an important role in the present structural evolution of the southern Oregon margin.

STRATIGRAPHY

Unconsolidated Sediments

The geologic history of the southern Oregon margin can be interpreted through a correlation of the various sedimentary units which occur on the margin and their continental counterparts. The stratigraphic work of Duncan (1968), Duncan, et al. (1970), and Griggs, et al. (1970) in the deep-sea environments west of the Oregon margin provide a basis for comparison with the results of this study and with other interpretations of the faunal stratigraphy of the Oregon margin.

Planktonic Foraminifera-Radiolaria Abundance

Duncan (1968) and Duncan, et al. (1970) reported the development of the first paleoclimatic stratigraphy for the deep-sea environments off Oregon, which is based mainly on the Radiolaria (R)/planktonic Foraminifera (P) ratios during the late Pleistocene and Holocene. Griggs (1969) and Griggs, et al. (1970) expanded this stratigraphy to give a more detailed paleoclimatic curve for the last 12,500 years in Cascadia Basin. The stratigraphy developed by both Duncan and Griggs closely matches the glacial advances and retreats noted by Armstrong, et al. (1965) on the continent. Since 35,000 years Before the Present (B.P.), there have been three warm periods recognized within the Pleistocene and marked by an increase in Radiolaria within the pre-dominant planktonic Foraminifera interval. These have been dated at

34,000 years B.P., 28,000 to 25,000 years B.P., and 18,000 to 16,000 years B.P. The most abrupt change in the fauna occurred about 12,500 years B.P. in Cascadia Basin and is considered the end of the Pleistocene and the beginning of the Holocene (or post-glacial) in this area (Duncan, 1968). The pelagic and hemipelagic sediments high in planktonic Foraminifera, principally Globigerina pachyderma and G. bulloides, characterize cooler or glacial periods, while Radiolaria-rich sediments characterize the warmer or interglacial periods. The abruptness of the transition depends on the sedimentation rate, which determines the length of the transitional interval between the Holocene and late Pleistocene.

Griggs (1969) and Griggs, et al. (1970) noted that several cooler periods, marked by Globigerina-rich intervals, occur within the Holocene since 12,500 years B.P. These have been dated at 5000 to 4000 years B.P. and 2000 years B.P.; the former can be dated precisely since it usually occurs just above a Mazema ash layer which dates at 6600 years B.P., while the latter is somewhat tenuous.

In an effort to determine whether or not these stratigraphic horizons occur in the continental margin deposits, an analysis similar to that performed by Griggs and Duncan was employed with the sediments examined in this study. Figure 25 illustrates the R/P ratios determined for five cores (6706-2, 6711-1, 6711-2, 6711-6, and 6711-8). In each core a combined count of at least 100 Radiolaria and/or planktonic Foraminifera were obtained. The high sedimentation rates,

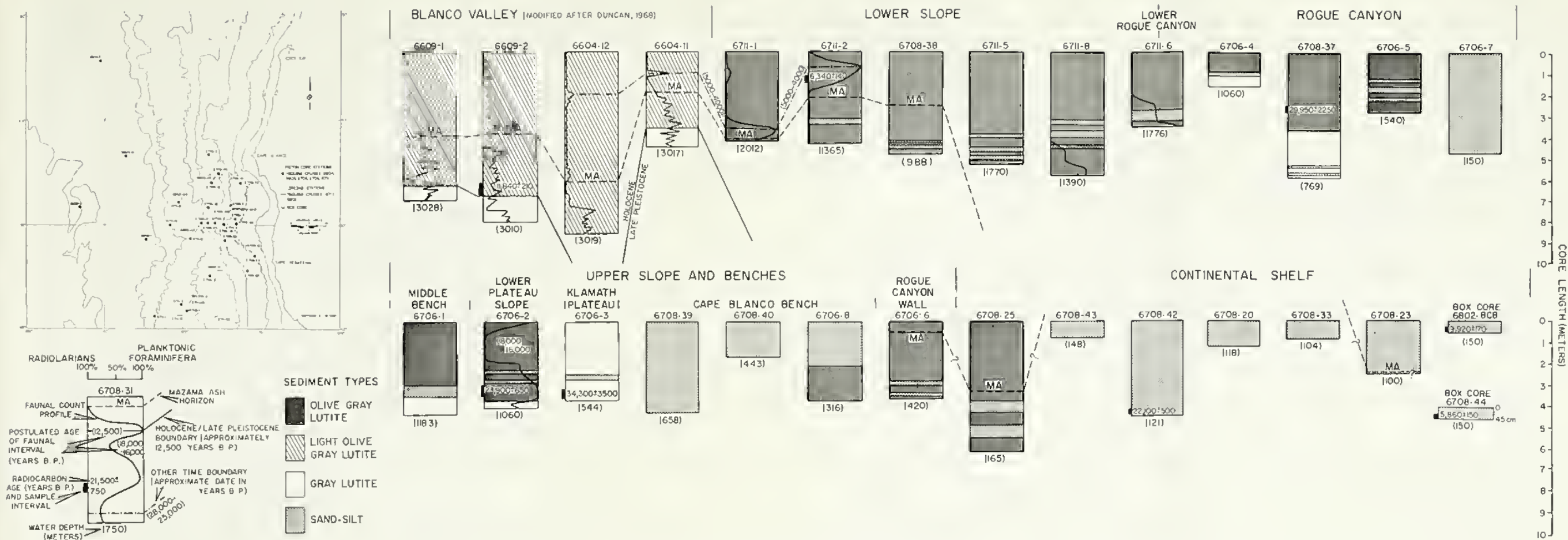


Figure 25. Summary of lithologic and stratigraphic information from piston cores from the continental margin and adjacent Blanco Valley. Data for box cores 6708-44 and 6802-BCB after Chambers (1968).

particularly evident in the lower slope cores, caused the dilution of the biologic material by detrital grains and precluded the calculation of R/P ratios in most other cores. The variation in the R/P ratio in cores 6706-2, 6711-1 and 6711-2 have been dated using radiocarbon dates and/or the presence of Mazama ash.

As can be noted from Figure 25, the R/P ratios in core 6706-2 (upper slope and benches) indicate an age for the core which ranges from 28,000 to 25,000 years B.P. near the bottom to 18,000 to 16,000 years B.P. near its surface. Since the top of the core is considered to be present, it appears that the surface sediment in this core and that from the surrounding area may be relict sediment of Pleistocene age. The low R/P ratio in cores 6711-1 and 6711-2 (lower slope) probably represents the 5000 to 4000 years B.P. interval of Griggs, et al. (1970). This interval correlates with a similar interval in cores 6604-12 and 6604-11 from Blanco Valley (Figure 25), and reflects similar sedimentation rates for the two environments. The ages inferred by the R/P ratios plotted for cores 6711-6 (lower Rogue Canyon) and 6711-8 (lower slope) have not been confirmed by dating. The topmost Foraminifera-rich zone in each core may represent the last cool period in the Holocene (2000 years B.P.); however, this would produce an unreasonably high rate of sedimentation. It is more reasonable to assume they represent the 5000 to 4000 years B.P. interval until more precise dating can confirm their age.

Mazama Ash

The Mazama ash which erupted from Mt. Mazama (Crater Lake, Oregon) 6600 years ago and blanketed large areas of the Pacific Northwest is a good stratigraphic horizon in deep-sea and continental margin sediments because of its widespread occurrence. Nelson, et al. (1968) describe the occurrence of the ash in the various deep-sea environments of Cascadia Basin and postulate that ash deposition was effected by turbidity currents and not through aerial fallout. They suggest that the ash accumulated on the continental margin prior to its transport to the deep sea. The ash identified in this study has been verified as Mazama ash through comparison of its refractive index (1.505) with known samples as identified by Nelson (1968), Duncan (1968) and others. The depth of maximum abundance of the ash has been used as the stratigraphic horizon dating approximating 6600 years B.P. in six cores (6711-1, 6711-2, and 6708-38, lower slope; 6706-6, upper slope; and 6708-23 and 6708-25, shelf) from the continental margin (Figure 25). While the depth of occurrence of the ash varies within the margin or deep-sea environments, it does reflect differences in sedimentation rates. It is significant to note that the ash was found in only one upper slope core (6706-6) which suggests that older sediments persist to the surface in upper slope environments, or at least that the sedimentation rate is markedly lower here.

Radiocarbon Dating

In order to establish the absolute ages of certain lithologic or biologic events recorded in the cores, and to facilitate correlation among cores, the radiocarbon (C^{14}/C^{12}) dating method was employed. Samples from five selected cores (6706-2 and 6706-3, upper slope; 6711-2, lower slope; 6708-37, Rogue Canyon; 6708-42, shelf) were dated utilizing the total carbon content (Figure 25; Appendix 2). Two other dates were obtained by Chambers (1968) from box cores taken on the southern Oregon shelf (6708-44 ($42^{\circ}35.1'N$, $124^{\circ}41.0'W$, 150 m) and 6802-BCB ($42^{\circ}35.1'N$, $124^{\circ}41.1'W$, 150 m)); these utilized carbonate carbon from mollusk shells found in the cores.

Faunal Stratigraphy of Consolidated Sediments

The benthic and planktonic Foraminifera in two selected dredge haul samples (6708-36-1 and 6802-D3-1) and from consolidated rock fragments in the basal 20 cm in one piston core (6706-3) were identified and described in detail by Fowler (1970). His conclusions regarding the faunal assemblages are shown in Table 1.

Both uplift and subsidence are inferred from the nature of the faunal assemblages in the consolidated rocks. In the two samples from the upper slope (6708-36-1 and 6706-3-11-2) the faunal data suggest that uplift has occurred on the southern Oregon margin. These data

Table 1. Age, correlation and paleo-depth of Foraminifera from selected consolidated sediments on the southern Oregon continental margin.^a

Sampling Data			Summary of Foraminiferal Data			
Sample No.	Location and Depth	Rock Type	Age	Correlation	Paleo-Depth ^b (meters)	Calculated Movement (minimum)
6706-3-11-2	Klamath Plateau (544 m)	Fossiliferous Mudstone	"mid-Pliocene" = Venturian Age of the "standard" California Pliocene section (approx. 6.5 million years B. P.) ^c	lower part of the Middle Rio Dell Fm., Wildcat Group, northern California	<u>500-1000</u> (625)	+ 80 meters (uplift)
6708-36-1	Upper Slope (250-330 m)	Lithic Wacke	"mid-Pliocene" = Venturian Age of the "standard" California Pliocene section (approx. 8 million years B. P.) ^c	lower part of the Middle Rio Dell Fm., Wildcat Group, northern California	<u>500-1000</u> (625)	+300 meters (uplift)
6802-D3-1	Lower Slope (1100 m)	Mudstone	"mid-Pliocene" = Venturian Age of the "standard" California Pliocene section (approx. 8.5 million years B. P.) ^c	Lower Rio Dell Fm., or Eel River Fm. (?), Wildcat Group, northern California	<u>500-1000</u> (875)	-225 meters (subsidence)

^a Identifications and correlations by Fowler (1970).

^b Number in parentheses is the weighted average midpoint of the paleo-depth range obtained by taking the difference between the dominant paleo-depth (underlined) and the average of the given depth range and adding or subtracting one-half of this difference to the dominant paleo-depth. (e. g. 750 m average (between 500 m and 1000 m); $750 - 500 = 250$; $250/2 = 125$; 500 + 125 = 625).

^c Estimates of absolute age after the time scale of Ingle, 1967.

corroborate the findings of Byrne, et al. (1966). Although the amount of uplift is less than the maximum reported by Byrne, et al., for the central Oregon margin (60 m to over 1000 m), it is within their lower range of values.

Faunal data from the lower slope sample (6802-D3-1) suggest that a significant amount of down-faulting or subsidence has occurred on the lower margin. Movement and deformation on the margin was subsequent to either "early Pliocene" or "mid-Pliocene." However, the three samples are all approximately the same age (Table 1). This suggests that both local uplift and subsidence could have occurred at about the same time, with the uplift restricted to the upper slope and shelf and the down-faulting or subsidence restricted to the deeper portions of the slope.

Rates of Sediment Accumulation

The stratigraphic horizons established at various depths within the unconsolidated sediment section permit the calculation of approximate rates of deposition. By noting the depth interval between a particular horizon and the surface (which is assumed to be at zero or present time) and by averaging this interval over the time represented, an estimate can be obtained of the sedimentation rates within the different depositional environments (Table 2).

The sedimentation rates determined for the upper slope, benches,

Table 2. Sedimentation rates from the southern Oregon continental margin

Core No.	Depositional Environment ^a	Stratigraphic Horizon and Date (yrs., B. P.)	Depth of Horizon (cm)	Sedimentation Rate within Interval (cm/1000 yrs.)	Average ^a Sedimentation Rates (cm/1000 yrs.)
6711-1	Lower Slope	Mazama Ash (6600) R/P shift (5000-4000)	405 390	62 59	60 (H)
6711-2	Lower Slope	Mazama Ash (6600) C-14 Date (6,340 ± 140) R/P shift (5000-4000)	200 117 80	30 19 18	22 (H)
6708-38	Lower Slope	Mazama Ash (6600)	250	38	38 (H)
6711-8	Lower Slope	R/P Shift (5000-4000)(?)	550	122(?) ^c	122(?) (H)
6711-6	Lower Rogue Canyon	R/P Shift (5000-4000)(?)	340	75(?)	75(?) (H)
6708-37	Upper Rogue Canyon	C-14 Date (29,950 ± 2250)	267	9	9 (LP-H)
6706-2	Upper Slope	R/P Shift (28,000-26,000) C-14 Date (23,900 ± 650) R/P Shift (18,000-16,000)	390 325 120	15 22 7	14 (LP-H)
6706-3	Upper Slope/Klamath Plateau	C-14 Date (34,300 ± 3500)	350	10	10 (LP-H)
6706-6	Upper Slope	Mazama Ash (6600)	45	7	7 (H)
6708-25	Shelf	Mazama Ash (6600)(?)	330	50(?)	50(?) (H)
6708-42	Shelf	C-14 Date (22,100 ± 500)	444	20	20 (LP-H)
6708-23	Shelf	Mazama Ash (6600)(?)	250	38(?)	38(?) (H)
6708-BCB	Shelf	C-14 Date (9920 ± 170)	45	5	5 (H)

^aIn most cases the depositional environment corresponds to the physiographic province.^bH = entirely within Holocene; LP-H = from late Pleistocene to Holocene.^c(?) indicates approximate sedimentation rate.

and the Upper Rogue Canyon are moderate, averaging about 10 cm/1000 years (Figures 29 and 31). In contrast, the lower slope is experiencing the highest rates of sediment accumulation, on the order of 40 to 50 cm/1000 years (Figures 30 and 31). Sedimentation on the shelf varies widely from a very low to a moderately high rate and ranges from 5 to approximately 50 cm/1000 years (Table 2; Figure 28). These comparisons assume that the surface of all cores represents present time, and that sedimentation continued uniformly at the calculated rate during the stated time interval. If the surface or near-surface sediment of the upper slope cores (670602, 6706-3, 6708-37) and the shelf core (6708-42) is assumed to be late Pleistocene in age as stratigraphic data suggest, then the calculated rates would have to be increased to about 15 cm/1000 years in each core (25 cm/1000 years in the case of core 6708-42) and would represent only late Pleistocene sedimentation. Consequently, the Holocene sedimentation rate for these shelf and upper slope cores would be nil. In any case, the upper slope environments appear to be receiving less sediment than the lower slope. This is also demonstrated in the Rogue Canyon, where the rate calculated in the lower Canyon (core 6711-6) is eight times greater than that determined from the upper Canyon (core 6708-37). This suggests that the lower Canyon may be more closely related to the rapidly-filling swale (core 6708-38) than to the upper Canyon, and hence the lower Canyon is filling much faster than the upper Canyon.

Estimates of the Holocene sedimentation rate on continental slopes vary widely. Gorsline and Emery (1959) calculated that the green muds of the southern California Borderland province deposit at a rate equivalent to 72 cm/1000 years, while the estimates given by Moore (1966) for the total basin-fill in the same area range from 4 to 160 cm/1000 years. Carlson (1968) notes that the rate of deposition on the floor of Astoria Canyon on the northern Oregon margin ranges from about 50 cm/1000 years near the mouth to more than 75 cm/1000 years near the head, but he estimates a 10 cm/1000 years average for the hemipelagic deposition on the adjacent protected continental slope. Duncan (1968) calculated postglacial (Holocene) rates of deposition ranging from 29 cm/1000 years to 100 cm/1000 years in the deep-sea area adjacent to the base of the continental slope. Thus the rates shown in Table 2, especially those from the lower slope, are not unreasonable when compared to the foregoing estimates. It is therefore suggested that the lower slope is presently accumulating sediment three to four times faster than the upper slope.

SEDIMENTOLOGY

The sedimentological character of continental margin deposits can provide important clues to the provenance and dispersal paths of the sediments, as well as to the physiographic and tectonic framework of sedimentation in the margin environment. In turn, a knowledge of margin sedimentation patterns, particularly with regard to the role of the continental slope as a temporary resting place for sediments during their transport from shelves to final deposition in deep-sea basins, is an essential link in the interpretation of the complete cycle of oceanic sedimentation.

Unconsolidated Sediments

Classification and Distribution of Sediment Types

Three main sediment types were observed in the cores taken on the southern Oregon margin. These are olive gray lutite, gray lutite, and sand-silt layers. Although not part of a particular classification, these terms have been used previously (Duncan, 1968; Griggs, 1969) to describe similar deposits, and are based primarily on characteristics observed by megascopic examination supplemented with the use of a binocular microscope. The term lutite (Ericson, et al. 1961; Heezen, et al., 1966) implies a sediment composed chiefly of silt-

and clay-size particles, or mud. The proportion of the two constituents may vary over a wide range from a nearly pure clay to a sediment composed almost entirely of silt, but most often the lutite in this study is a clayey silt ($< 50\%$ clay) or silty clay ($< 50\%$ silt) according to Shepard's classification (1954). The distinction between olive gray lutite and gray lutite is based solely on color. Sand-silt layers refer to terrigenous sand or coarse silt-size particles composed chiefly of detrital mineral grains.

At this point it is important to note that in most cases a physiographic province corresponds to an environment of deposition. Therefore, in subsequent discussions relating to the margin sediments, the term "physiographic province" will also imply the depositional environment represented by that province, and conversely, the term "depositional environment" will also imply the particular physiographic province which includes that depositional environment. Any exception to this will be explained fully in subsequent discussion.

Using the data from the textural analysis, and plotting each sample according to its sediment type, depositional environment and age, the sediments were grouped according to the textural classification of Shepard (1954) (Figure 26). Similarly, the coarse-fraction constituents of each sample are plotted on a triangular diagram whose three end-members are grouped according to origin and hydrodynamic character: the detrital group consists of those mineral grains and

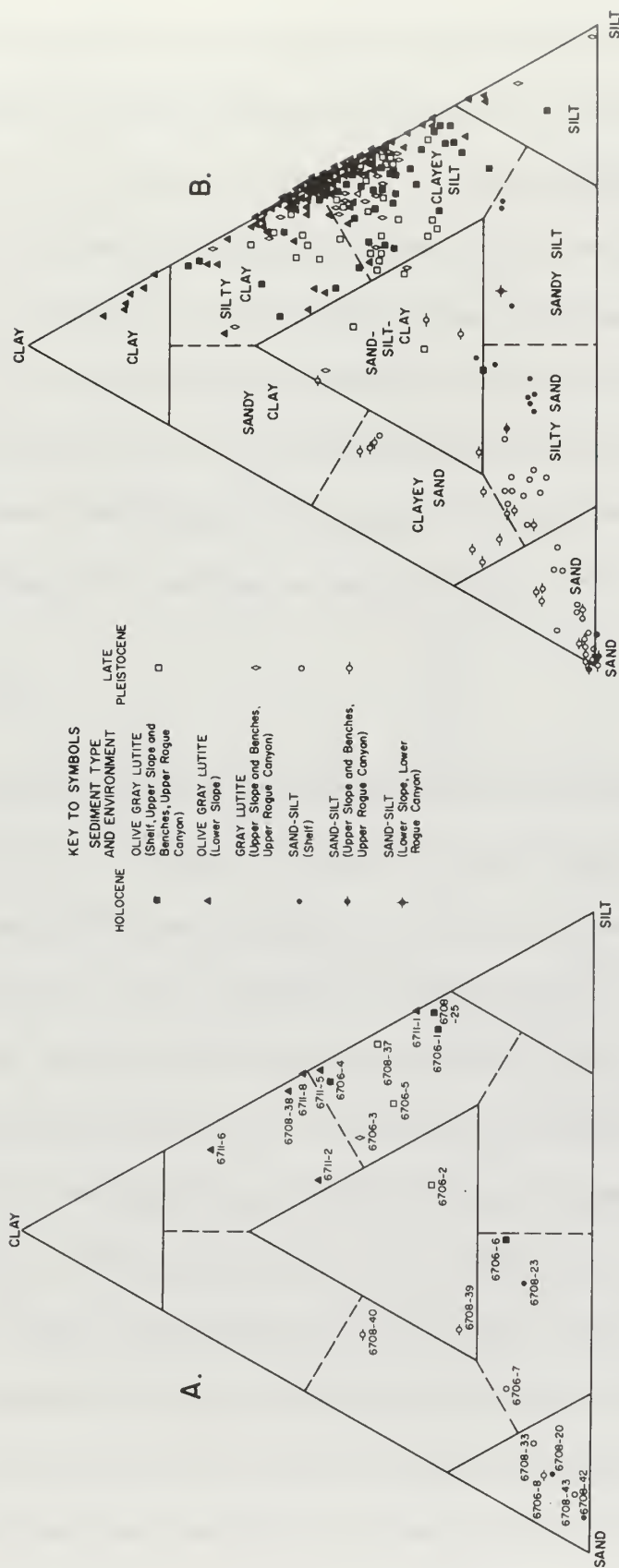


Figure 26. Textural classification of unconsolidated sediments (after Shepard, 1954) plotted according to type, depositional environment, and age. A. Surface sediments. B. Subsurface sediments.

rock fragments (except mica) requiring strong transporting currents; mica-plant fibers-volcanic glass are platy and/or low-density grains sensitive to current action; the biologic-authigenic group consists of material which accumulates in situ such as benthic and planktonic Foraminifera, Radiolaria, fecal pellets, glauconite and pyrite (Figure 27). The location and distribution of the major and minor sediment types within each core illustrated for the four main physiographic provinces: shelf (Figure 28), upper slope and benches (Figure 29), lower slope (Figure 30) and Rogue Canyon (Figure 31).

Olive Gray Lutite

Olive gray lutite is the most widespread and abundant sediment type (Figures 28-31). It varies slightly in color, from olive gray (5Y 3/2, Geological Society of America Rock Color Chart, 1963) to light olive gray (5 Y 4/2). The texture also varies, but it is typically a homogeneous, poorly sorted silty clay or clayey silt, with occasional coarse constituents (Figure 26). The olive gray lutite is characteristically poorly consolidated and relatively high in organic matter and moisture content. Although found in every environment, it especially dominates the lower slope (Figure 30), where the coarse fraction commonly is composed of more than 50% biologic material (Figure 27). In contrast, the majority of the coarse fraction in samples from the upper slope and benches consists of detrital minerals (Figure 27).

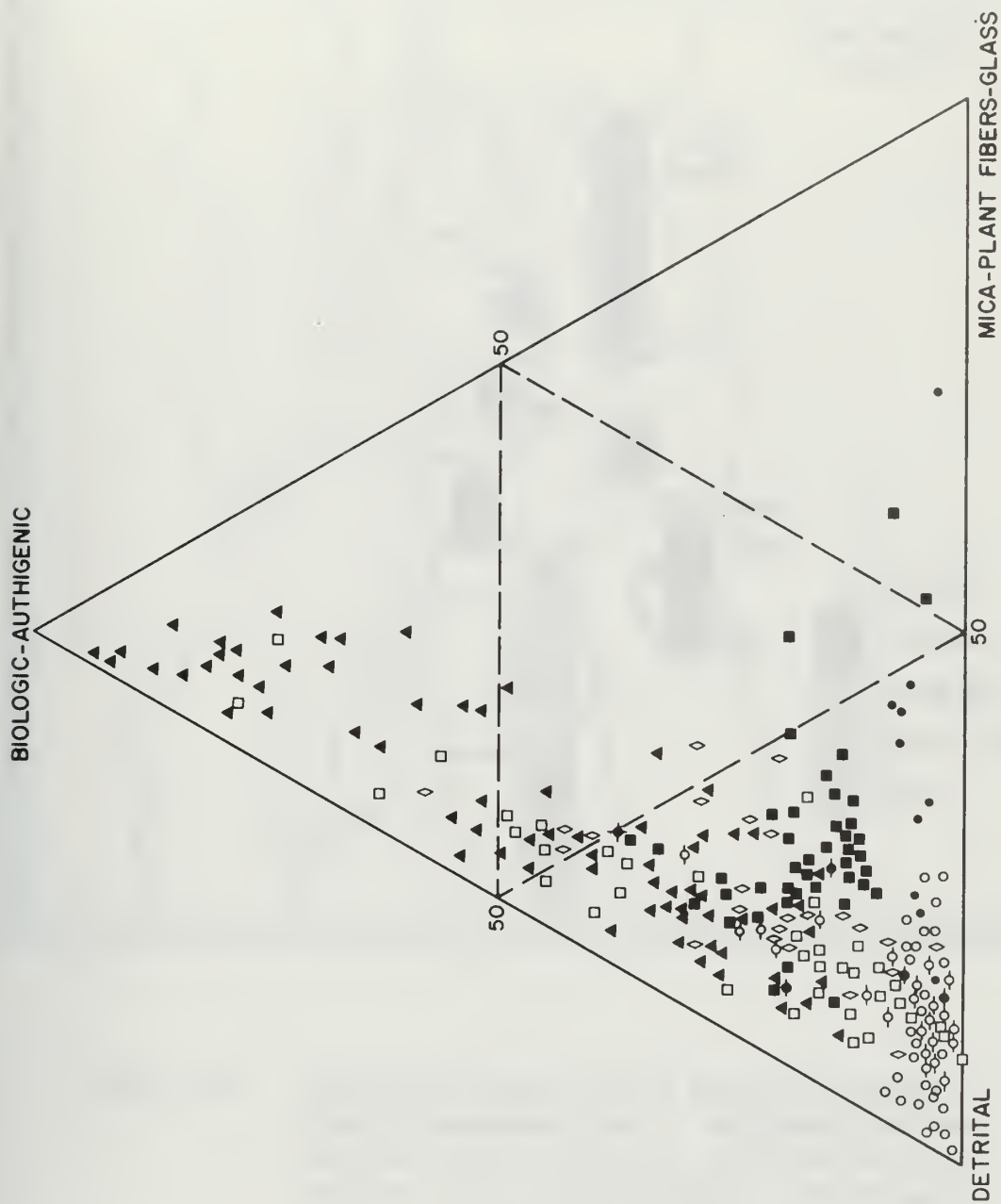


Figure 27. Coarse-fraction constituents of unconsolidated sediments, plotted according to type, depositional environment, and age. See Figure 26 for legend.

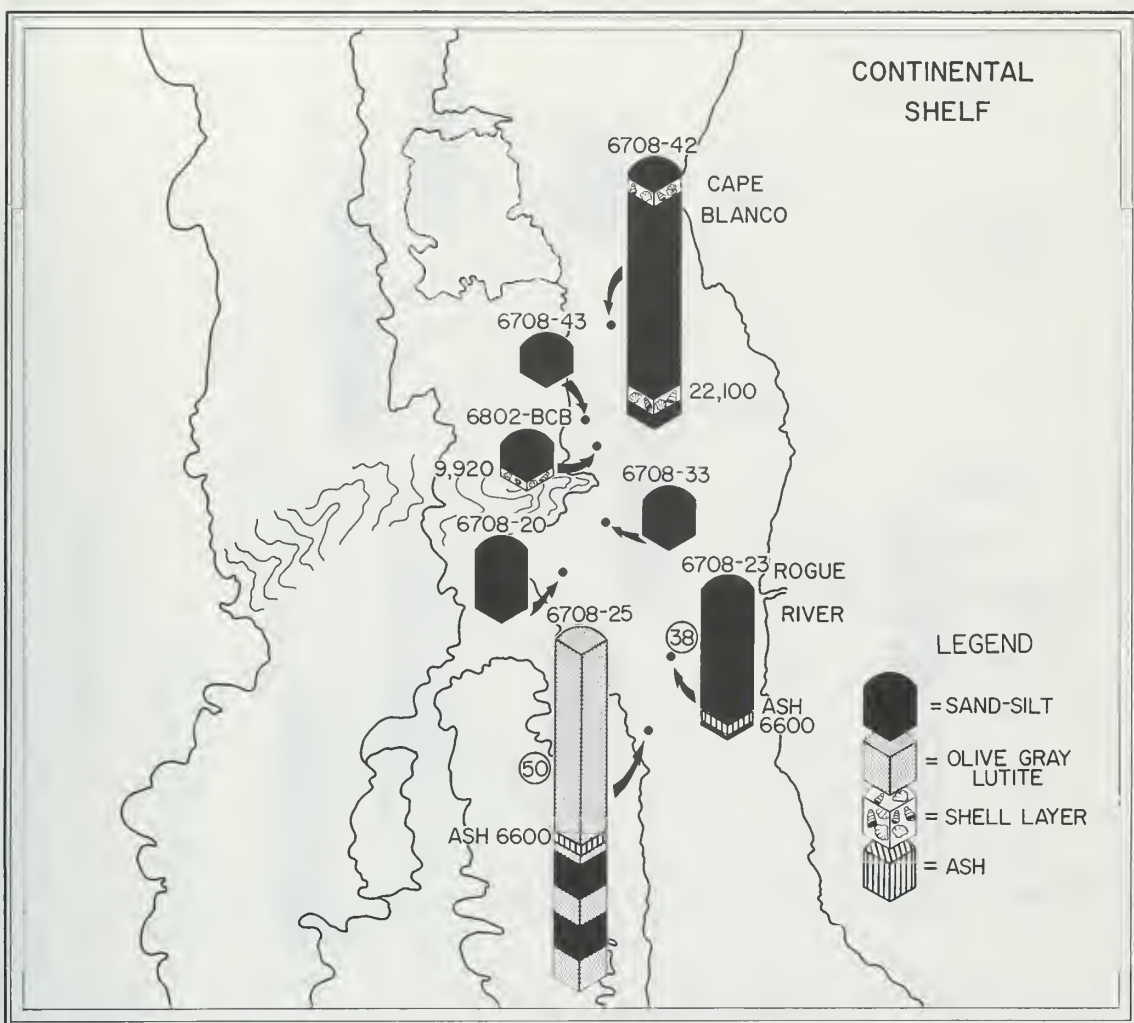


Figure 28. Lithology of piston cores from the southern Oregon continental shelf. Sediment ages are indicated next to the core. Circled numbers indicate rates of sedimentation. Physiographic province boundaries reflect present dissected surface of margin. Data for box core 6802-BCB after Chambers (1968).

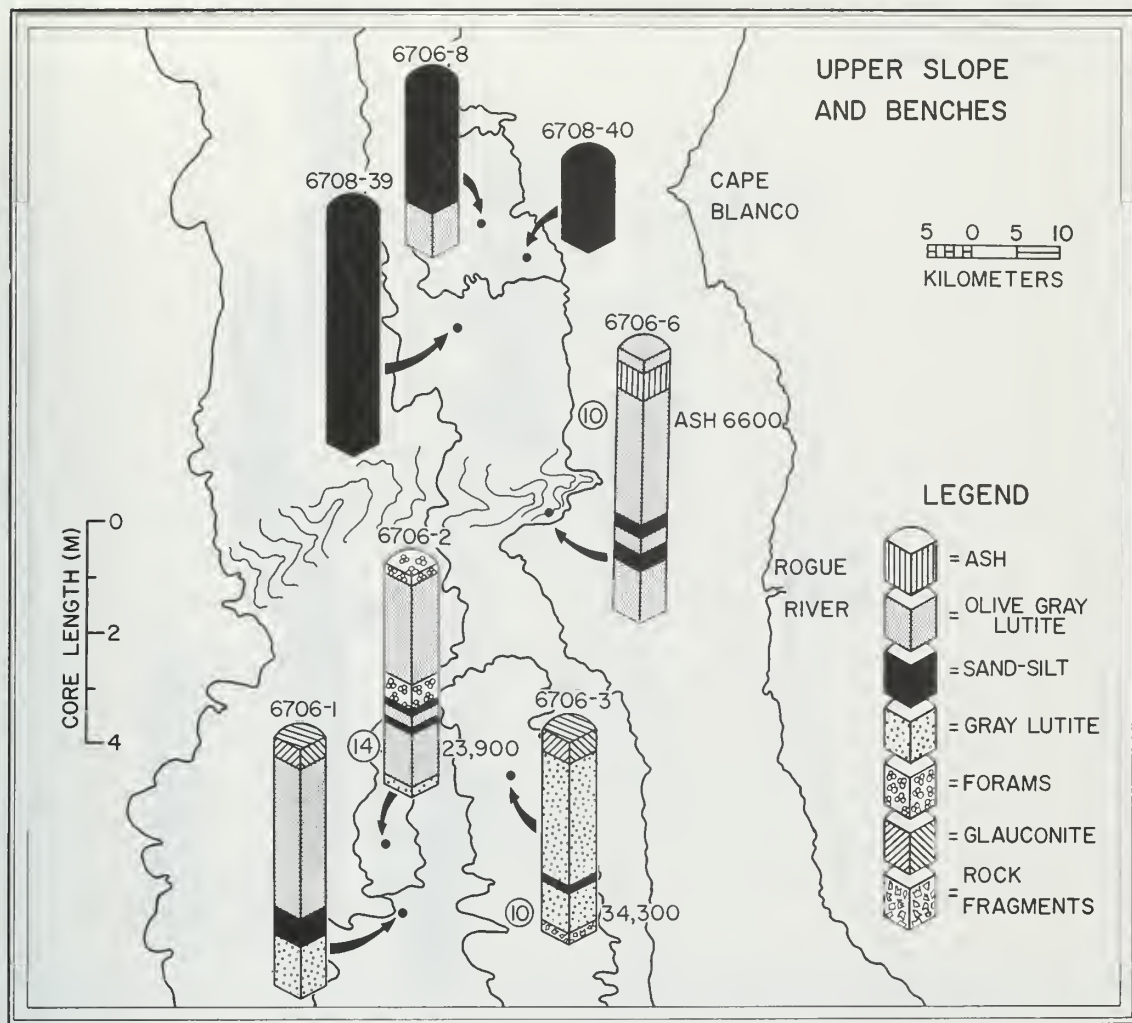


Figure 29. Lithology of piston cores from the upper continental slope and benches. Sediment ages are indicated next to the core. Circled numbers indicate rates of sedimentation. Physiographic province boundaries reflect present dissected surface of margin.

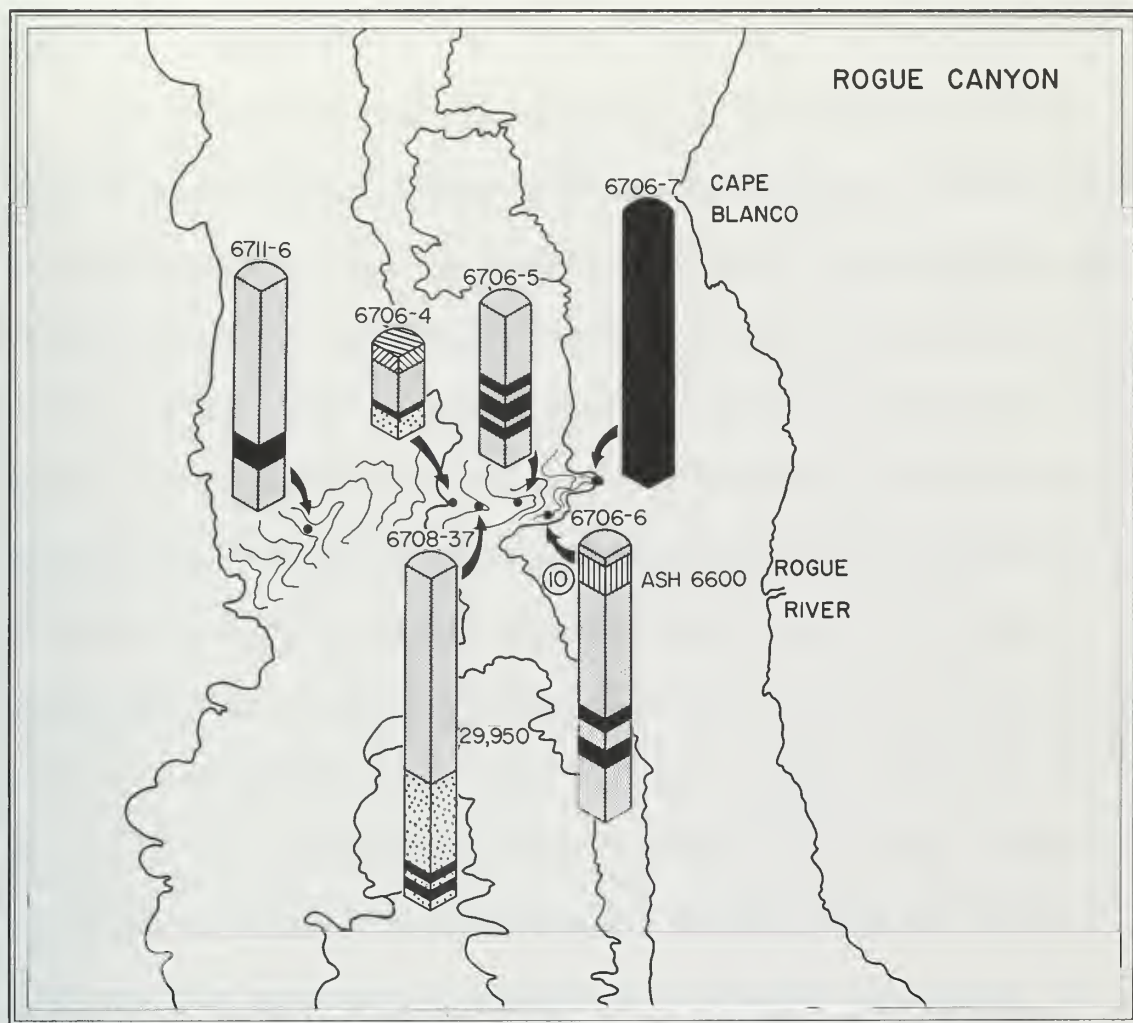


Figure 31. Lithology of piston cores from the Rogue Submarine Canyon. See legend and caption of Figure 29 for explanation.

Mica, plant fibers and glass are rarely more than 20% of the coarse fraction in any sample.

All of the olive gray lutite observed by Duncan (1968) in the adjacent deep sea was postglacial (Holocene); however, at least some of that sampled from the upper slope and Upper Rogue Canyon (cores 6706-2 and 6708-37, Figures 25, 29 and 30) may be late Pleistocene in age. In both cases gray lutite occurs at the base of the core. As Duncan (1968), Carlson (1968) and Nelson (1968) have observed, the change from gray lutite to olive gray lutite may mark a significant time boundary, the transition from late Pleistocene to postglacial (Holocene) time. If the R/P faunal ratio indicates that this transition took place about 12,500 years B.P. (Duncan, et al., 1970) then the gray to olive transition should have occurred at about the same time and would be observed at approximately the same depth as the shift from abundant planktonic Foraminifera to abundant Radiolaria. A transitional type sediment, light olive gray, lutite often occurs between the gray and olive varieties in the deep sea, but appears to be restricted to postglacial time (Duncan, 1968).

The color transition has been noted in four slope cores (6706-1 and 6706-2 from the upper slope; 6706-4 and 6708-37 from the Upper Rogue Canyon), with one other core (6706-3 from the Klamath Plateau) composed almost entirely of gray lutite (Figures 25, 29 and 31). Two of these cores (6706-1 and 6706-4) lack sufficient stratigraphic

information to confirm the above hypothesis. However, a core adjacent to each of these from a similar environment (6706-2 and 6708-37, Figures 29 and 31, respectively) clearly indicates that the color shift occurs earlier than 12,500 years B.P. (Figure 26). This indicates that either the deposition of olive gray lutite began much earlier in the upper margin environments than in the deep sea and hence may be as old as late Pleistocene, or that the olive gray lutite in cores 6708-37 and 6706-2 should have been classed as gray lutite, a distinction not apparent from either megascopic examination or subsequent analyses (Figures 26 and 27).

Gray Lutite

Gray lutite commonly occurs as a clayey silt or silty clay (Figure 27) and varies in color from olive gray (5Y 4/1) to dark greenish gray (5GY 4/1) or medium dark gray (N4). It is generally cohesive and stiffly compacted, and hence tends to be better consolidated than the olive gray lutite. The coarse fraction content of the gray lutite comprise only two or three percent of the total sediment, and consist mainly of detrital grains with only 25 to 40% biologic material (Figure 27). As noted above, gray lutite was penetrated only in cores from the upper slope and Upper Rogue Canyon. If it is indicative of the late Pleistocene, it probably underlies the thicker accumulation of Holocene sediment on the lower slope.

In continental margin environments, gray lutite cannot be distinguished from olive gray lutite on the basis of texture (Figure 26) or coarse fraction (Figure 27). It may be distinctive initially only in its color until its age can be established. Gray lutite from the continental margin is similar texturally to that found by Duncan (1968) in adjacent deep-sea environments, and closely resembles the gray clay found by Griggs (1969) in Cascadia Channel. However, the coarse fraction in these latter types often contains 75% or more biologic material, principally planktonic Foraminifera and Radiolaria, as compared to the lesser amounts found in gray lutite from the margin. This reflects the increased pelagic rain of shells and tests and the smaller amount of detrital material found in deeper and more distant environments.

Sand-Silt Layers

Terrigenous sand and coarse silt occur in all environments and in all cores except 6711-1 (Figures 28-31). It is the dominant sediment type in cores from the continental shelf (including 6706-7 from the head of the Rogue Canyon) and from the Cape Blanco Bench. It occurs in these latter environments in thick sequences, and in all other environments as distinct layers with sharp and well-defined contacts interbedded with olive gray lutite or gray lutite. X-radiographs revealed that all of the sands sampled were essentially featureless and structureless with no grading observed within a unit or layer except for some minor

grading noted in core 6706-5 from the Upper Rogue Canyon. Texturally, this type varies from sandy silt to sand, but still can easily be distinguished from the lutites (Figure 26). Generally the coarse fraction consists of more than 75% detritals.

The age of the sand-silt layers in the various environments is more difficult to determine, and can be either Holocene or late Pleistocene. Coarse fraction analyses reveal an abundance of iron-staining, solution pitting, and alteration in the sand-silt materials from the surface of both the shelf and Cape Blanco Bench, but these characteristics are absent from other parts of the slope. The thick accumulations of sand-silt on Cape Blanco Bench are more suggestive of shelf sands than of the thinner sand-silt layers on the lower slope. Chambers (1968) recognized staining and alteration in sands from the southern Oregon shelf; Emery (1965, 1968) notes that staining and alteration of shelf sands may be indicative of their relict nature. It is postulated here that the sand-silt on the surface of Cape Blanco Bench is also of a relict nature, and may be late Pleistocene in age. However, all of the sand-silt layers in the cores from the lower slope are Holocene.

Minor Sediment Types

Several minor sediment types were observed which were distinctly different from the three main types just described, but were not

widespread enough either vertically or areally to warrant their classification as major sediment types. These types usually consist of sediments whose coarse fractions contain appreciable amounts of distinctive constituents. The most important of these were:

Foraminifera-rich lutite (6706-2 from the upper slope; 6711-1 and 6711-2 from the lower slope);

volcanic ash-rich layers, usually lutite (6708-23 and 6708-25 from the shelf; 6706-6 from the wall of the Upper Rogue Canyon; 6711-1, 6711-2, and 6708-38 from the lower slope);

shell layers (6708-42 from the shelf);

rock fragments (6706-3 from the Klamath Plateau); and

glauconitic layers, usually sandy (6706-1 from Middle Bench, 6706-3 from the Klamath Plateau, and 6706-4 from the Upper Rogue Canyon).

The glauconitic layers occur at the surface of two cores from the upper slope close to the relict surface sediments. Glauconite is normally authigenic, or formed in place, and is often relict (Emery, 1968). Because of its association with relict, or possibly relict sediments, it is postulated that the glauconite found in the upper slope cores is also relict (i.e. a sediment formed out of equilibrium with existing conditions). The tentative relict age of the olive gray lutite at the surface of core 6706-2 may also apply to the adjacent olive gray lutite and surface glauconite in core 6706-1. Similarly, the late

Pleistocene age of the gray lutite in core 6706-3 (Figure 25) also suggests that the surface glauconite in this core is not modern but relict. The coarse sand in core 6706-7 from the head of the Upper Rogue Canyon, the late Pleistocene age of the olive gray lutite in core 6708-37, and the surface glauconite in core 6706-4 (Figure 31), all suggest that the Upper Rogue Canyon may be another relict area on the upper slope.

Without additional evidence for the absolute ages of the surface sediment in cores 6706-1, 6706-3, and 6706-4, it is difficult to state with certainty that these sediments are late Pleistocene in age, although the existing evidence suggests that they may be. Relict sediments need not all be of late Pleistocene age, they could have formed early in Holocene time under different conditions than those encountered today.

The Present Sediment Pattern

The stratigraphic and sedimentological evidence from the upper slope environments, especially the benches, strongly suggests that the surface sediment in these areas is both modern and relict in nature. Certain areas, such as Cape Blanco Bench and the Klamath Plateau, may be covered entirely with relict sediment while other upper slope areas contain patches of both modern and relict material. The data of Chambers (1968) suggest that the continental shelf off southern

Oregon is also surfaced with both modern and relict sediment. In contrast, the lower slope appears to be completely mantled by modern mud.

By combining the data available on the surface sediments of the southern Oregon margin, a generalized genetic classification emerges. Figure 32 illustrates six types thought to be present on the margin. Modern sand occurs on the inner shelf and modern mud is found on both the central shelf and lower slope. Mixed sand and mud and the relict sand found on the shelf have their analogs in the mixed modern and relict deposits and the relict sand found on the upper slope. The shelf, upper slope, and lower slope are distinct physiographically and as sedimentary environments. The upper slope appears to be more closely related to the shelf than to the lower slope, and could be thought of as a transition zone between the two, not unlike the sedimentary regime of the Borderland province off southern California (Gorsline and Emery, 1959; Moore, 1966).

Textural Relationships

Certain statistical measures related to the texture of the sediment have been examined in an attempt to test whether or not the three environments (shelf, upper slope, lower slope) can be distinguished more precisely. Mean diameter (M_ϕ) has been plotted against both the phi deviation (σ_ϕ) and phi skewness (a_ϕ) with respect

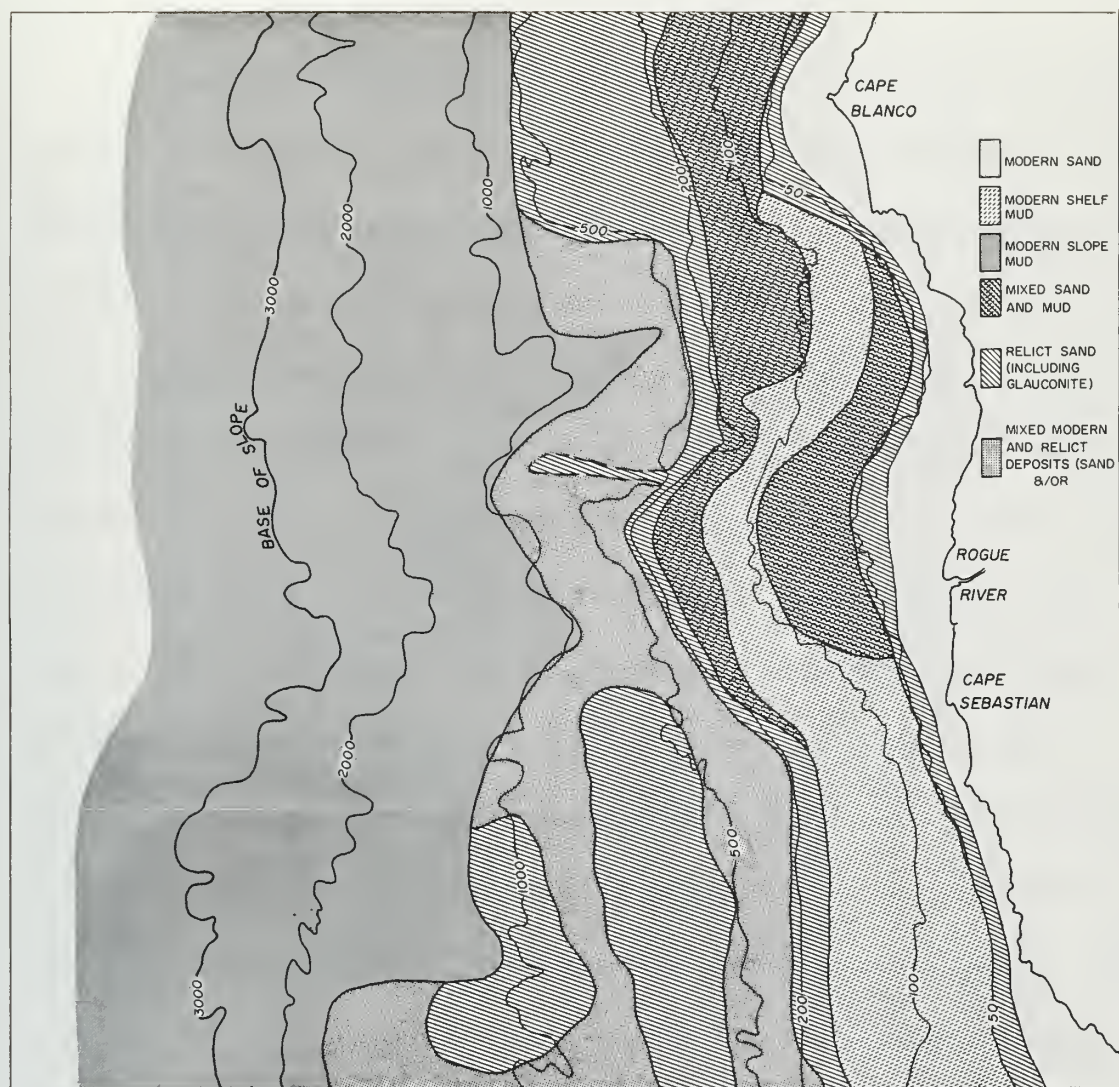


Figure 32. Distribution of surface sediment types on the southern Oregon margin.

to environment (Figures 33, A and 34) and sediment type (Figures 33, B and 35).

The sorting of the majority of sediments, particularly the olive gray lutites from the lower slope, is generally poor (Figure 33). No sharp demarcation can be made between sand-silt layers and lutites on this basis, either environmentally or by sediment type. A division of the sediments into two groups is apparent in both Figures 34 and 35. One group represents sand-silt layers, which are coarse-grained and extremely fine-skewed, and both olive gray and gray lutite appear as another group which is fine-grained and coarse-skewed. The coarse (negative) skewness of the lutite may be attributable to the presence of sand-sized tests or shells of Foraminifera or other pelagic organisms. No environmental distinction can be made among any of the three sediment types which would indicate their particular environment of deposition. Conversely, it also appears that no clear textural subdivisions can be made among the various environments which would indicate the presence of a distinct sediment type.

Mineralogy

An analysis of the mineralogy of the margin sediments can be most useful, not only in distinguishing among the various sediment types, but also in determining the provenance of the sediment and its dispersal patterns.

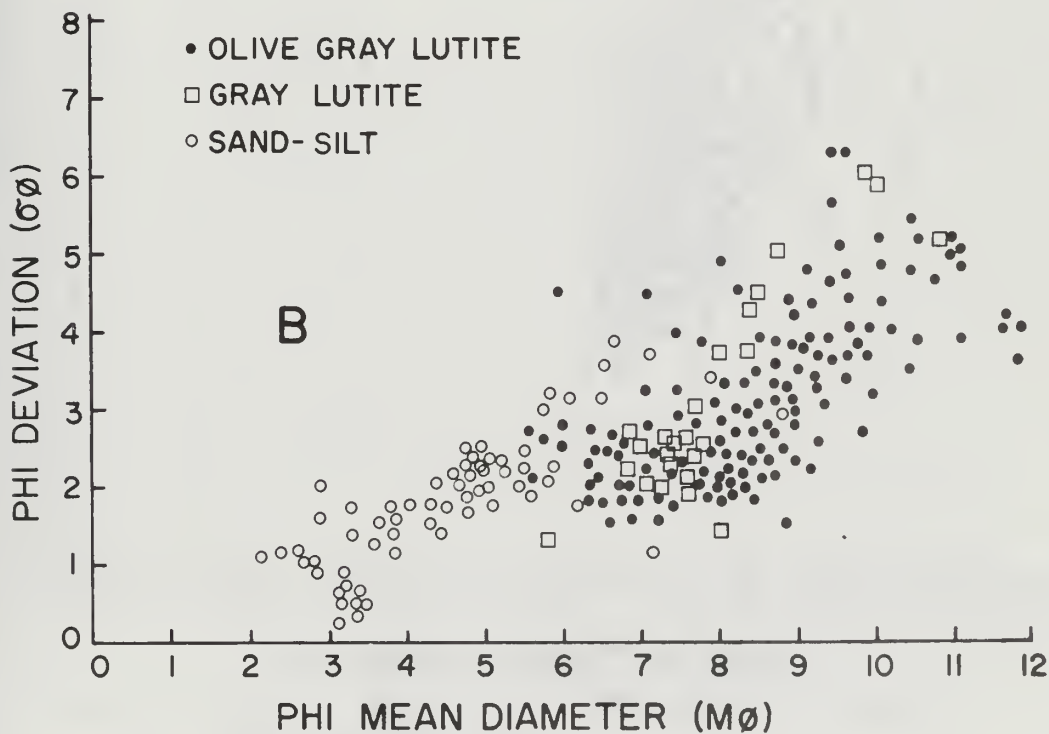
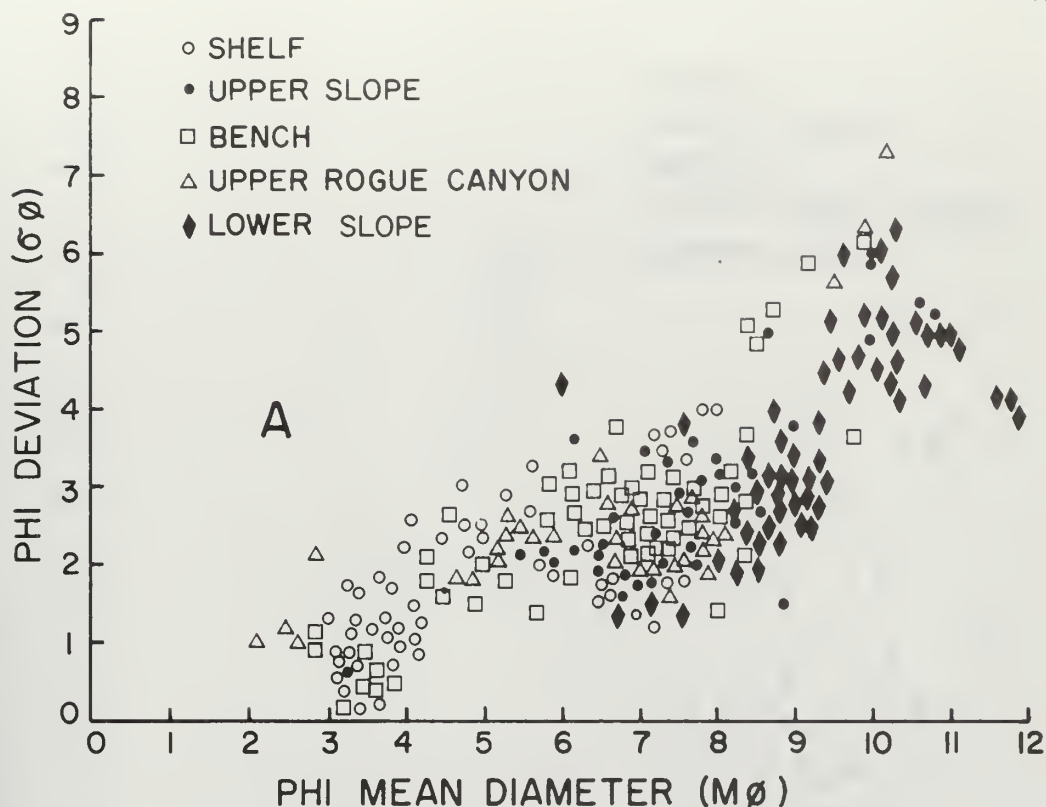


Figure 33. Phi Mean Diameter versus Phi Deviation according to (A) depositional environment and (B) sediment type.

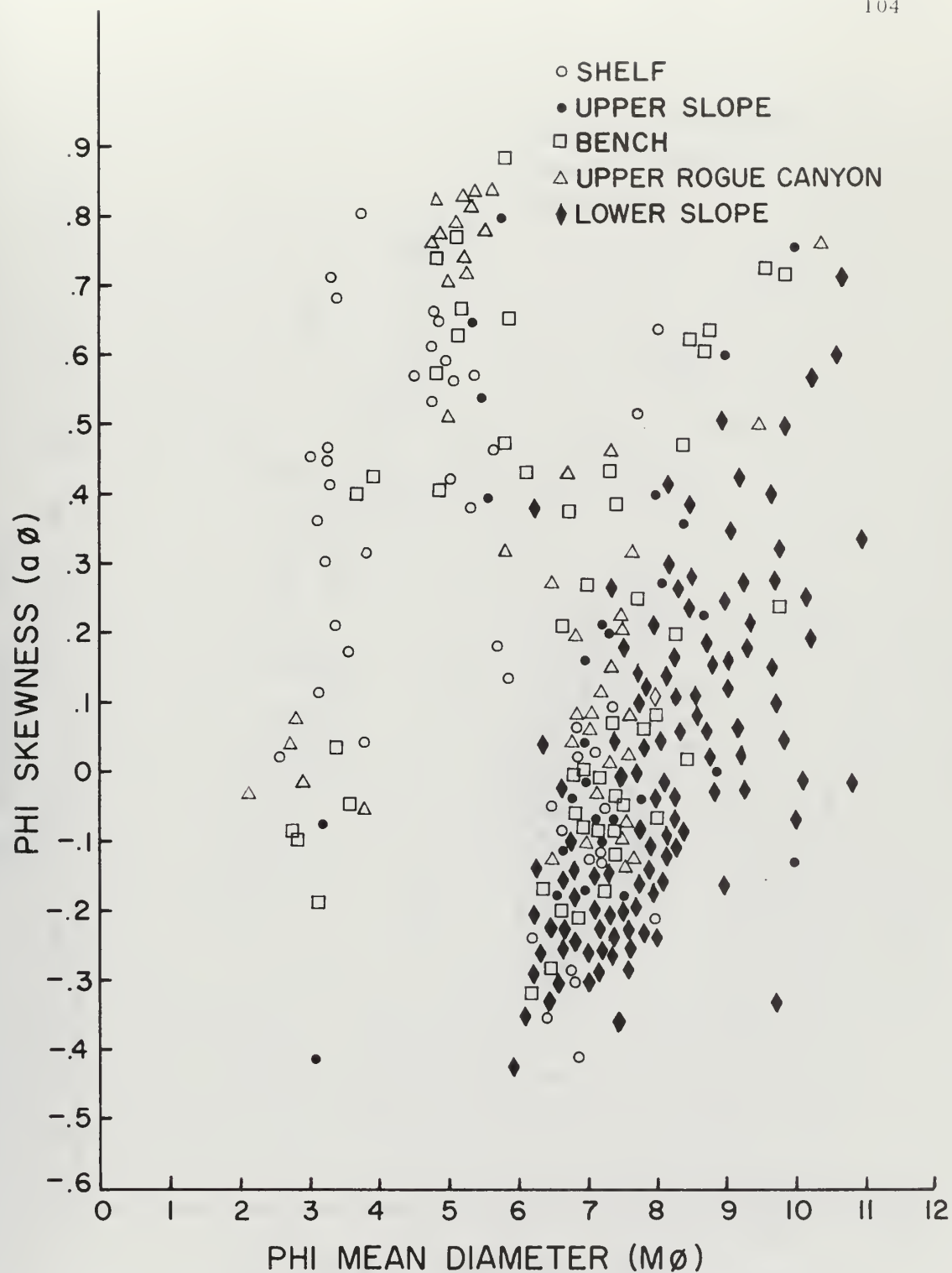


Figure 34. Phi Mean Diameter versus Phi Skewness according to depositional environment.

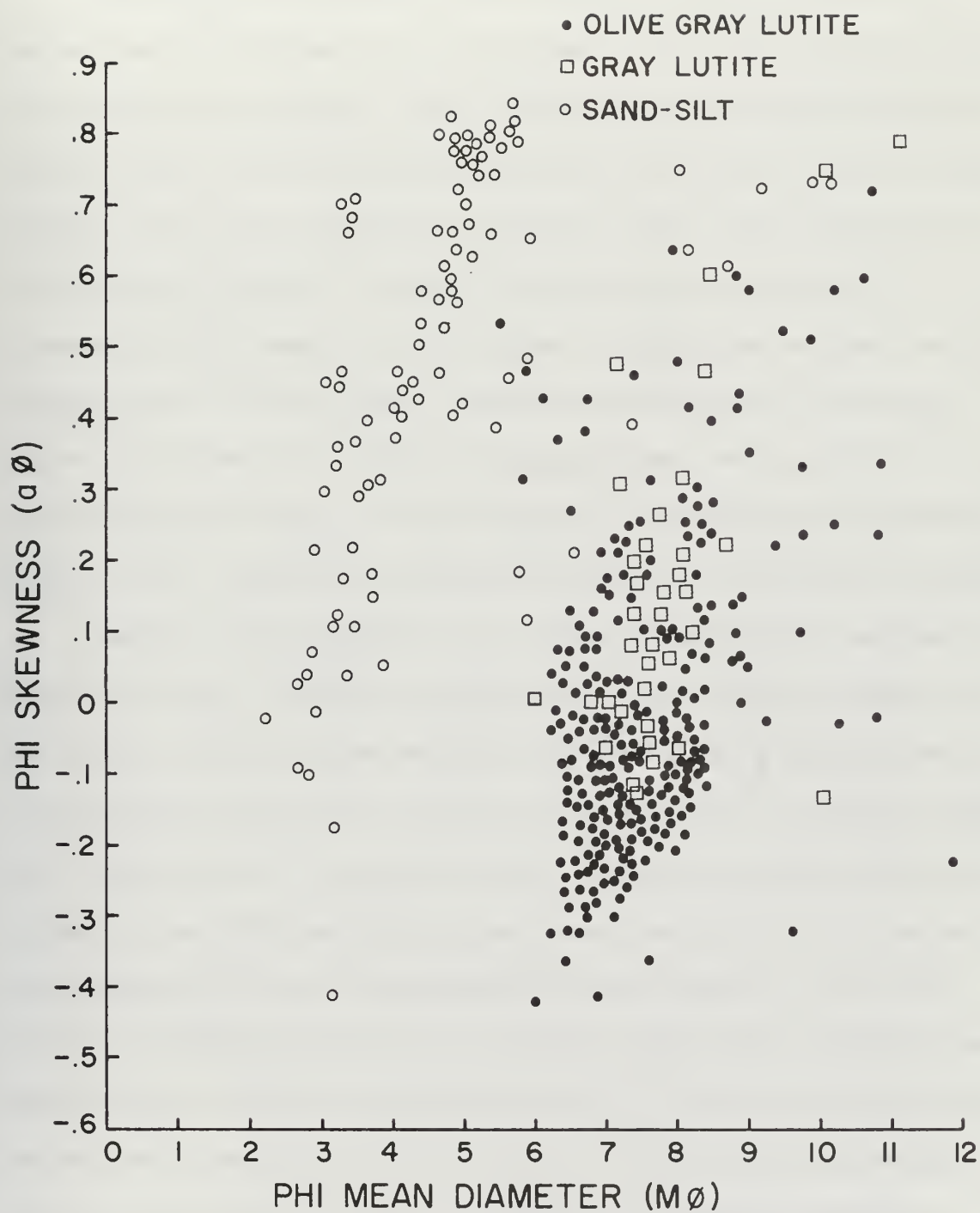


Figure 35. Phi Mean Diameter versus Phi Skewness according to sediment type.

Light Minerals

Inasmuch as the texture of the sediments tends to reflect the depositional environment for the most part, rather than the source area of the sediment (van Andel, 1964), an examination of light minerals of the sediment coarse fraction can provide a better clue to the rock composition and tectonic stability of the source areas. The light mineral suites from 12 samples selected from the various physiographic provinces include quartz, potash feldspar, plagioclase feldspar, rock fragments and volcanic glass. Using the classification of Williams, Turner and Gilbert (1954), these constituents have been plotted on a ternary diagram (Figure 36, A) to show the relative amounts of stable (quartz, chert, quartzite) and unstable (feldspar, rock fragments) grains.

The light mineral fraction of southern Oregon margin sediments is chiefly arkosic, volcanic or lithic sand, with the arkosic sands predominating. All sediments have less than 50% stable grains (Figure 36, A) suggesting a tectonically unstable source area that has possibly undergone rapid erosion. The unconsolidated sediments contain higher percentages of unstable constituents than those found in various Jurassic and Cretaceous rocks of southwestern Oregon (Figure 36, B) by Dott (1965). His analysis indicates an increase in both potash feldspars and total feldspars with decreasing age (Table 3). This trend is continued in the unconsolidated sediments (Figure 36, A; Table 3) which are younger than the rocks and which contain an even higher percentage of feldspars.

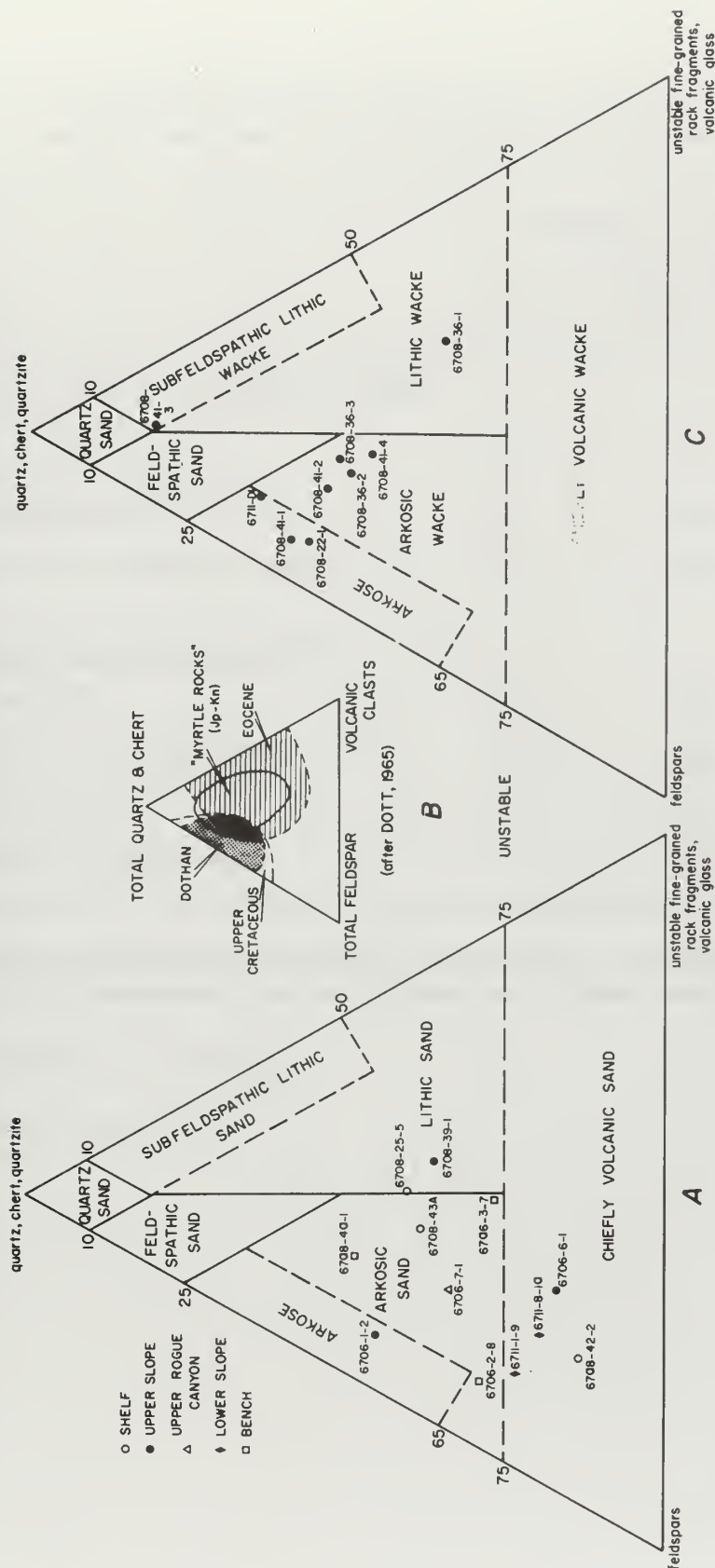


Figure 36. Light mineral composition of selected sediments (A) and sedimentary rocks (C). Petrographic classification of impure sands and sandstone types after Williams, Turner and Gilbert (1954). Composition of southwestern Oregon rocks (B) after Dott (1965).

Table 3. A comparison of the light mineral composition of selected margin sediments with southwestern Oregon sandstones.

Location	Percent of Composition ^a		
	Quartz	Plagioclase Feldspar	Potash Feldspar
<u>Southern Oregon Continental Margin</u>			
Shelf sediments (3) ^b	30	30	15
Upper slope and bench sediments (7)	33	26	21
Lower slope sediments (2)	21	15	42
<u>Southwestern Oregon Rocks^c</u>			
Eocene (38)	25	14	6-25
Upper Cretaceous (42)	48	20	10-20
"Myrtle Rocks"	--	--	1-10
Dothan Formation (50)	17	18	< 1

^a Composition does not total 100% because other constituents not listed here (rock fragments, volcanic glass, etc.) have been excluded.

^b(N) - Number of samples.

^cData from Dott (1965).

Heavy Minerals

One of the best indicators of the provenance of continental margin sediments is the heavy mineral assemblage. The distinctive assemblage found in the sediments from the southern Oregon margin provides a particularly clear indication of their source area and source rocks.

The dominant heavy mineral groups observed were the amphiboles (especially blue-green hornblende and actinolite-tremolite), epidote, and opaque minerals (including hematite and limonite). Next in importance were the pyroxenes, olivine and garnets. Glaucophanite, a mineral diagnostic of metamorphic provenance (Kulm, et al., 1968), was also present in minor amounts in the assemblage.

The four continental drainage basins providing sediment to the Oregon continental margin are the Columbia River Basin, the North Coast Basin, the Umpqua Mid-Coast Basins, and the Klamath-South Coast Basins (Figure 37). The various rivers in each of the basins have been examined to determine their heavy mineral assemblages and source rocks (Kulm, et al., 1968b; Duncan, 1968). The Klamath-South Coast Basins, particularly those of the Rogue and Klamath Rivers, are the principal basins draining southwestern Oregon and northern California. They appear to be the principal contributors of sediment to the southern Oregon continental margin.

The Paleozoic and Mesozoic meta-sedimentary, meta-volcanic, and sedimentary rocks of the Klamath Mountains which have been intruded by granitoid and ultrabasic rocks (Baldwin, 1964) are responsible for the distinctive mineralogy found in Klamath-South

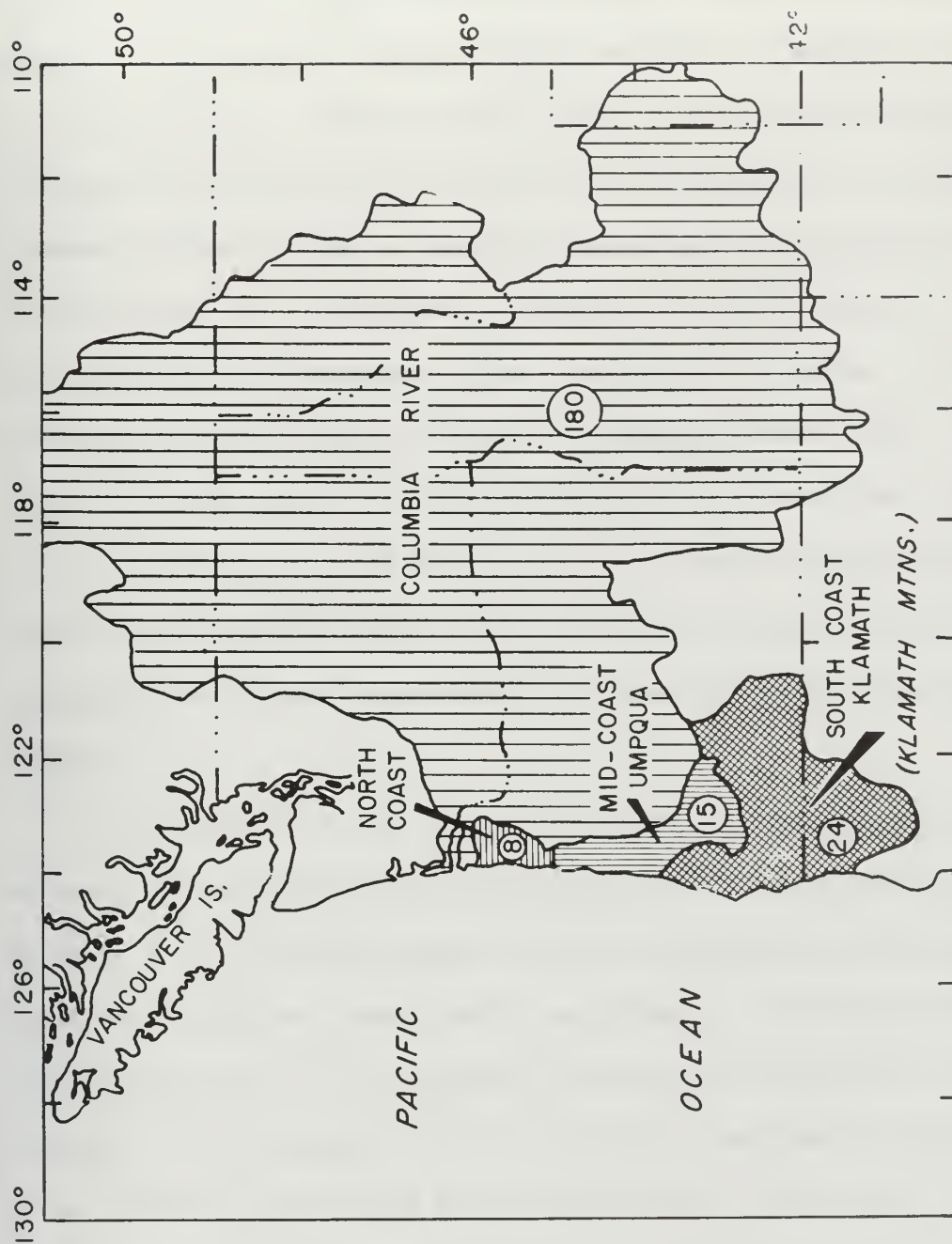


Figure 37. Major drainage basins of northwestern United States. Circled numbers indicate average annual runoff in millions of acre feet for each basin. Modified after Duncan (1968).

Coast drainages. The rivers of the Klamath-South Coast Basins are characterized by an amphibole assemblage, consisting principally of blue-green hornblende and actinolite-tremolite. In addition to these, the epidote group is also present in nearly all the rivers. Glaucophane, although present only in small amounts, occurs only in the Rogue and Klamath drainages, and is therefore diagnostic of the Klamath-South Coast Basins. The glaucophane probably is derived from the glaucophane-bearing schists of the Franciscan Formation of northern California and the Dothan Formation of Oregon (Irwin, 1966). Some rivers of the Klamath-South Coast Basins such as the Coos, Coquille, Sixes and Elk Rivers, and the major rivers of the Umpqua Mid-Coast Basins drain the late Tertiary and Quaternary volcanic and sedimentary formations of the central and southern Oregon Coast Range (Figure 7).

The similarity of the heavy mineral assemblages from the southern Oregon margin and the Klamath-South Coast Basins is shown in Table 4. The low percentage of pyroxene minerals in the margin sediments compares closely with that present in the Klamath-South Coast Basins, and is very close to the amount present in the adjacent deep sea. The average amount of blue-green hornblende (29%) present in the Klamath-South Coast Basins assemblage (Kulm, et al., 1968b) is very close to the average obtained from the margin assemblages (25%). Glaucophane, found only in the Klamath-South Coast Basins, is present in at least one sample from every margin environment.

Table 4. Comparison of the heavy mineral suites and pyroxene/amphibole ratios of southern Oregon margin environments with continental drainage basins.

Locality	Major Heavy Mineral Groups					Pyroxene/ Amphibole Ratio		
	Amphibole ^b	Pyroxene	Epidote	Garnet	Olivine			
Continental Margin Environment	Shelf (6) ^a	35 (30) ^c	13	16	2	4	30 (30) ^f	0.4
	Benches (11)	23 (20)	7	11	4	2	53 (50)	0.3
	Upper Slope (4)	31 (25)	11	10	3	3	42 (36)	0.4
	Upper Rogue Canyon (7)	33 (27)	6	6	3	3	48 (43)	0.2
	Lower Slope (5)	26 (18)	19	11	4	1	39 (31)	0.7
Deep Sea	Blanco Valley (13) ^d	(52)	19 ^e	8	1	1	1 ^g	0.37 ^h
Continental ⁱ Drainage Basins	Klamath-South Coast	65 (59)	19	4	2	4	6 ^g	0.3
	Umpqua Mid-Coast	20 (19)	61	4	5	1	9	3.1
	North Coast	2 (2)	96	--	--	1	1	48.0
	Columbia River	28 (27)	64	1	2	2	3	2.3

^a Number of samples examined is indicated in parentheses ().^b Includes glaucophane which is present in all margin environments and the Klamath-South Coast Basins.^c Percent hornblende (all types) is indicated in parentheses ().^d Data from Duncan (1968). Includes only non-opaque, non-micaceous minerals.^e Includes clinopyroxenes only.^f Percent of weathered grains + opaque grains is indicated in parentheses ().^g Excluding weathered and opaque grains^h Clinopyroxene/hornblende ratioⁱ Data from Kulm, et al. (1968b).

The relative abundance of pyroxene and amphibole is a consistent indicator of the source area contributing sediment to the margin environments. The minerals included in the pyroxene to amphibole ratio (P/H ratio) constitute the majority of the non-opaque, non-micaceous and unweathered constituents and therefore adequately represent the entire heavy mineral suite. The average P/A ratio in the margin environments is similar to that obtained for the Klamath-South Coast Basins (Table 4).

The P/A ratios indicate that the sediments in all margin environments are influenced more by the mineral assemblages in the Klamath-South Coast Basins than those from any other basin. Despite the fact that the river runoff of the Columbia Basin is over seven times that for the Klamath-South Coast Basin (Figure 37), the distinctive assemblage of the latter basin still appears to dominate the southern Oregon margin environments. It may be argued from the data of Table 4 that the lower slope, which has a relatively high P/A ratio of 0.7, is also influenced by sediments from the Umpqua Mid-Coast Basins and/or the Columbia River. However, the clay mineralogy suggests that only the sediments from the Umpqua Mid-Coast Basins have any noticeable effect on the lower slope off southern Oregon.

In general, surface sediments from the benches and upper slope exhibit higher percentages of hematite and limonite in their heavy mineral fractions than do sediments of other environments.

Considerable iron staining, pitting, and alteration is also evident in the light mineral fractions from these environments, especially from the benches. As previously noted, this evidence may be an indication of the relict nature of the benches sediments, and to a lesser extent of most upper slope sediments. Shelf sediments show a higher average percentage of heavy minerals, particularly opaque grains, than do the other environments. Chambers (1968) has plotted the zones of high heavy mineral concentration on the shelf; he has also noted that opaque grains may be indicative of stillstands of sea level due to their high specific gravity and resistance to offshore transport. The shelf samples examined in this study are within, or adjacent to, high heavy mineral zones mapped by Chambers and the results from these samples appear to be consistent with his data.

Clay Minerals

The clay mineralogy reinforces the hypothesis that the Klamath-South Coast Basins are the most important source for the sediments of the southern Oregon margin. The clay fraction from 18 sediment samples representing shelf, upper slope and lower slope environments, and from three rock dredges was examined to determine the percentages of the various clay minerals present (Figure 38). The clay minerals from all the environments on the southern Oregon margin consist predominantly of chlorite and illite, with only minor amounts

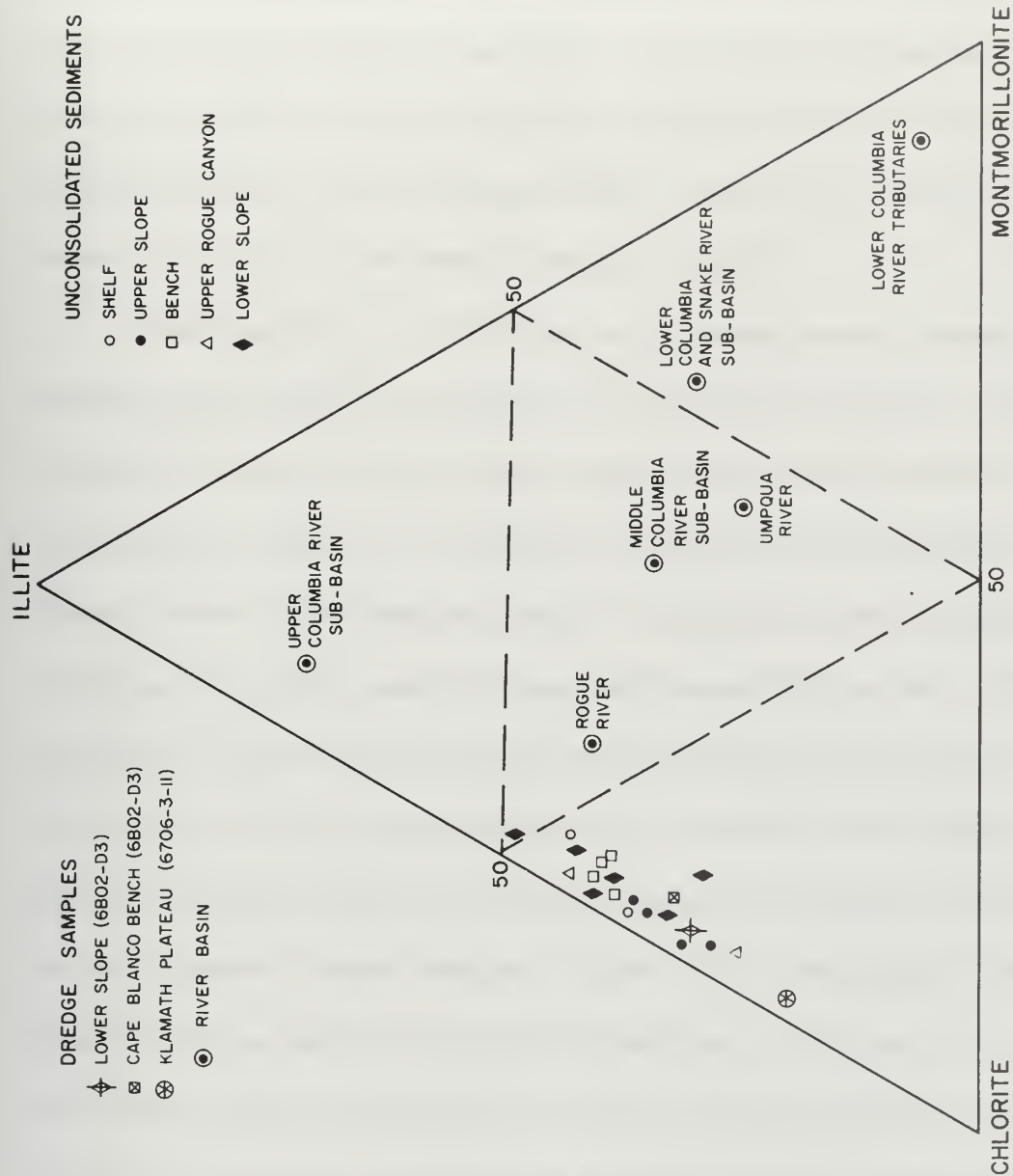


Figure 38. Clay mineral composition of selected sediments from the continental margin and major Oregon rivers. Clay mineral data for the Columbia River sub-basins after Knebel, et al. (1968); data for Rogue and Umpqua Rivers after Drake (1969).

of montmorillonite. No kaolinite was found. The presence of amphiboles of clay size was also noted in six of the sediment samples and all the rock samples examined. In all sediments and sedimentary rocks, chlorite is the most abundant mineral (average 60%), with lesser amounts of illite (average 35%). Only minor amounts of montmorillonite occur in the sediments (average 5%).

The Rogue River, which drains the metamorphic terrane of the Klamath Mountains, is noted for its high chlorite content. Duncan (1968) and Duncan, et al. (1970) examined the clays from this river and obtained values of 51 % chlorite, 26% illite, and 23% montmorillonite; Drake (1969) obtained similar values in her analysis (43% chlorite, 38% illite, and 19% montmorillonite) (Figure 38). When compared to the clay mineralogy of the Umpqua River of any of the Columbia River sub-basins (Figure 38), the Rogue River appears to be the dominant influence affecting the clay mineralogy of all sediments on the southern Oregon margin. Other rivers draining the Klamath Mountains may also be chlorite-rich and may contribute to the relative uniformity of the clay mineral content of margin sediments. The fact that all the samples examined are so nearly alike in clay mineral composition attests to the pervasive influence of chlorite-rich sediments from the Klamath Mountains, which masks any influence from the Columbia sub-basins, and to a lesser extent, from the Umpqua Mid-Coast Basins.

Russell (1967), Duncan (1968), Duncan, et al. (1970), and Harlett (1969) have all noted that diffractograms of late Pleistocene deep-sea clays exhibit sharper peaks than those of Holocene deep-sea clays. Duncan et al. (1970) report that more illite than chlorite is present in late Pleistocene deep-sea clays than in the Holocene clays. They postulate that the change in character between the late Pleistocene and Holocene clays is probably due to variations in the relative rates at which the Columbia River and Snake River sub-basins contributed their clay mineral assemblage to the sediment load of the Columbia River. They state further that the Upper Columbia River sub-basin was a major source for the illite-rich deep-sea sediments during the Pleistocene, but as the region emerged from glaciation montmorillonite-rich sediments of the Lower Columbia and Snake River sub-basins began to dominate the sediment load. This change is abrupt, and not due to more gradual marine diagenetic processes; it is associated with the late Pleistocene-Holocene faunal boundary (ca. 12,500 years B.P.) and has been verified quantitatively by similar abrupt increases in the chlorite-illite and montmorillonite-illite ratios (Duncan, 1968; Duncan, et al., 1970). Chlorite-illite ratios were calculated for the samples examined in this study; the samples represent the tops and bottoms of nine cores from the various environments (Appendix 7). Although the Pleistocene-Holocene boundary was not evident in the cores examined the chlorite-illite ratio

did increase upward in all but two cores, a trend which is in general agreement with Duncan's data.

In addition to determining the change in clay mineral character with depth, Duncan (1968) noted that three Holocene clay mineral groups are evident in the deep-sea which radiate outward from the Columbia River. The montmorillonite content decreases while chlorite, and to a lesser extent, illite, increase with distance from the river. Group three, in the deep sea off central and southern Oregon, contains the most chlorite (mean value 40%) and the least montmorillonite (mean value 32%). The clay minerals from the continental margin appear to belong to this group. However, the higher chlorite content of margin sediments compared to those in group three suggest either that a significant amount of chlorite is retained on the margin and may never reach the deep-sea environment, or that the chlorite is diluted as the clays move seaward.

The occurrence of amphibole in the clay mineral fraction from three cores and three dredge samples (Appendix 7), representing mostly upper slope environments, may be significant. Heath (1969) suggests that the amphibole may have been produced as glacial rock flour during the late Pleistocene and may have deposited on the margin in that form. However, except for a few valley glaciers that may have been present, the region was not glaciated during the Pleistocene. In addition, the sediment in these samples is not all Pleistocene in

age. A fuller explanation for the presence of amphibole must await a more detailed examination.

Organic Carbon

Sedimentation rates in late Pleistocene was at least six times higher than that in the Holocene in the deep-sea environments off Oregon (Duncan, 1968). Duncan found that the organic carbon content of postglacial lutite is up to five times higher than that of the late Pleistocene lutites. He attributed this apparently reversed trend to the higher influx of sediments in the late Pleistocene masking the organic carbon content of these older sediments. Peterson (1969) reached the same conclusion by calculating sediment and organic carbon accumulations in terms of $\text{gm/cm}^2/1000$ years. From his calculations, Peterson found that although the sedimentation rate and organic carbon influx was higher during the late Pleistocene, the absolute amount of organic carbon preserved in the older sediments was less due to dilution, differences in preservation, and depth of burial.

In this study, samples from near the top and bottom of eight cores representing different depositional environments were analyzed for their percent total carbon, organic carbon, and calcium carbonate (Table 5). Two additional cores were more fully examined by Peterson (1969).

Table 5. Total carbon, organic carbon and calcium carbonate in selected margin sediments.

Sample number	Depth in core (cm)	Depositional environment	Age ^b	Sediment type ^c	Percent total carbon	Percent organic carbon	Percent CaCO ₃ ^a
6708-25-4	230	Shelf	H	OGL	1.16	0.90	2.17
6708-25-16	583		H	OGL	0.95	0.63	2.67
6708-42-1	230	Shelf	H	S-S	0.53	0.44	0.76
6708-42-2	454		LP	S-S	1.02	0.54	3.97
6706-5-(1) ^d	17	Upper Rogue Canyon	LP	OGL	1.41	1.36	0.48
6706-5-(2)	183		LP	OGL	0.69	0.47	1.77
6706-5-(3)	255		LP	OGL	0.70	0.53	1.35
6708-37-1	15	Upper Rogue Canyon	LP	OGL	1.70	1.57	1.03
6708-37-7	575		LP	GL	1.56	1.14	3.50
6706-3-1	5	Klamath Plateau	LP	GL	1.00	0.95	0.41
6706-3-10	377		LT	GL	0.84	0.67	1.44
6706-2-12	302	Middle	LP	OGL	1.34	0.85	4.08
6706-2-17	375	Bench	LP	GL	1.18	0.74	3.66
6706-6-8	155	Upper	H	OGL	1.14	0.94	1.53
6706-6-15	355+	Slope	H	OGL	1.18	0.89	2.47
6711-6-1	10	Lower Rogue Canyon	H	OGL	2.30	2.00	2.45
6711-6-8	340+		H	OGL	2.22	1.84	3.00
6708-38-1	5	Lower	H	OGL	1.82	1.60	1.82
6708-38-21	472	Slope	H	OGL	1.52	1.32	1.62
6711-2-(1) ^d	19	Lower	H	OGL	2.06	1.42	5.32
6711-2-(5)	154	Slope	H	OGL	1.06	0.97	0.62
6711-2-(10)	410		H	OGL	1.33	1.20	1.16

^a Percent by weight^b LP - late Pleistocene, H - Holocene, LT - Late Tertiary.^c OGL - olive gray lutite, GL - gray lutite, S-S - sand-silt layers.^d Data and sample number designations after Peterson (1969)

In those margin cores where the surface, or near-surface, samples were examined, the average percent organic carbon was found to be 1.3, with surface samples from the lower slope being among the highest values recorded (1.6% and 2.0%). These values compare favorably with the 1.6% median value from the adjacent continental slope at 41°59'N, reported by Gross, et al. (1970). Sediments accumulating on the continental slope are thought to have high organic-carbon concentrations where the oxygen-minimum zone impinges on the bottom. Off Oregon the oxygen minimum zone extends to depths of 500 to 2000 m and appears to coincide with the high organic carbon content of slope sediments in this depth range.

All but one core (6708-42, a sandy core from the shelf) showed an increasing percentage of organic carbon upwards, and all but three cores (6711-2, 6708-38, and 6706-2) showed a decreasing percentage of calcium carbonate upwards in the core. In terms of absolute values of organic carbon, samples from cores considered to be entirely Holocene in age showed generally higher values of organic carbon and lower values of calcium carbonate than cores considered to be entirely late Pleistocene in age. It is not possible to determine whether this increase is abrupt. Although the Holocene sedimentation rates computed in this study are high (Table 2), it is possible, as Duncan has noted, that Pleistocene rates could have been several times higher both on the margin and in the deep sea. If this hypothesis is correct,

then the decrease in sedimentation rate from Pleistocene to Holocene time may not have occurred as abruptly on the margin as in the deep sea.

Consolidated Sediments

Classification and Distribution of Rock Types

A comparison of the consolidated rocks recovered from the dredge hauls with the unconsolidated sediments from the cores reveals certain trends which may provide a clearer understanding of the geological events that have occurred on the margin. Figure 39 shows the location and major lithology of the rock types collected in the ten dredge hauls. Samples from nine of the rock types were sufficiently coarse-grained to permit a detailed petrographic examination (Appendix 8); these have been grouped according to the classification of Williams, Turner and Gilbert (1954) and are shown in Figure 36, C. The remaining samples were too fine-grained for petrographic identification (Figure 39; Appendix 8).

The lithified samples fall into two groups: coarse-grained impure sandstones, mostly arkosic and lithic wacke (Figure 36, C), all but one of which are from the shelf and upper slope, and fine-grained mudstones and siltstones from the lower slope (Figure 39), some of which are calcareous. When one compares the light mineral

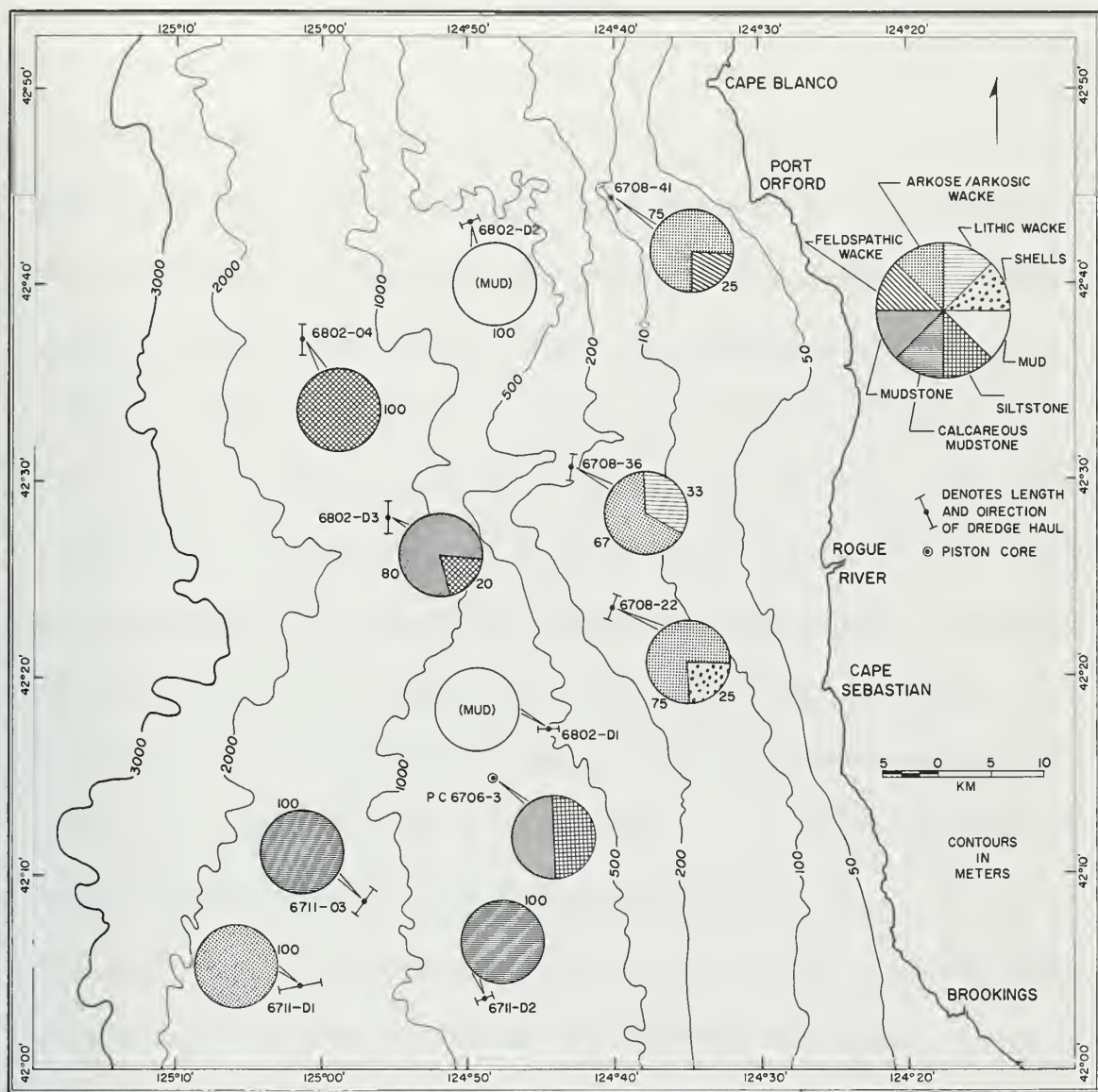


Figure 39. Rock types from the southern Oregon margin. Numbers next to circles denote percent of each rock type.

composition of the unconsolidated sediments (Figure 36, A) with that of the consolidated sediments (Figure 36, C), it is apparent that the unconsolidated sediments have a higher percentage of unstable grains than do the lithified sediments. This would seem reasonable since the sediments lose much of their unstable elements during the various stages of diagenesis and repeated cycling as they become lithified. In general, both the unconsolidated and consolidated sediments are arkosic in character. A comparison of the light mineralogy of the consolidated sediments on the margin with that of southwestern Oregon continental rocks examined by Dott (1965) (Figure 36, B) shows that the composition of the shelf and upper slope sedimentary rocks are similar to those of the Upper Cretaceous Series and the Dothan Formation. This suggests that the late Tertiary rocks of the shelf and upper slope could have been derived from either the Jurassic or Late Cretaceous rocks of the Klamath Mountains.

A complex of Tertiary and pre-Tertiary strata crop out in the coastal and near-coastal regions of southwestern Oregon. These have been described in detail previously (see Regional Geology). The early Tertiary strata exposed along the southern Oregon Coast Range were folded and faulted during the late Tertiary Cascadian orogeny (Dott, 1965), and the resulting north-south-trending anticlines and synclines probably extend westward from the coast offshore and underlie the shelf and upper slope, and perhaps the lower slope. All but the most

resistant Tertiary strata probably occur only in synclinal basins or down-faulted blocks, and most likely only the younger Mio-Pliocene strata are widespread, or exposed, on the upper margin. Maloney (1965) reports only Miocene and Pliocene rocks from the shelf, banks, and slope off central Oregon. The age of three rocks recovered from the margin off southern Oregon date back to the early or mid-Pliocene (Table 1). Most, if not all, of the predominantly arkosic rocks from the shelf and upper slope (6708-22, 6708-36, 6708-41, 6711-D1; Figure 39) may also be Mio-Pliocene in age, although it cannot be stated with certainty that they are from contiguous strata.

The calcareous, nodular mudstones (6711-D2 and 6711-D3) may be widespread on the upper slope, particularly on the Klamath Plateau, since similar rocks have been recovered by Silver (1969a) on the Klamath Plateau off northern California. The rocks are probably concretionary in origin, but the time of their formation is unknown. Rock fragments in the base of core 6706-3 (Figure 39) have been dated as mid-Pliocene (Table 1). This suggests that a distinct unconformity, probably a result of tectonism, exists between the Tertiary rocks at the base of the core and the overlying late Pleistocene sediments. In general, the lithology and age of the rocks recovered by Silver (1969a) from the northern California margin are similar to those found in this study.

Clay mineral contents of the three rock samples from the slope

(6802-D3-1, 6802-D2, and 6706-3-11-1; Figure 38) show the same high chlorite percentages as unconsolidated sediments from the slope, which indicates that the contribution of the chlorite-rich sediments from the Klamath Mountains has been strong, at least since the Miocene. The large difference in the chlorite-illite ratio in core 6706-3 between the mudstone fragments at the base ($C/I = 3.9$) and the immediately overlying gray lutite ($C/I = 1.5$) reinforces the evidence of a distinct erosional boundary at that depth in the core.

In general, the grain-to-matrix ratio of the consolidated sediments from the margin approximates the sand-mud ratio of the overlying sediments. On the shelf, the grain-matrix ratio of the rocks approaches one and the sand-mud ratio of shelf sediments is also commonly one or slightly greater. In the remaining margin environments, both the grain-matrix ratio of the rocks and the sand-mud ratio of the overlying sediments are usually less than one, reflecting an absence of coarse constituents in these environments.

In examining the composition of the consolidated and unconsolidated sediments of the southern Oregon margin, certain generalizations can be made. First, the light mineral composition of the sediment samples is generally similar to the rocks, but the latter have more stable constituents. Second, the upper slope sediments and rocks have a composition more closely approaching that of the Upper Cretaceous Series and Dothan Formation of the Klamath Mountains

than that of the Eocene or other early Tertiary strata of the southern Oregon Coast Range. Third, the lower slope sediments and rocks have a higher percentage of unstable constituents, particularly feldspars, than do those of the upper slope. They tend to reflect the influence of the early Tertiary strata of the southern Oregon Coast Range as well as that of the Klamath Mountains.

These relationships suggest an orderly sequence of events. The Mio-Pliocene strata exposed or underlying the shelf and upper slope were apparently derived from the uplift and erosion of pre-Tertiary Klamath Mountain strata, probably during the Nevadan orogeny or late Cretaceous disturbance. The Quaternary sediments exposed or underlying the lower slope were probably derived in part from a later uplift and erosion of mid- and late Tertiary sediments, probably during the Cascadan orogeny, and in part from the pre-existing Klamath Mountain strata.

PROCESSES OF SEDIMENTATION

A Proposed Model for Modern Sediment Transport on the Southern Oregon Continental Margin

Many factors influence sedimentation on the southern Oregon continental margin. These include the character of the source rocks, climatic effects, the quantity of sediment supplied by the continental drainage, the influence of coastal morphology and submarine topography, and the various oceanographic conditions which prevail over the margin. A generalized model of modern sediment transport processes (Figure 40) is proposed which attempts to relate these factors to the sediment distribution pattern presently found on the margin, and to that present during the late Pleistocene and early Holocene.

The Initial Regime of Sedimentation

The major sources of the unconsolidated sediments on the southern Oregon margin lies in the adjacent coastal complex of pre-Tertiary and Tertiary rocks of the Klamath Mountains and southern Oregon Coast Range. The relative dominance of sediments from the metamorphic terrane of the Klamath Mountains throughout the entire margin has already been shown. To a lesser extent, sediments from the Tertiary rocks of the southern Oregon Coast Range are contributed to the margin, but this contribution is more noticeable on the lower

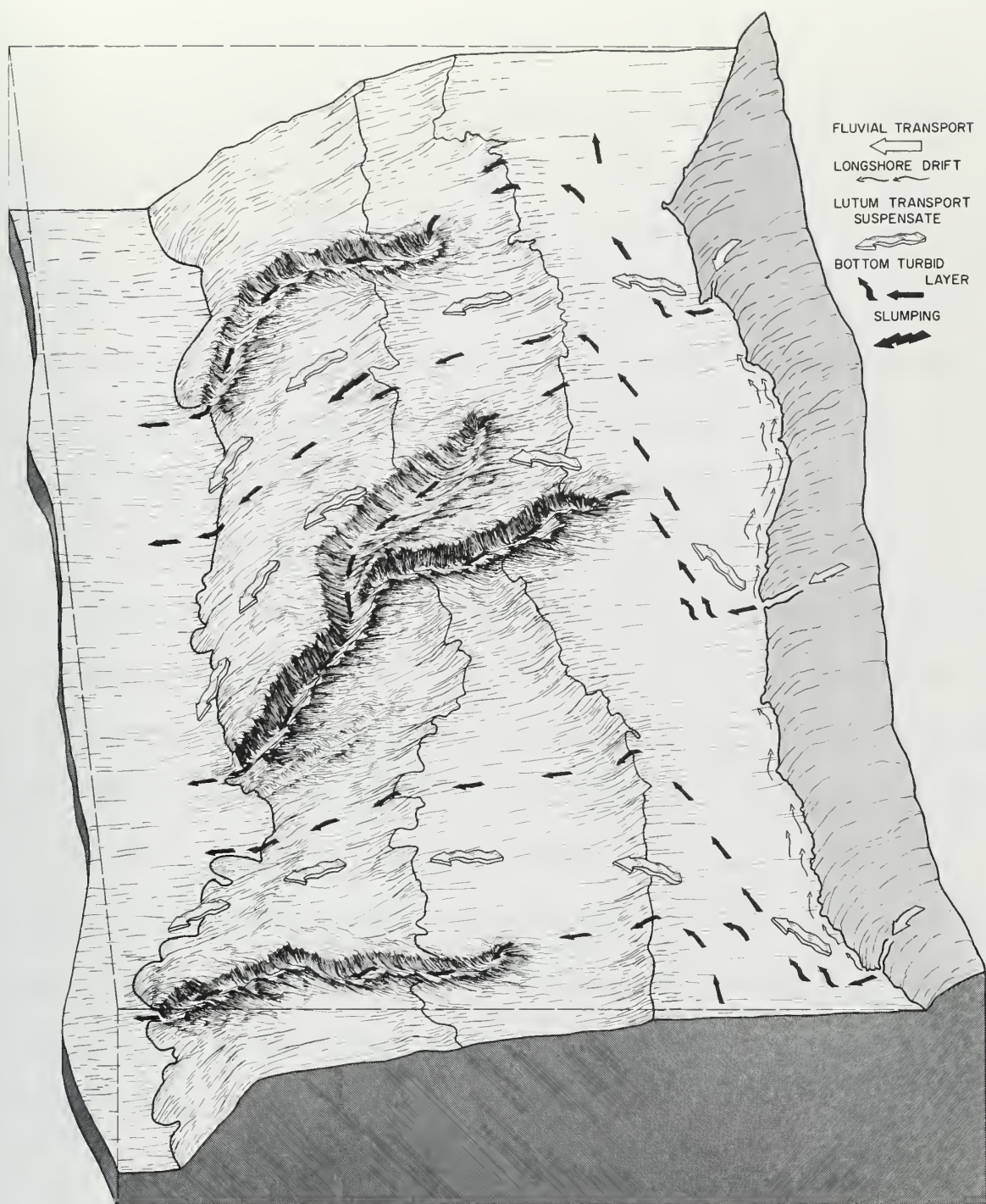


Figure 40. Schematic model of modern sediment transport processes on the southern Oregon margin.

slope than in other margin environments.

The major drainage complex supplying sediment to the margin is that of the Klamath-South Coast Basins. Additional sediment may be added to the southern Oregon margin by the major streams of the Umpqua Mid-Coast Basins, particularly by the Umpqua River, which drains portions of the northern edge of the Klamath Mountains as well as the southern Oregon Coast Range. River runoff data for these streams has been compiled by Hagenstein, et al. (1966) and by the U. S. Geological Survey (1964, 1966). Over 87% (21.5 million acre feet) of the total runoff of the Klamath-South Coast Basins comes from the Klamath and Rogue Rivers; one-half (7.5 million acre feet) of the total runoff of the Umpqua Mid-Coast Basins is supplied by the Umpqua River (Figure 37). The runoff of all the streams in both basins is only 20-25% of that supplied by the Columbia River (Lockett, 1965). However, mineralogical analyses in this study have shown that the influence of the Columbia River, and that of the North Coast Basins to the south of it, have a relatively minor affect on the sediments of the southern Oregon margin.

The amount of rainfall over southwestern Oregon varies widely with seasons, but is greatest during winter months, which is reflected in the stream runoff. For example, although the average discharge at the mouth of the Rogue River is approximately 3000 to 4000 cubic feet per second (cfs) for the entire year, it reaches a maximum of 15,000

to 16,000 cfs in January, and a minimum of 1500 cfs in September, following the low summer rainfall season. Since the amount and size of sediment discharge from a river is a function of the rate of flow of the river (Postma, 1967), the Rogue River discharges more sediment in winter, by an order of magnitude, than in summer.

The last rise of sea level has created numerous bays and estuaries at the mouth of the major streams along the northern California and southern Oregon coasts. These features have a marked influence on the supply of sediment to the southern Oregon margin. Fluctuating tides influence the interaction of the discharging fresh river water and the encroaching oceanic salt water within these bays and estuaries. According to Postma (1967) various accumulation mechanisms, particularly settling- and scour-lag effects, tend to trap sediment inside these basins or at least restrict their movement to the near-shore regions. Kulm and Byrne (1966) have shown this to be the case in Yaquina Bay, Oregon. Postma noted that this sediment trapping is most effective for relatively fine-grained sediment, but may vary between wide limits depending on local conditions to any size between five to ten μ and 100 μ .

As Chambers (1968) has noted, the Holocene sea level rise has caused the trapping and restriction of sand-sized sediment on the continental shelf off the Rogue River. A belt of sand is present from the shoreline to a depth of about 50-75 m, but only sand shoaler than

15-20 m (modern sand) is considered to be in equilibrium with the present environment (Figure 32). The sand between 20 and 70 m is probably relict sand of Pleistocene age. Dietz (1963) and Vernon (1966) conclude that modern beach sand is generally not transported offshore to depths greater than 20 m, except where the heads of submarine canyon extend into this depth. No work later than that of Chambers, including the present study, has detected any appreciable quantities of modern Holocene sand at the surface in margin environments deeper than the inner shelf, although Roush (1970) and Neudeck (1970) have cited evidence from sedimentary structures and from oceanographic conditions which indicate that sand movements to depths of 80-90 m or deeper may be possible.

The Holocene sea-level rise on the southern Oregon margin produced the following: 1. large accumulations of relict Pleistocene sand on the submerged benches and the deposition of large quantities of Holocene mud on the lower slope; 2. a six-times greater Pleistocene sedimentation rate in the deep sea compared to the Holocene (Duncan, 1968); 3. non-deposition of Holocene and modern sands on much of the outer shelf due to trapping in the bays and estuaries. This evidence all points to a large influx of coarse-grained sediment on the margin during the late Pleistocene when sea level was lower, followed by a greatly reduced and finer-grained influx of sediment deposited in Holocene time as a consequence of rising sea level.

The Concept of Lutum Transport

The initial premise upon which the present sediment transport model (Figure 40) is based is that since the modern time (3000 years B.P. to the present, when sea level is assumed to have been at about the same level it is today), and indeed since the beginning of Holocene time (12,500 years B.P.), the sediment influx to the margin has been primarily one of fine-grained silts and clays, or lutum. Lutum here refers to fine-grained sediment still in transport or suspension, as distinguished from lutite, which is fine-grained sediment that has been deposited. As opposed to the late Pleistocene, when great quantities of coarse sediment blanketed the margin and deep sea, very little modern sand reaches depths greater than 20-30 m. As this study has shown, Holocene (including modern) lutites are ubiquitous on the margin, but the thickest accumulations are found on the lower slope. These lutites are generally uniform in character with no visible grading, as are the sand-silt layers interbedded with them. These sand-silt layers were probably deposited by mass downslope gravity movements, such as slumping; it is also possible that they are winnowed deposits, or even the finer-grained tails of unrecognizable turbidites. However, the evidence precludes a turbidity current origin for much, if not all, of the Holocene deposits, and suggests instead that a process of large-scale lutum transport must be called for to account for the Holocene

and modern deposits. Such a process has been described by Moore (1970) to account for much of the basin-filling occurring on the southern California Borderland. A similar process is postulated to occur on the southern Oregon margin.

The Oceanographic Regime

In order to fully understand lutum transport on the southern Oregon margin, it is also necessary to understand the oceanographic regime in which it operates. The oceanographic factors play a major role in determining the routes of sediment transport and dispersal, and consequently the ultimate sites of deposition. Many of the oceanographic factors that are important to sediment transport vary seasonally and shift in direction in response to the changing wind patterns. Sea and swell and many of the currents on the margin change direction in this manner; therefore, it is important to distinguish between the oceanographic regime in the winter (Figure 41, left) and that which exists in the summer (Figure 41, right).

The Westwind Drift is a major ocean surface current which moves eastward across the North Pacific Ocean. As it approaches North America at a point about 500 km west of the continent near 45° N latitude it divides into two parts: one part of the Drift flows north and one part south as the California Current (Dodimead, Favorite, and Hirano, 1963). The Davidson Current flows northward as a subsurface

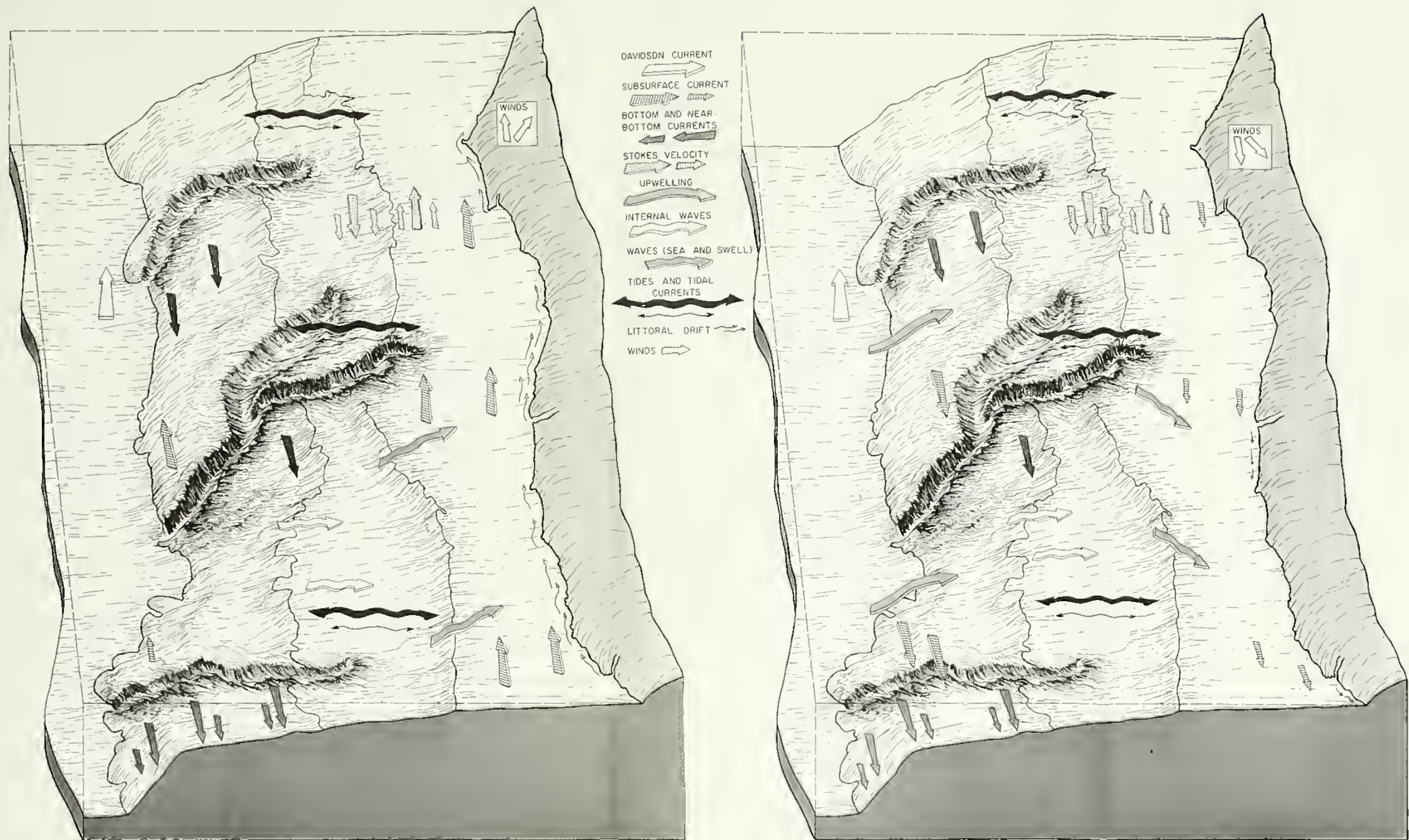


Figure 41. Schematic diagram of the major ocean currents on the southern Oregon margin. Left, represents winter conditions; right, summer conditions.

current on the coastal side of the California Current (Figure 41) and breaks through to the surface during the winter months (Sverdrup, et al., 1942); it has been reported as far north as 50° during January and February (Burt and Wyatt, 1964).

Stevenson, et al. (1969) report a subsurface current flowing about 70 km offshore from Oregon which has a southerly component of movement from the surface to 500 m during the entire year except for some slight northward movement during the winter months (Figure 41, left). They measured velocities averaging 5-10 cm/sec, but reported no velocities greater than 18 cm/sec below 50 m. Maughan (1963) measured velocities as great as 25.8 cm/sec at a depth of 10 m over the central Oregon continental slope. Collins (1967) measured northerly subsurface currents with velocities of 13 to 27 cm/sec on the central Oregon shelf at depths of 10, 20, and 60 m during the winter months (Figure 41, left), but reported a southerly movement at these same depths during the summer (Figure 41, right). However, throughout any year the net movement was to the north over the shelf.

Longuet-Higgins (1969a), in studying mass transport by time-varying ocean currents, determined that in regions of large bottom gradient the Stokes velocity factor (the difference between Eulerian mean velocity and Lagrangian mean velocity at a given point) may be an important consideration. He stated that the Stokes velocity may at times be opposite in direction to that of the surface wave propagation

direction, and hence the resulting mass transport may be opposite in direction to that expected from the wave propagation direction. He further reasoned (1969b) that such a situation may exist along the continental shelf-slope transition off Oregon, where a significant Stokes jet may give rise to a southerly mass transport along the upper slope with the flow being opposite to the wave-generated northerly mass transport over the shelf (Figure 41).

Upwelling has been noted to occur along the Oregon coast (Smith, 1964), and is particularly well developed off southern Oregon (Pattullo and Denner, 1965; Smith, et al., 1966). The upwelling is explained by the seasonal shift in wind direction off the Oregon coast. During the late spring and summer, the predominant winds are from the north-northwest and blow onshore to drive the surface water offshore. This surface water is then replaced by upwelling subsurface water (Figure 41). During the winter the winds and surface water movement reverses direction and the upwelling ceases. Neudeck (1970) has postulated that upwelling may be a significant factor in inhibiting the offshore and down-slope flow of bottom turbid layers.

The strongest winds occur off Oregon during the winter months, when severe storms produce high energy wind and wave conditions (Cooper, 1958; Kulm and Byrne, 1966). Neudeck (1970) has related the occurrence of greater amounts of more competent waves in winter to an increase in the maximum depth of rippling of bottom shelf sediment.

He has shown that rippling occurs roughly parallel to the coastline to maximum depths of about 200 m in winter and only 50-100 m in summer.

The seasonal shift in winds produces similar shifts in the pattern of waves and in the resulting littoral drift directions along the coast. During the winter months wave directions due to sea are from the south-southwest (Figure 41); however, the prevailing swell comes from the south-southwest a majority of the time only during January and February (Kulm and Byrne, 1966). During the summer, both sea and swell come from the north-northwest a majority of the time (Figure 41, right). Thus, it can be inferred that littoral drift along the Oregon coast is to the south during the summer and north during the winter (Figure 41). Quantitatively, the northerly drift in winter appears to be greater due to the larger sediment influx during this season and the higher energy waves available to move it. The existence of a net northward littoral drift over the Oregon shelf has been verified by textural studies (Gross and Nelson, 1966; Gross, et al., 1967) and heavy mineral patterns (Kulm, et al., 1968b; Chambers, 1968). The work of Collins, cited above, and Mooers, et al. (1968) also suggest that a net northward movement exists over the Oregon shelf during the year.

Tides along the Oregon coast are mixed semi-diurnal with a range of 6 to 10 feet (Pattullo and Burt, 1962). Mooers, et al. (1968) believe that the tidal influence accounts for a large percentage of the current

speeds measured on the Oregon shelf, and although these tidal current speeds average less than 10 cm/sec, they may cause turbulence or instability at the pycnocline due to shear. Tidal currents may be related to internal waves and internal tides which Mooers (1968) believes may be a contributing factor to subsurface turbulence at the shelf edge. Normal alternating tides and tidal currents may have a pronounced effect on the movement of suspended sediment within the water column and on the bottom sediment down as far as abyssal depths (Swift, 1969; Johnson and Belderson, 1969). However it is significant to note that Neudeck (1970) has considered these normal tides relatively un-important compared to the influence of surface waves, especially long-period swell, in forming ripples and in generating a turbid transport system on the Oregon shelf. Storm tides may affect the bottom; however, these are exceptions to the normally predicted tides.

Bottom photographic studies have been made by Neudeck (1970) on the Oregon margin to determine the extent of bottom current activity. He found indirect evidence of current directions (no current velocity measurements were made) in the trends of rippling, scouring, and in the movements of benthic organisms. On the upper slope off southern Oregon, Neudeck found indications of both a southwest-moving bottom current and scouring at a depth of 1000 m in two nearby stations within the swale to the north of the Upper Rogue Canyon (Kulm, 1969).

Korgen (1969) has actually measured near-bottom current velocities (but not directions) on the central Oregon slope. He recorded velocities at depths of 700-900 m which range from 8.4-17.4 cm/sec (at 75 cm above the bottom) to 9.6-45.0 cm/sec (at 300-350 cm above the bottom). At another station, at a depth of 1600 m, he recorded velocities of 0.4-12.9 cm/sec (at 150-200 cm above the bottom). Harlett (1970) has verified a southerly bottom current direction on the upper slope, but was unsuccessful in recording its velocity.

Neudeck has observed many areas of north-south trending bottom ripples on the southern Oregon shelf, which he has related to long-period swell. He also observed extensive areas of near-bottom turbid layers over the southern Oregon shelf and slope. His results show that: 1. in general the turbidity decreases with distance offshore, but increases sharply within 10 to 20 m off the bottom; 2. relatively turbid waters were observed on the upper slope in the swale north of the Upper Rogue Canyon, and in the Upper Canyon itself, while the water over submarine banks was relatively clear; 3. marked seasonal changes were evident in the turbidity of surface waters due to planktonic organisms, but the turbidity was usually higher during summer upwelling; 4. although near-bottom turbid layers were dense over the shelf during the entire year, bottom turbidity was more evident over the upper slope in winter when its generation by waves was greater and when the downslope movement of the bottom turbid layers was

unopposed by upwelling.

Based on all previous work it is evident that the predominant surface, subsurface, and bottom current direction, as well as the resultant net transport, is to the south on the upper slope, while the predominant current directions at all depths over the shelf are to the north (Figure 41). Normal tides superimpose an oscillatory east-west component of movement on this system, possibly at all depths, while upwelling superimposes a west-to-east, subsurface to surface transport during the summer.

Turbid Layer Formation and Transport Across the Shelf

The mechanism of lutum transport described by Moore (1970) calls for the downslope transport of fine-grained lutum as bottom or near-bottom low-density turbid layers. These turbid layers are often thin and relatively slow-moving, without sufficient erosive power to remove fine sand or the tests of Foraminifera into deeper water. Depending on topographic or other conditions, they may be channelized into thicker, faster flows, or may remain as un-channelized sheet flows.

In the initial formation of turbid layers mixed sand and mud of the southern Oregon rivers reaches the bays and estuaries. Much of the coarse material is separated from the lutum in the bay immediately seaward of the river mouth; part of the sand is restricted to channel

banks or tidal flats inside the bay (Kulm and Byrne, 1966), or subjected to alternating littoral drift and restricted to the beaches or the inner shelf shallower than 20-30 m (modern shelf sand, Figure 32). The lutum fraction is separated into a very fine-grained clay and colloidal suspensate (Figure 40) which often contains entrapped organic debris, and a silt, clayey silt, or silty clay fraction which eventually becomes the bottom turbid layer. The finest fraction (the suspensate) is carried slowly westward in suspension in the water column by alternating tidal currents, by-passing the shelf and upper slope and settling in the manner of hemipelagic sediments to deposit on the lower slope or adjacent deep sea (Figure 40).

Part of the lutum fraction may remain in the bay or estuary; however, most of it deposits over a wide area relatively near the river mouth (Modern Shelf Mud, Figure 32). This newly deposited lutum is subjected to re-suspension by long-period swell, and if the re-suspended cloud is of sufficient density, it will form a bottom or near-bottom turbid layer. Since long-period swell is most dominant during the winter when the sediment supply is greatest, turbid layers are most apt to form during this season. Long-period swell is a more effective agent for re-suspending the lutum than normal sea waves. It is mostly this former type of wave, with a period of 8-12 sec and frequently greater than 14 sec off Oregon (National Marine Consultants, 1961), that may attain sufficient bottom orbital velocity over all shelf depths

to erode fine sand and the finer-grained sediment. Inman (1957) has demonstrated that it is the long-period waves, of both sea and swell, which most often attain the critical orbital velocity of 10 cm/sec necessary to erode or ripple fine sand. Moore (1966) has also suggested that the long-period swell is the prime agent responsible for re-suspending lutum. Neudeck (1970) suggests that certain trends are evident when the frequency of long-period swell increases during the winter, among these is a corresponding increase in turbidity and turbid layer formation.

Sundborg (1956) calculated that a minimum velocity of 10 cm/sec is necessary to erode very fine sand ($62\ \mu$). Postma (1967) notes that the "critical erosion velocity" for fine-grained silt and clay varies according to its degree of consolidation (i.e., water content). For example, a freshly deposited medium silt ($30\ \mu$ diameter) containing 90% water would require a velocity of 15-20 cm/sec to initiate movement, whereas the same size sediment containing 50% water would require a velocity over 100 cm/sec. In each case, a somewhat lower velocity is required to maintain the sediment in suspension. Thus, it is only the long-period waves, mostly swell, which can provide the necessary velocity for re-suspending recently deposited lutum on the southern Oregon shelf.

Once the lutum is re-suspended into the water column as a near-bottom turbid cloud, it is subjected to the influence of coastal currents. A small part may move south over the shelf in the summer, but the

bulk of the material moves north in response to the net mass transport over the shelf (Figure 40). During the winter, when the sediment supply and coastal current velocities are greatest, the near-bottom turbid cloud more nearly approaches a very low-density current which moves northward under the action of coastal currents and westward across the relatively steep shelf under the action of gravity.

The bottom turbid current continues to move in this fashion until one of several events occurs. It may continue to move north until it impinges against a natural topographic barrier, such as a headland or a rock reef. Numerous resistant headlands, chains of sea stacks, and rock reefs, are present along the southern Oregon coast. Cape Blanco, Humbug Mountain, Cape Sebastian, and Cape Ferrelo are examples of the first, and the rock reefs off the southern end of Cape Blanco and off the Rogue River are examples of the last (Figure 2). These barriers may tend to constrict the northward flow and temporarily increase the density of the current, or they may disperse or divert the flow. In either of these cases, the action of alternating tides together with the shelf gradient will gradually move the turbid water outward to the shelf edge. In summer when the northward coastal currents are weak, or if the re-suspended turbid cloud is initially in a less-dense dispersed state, the westward component of movement may be stronger than the northern component. In this event, the turbid cloud will move as a sheet flow directly, but more slowly, westward across the shelf to the

shelf edge. Thus as a consequence of the various oceanographic conditions in both winter and summer, together with the influence of bottom topography, the bottom turbid layer may reach the shelf edge most often as a broad sheet-like cloud (Moore, 1966).

Transport Down the Slope

Upon reaching the edge of the shelf the turbid cloud is subjected to: 1. the increased gradient of the upper slope; 2. the influence of a predominantly southerly mass transport and a resulting component of southwesterly bottom currents; and 3. possible turbulence arising from internal waves, a factor which may keep the turbid layer stirred up enough to prevent deposition on the outer edge of the shelf. In addition, topographic features may be present which would tend to channel or divert the flow.

The submarine topography of the southern Oregon continental slope reveals many features which may serve as natural barriers or channelways to sediment movement (Figures 2, 4 and 5). The most obvious of these are the numerous east-west trending submarine valleys, especially the Rogue Canyon, Brookings Seavalley and Blanco Seavalley. These valleys serve to channel sediment from the upper to the lower slope. Another important valley is the unnamed swale to the north of the Upper Rogue Canyon; this swale trends northeast-southwest and probably feeds sediment into the Lower Rogue Canyon.

The topography of the southern end of Cape Blanco Bench (Figure 5) strongly suggests that a system of north-south channels is present which may also serve to channel sediment. Less obvious, but perhaps as important, is the character of the continental slope itself. The downslope gradient of the continental slope gives rise to normal downward gravity flow and slumping of sediment from the shelf edge to the upper slope, and from the upper to the lower slope.

The benches on the upper slope, which interrupt the steadily descending gradient of the continental slope, can be considered as relative "highs" because of their less steep gradient (approximately 1° - 2° versus an average of $3^{\circ}37'$). In effect, this may have several consequences depending on the direction and velocity of sediment-laden currents or water masses which may move over such "highs."

Downslope-moving bottom or near-bottom sediment loads tend to deposit coarser-grained particles on these benches upon reaching the abruptly decreased gradient. Any other slope currents would tend to flow faster over these "highs" than over the lower slope, since the "high," in effect, has constrained the current to a narrower space in the water column. From a topographic viewpoint, the benches, and much of the upper slope, may be regimes of coarse sediment from which the fine sediment is being continually removed or winnowed.

As the turbid bottom layer progresses down the slope it is often 5-10 m thick (Neudeck, 1970), and may become channelized by entering

sea valleys such as the Upper Rogue Canyon, the swale, or other valley systems (Figure 40). Neudeck has found high turbidity in both the swale and the Upper Rogue Canyon. In the swale, he also observed indications of southwest-trending bottom currents and scouring at the same station (970 m) where a significant amount of turbid water was observed. He postulates that the scouring and current activity were probably generated by the turbid, more dense, near-bottom waters flowing down the swale in response to gravity. This explains the relatively low Holocene sedimentation rate (9 cm/1000 years, Table 2) determined for the Upper Rogue Canyon, as well as the scouring observed in the swale to the north of the Canyon. One must assume that the velocity of the turbid layer increases down-canyon due to an increased thickness and density of the layer, and/or due to an increased gradient.

Moore (1970) suggests that the velocity of the turbid layer increases only slightly above 10 cm/sec in its transit, and this is not sufficient to transport shallow-water foraminiferal tests into deeper water. But Neudeck and others (Owens and Emery, 1967; Stanley and Kelling, 1968) suggest that the velocity of such turbid layers may increase enough to cause distinct scouring. It is evident that whatever the resultant velocity of the turbid layer may be, it is enough to prevent significant deposition of lutum in the upper reaches of the Rogue Canyon, and perhaps in the shoaler portions of other valleys. The

northward-flowing lutum may have sufficient velocity to by-pass the Canyon head and eventually divert into the swale to the north. In any case, large quantities of lutum do become funneled, or channelized, and eventually deposit on the lower slope. This process may be the most important mode of supply for the fine-grained sediment on the lower slope. When combined with the by-passed suspensate fraction, the two probably account for the total Holocene and modern lutite cover on the lower slope.

That portion of the bottom turbid layer which does not become channelized probably flows down the upper slope in a sheet-like manner. It has been established that the Holocene sediment cover on the upper slope is thin, and often patchy enough to reveal "windows" of older, late Pleistocene, relict sediment (Figure 32). This is true of the Upper Plateau Slope as well as the benches. Moore (1966) contends that once lutum has deposited, it forms a fairly stable mass and is not prone to failure by slumping. If this assumption is correct, then the slumping observed on the Upper Plateau Slope (Figures 21 and 22) is probably a Pleistocene phenomenon, due to the failure of great masses of sediment deposited there during lowered sea level. It is postulated that this process did occur, which left large areas of still older Pleistocene material exposed on the upper slope. The unchannelized flows of Holocene and modern lutum do not deposit at as high a rate as the channelized flows reaching the lower slope (10 cm/1000 years

versus 50 cm/1000 years); hence they have failed to cover the underlying Pleistocene material completely, leaving a patchy sediment distribution pattern. In addition, the increased gradient from the shelf edge to the Upper Plateau Slope and the possibility of a Stokes "jet" here may be sufficient to prevent deposition of all but the coarsest lutum fraction on the Upper Plateau Slope.

The greater portion of the un-channelized lutum reaches the less-steep bench areas on the upper slope, and is subjected to further diversion, mostly in a southerly direction. The channels on the Cape Blanco Bench may serve as routes of north-south transport for lutum from the Umpqua drainage. Whatever quantity does move south within these channels is fed into the swale to the north of the Rogue Canyon. Silver (1969a) has observed similar channels on the southern Klamath Plateau which empty into Trinidad Seavalley. He believes that they are routes of sediment transport into Gorda Basin. Although no such channels are evident on the Klamath Plateau off southern Oregon, the southerly mass transport over this region may sweep much of the lutum into Brookings Seavalley, which carries it to the lower slope. Core 6711-1, from Brookings Seavalley, shows the highest rates of deposition (60 cm/1000 years) of any core on the lower slope.

Although it appears that the abruptly decreased gradient from the Upper Plateau Slope to the benches on the upper slope would give rise to the deposition of much of the lutum, several facts contradict

this. First, the southerly mass transport mentioned previously may sweep the lutum into an available downslope valley; second, the sediment distribution pattern itself (Figure 32) shows that little Holocene or modern lutite is present on the benches; third, the near-bottom current velocities measured by Korgen (8.4 to 45.0 cm/sec at a depth of 700-900 m) indicate that the velocities are high enough on the upper slope to keep the bottom turbid layer in transit, or even to winnow any newly deposited lutum from the bench surface. Topographic highs, such as those at the western edge of the Klamath Plateau are another factor which affects turbid layer movement. These highs effectively dam any westward-flowing lutum, and give rise to a thicker ponded accumulation behind the high. Although this undoubtedly occurs, part of this accumulation may also be winnowed and diverted into downslope channels.

Deposition of Lutum on the Lower Slope

The distribution of Holocene and modern lutite on the lower slope and the computed Holocene sedimentation rates (50 cm/1000 years average, Table 2) attest to the fact that the lower slope receives the major portion of lutum generated from southern Oregon drainages. Lutum reaching the upper slope is either channelized directly and funneled onto the lower slope, or it may deposit on the upper slope for a brief period and later become re-suspended and channelized. In

either case, much of the lutum eventually funnels into the major distributary channels and accumulates on the lower slope.

Much of the lutum from the Upper Rogue Canyon and from the swale to the north feeds into the Lower Rogue Canyon. Sedimentation rates suggest that the Lower Rogue Canyon (core 6711-6, approximately 75 cm/1000 years), the swale (core 6708-38, 38 cm/1000 years), and Brookings Seavalley (core 6711-1, 60 cm/1000 years) are rapidly filling with lutum. Thus it is not unreasonable to assume that all the seavalleys on the lower slope, and the inter-valley areas as well, are also filling as rapidly. The entire lower slope is growing and outbuilding in this manner. Duncan (1968) has examined the Holocene sediment in Blanco Valley adjacent to the southern Oregon slope, and has calculated Holocene sedimentation rates ranging from 44 to 100 cm/1000 years in four cores from this area. The Holocene section in these cores suggests that a distinct bulge of Holocene sediment is building up at the base of the southern Oregon slope. Data presented here indicates that the lower slope is upbuilding in a similar manner.

Downslope gravitational processes, both within valleys and in intervalley areas, are the dominant mechanism for transport of lutum on the lower slope (Dott, 1963; Shepard, 1965; Moore, 1970). Although bottom currents are probably present in the lower slope valleys, none have been adequately measured. The newly-deposited lutum may be a stable mass, as Moore (1970) has suggested. However, the margin is

relatively active tectonically, and the lower slope possesses a fairly steep gradient (up to 8°); both of these facts suggest that considerable slumping may occur on the lower slope, such as that observed in Figure 21. This slumping is not as large-scale as that postulated to have occurred on the upper slope during the Pleistocene, but it still may be quantitatively important. Locally, the numerous small anticlines on the lower slope may serve as dams which give rise to a number of thickly ponded areas behind them. This is similar to the ponding noted on the upper slope, but on a smaller scale.

The mineralogy of the lower slope sediments indicates a greater influence from Tertiary rocks than do the sediments from other environments. Much of this may come from the Umpqua Mid-Coast Basins, especially from the Umpqua River. If this assumption is correct, and a similar turbid transport mechanism operates north of Cape Blanco, as Neudeck (1970) suggests, then some Umpqua sediments may be diverted to the south around Coquille Bank and onto the southern Oregon margin. Blanco Seavalley would be expected to collect much of this sediment and funnel it into the deep sea. However, no core has been taken in Blanco Seavalley to test this hypothesis, and Duncan's cores (1968) in the adjacent deep sea do not reflect this. However, it is significant to note that one core near the mouth of Blanco Seavalley (6604-12, Figure 25) exhibits the thickest Holocene section of any of Duncan's cores. Consequently, it is not unreasonable to suggest that

Blanco Seavalley contributes the major portion of this Holocene material in the form of lutum.

The Late Pleistocene and Holocene Sedimentation Patterns

The great influx of sediments during the Pleistocene originally covered much of the southern Oregon shelf, upper slope, and lower slope (Figure 42). The benches are primarily Pleistocene phenomena, having formed by the ponding of Pleistocene sediment behind anticlinal folds on the upper slope. The Upper Rogue Canyon, although structurally controlled, was primarily cut during the Pleistocene, as were the majority of channels and valleys. Evidence from glacial marine sediments in the adjacent deep sea (Griggs and Kulm, 1969) suggests that the paleo-oceanographic regime was essentially the same in the late Pleistocene as it is today. If the major winds and currents were essentially the same, then it is not unreasonable to assume that the paleo-oceanographic regime over the continental margin was also similar.

As a consequence of the rise of sea level during the Holocene, the deposition of coarse-grained material was greatly reduced. Even so, a uniform Holocene sedimentation rate of 50 cm/1000 years over the entire margin should have covered all the environments with a sediment cover approximately six meters thick since the start of Holocene time. However, the model of lutum transport just described

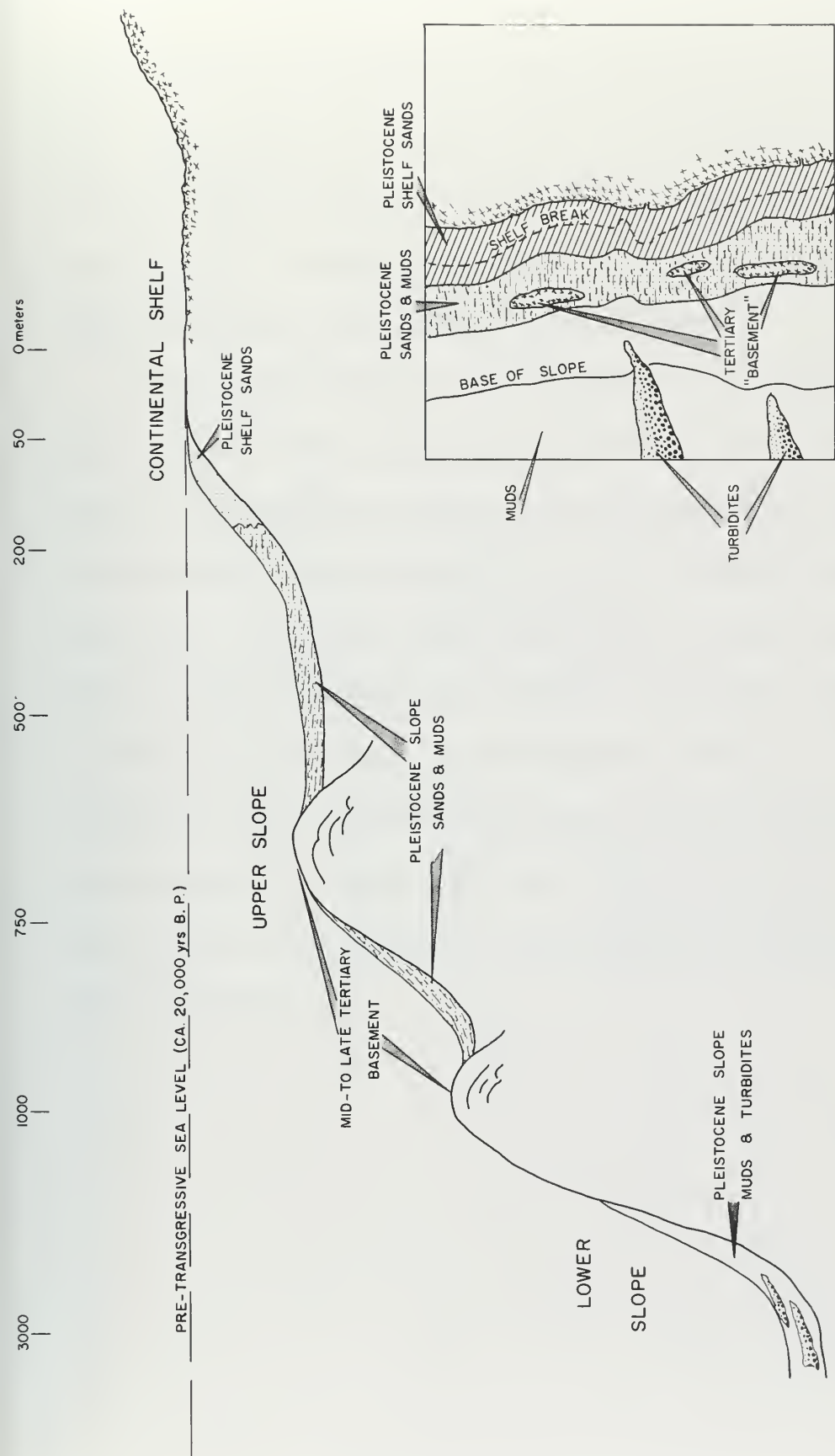


Figure 42. Idealized cross-section of the late Pleistocene sediment distribution on the southern Oregon margin. Inset map shows idealized areal distribution. Not to scale.

has shown that such a uniform sediment distribution does not exist. A thin Holocene cover, averaging only about 3-4 m thick, is present on the upper slope, benches, and in the Upper Rogue Canyon, and a much thicker cover, probably averaging 10 meters exists over the lower slope, especially in the seavalleys (Figure 43).

Pleistocene sediments were laid down over a longer time period, and at a higher rate, than Holocene sediments. Hence the Pleistocene section is probably more widespread and thicker than the present Holocene cover, perhaps as thick as several hundred meters or more (Figure 43). The uneven deposition of lutum during the Holocene has left large areas of Pleistocene sediment still exposed on the surface of the shelf and upper slope. This sediment is now relict, being out of equilibrium with the present environment. Even though Holocene and modern lutum now dominate the lower slope, the total thickness of these deposits is not great, and would probably be penetrated frequently below 10 meters.

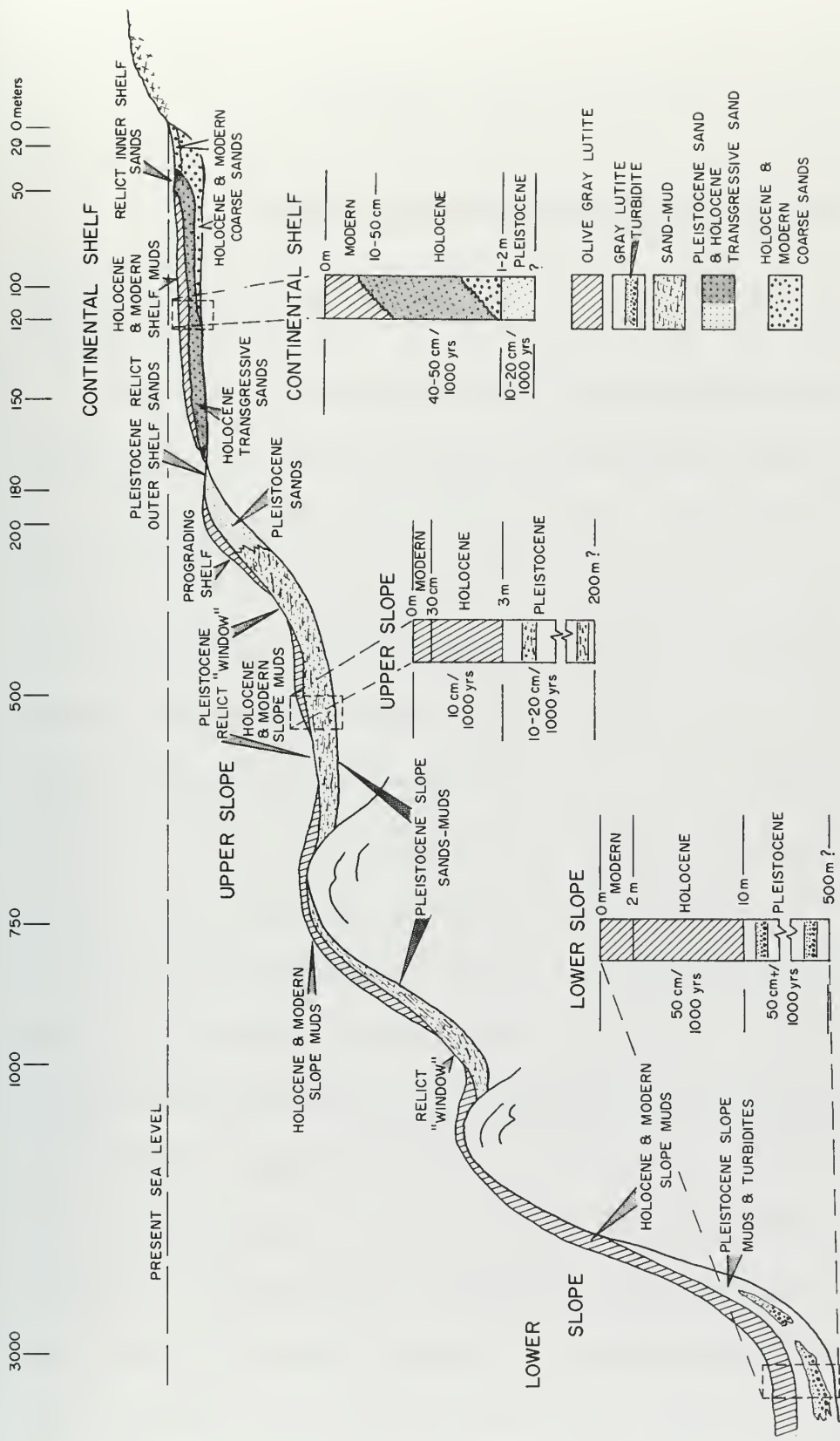


Figure 43. Idealized cross-section of the Holocene and modern sediment distribution on the southern Oregon margin. Not to scale. See Figure 32 for areal distribution.

SUMMARY AND CONCLUSIONS

Development of the Structural Framework

Pre-Tertiary History

The present structural pattern of the southern Oregon continental margin is the end result of several large-scale orogenic events which have occurred mostly since Mesozoic time. Southwestern Oregon and northern California lie at the westernmost edge of the Cordilleran mobile belt. This belt extends to the continental margin in these areas and has been generally eugeosynclinal throughout most of the Paleozoic and Mesozoic to late Cenozoic time (Dott, 1965). Initially, during Paleozoic and much of Mesozoic time, the area over what is now the present margin received thousands of feet of sediment, which formed graywackes and associated volcanics. During the Nevadan orogeny of late Jurassic and the later Mesozoic orogenies the area reached a peak of metamorphism and plutonism and the geosynclinal sediments, such as the Dothan, Rogue and Galice formations, were uplifted, intruded, and metamorphosed to form the present Klamath Mountains. A distinctive arcuate low-angle thrust pattern was developed in these mountains (Irwin, 1966) which remained intact despite the further warping that took place at the end of Mesozoic time. Marine sedimentation continued into Cretaceous time, but by the Late Cretaceous volcanism

had ceased and the deposition of the more mature non-turbidite sand and mud ensued (Dott, 1965). Irwin (1966) has called these rocks the superjacent sequence. The complex Mesozoic strata which probably extend westward to form the underlying basement of the present southern Oregon and northern California margins is believed to be the result of the underflow of oceanic mantle beneath the earlier margin of the continent (Hamilton, 1969; Silver, 1969a).

Tertiary History

Early in the Tertiary, probably beginning during Eocene time, the sea transgressed to the northwestern edge of the Klamath Mountains. This was followed by the deposition of mud and sand and was accompanied by minor volcanism. Deposition continued throughout the Eocene and Oligocene and resulted in the formation of many rhythmically-bedded units, including turbidites such as those found in the Tyee Formation. The source for this material was the pre-Tertiary complex of the Klamath Mountains; these mountains no doubt supplied all of the sediments during the Tertiary.

Rocks dredged from the continental shelf and slope indicate that the Tertiary strata extend westward under the southern Oregon margin and lie between the older Mesozoic basement and the younger Quaternary sediments. They may be exposed, or only thinly covered by overlying sediments, atop several of the anticlinal folds which mark

the western edge of benches on the upper slope. The older Tertiary strata, however, may be deeply buried beneath the southern Oregon margin since the rocks recovered from that part of the margin are all Pliocene in age, and no rocks older than middle Miocene have been recovered from the Oregon margin to date (Kulm and Fowler, 1970).

The rocks recovered from the southern Oregon margin have a lower percentage of unstable constituents than the overlying sediments and fall into two groups. The first group consist of coarse-grained impure sandstones, mostly arkosic and lithic wacke, from the shelf and upper slope. The composition of these sandstones is similar to the pre-Tertiary complex of Klamath Mountains, particularly the Upper Cretaceous Series and the Dothan Formation, which suggests that the source for the late Tertiary upper slope rocks was either the Jurassic or Late Cretaceous strata of the Klamath Mountains. The second group consists of fine-grained siltstones and mudstones from the lower slope, some of which are calcareous. They have a higher percentage of unstable constituents than the upper slope sediments and rocks and their composition reflects the influence of the early Tertiary strata of the southern Oregon Coast Range as well as that of the Klamath Mountains.

Minor uplifting and folding began early in the Tertiary, and although it continues on the margin and in coastal areas today, it reached its peak during mid- and late Tertiary time (Mio-Pliocene)

with the onset of the Cascadan orogeny and the beginning of formation of the southern Oregon Coast Ranges. A marked change in the structure and in the pattern of coastal faults occurred during the mid- to late Tertiary orogeny. Intense high-angle, north-south shears developed in the Klamath Mountains and Coast Ranges, probably as a result of a major shift in the direction of movement of the Pacific plate in relation to the North American plate (i. e. a change in the direction of sea-floor spreading). The direction of spreading shifted from a primarily west-to-east direction to one that was primarily northwest-southeast; Atwater and Menard (1970) have documented this shift as beginning as early as 55 million years ago (Eocene time). Silver (1969a) has calculated that the present relative motions between the Gorda and North American plates is still in a northwest-southeast direction. The intense shears developed on the continent, such as the Gold Beach Shear Zone (Dott, 1962), superimposed a north-south pattern upon the arcuate low-angle thrusts of the Klamath Mountains. Coastal rocks became increasingly fragmented by this intense faulting. The Franciscan complex of California was structurally juxtaposed against the Klamath Mountains by shearing within the California Coast Ranges.

A renewed episode of sea-floor spreading and underthrusting began in late Tertiary time, perhaps as late as Plio-Pleistocene (Silver, 1969a). This resulted in compression against the continent from the west and probably produced the north-south pattern of folds

on the southern Oregon and northern California margins. The high-angle normal faults which cut the margin strata developed simultaneously, or shortly thereafter during the latest Pliocene and early Pleistocene.

Evidence suggests that the continental crust of the western United States and the adjacent oceanic crust have been undergoing tension and extension since early in the Cenozoic (Hamilton, 1969). However, it has been postulated that both underthrusting, producing compressional features, and extension of the crust, producing high-angle normal gravity faults, can co-exist over an oceanic-island arc complex (Malahoff, 1970) or a continental margin-oceanic complex (Silver, 1969a). This explanation would appear to fit the structural patterns observed on the southern Oregon margin.

Byrne, et al. (1966) calculated that significant uplift of late Tertiary sediments (as much as 1000 m) occurred along the seaward portion of the central Oregon continental margin, and they suggested that appreciable accretion to the continent has taken place during, and since, the Pliocene. This evidence is in agreement with Silver's hypothesis of underthrusting along the northern California and southwestern Oregon margins. Continued tectonic and structural mobility is evidenced on the southern Oregon margin by the rocks which have been recovered from it. From 80 to 300 m of uplift, and up to 225 m

of downwarp, are indicated from paleo-depth determinations using the Pliocene fauna in these rocks.

Quaternary History of Sedimentation

Pleistocene

Although tectonic activity has continued on the margin since the end of the Tertiary period to the present time, the history of the Quaternary period on the southern Oregon margin is characterized by a record of extensive deposition, changing regimes of sedimentation, and sedimentary out-building and up-building. The glacial and interglacial stages in the Pleistocene were accompanied by retreats and advances of the sea, the latter are recorded in the elevated marine terraces along the southern Oregon coast. At no time could the sea level have been 500 m above its present level, which is the elevation of the highest terrace level along the southern Oregon coast. Faunal studies and radiometric dating indicate a rate of uplift of 2 m/1000 years has accompanied the formation of the terraces.

Sea level was lowered about 120-130 m below its present level during the last stage of glaciation in the late Pleistocene, and vast quantities of coarse clastics were deposited on the outer continental shelf and slope. Reflection profiles indicate numerous truncated structures. One or more unconformities exist beneath the southern

Oregon shelf and at the shelf edge. These unconformities, particularly the one at the edge of the shelf, are probably Plio-Pleistocene (Bales and Kulm, 1969). The wedge of sediment which unconformably overlies the truncated shelf edge was probably deposited during the last major regression associated with the Wisconsin glaciation, and suggests that the shelf began prograding at that time.

The coarse-grained sediments deposited on the margin during the late Pleistocene continued to reflect a Klamath Mountain source; this source probably still provided the greatest amount of sediment to the margin. The development of the marginal plateau physiography began in the Pleistocene when large quantities of coarse sediment began filling in synclinal basins and down-faulted structures on the upper slope. The Upper Rogue Canyon began forming as a channel which was cut along the trace of the older east-west fault at the shelf edge. Many of the lower slope valleys also developed during this time.

Turbidity current deposition was prevalent during the Pleistocene and many of the sand-silt layers which dominate the Pleistocene section were probably laid down in this manner. Lesser amounts of mud (which is now found as gray lutite) accompanied the sand-silt deposition. Slumping of large sediment masses occurred during the late Pleistocene, especially along what is now the Upper Plateau Slope. Pleistocene sediments accumulated at about six times the rate of Holocene sediments, and may reach thicknesses of 100-200 m or more on the upper

continental slope and several hundred meters or more on the lower continental slope.

Holocene and Modern

The rise of sea level during the Holocene, probably began about 15,000 years B.P. and may have been interrupted by several minor regressions. The submerged terrace levels identified on the southern Oregon shelf may reflect these periods of regression. Coarse-clastic deposition on the outer margin ceased about 7,000 years B.P., as much of it was trapped in newly-formed bays and estuaries. As a result, the regime of sedimentation changed to one that was mainly characterized by the transport and deposition of fine-grained silts and clays by bottom turbid layers and a fine-particle suspensate (i. e. lutum transport). This process produced the large quantities of olive gray lutite now found on the margin.

The changes in Radiolaria/planktonic Foraminifera abundance which mark late Pleistocene-Holocene boundary and other stratigraphic horizons in deep-sea are also evident on the margin. Although all the faunally-determined horizons within the late Pleistocene and Holocene are probably present in margin sediments, only two late Pleistocene horizons and one Holocene horizon were identified. The latter, the 5000-4000 years B.P. horizon, was the only one useful in correlation.

Volcanic ash from the eruption of Mt. Mazama (6600 years B.P.)

is present in several cores from both the shelf and slope off southern Oregon; its occurrence suggests that the margin was an area of accumulation for the ash prior to its eventual deposition on the deep sea (Nelson, et al., 1968). The Mazama ash is a distinct stratigraphic horizon in margin sediments and has been used for correlating upper slope and shelf cores.

The abundance of blue-green hornblende and other minerals indicative of metamorphic sources, together with an abundance of chlorite in the clay fraction, indicate that the Klamath Mountains are still the dominant source of sediments on the margin. However, the mineralogy of Holocene sediments on the lower slope suggest that this environment is receiving sediments from the Tertiary strata of the southern Oregon Coast Range to a greater extent than other margin environments. Lower slope sediments have a relatively high feldspar content and exhibit a higher pyroxene to amphibole ratio than the other environments.

This latter trend is significant, since finer-grained lower slope sediments normally should exhibit low P/A ratios because of the tendency for amphiboles to be found in the finer sediment sizes. Hence a source other than the Klamath Mountains must be supplying pyroxene to the lower slope in sufficient quantities to effect a noticeable change in the P/A ratio. In addition to these trends, the only sample in which the percent illite exceeded chlorite was that from a lower

slope core (6711-6-8).

The Columbia River, because of its large runoff, would normally be thought of as a sediment contributor to the southern margin; however, the mineralogy of lower slope sediments more strongly suggests that nearby Tertiary strata of the southern Coast Ranges are the more probable secondary source, and that since Holocene time Columbia River sediments have not reached far enough south to affect either the southern margin, or the adjacent deep sea (Duncan, 1968).

Organic carbon preserved in margin sediments averages 1.3%, with lower slope sediments containing higher values than sediments from other environments. The percent organic carbon increases upwards in margin cores, but only gradually; this fact may not reflect an abrupt decrease in margin sedimentation from late Pleistocene to Holocene time similar to that observed in the deep sea by Duncan (1968).

Sedimentation rates obtained from margin cores suggest that the lower slope is accumulating sediment, mostly of the olive gray lutite type, at an average rate four to five times faster than the upper slope environment (50 cm/1000 years versus 10 cm/1000 years). The resulting Holocene cover is unevenly distributed: an average of 3 m on the upper slope versus 10 m on the lower slope. As additional evidence, the transport processes which have operated during the Holocene have given rise to a patchy Holocene cover on the surface of the upper slope and benches, where large areas of relict Pleistocene (?) sediments

are still exposed which have not been covered by later Holocene or modern deposits.

Oceanographic conditions existing today indicate that the net transport over the southern Oregon shelf is to the north and that over the upper slope and much of the lower slope is to the south. In addition, documented seasonal changes in the river runoff and oceanographic conditions together with a knowledge of bottom topography suggest the formation and net transport of lutum by bottom turbid layers can be traced adequately throughout the margin.

A model of modern lutum transport by bottom turbid layers and fine-particle suspensate is proposed for the southern Oregon margin. Bottom turbid layers are formed on the southern Oregon shelf and move north and west under the influence of shelf currents and long-period swell. The turbid layers are funnelled into submarine valleys and transported to the lower slope. Lutum deposited on the upper slope is eventually winnowed by southerly bottom currents and fed to available downslope valleys and very little remains on the upper slope. Slumping and other gravitational processes contributes additional lutite deposits to the lower slope. The end result of modern lutum transport is the continual up-building and out-building of the lower slope.

BIBLIOGRAPHY

- Addicott, W. O. 1964. Late Pleistocene invertebrate fauna from southwestern Oregon. *Journal of Paleontology* 38:650-661.
- Armstrong, J. E., D. R. Crandell, D. J. Easterbrook and J. Noble. 1965. Late Pleistocene stratigraphy and chronology in southwestern British Columbia and northwestern Washington. *Geological Society of America, Bulletin* 76:321-330.
- Arrhenius, G. 1952. Sediment cores from the east Pacific. *Swedish Deep-Sea Expedition Reports, 1947-1948*, 5:1-227.
- Atwater, T. and H. W. Menard. 1970. Magnetic lineations in the northeast Pacific. *Earth and Planetary Science Letters* 7:445-451.
- Bailey, E. H. and R. E. Stevens. 1960. Selective staining of K-feldspar and plagioclase on rock slabs and thin sections. *American Mineralogist* 45:1020-1025.
- Bailey, E. H., W. P. Irwin, and D. L. Jones. 1964. Franciscan and related rocks and their significance in the geology of western California. *California Division of Mines and Geology, Bulletin* 184, 177 p.
- Baldwin, E. M. 1945. Some revisions of the Late Cenozoic stratigraphy of the southern Oregon coast. *Journal of Geology* 52:32-46.
- Baldwin, E. M. 1964. *Geology of Oregon*. 2d ed. Eugene, Oregon, University of Oregon Cooperative Book Store. 165 p.
- Bales, W. E. 1969. Research Associate. Oregon State University, Department of Oceanography. Personal communication. Corvallis, Oregon.
- Bales, W. E. and L. D. Kulm. 1969. Structure of the continental shelf off southern Oregon. (Abstract). *American Association of Petroleum Geologists, Bulletin* 53:471-472.

- Bandy, O. L. 1960. The geologic significance of coiling ratios in the foraminifer Globigerina pachyderma (Ehrenberg). *Journal of Paleontology* 34:671-681.
- Biscaye, P. E. 1964. Distinction between kaolinite and chlorite in Recent sediments by X-ray diffraction. *American Mineralogist* 49:1281-1289.
- Biscaye, P. E. 1965. Mineralogy and sedimentation of Recent deep-sea clay in the Atlantic Ocean and adjacent seas and oceans. *Geological Society of America, Bulletin* 74:803-832.
- Bolt, B. A., C. Lomnitz, and T. V. McEvilly. 1968. Seismological evidence on the tectonics of central and northern California and the Mendocino escarpment. *Seismological Society of America, Bulletin* 58:1725-1767.
- Burt, W. V. and B. Wyatt. 1964. Drift bottle observations of the Davidson Current off Oregon. In: *Studies on oceanography, a collection of papers dedicated to Kaji Hidaka*. Seattle, University of Washington Press. p. 156-165.
- Byrne, J. V. 1962. Geomorphology of the continental terrace off the central coast of Oregon. *Ore Bin* 24:65-74.
- Byrne, J. V. 1963a. Geomorphology of the continental terrace off the northern coast of Oregon. *Ore Bin* 25:201-209.
- Byrne, J. V. 1963b. Geomorphology of the Oregon continental terrace south of Coos Bay. *Ore Bin* 25:149-157.
- Byrne, J. V., G. A. Fowler and N. J. Maloney. 1966. Uplift of the continental margin and possible continental accretion off Oregon. *Science* 154:1654-1656.
- Carlson, P. R. 1968. Marine geology of Astoria Submarine Canyon. Ph.D. thesis. Corvallis, Oregon State University. 259 numb. leaves.
- Chambers, D. M. 1968. Holocene sedimentation and potential placer deposits on the continental shelf off the Rogue River, Oregon. Master's thesis. Corvallis, Oregon State University. 102 numb. leaves.

- Chambers, D. M. and L. D. Kulm. 1969. Holocene sedimentation on a narrow continental shelf. (Abstract) 1968 Annual Meeting, Geological Society of America, Mexico City, In: Abstracts for Geological Society of America, Special Paper No. 121, p. 51.
- Christensen, M. N. 1966. Quaternary of the California coast ranges. California Division of Mines and Geology, Bulletin 190: 305-313.
- Clifton, H. E. 1968. Gold distribution in surface sediments on the continental shelf off southern Oregon: a preliminary report. Washington, D. C. 6 p. (U. S. Geological Survey Circular No. 587).
- Collins, C. A. 1967. Description of measurements of current velocity and temperature over the Oregon continental shelf, July 1965-February 1966. Ph.D. thesis. Corvallis, Oregon State University. 154 numb. leaves.
- Cooper, W. S. 1958. Coastal dunes of Oregon and Washington. New York. 169 p. (Geological Society of America, Memoir 72).
- Couch, R. 1970. Assistant Professor. Oregon State University, Department of Oceanography. Personal communication. Corvallis, Oregon.
- Curray, J. R. 1964. Transgressions and regressions. In: Papers in Marine Geology (Shepard Commemorative volume) p. 175-201. ed. by R. L. Miller. New York, Macmillan Company.
- Curray, J. R. 1966. Geologic structure of the continental margin, from subbottom profiles, northern and central California. California Division of Mines and Geology, Bulletin 190:337-342.
- Dehlinger, P. 1969. Evidence regarding the development of Juna de Fuca and Gorda Ridges in the northeast Pacific Ocean. Transactions of the New York Academy of Sciences, series II, v. 31:379-403.
- Dehlinger, P., R. W. Couch and M. Gemperle. 1967. Gravity and structure of the eastern part of the Mendocino escarpment. Journal of Geophysical Research 72:1233-1247.
- Dehlinger, P., R. W. Couch and M. Gemperle. 1968. Continental and oceanic structure from the Oregon coast westward across the Juan de Fuca Ridge. Canadian Journal of Earth Sciences 5:1079-1090.

- Dehlinger, P., R. W. Couch, D. A. McManus and M. Gemperle. 1970. Oceanic structures: northern California to British Columbia. In: *The Sea*, vol. 4 (In press).
- Dietz, R. S. 1963. Wave base, marine profile of equilibrium, and wave-built terraces: a critical appraisal. *Geological Society of America, Bulletin* 74:971-990.
- Diller, J. S. 1902. Topographic development of the Klamath Mountains. Washington, D. C. 69 p. (U. S. Geological Survey Bulletin No. 196).
- Dodimead, A. J., F. Favorite and T. Hirano, 1963. Salmon of the North Pacific Ocean. Part II. Review of oceanography of the Subarctic Pacific region. *International North Pacific Fisheries Commission, Bulletin* 13:1-195.
- Dott, R. H., Jr. 1962. Geology of the Cape Blanco area, southwest Oregon. *Ore Bin* 24:121-133.
- Dott, R. H., Jr. 1963. Dynamics of subaqueous gravity depositional processes. *American Association of Petroleum Geologists, Bulletin* 47:104-128.
- Dott, R. H., Jr. 1964. Ancient deltaic sedimentation in eugeo-synclinal belts. In: *Developments in Sedimentology - Deltaic and Shallow Marine Deposits*. Amsterdam, Elsevier Publishing Company. p. 105-113.
- Dott, R. H., Jr. 1965. Mesozoic-Cenozoic tectonic history of the southwest Oregon coast in relation to Cordilleran orogenesis. *Journal of Geophysical Research* 70:4687-4708.
- Drake, E. T. 1969. An evaluation based on a comparison of X-ray diffraction mounting techniques of the reliability of some reported clay mineral data. Unpublished research. Oregon State University, Corvallis, Oregon. 13 p.
- Duncan, J. R., Jr. 1968. Late Pleistocene and postglacial sedimentation and stratigraphy of deep-sea environments off Oregon. Ph.D. thesis. Corvallis, Oregon State University. 222 numb. leaves.
- Duncan, J. R., Jr., L. D. Kulm and G. B. Griggs. 1970. Clay mineral composition of Late Pleistocene and Holocene sediments of Cascadia Basin, northeastern Pacific Ocean. *Journal of Geology* 78:213-221.

- Eittreim, S., M. Ewing, and E. M. Thorndike. 1969. Suspended matter along the continental margin of the North American Basin. *Deep-Sea Research* 16:613-624.
- Emery, K. O. 1938. Rapid method of mechanical analysis of sand. *Journal of Sedimentary Petrology* 8:105-111.
- Emery, K. O. 1965. Geology of the continental margin off eastern United States. In: *Submarine Geology and Geophysics*, ed. by W. F. Whittard and R. Bradshaw. London, Butterworths, p. 1-20.
- Emery, K. O. 1968. Relict sediments on continental shelves of the world. *American Association of Petroleum Geologists, Bulletin* 52:445-464.
- Emilia, D. A., J. W. Berg and W. E. Bales. 1968. Magnetic anomalies off the northwest coast of the United States. *Geological Society of America, Bulletin* 79:1053-1062.
- Emiliani, C. 1966. Paleotemperature analysis of Caribbean cores P6304-8 and P6304-9 and a generalized temperature curve for the past 425,000 years. *Journal of Geology* 74:109-124.
- Ericson, D. B. 1959. Coiling directions of Globigerina pachyderma as a climatic index. *Science* 130:219-220.
- Ericson, D. B., M. Ewing, G. Wollin and B. C. Heezen. 1961. Atlantic deep-sea sediment cores. *Geological Society of America, Bulletin* 72:193-286.
- Ewing, M. and E. M. Thorndike. 1965. Suspended matter in deep-ocean water. *Science* 147:1291-1294.
- Fowler, G. A. 1970. Assistant Professor. Unpublished research. Oregon State University, Corvallis, Oregon.
- Fowler, G. A. and L. D. Kulm. 1966. A multiple corer. *Limnology and Oceanography* 11:630-633.
- Geological Society of America. 1963. Rock color chart. New York. 6 p.
- Gorsline, D. S. and K. O. Emery. 1959. Turbidity current deposition in San Pedro and Santa Monica Basins off southern California. *Geological Society of America, Bulletin* 70:279-290.

- Griggs, A. B. 1945. Chromite bearing sands of the southern part of the coast of Oregon. Washington, D. C. p. 113-150 (U. S. Geological Survey Bulletin 945-E).
- Griggs, G. B. 1969. Cascadia Channel: the anatomy of a deep-sea channel. Ph.D. thesis. Corvallis, Oregon State University, 183 numb. leaves.
- Griggs, G. B. and L. D. Kulm. 1969. Glacial marine sediments from the northeast Pacific. *Journal of Sedimentary Petrology* 39:1142-1148.
- Griggs, G. B., L. D. Kulm, J. R. Duncan, and G. A. Fowler. 1970. Holocene faunal stratigraphy and paleoclimatic implications of deep-sea sediments in Cascadia Basin. *Paleogeography, Paleoclimatology, Paleoecology* 7:5-12.
- Gross, M. G. and J. L. Nelson. 1966. Sediment movement on the continental shelf near Washington and Oregon. *Science* 154: 879-881.
- Gross, M. G., D. A. McManus and Hsin-Li Ling. 1967. Continental shelf sediment, northwestern United States. *Journal of Sedimentary Petrology* 37:790-795.
- Gross, M. G., A. G. Carey, Jr., G. A. Fowler and L. D. Kulm. 1970. Distribution of organic carbon in surface sediments, northwest Pacific Ocean. (In press)
- Hagenstein, W. D., et al. 1966. Sixth biennial report. Salem, Oregon, State Water Resources Board. 50 p.
- Hamilton, W. 1969. Mesozoic California and the underflow of Pacific mantle. *Geological Society of America, Bulletin* 80:2409-2430.
- Hanna, G. D. 1952. Geology of the continental slope off central California. *California Academy of Sciences, Proceedings*, 4th series, 27:325-358.
- Harlett, J. C. 1969. An investigation of the character of the Late Pleistocene and Holocene clays off southern Oregon. Unpublished term paper. Department of Oceanography, Oregon State University, Corvallis, 20 p.

- Harlett, J. C. 1970. Unpublished research. Department of Oceanography, Oregon State University, Corvallis.
- Heath, G. R. 1968. Mineralogy of Cenozoic deep-sea sediments from the equatorial Pacific Ocean. Ph.D. thesis. Scripps Institution of Oceanography, University of California, San Diego. 186 numb. leaves.
- Heath, G. R. 1969. Assistant Professor. Oregon State University, Department of Oceanography. Personal communication. Corvallis, Oregon.
- Heezen, B. C., M. Tharp and M. Ewing. 1959. The floors of the oceans, I. The North Atlantic. Geological Society of America, Special Paper No. 65, 122 p.
- Heezen, B. C., C. Hollister and W. F. Ruddiman. 1966. Shaping of the continental rise by deep geostrophic contour currents. *Science* 152:502-508.
- Highsmith, R. M., Jr., 1962. Water. In: Atlas of the Pacific Northwest resources and development, ed. by R. M. Highsmith, Jr. 3d ed. Corvallis, Oregon State University Press. p. 38-42.
- Holmes, A. 1965. Principles of Physical Geology. Rev. ed. New York, Ronald Press. 1288 pp.
- Ingle, J. C., Jr., 1967. Foraminiferal biofacies variation and the Miocene-Pliocene boundary in southern California. *Science reports, new series, Geology*. Tohoku University, Japan.
- Inman, D. L. 1952. Measures for describing the size distribution of sediments. *Journal of Sedimentary Petrology* 22:125-145.
- Inman, D. L. 1957. Wave-generated ripples in nearshore sands. Department of the Army, Beach Erosion Board. 66 p. (Corps of Engineers, Technical Memorandum No. 100; Scripps Institution of Oceanography New Series No. 947)
- Irwin, W. P. 1966. Geology of the Klamath Mountains province. California Division of Mines and Geology, Bulletin 190:19-38.
- Isacks, B., J. E. Oliver and L. R. Sykes. 1968. Seismology and the new global tectonics. *Journal of Geophysical Research* 73:5855-5899.

- Janda, R. J. 1969. Age and correlation of marine terraces near Cape Blanco, Oregon. (Abstract) Program of the 65th Annual Meeting, Cordilleran Section, Geological Society of America, Eugene, Oregon.
- Johnson, M. A. and Belderson, R. H. 1969. The tidal origin of some vertical sedimentary changes in epicontinental sea. *Journal of Geology* 77:353-357.
- Knebel, H. J., J. C. Kelly and J. T. Whetten. 1968. Clay minerals of the Columbia River: A qualitative, quantitative, and statistical evaluation. *Journal of Sedimentary Petrology* 38:600-611.
- Korgen, B. J. 1969. Temperature and velocity fields near the deep ocean floor west of Oregon. Ph.D. thesis. Oregon State University, Corvallis, Oregon. 166 numb. leaves.
- Krumbein, W. C. and F. J. Pettijohn. 1938. *Manual of Sedimentary Petrography*. New York, D. Appleton-Century. 549 p.
- Kulm, L. D. 1969. (Compiler) Study of the continental margin off the state of Oregon. Technical report 1 February 1968 through 31 January 1969. 134 numb. leaves. (Oregon State University. Department of Oceanography. Reference 69-1. U. S. Geological Survey Office of Marine Geology and Hydrology Contract No. 14-08-0001-10766).
- Kulm, L. D. and W. E. Bales. 1969. Shallow structure and sedimentation on the upper continental slope off southern and central Oregon: a preliminary investigation. (Abstract) *American Association of Petroleum Geologists, Bulletin* 53:472.
- Kulm, L. D. and J. V. Byrne. 1966. Sedimentary response to hydrography in an Oregon estuary. *Marine Geology* 4:85-118.
- Kulm, L. D. and G. A. Fowler (Compilers). 1970. Study of the continental margin off the state of Oregon. Technical Report 1 February 1969 to 31 January 1970. 43 numb. leaves. (Oregon State University. Department of Oceanography. Reference 70-2. U. S. Geological Survey technical report no. 4 on U. S. Geological Survey Office of Marine Geology and Hydrology Contract No. 14-08-001-11941).
- Kulm, L. D., D. F. Heinrichs, R. M. Buehrig, and D. M. Chambers. 1968a. Evidence for possible placer accumulations on the southern Oregon continental shelf. *Ore Bin* 30:81-104.

- Kulm, L. D., K. F. Scheidegger, J. V. Byrne and J. J. Spigai. 1968b. A preliminary investigation of the heavy mineral suites of the coastal rivers and beaches of Oregon and northern California. *Ore Bin* 30:165-181.
- Lane, R. K. 1965. Climate and heat exchange in the oceanic region adjacent to Oregon. Ph.D. thesis. Corvallis, Oregon State University. 115 numb. leaves.
- Le Pichon, X. 1968. Sea floor spreading and continental drift. *Journal of Geophysical Research* 73:3661-3698.
- Lockett, J. B. 1965. Some indications of sediment transport and diffusion in the vicinity of the Columbia estuary and entrance, Oregon and Washington. Presented before the International Association for Hydraulic Research. Portland, U. S. Army Engineer Division, North Pacific. 7 numb. leaves.
- Longuet-Higgins, M. S. 1969a. On the transport of mass by time-varying ocean currents. *Deep-Sea Research* 16:431-447.
- Longuet-Higgins, M. S. 1969b. Professor. Oregon State University. Department of Oceanography. Personal communication. Corvallis, Oregon.
- Mackay, A. J. 1969. Continuous seismic profiling investigations of the southern Oregon continental shelf between Coos Bay and Cape Blanco. Master's thesis. Corvallis, Oregon State University. 118 numb. leaves.
- Malahoff, A. 1970. Some possible mechanisms for gravity and thrust faults under oceanic trenches. *Journal of Geophysical Research* 75:1992-2001.
- Maloney, N. J. 1965. Geology of the continental terrace off the central coast of Oregon. Ph.D. thesis. Corvallis, Oregon State University. 233 numb. leaves.
- Maughan, P. M. 1963. Observations and analysis of ocean currents above 250 meters off the Oregon coast. Master's thesis. Corvallis, Oregon State University. 49 numb. leaves.
- McKenzie, D. P. and W. J. Morgan. 1969. Evolution of triple junctions. *Nature* 224:125-133.

- McManus, D. A. 1964. Major bathymetric features near the coast of Oregon, Washington and Vancouver Island. *Northwest Science* 38:65-82.
- McManus, D. A. 1965. Blanco Fracture Zone, Northeast Pacific Ocean. *Marine Geology* 3:429-455.
- McManus, D. A. 1967. Physiography of Cobb and Gorda Rises, northeast Pacific Ocean. *Geological Society of America, Bulletin* 78:527-546.
- Meade, B. K. and Small, J. B. 1966. Current and recent movement on the San Andreas Fault. *California Division of Mines and Geology, Bulletin* 190:385-391.
- Menard, H. W. and T. Atwater. 1968. Changes in direction of sea floor spreading. *Nature* 219:463-467.
- Menard, H. W. and T. Atwater. 1969. Origin of fracture zone topography. *Nature* 222:1037-1040.
- Mesecar, R. S. 1968. Oceanic vertical temperature measurements across the water-sediment interface at selected stations west of Oregon. Ph.D. thesis. Corvallis, Oregon State University. 99 numb. leaves.
- Milliman, J. D. and K. O. Emery. 1968. Sea levels during the past 35,000 years. *Science* 162:1121-1123.
- Mooers, C. N. K. 1968. The interaction of an internal tide with the frontal zone in a coastal upwelling region. Ph.D. thesis. Corvallis, Oregon State University. 480 numb. leaves.
- Mooers, C. N. K., and R. L. Smith. 1968. Continental shelf waves off Oregon. *Journal of Geophysical Research* 73:549-557.
- Moore, D. G. 1966. Structure, litho-orogenic units, and post-orogenic basin fill by reflection profiling: California Continental Borderland. Ph.D. thesis. University of Groningen, Netherlands. 151 p.
- Moore, D. G. 1970. Reflection profiling studies of the California Continental Borderland structure and Quaternary turbidite basins. *Geological Society of America, Special paper* 107. 142 p.

- National Marine Consultants, Inc. 1961. Wave statistics for three deep water stations along the Oregon-Washington coast. Santa Barbara, California. 17 numb. leaves. (Prepared for U. S. Army Engineers District, Portland, Oregon).
- Nayudu, Y. R. 1964. Carbonate deposits and paleoclimatic implications in the northeast Pacific Ocean. *Science* 146:515-517.
- Nelson, C. H. 1968. Marine geology of Astoria deep sea fan. Ph.D. thesis. Corvallis, Oregon State University. 287 numb. leaves.
- Nelson, C. H., L. D. Kulm, P. R. Carlson and J. R. Duncan. 1968. Mazema Ash in the northeastern Pacific. *Science* 161:47-49.
- Neudeck, R. H. 1970. Photographic investigation of sediment transport mechanics on the Oregon continental margin. Master's thesis. Corvallis, Oregon State University. (In preparation)
- Ogle, B. A. 1953. Geology of Eel River Valley area, Humboldt County, California. California Division Mines, Bulletin 164. 128 p.
- Owen, D. M. and K. O. Emery. 1967. Current markings on the continental slope. In: Deep-sea Photography, ed. by J. B. Hersey, Johns Hopkins Oceanographic Studies No. 3:167-172.
- Page, B. M. 1966. Geology of the Coast Ranges of California. California Division of Mines and Geology, Bulletin 190:255-276.
- Pattullo, J. G. and W. V. Burt. 1962. The Pacific Ocean. In: Atlas of the Pacific Northwest resources and development, ed. by R. M. Highsmith, Jr. 3d ed. Corvallis, Oregon State University Press. p. 93-95.
- Pattullo, J. G. and W. Denner. 1965. Processes affecting sea water characteristics along the Oregon coast. *Limnology and Oceanography* 10:443-450.
- Peck, D. L., A. B. Griggs, H. G. Schlicker, F. G. Wells, and H. M. Dole. 1964. Geology of the central and northern parts of the western Cascade Range in Oregon. U. S. Geological Survey, Professional paper 449, 56 p.
- Peterson, R. E. 1969. Calcium carbonate, organic carbon, and quartz in hemipalagic sediments off Oregon: a preliminary investigation. Master's thesis. Corvallis, Oregon State University. 44 numb. leaves.

- Poole, D. M. 1957. Size analysis of sand by a sedimentation technique. *Journal of Sedimentary Petrology* 27:460-468.
- Postma, H. 1967. Sediment transport and sedimentation in the estuarine environment. In: *Estuaries*, ed. by G. H. Lauf. Washington, D. C., p. 158-179. (American Association for the Advancement of Science. Publication 83).
- Raff, A. D. 1966. Boundaries of an area of very long magnetic anomalies in the northeast Pacific. *Journal of Geophysical Research* 71:2631-2636.
- Raff, A. D. and R. G. Mason. 1961. A magnetic survey off the west coast of North America, 40°N to 52 1/2°N. *Geological Society of America, Bulletin* 72:1259-1265.
- Reed, R. D. 1933. *Geology of California*. Tulsa, Oklahoma, American Association of Petroleum Geologists, 355 p.
- Richards, H. G. and D. L. Thurber. 1966. Pleistocene age determinations from California and Oregon. *Science* 152:1091-1092.
- Roush, R. C. 1970. Sediment textures and internal structures: a comparison between central Oregon continental shelf sediments and adjacent coastal sediments. Master's thesis. Corvallis, Oregon State University. 75 numb. leaves.
- Rusnak, G. A. 1966. The continental margin of northern and central California. *California Division of Mines and Geology, Bulletin* 190:325-335.
- Russell, K. L. 1967. Clay mineral origin and distribution on Astoria Fan. Master's thesis. Corvallis, Oregon State University. 47 numb. leaves.
- Shepard, F. P. 1954. Nomenclature based on sand-silt-clay ratios. *Journal of Sedimentary Petrology* 24:5;-158.
- Shepard, F. P. 1963. *Submarine Geology*. 2d ed. New York, Harper and Row. 557 p.
- Shepard, F. P. 1965. Importance of submarine valleys in funneling sediments to the deep sea. In: *Progress in Oceanography*, v. 3:321-332.

- Shepard, F. P., R. F. Dill and V. von Rad. 1969. Physiography and sedimentary processes of La Jolla submarine fan and fan valley. American Association of Petroleum Geologists, Bulletin 53:390-420.
- Shor, G. G., Jr., P. Dehlinger, H. K. Kirk and W. S. French. 1968. Seismic refraction studies off Oregon and northern California. Journal of Geophysical Research 73:2175-2194.
- Silver, E. A. 1969a. Structure of the continental margin off northern California, north of the Gorda escarpment. Ph.D. thesis. San Diego, California, Scripps Institution of Oceanography. 123 numb. leaves.
- Silver, E. A. 1969b. Late Cenozoic underthrusting of the continental margin off northernmost California. Science 166:1265-1266.
- Smith, R. L. 1964. An investigation of upwelling along the Oregon coast. Ph.D. thesis. Corvallis, Oregon State University. 83 numb. leaves.
- Smith, R. L. 1968. Upwelling. In: Oceanography and Marine Biology Annual Review. ed. by H. Barnes, v. 6:11-46. New York, Hafner Publishing Co.
- Smith, R. L., J. G. Pattullo and R. K. Lane. 1966. An investigation of the early stage of upwelling along the Oregon coast. Journal of Geophysical Research 71:1135-1140.
- Spigai, J. J. and L. D. Kulm. 1969. Patterns of Holocene sedimentation on the continental slope off southern Oregon. (Abstract) 1969 Annual Meeting of the Geological Society of America, Atlantic City, N. J., In: Abstracts for 1969 Geological Society of America Meeting, part 7, p. 212.
- Stanley, D. J. (ed.). 1969. The new concepts of continental margin sedimentation; application to the geologic record. American Geological Institute Short Course Lecture Notes, Philadelphia, 7-9 November 1969. Washington, D. C., American Geological Institute. 254 numb. pages.
- Stanley, D. J. and G. Kelling. 1968. Photographic investigation of sediment texture, bottom current activity and benthonic organisms in the Wilmington Submarine Canyon. U. S. Coast Guard, Oceanography Report 22, 95 p.

- Stevenson, M. R., J. G. Pattullo and B. Wyatt. 1969. Subsurface currents off the Oregon coast as measured by parachute drogues. *Deep-Sea Research* 16:449-461.
- Sundborg, A. 1956. The river Klaralven, a study of fluvial processes. *Geografiske Annalav* 38:127-316.
- Sverdrup, H. U., M. W. Johnson and R. H. Fleming. 1942. *The Oceans: their Physics, Chemistry and General Biology*. New York, Prentice Hall 1087 p.
- Swift, D. J. P. 1969. Outer shelf sedimentation: processes and products. In: *The new concepts of continental margin sedimentation; application to the geological record*. ed. by D. J. Stanley. American Geological Institute Short Course Lecture Notes, Philadelphia, 7-9 November 1969. Washington, D. C., American Geological Institute. p. DS-5-1 to DS-5-26.
- Taliaferro, N. L. 1943. Franciscan-Knoxville problem. *American Association of Petroleum Geologists, Bulletin* 27:109-219.
- Tobin, D. G. and L. R. Sykes. 1968. Seismicity and tectonics of the northeast Pacific Ocean. *Journal of Geophysical Research* 73: 3821-3845.
- Uchupi, E. and K. O. Emery. 1963. The continental slope between San Francisco, California and Cedros Island, Mexico. *Deep Sea Research* 10:397-447.
- U. S. Coast and Geodetic Survey. 1968. Umpqua River to Cape Ferrelo. U. S. Coast & Geodetic Survey bathymetric map 1308N-17. 1 sheet.
- U. S. Geological Survey. Water Resources Division. 1964. Surface water records of California 1:1-498.
- U. S. Geological Survey. Water Resources Division. 1966. Surface water records of Oregon 1:1-355.
- van Andel, T. H. 1964. Recent marine sediments of the Gulf of California. In: *Marine geology of the Gulf of California*, ed. by T. H. van Andel, and G. C. Shor, Jr., Tulsa, Oklahoma, p. 216-310. (American Association of Petroleum Geologists, Memoir No. 3).

- Vernon, J. W. 1966. Shelf sediment transport system. Ph.D. thesis. Los Angeles, University of Southern California. 135 numb. leaves.
- Vine, F. J. 1966. Spreading of the ocean floor: new evidence. *Science* 154:1405-1415.
- Vine, F. J. and J. T. Wilson. 1965. Magnetic anomalies over a young oceanic ridge off Vancouver Island. *Science* 150:485-489.
- Wells, D. L. and F. G. Peck. 1961. Geological map of Oregon west of the 121st meridian. U. S. Geological Survey, Miscellaneous Geological Investigation Map I-325.
- Williams, H., F. J. Turner and C. J. Gilbert. 1954. Petrography; an Introduction to the Study of Rocks in Thin Sections. San Francisco, Freeman. 406 p.
- Wilson, J. T. 1965a. Transform faults, oceanic ridges, and magnetic anomalies southwest of Vancouver Island. *Science* 150:482-485.
- Wilson, J. T. 1965b. A new class of faults and their bearing on continental drift. *Nature* 207:343-347.

LEGEND FOR APPENDICES

Sediment Age	H Holocene
	LP Late Pleistocene
Sediment Type	OGI Olive Gray Lutite
	GL Gray Lutite
	S-S Sand-Silt Layers
Physiographic Province	SH Continental Shelf
	US Upper Continental Slope
	CBB Cape Blanco Bench
	KP Klamath Plateau
	LS Lower Continental Slope
	URC Upper Rogue Canyon
	LRC Lower Rogue Canyon
	MB Middle Bench
	LB Lower Bench
	UPS Upper Plateau Slope
	LPS Lower Plateau Slope
	URCW Upper Rogue Canyon Wall

"T" denotes less than one percent (trace).

APPENDIX 1. PISTON CORE AND ROCK DREDGE STATION LOCATIONS

OSU Station number	Latitude (north)	Longitude (west)	Water depth (meters)	Physiographic province	Length of core (cm)
PISTON CORE STATIONS					
6706-1	42°05.5'	124°56.0'	1183	US	430
6706-2	42°09.6'	124°56.2'	1060	MB	390
6706-3	42°14.5'	124°47.8'	544	KP	377
6706-4	42°31.5'	124°52.0'	1060	URC	150
6706-5	42°31.3'	124°45.7'	540	URC	273
6706-6	42°31.0'	124°45.0'	420	URCW(US)	355
6706-7	42°32.2'	124°39.0'	150	URC(SH)	465
6706-8	42°49.4'	124°48.6'	316	CBB	375
6708-20	42°26.4'	124°42.5'	118	SH	110
6708-23	42°21.6'	124°33.3'	100	SH	243
6708-25	42°17.1'	124°35.0'	165	SH	610
6708-33	42°29.8'	124°38.6'	104	SH	65
6708-37	42°30.4'	124°50.3'	769	URC	583
6708-38	42°35.2'	124°50.4'	988	LS	472
6708-39	42°42.1'	124°50.0'	658	CBB	427
6708-40	42°45.8'	124°45.5'	443	CBB	152
6708-42	42°41.9'	124°37.3'	121	SH	455
6708-43	42°35.9'	124°41.0'	148	SH	50
6711-1	42°03.8'	125°06.9'	2012	LS	408
6711-2	42°07.3'	124°58.7'	1365	LS	430
6711-5	42°25.3'	124°56.9'	1770	LS	516
6711-6	42°29.8'	125°04.8'	1776	LRC(LS)	340
6711-8	42°36.6'	125°01.5'	1390	LS	560
ROCK DREDGE STATIONS					
6708-22	42°23.2'	124°40.3'	125-130	SH	---
	42°24.2'	124°40.1'			
6708-36	42°30.5'	124°43.2'	250-330	URCW(US)	---
	42°29.7'	124°43.4'			
6708-41	42°44.0'	124°40.0'	110-150	SH	---
	42°44.7'	124°40.8'			
6711-D1	42°04.2'	125°03.5'	1450-1200	LS-MB	---
	42°04.5'	124°59.7'			
6711-D2	42°03.9'	124°49.3'	730-640	LPS-KP	---
	42°03.9'	124°48.7'			
6711-D3	42°08.1'	124°57.8'	1000-1200	MB	---
	42°09.0'	124°56.8'			
6802-D1	42°17.5'	124°48.5'	550-450	KP-UPS	---
	42°17.5'	124°45.0'			
6802-D2	42°43.0'	124°50.8'	460-550	CBB	---
	42°43.4'	124°49.6'			
6802-D3	42°27.3'	124°55.6'	1100	LS	---
	42°29.1'	124°54.7'			
6802-D4	42°36.8'	125°01.4'	1100	LS	---
	42°37.7'	125°00.0'			

APPENDIX 2. RADIOCARBON AGE DETERMINATIONS FROM SELECTED CORES^a

Sample Number ^b	Depth of core (meters)	Depth of interval sampled (cm) ^c	C ¹⁴ age (years B. P.) ^d
6706-2	1060	300-350 (325)	23,900 ± 650
6706-3	544	325-375 (350)	34,300 ± 3500
6708-37	769	250-283 (267)	29,950 ± 2250
6708-42	121	434-454 (444)	22,100 ± 500
6711-2	1365	108-126 (117)	6,340 ± 140
6708-44	150	whole core	5,860 ± 150
6802-BCB	150	whole core	9,920 ± 170

^aAll analyses made by Isotopes, Inc., Westwood, New Jersey.

^bAll samples are from piston cores, except 6708-44 and 6802-BCB which are box core samples.

^cNumber in parentheses indicates the mid-point of the sampled interval where the radiocarbon age datum level has been centered.

^dAll analyses are based on total carbon except for box cores 6708-44 and 6802-BCB which were based on calcium carbonate carbon and mollusk shells in these samples.

APPENDIX 3. COARSE-FRACTION COMPOSITION OF SEDIMENT SAMPLES

Sample number	Depth in core (cm)	Age	Sediment Type	Percent of coarse fraction by number				Total grains counted	Detrital grains	Mica	Volcanic glass	Plant fibers	Radiolarians	Diatoms	Planktonic foraminifera	Benthic foraminifera	Fecal pellets	Glauconite
				% sand	% silt	% clay												
6706-1-1-phl ^a	0	H	O	--	--	--		334	66	9	1	3	6	1	--	9	2	3
6706-1-1	5	H	OGL	5	68	27		370	61	7	2	1	6	2	--	12	6	7
6706-1-2	11	H	S-S	55	29	16		302	74	4	2	1	5	1	--	7	4	1
6706-1-3	60	H	OGL	9	51	41		311	66	5	5	2	4	2	--	8	6	3
6706-1-4	105	H	OGL	2	55	43		298	70	7	4	2	6	3	--	5	4	2
6706-1-5	150	H	OGL	3	48	49		307	52	10	1	3	15	4	2	8	2	2
6706-1-6	205	H	OGL	2	26	72		300	60	5	3	2	13	2	2	5	3	1
6706-1-7	255	H	OGL	2	28	70		290	74	4	1	1	10	1	1	4	1	2
6706-1-8	305	H	OGL	2	59	40		304	71	5	2	1	11	3	1	3	2	3
6706-1-9	352	LP	GL	30	22	48		391	68	8	--	4	11	2	--	3	3	2
6706-1-10	410	LP	GL	15	21	64		329	73	9	--	1	14	1	--	5	2	1
6706-1-11	430	LP	GL	2	98	0		344	64	11	--	2	11	2	--	6	3	1
6706-1-12	430+ ^b	LP	GL	1	31	67		392	65	5	1	--	7	1	2	3	4	12
6706-2-1-phl	0	LP	OGL	--	--	--		322	14	1	1	1	8	2	32	36	T	6
6706-2-1	5	LP	OGL	29	43	28		380	18	3	T	1	4	1	42	21	T	9
6706-2-2	50	LP	OGL	3	67	30		350	45	5	--	2	37	4	--	1	1	5
6706-2-3	115	LP	OGL	6	49	45		356	58	4	--	3	24	2	--	6	1	2
6706-2-4	155	LP	OGL	4	39	56		352	53	6	2	2	19	3	--	4	10	1
6706-2-5	190	LP	OGL	4	35	62		322	52	6	1	3	11	2	--	9	14	2
6706-2-6	198	LP	OGL	--	--	--		396	59	10	1	2	11	4	--	12	1	2
6706-2-7	205	LP	OGL	6	49	45		391	55	6	T	3	8	3	15	8	2	T
6706-2-8	224	LP	S-S	100	0	0		353	79	13	T	1	1	1	2	1	1	T
6706-2-9	250	LP	OGL	22	46	32		333	51	5	--	--	4	T	16	20	3	--

APPENDIX 3. (Continued)

Sample number	Depth in core (cm)	Age	Sediment Type	Percent of coarse fraction by number										Total grains counted	Detrital grains	Mica	Volcanic glass	Plant fibers	Radiolarians	Diatoms	Planktonic foraminifera	Benthic foraminifera	Fecal pellets	Glauconite
				% sand	% silt	% clay																		
6706-2-10	254	LP	OGL	19	42	38	305	34	7	--	2	2	1	1	1	31	8	14						
6706-2-11	283	LP	S-S	--	--	--	310	66	7	--	2	1	1	11	6	5	1							
6706-2-12	302	LP	OGL	4	55	41	469	48	5	--	2	2	T	35	3	4	1							
6706-2-13	315	LP	OGL	6	51	43	438	14	9	--	3	2	T	48	23	1	--							
6706-2-14	321	LP	OGL	16	49	35	458	43	5	--	3	2	--	25	9	8	6							
6706-2-15	335	LP	OGL	16	49	35	325	56	6	--	3	2	1	25	9	5	1							
6706-2-16	360	LP	OGL	4	49	46	309	34	3	--	--	4	--	46	13	1	--							
6706-2-17	375	LP	OGL	3	43	54	419	49	6	--	2	5	1	24	12	1	1							
6706-2-18	390	LP	GL	5	51	43	312	47	10	--	--	11	1	13	10	7	1							
6706-2-19	390+	LP	GL	5	50	46	320	36	6	--	--	5	1	31	19	1	1							
6706-3-1	5	LP	GL	15	46	39	305	49	5	3	3	1	3	3	11	--	25							
6706-3-2	55	LP	GL	7	56	37	311	66	12	--	1	5	1	--	5	2	8							
6706-3-3	105	LP	GL	2	86	12	347	46	13	13	1	5	--	--	11	--	11							
6706-3-5	155	LP	GL	4	57	39	292	52	14	11	3	5	2	--	3	--	13							
6706-3-6	205	LP	GL	5	49	46	284	62	10	--	4	6	2	--	4	2	9							
6706-3-7	255	LP	GL	6	51	43	305	56	13	5	3	4	1	--	7	--	11							
6706-3-8	305	LP	GL	6	56	38	317	68	12	1	2	5	1	--	1	T	10							
6706-3-9	355	LP	GL	7	52	41	358	52	12	5	3	5	--	2	11	1	9							
6706-3-10	377	LT	GL	11	51	38	307	70	9	1	T	3	--	T	11	1	4							
6706-3-11	377+	LT	GL	21	45	34	309	86	7	--	--	--	--	--	--	7	1							
6706-4-1-phl	0	H	OGL	4	50	47	293	60	11	2	7	1	2	--	2	7	8							
6706-4-2	65	H	OGL	5	41	55	299	63	9	4	6	1	1	--	2	7	7							
6706-4-3	97	H	OGL	3	53	45	416	60	16	--	13	2	1	T	5	2	1							

APPENDIX 3. (Continued)

Sample number	Depth in core (cm)	Age	Sediment Type	Percent of coarse fraction by number				Total grains counted	Detrital grains	Mica	Volcanic glass	Plant fibers	Radiolarians	Diatoms	Planktonic foraminifera	Benthic foraminifera	Fecal pellets	Glauconite
				% sand	% silt	% clay												
6706-5-17	273	LP	OGL	12	41	48		237	71	3	--	1	1	2	--	2	3	18
6706-5-18	273+	LP	OGL	9	51	40		234	77	4	2	--	3	1	1	3	2	9
6706-6-1	5	H	OGL	44	41	15		404	78	5	3	2	2	1	--	1	0	9
6706-6-2	20	H	OGL	6	61	32		327	42	2	24	14	5	2sp	2	5	2	2
6706-6-3	50	H	OGL	6	61	33		288	45	7	40	6	2	--	sp	--	1	1
6706-6-4	65	H	OGL	2	69	29		264	55	1	24	8	2	3sp	3	2	2	2
6706-6-5	83	H	OGL	3	71	26		354	57	6	14	3	5	1	--	6	5	4
6706-6-6	103	H	OGL	15	57	28		346	69	7	9	6	2	1	1	2	1	3
6706-6-7	127	H	S-S	100	0	0		314	65	7	8	6	2	5sp	--	2	2	2
6706-6-8	155	H	OGL	5	58	37		306	70	3	5	10	2	1	1	4	1	3
6706-6-9	193	H	OGL	12	50	38		313	64	8	5	1	1	2	--	5	3	2
6706-6-10	201	H	S-S	100	0	0		355	79	7	4	4	2	--	--	3	1	1
6706-6-11	255	H	OGL	7	56	37		316	66	8	5	8	2	2	T	5	1	T
6706-6-12	288	H	OGL	8	68	25		351	67	5	6	7	5	3	--	3	2	2
6706-6-13	323	H	OGL	14	46	40		291	61	3	3	8	14	5	1	3	1	2
6706-6-14	355	H	OGL	10	54	35		258	63	4	2	10	7	3	5	4	--	1
6706-6-15	355+	H	OGL	9	56	34		314	62	5	2	6	9	4	T	6	4	2
6706-7-1	5	LP	S-S	67	18	14		356	77	2	13	2	--	--	--	--	2	3
6706-7-2	45	LP	S-S	45	17	38		355	76	2	17	1	--	--	--	--	1	2
6706-7-3	75	LP	S-S	63	22	15		389	82	2	11	1	--	--	--	--	--	4

APPENDIX 3. (Continued)

Sample number	Depth in core (cm)	Age	Sediment Type	Percent of coarse fraction by number			Total grains counted	Percent of coarse fraction by number																	
				% sand	% silt	% clay		Detrital grains	Mica	Volcanic glass	Plant fibers	Radiolarians	Diatoms	Planktonic foraminifera	Benthic foraminifera	Fecal pellets	Glauconite								
6706-7-4	125	LP	S-S	65	20	15	312	77	3	16	1	--	--	--	--	--	--	--	--	--	--	--	--	1	1
6706-7-6	200	LP	S-S	72	16	12	340	74	2	19	2	--	--	--	--	--	--	--	--	--	--	--	--	2	2
6706-7-8	253	LP	S-S	65	19	17	317	73	2	20	3	T	--	--	--	--	--	--	--	--	--	--	1	1	1
6706-7-10	290	LP	S-S	64	25	11	328	87	3	5	1	--	--	--	--	--	--	--	--	--	--	--	T	4	4
6706-7-11	320	LP	S-S	65	23	13	368	78	1	12	3	--	--	1	--	--	--	--	--	--	--	--	--	5	5
6706-7-13	390	LP	S-S	67	20	13	329	74	4	14	2	T	--	--	--	--	--	--	--	--	--	--	--	5	5
6706-7-14	415	LP	S-S	66	25	9	424	78	3	14	1	--	--	--	--	--	--	--	--	--	--	--	--	4	4
6706-7-15	450	LP	S-S	68	22	10	363	71	5	19	2	--	--	--	--	--	--	--	--	--	--	--	--	3	3
6706-7-16	465	LP	S-S	56	28	16	318	80	3	14	1	--	--	--	--	--	--	--	--	--	--	--	--	2	2
6706-8-1-phl	0	LP	S-S	84	8	8	325	82	5	--	T	--	--	--	--	--	--	--	--	--	--	--	--	13	13
6706-8-2	40	LP	S-S	63	17	20	257	79	6	--	5	--	--	--	--	--	--	--	--	--	--	--	2	8	8
6706-8-3	100	LP	S-S	90	8	2	310	82	7	--	2	2	--	--	--	--	--	--	--	--	--	2	2	4	4
6706-8-4	255	LP	OGL	18	52	30	304	76	7	--	2	2	1	--	--	--	--	--	--	--	--	4	4	5 ^{py}	5 ^{py}
6706-8-5	360	LP	OGL	36	34	31	329	74	6	--	5	2	1	--	--	--	--	--	--	--	--	4	5	4	4
6706-8-6	375	LP	OGL	17	45	38	351	57	12	--	14	3	1	1	--	--	--	--	--	--	--	5	3	3	3
6708-23A	6	H	S-S	52	36	72	333	82	10	--	7	--	--	--	--	--	--	--	--	--	--	T	--	2	2
6708-23B	52	H	S-S	43	42	15	388	72	10	7	6	--	--	--	--	--	--	--	--	--	--	2	1	2	2
6708-23C	77	H	S-S	49	39	12	325	74	7	11	4	--	--	--	--	--	--	--	--	--	--	1	1	2	2
6708-23D	100	H	S-S	53	35	12	301	65	4	22	5	--	--	--	--	--	--	--	--	--	--	T	2	2	2
6708-23E	126	H	S-S	44	42	14	328	64	4	23	4	--	--	--	--	--	--	--	--	--	--	1	1	2	2
6708-23F	170	H	S-S	36	49	15	339	53	4	33	6	--	--	--	--	--	--	--	--	--	--	T	2	2	2
6708-23G	202	H	S-S	54	35	11	336	54	6	28	5	--	--	--	--	--	--	--	--	--	--	1	4 ^{sh frg}	2	161
6708-23H	207	H	S-S	53	37	11	361	59	3	28	4	--	--	--	--	--	--	--	--	--	--	T	3	2	2

APPENDIX 3. (Continued)

Sample number	Depth in core (cm)	Age	Sediment Type	% sand	% silt	% clay	Total grains counted	Percent of coarse fraction by number									
								Detrital grains	Mica	Volcanic glass	Plant fibers	Radiolarians	Diatoms	Planktonic foraminifera	Benthic foraminifera	Fecal pellets	Clauconite
6708-23I	215	H	S-S	20	63	17	306	53	4	37	2	--	--	--	1	2	1
6708-23J	243	H	S-S	19	66	14	309	26	2	69	1	--	--	--	T	2	1
6708-25-1	5	H	OGL	2	70	28	248	63	8	2	11	2	1	--	4	5	6
6708-25-2	80	H	OGL	9	59	33	330	64	10	3	12	T	T	--	3	4	2
6708-25-3	155	H	OGL	4	55	41	315	62	12	6	7	3	1	--	5	1	3
6708-25-4	230	H	OGL	6	69	25	305	56	9	10	13	4	1	--	4	2	2
6708-25-5	289	H	OGL	13	68	20	292	63	8	10	8	7	2	--	2	1	2
6708-25-6	325	H	OGL	3	59	38	356	35	9	39	10	5	--	--	1	1	1
6708-25-7	355	H	OGL	4	65	31	341	51	14	7	11	5	4sp-	--	6	2	1
6708-25-8	400	H	OGL	10	82	9	308	59	11	5	8	4	4	--	6	3	1
6708-25-9	423	H	OGL	5	59	35	334	64	8	3	8	6	2	--	4	5	1
6708-25-10	443	H	OGL	7	56	37	332	65	8	3	7	6	1	--	3	4	2
6708-25-11	463	H	OGL	9	48	43	342	68	13	4	5	5	2	--	2	1	1
6708-25-12	483	H	OGL	17	47	36	327	66	11	4	1	6	2	--	4	5	1
6708-25-13	505	H	OGL	11	30	60	288	59	18	2	7	7	1	--	2	1	1
6708-25-14	525	H	OGL	16	47	37	299	64	16	1	6	6	1	--	2	2	1
6708-25-15	545	H	OGL	18	36	46	266	66	14	2	7	5	T	--	2	4	1
6708-25-16	583	H	OGL	17	41	42	308	68	13	1	9	6	T	--	2	2	--
6708-25-17	610	H	OGL	18	27	56	282	68	7	1	12	6	1	--	2	1	1
6708-33A	3	LP	S-S	82	12	06	301	96	3	--	--	1	--	--	1	--	--
6708-33B	23	LP	S-S	78	15	07	284	91	4	T	1	1	--	--	1	--	1
6708-33C	43	LP	S-S	91	2	7	280	97	2	--	T	1	--	--	T	--	--

Sample number	Depth in core (cm)	Age	Sediment Type	Percent of coarse fraction by number			Total grains counted	Percent of coarse fraction by number										
				% sand	% silt	% clay		Detrital grains	Mica	Volcanic glass	Plant fibers	Radiolarians	Diatoms	Planktonic foraminifera	Benthic foraminifera	Fecal pellets	Clauconite	
6708-33D	63	LP	S-S	82	11	7	287	98	1	--	--	--	--	--	--	T	--	--
6708-37-1	15	LP	OGL	2	60	38	290	66	10	--	7	8	4	4	--	1	2	4
6708-37-2	105	LP	OGL	3	59	39	336	69	10	--	4	8	4	4	--	--	1	4
6708-37-3	205	LP	OGL	4	62	35	348	71	12	--	4	6	3	3	--	--	T	3
6708-37-4	310	LP	OGL	3	62	36	279	79	8	--	6	3	2	2	--	--	T	2
6708-37-5	405	LP	GL	2	61	38	254	75	13	--	5	4	1	1	--	--	--	2
6708-37-6	510	LP	GL	3	59	38	315	75	12	--	5	5	2	2	--	--	1	--
6708-37-7	575	LP	GL	1	57	42	243	70	8	--	9	8	4sp	4sp	--	--	1	--
6708-37-8	583	LP	GL	1	60	39	274	78	8	--	2	8	4	4	--	--	--	--
6708-38-2	13	H	OGL	c	c	c	344	41	2	2	4	32	8	4	3	2	2	4
6708-38-4	63	H	OGL				332	57	7	4	7	9	8sp	1	1	2	2	2
6708-38-6	113	H	OGL				322	45	6	6	10	12	14sp	1	2	2	2	1
6708-38-8	163	H	OGL				328	57	5	6	9	7	12	sp	5	1	4	4
6708-38-10	205	H	OGL				350	78	7	6	1	2	2	--	1	--	--	4
6708-38-12	263	H	OGL				331	58	5	8	7	8	7	T	3	2	2	2
6708-38-14	313	H	OGL				280	65	5	3	9	6	3	--	4	2	2	2
6708-38-16	363	H	OGL				286	66	7	1	7	8	6	--	2	1	2	2
6708-38-18	413	H	OGL				346	82	3	1	2	2	1	--	1	--	--	6
6708-38-20	463	H	OGL				343	67	4	--	10	6	5	--	2	1	1	1

APPENDIX 3. (Continued)

Sample number	Depth in core (cm)	Age	Sediment Type	% sand	% silt	% clay	Total grains counted	Percent of coarse fraction by number									
								Detrital grains	Mica	Volcanic glass	Plant fibers	Radiolarians	Diatoms	Planktonic foraminifera	Benthic foraminifera	Fecal pellets	Clauconite
6708-39-1-phl	0	LP	S-S	56	23	21	332	88	9	--	1	--	--	--	--	2	--
6708-39-2-phl	25	LP	S-S	31	39	30	311	88	9	--	1	--	1	--	--	1	1
6708-39-3	70	LP	S-S	72	12	16	386	80	14	--	4	--	1	--	--	1	1
6708-39-4	115	LP	S-S	71	8	21	305	82	14	--	3	--	--	--	--	T	--
6708-39-5	130	LP	S-S	5	55	41	281	85	10	--	3	--	--	--	--	T	--
6708-39-6	135	LP	S-S	85	6	9	255	87	8	--	2	--	1	--	--	1	--
6708-39-7	185	LP	S-S	36	40	24	252	89	8	--	2	--	T	--	--	1	--
6708-39-8	235	LP	S-S	16	50	34	253	87	9	--	4	--	T	--	--	1	--
6708-39-9	285	LP	S-S	83	7	10	322	85	10	--	4	--	1	--	--	--	1
6708-39-10	335	LP	S-S	74	6	20	277	87	9	--	2	--	1	--	--	1	--
6708-39-11	385	LP	S-S	68	17	14	250	89	7	--	1	--	1	--	--	1	1
6708-39-12	417	LP	S-S	22	43	35	229	92	6	--	1	--	--	--	--	--	--
6708-39-13	427	LP	S-S	68	16	17	243	88	9	--	2	--	--	--	--	T	--
6708-40-1	5	LP	S-S	46	14	40	269	83	12	--	--	--	--	--	3	T	2
6708-40-2	35	LP	S-S	29	20	51	291	84	13	--	--	--	--	--	1	T	2
6708-40-3	42	LP	S-S	73	17	11	288	88	7	--	--	--	--	--	2	3	2
6708-40-4	92	LP	S-S	46	13	41	282	85	10	--	--	--	--	--	2	--	3 py
6708-40-5	127	LP	S-S	46	15	39	322	84	11	--	--	--	--	--	3	T	2
6708-42-1	230	H	S-S	94	5	2	323	91	6	--	--	--	--	--	1	T sh frg 1	1
6708-42-2	454	LP	S-S	99	1	0	274	92	6	--	--	--	--	--	1	T sh frg 1	1
6708-43A	10	LP	S-S	90	8	3	305	89	5	--	--	--	1	--	--	5 sh frg 1	193
6708-43B	20	LP	S-S	94	4	2	327	90	3	--	--	--	1	--	--	4 sh frg 2	2

Sample number	Depth in core (cm)	Age	Sediment Type	% sand	% silt	% clay	Total grains counted	Percent of coarse fraction by number										Fecal pellets	Glauconite
								Detrital grains	Mica	Volcanic glass	Plant fibers	Radiolarians	Diatoms	Planktonic foraminifera	Benthic foraminifera				
6708-43C	30	LP	S-S	89	8	3	338	96	2	--	--	--	T	--	--			1	T
6708-43D	40	LP	S-S	91	7	2	306	92	5	--	--	--	--	--	--			1	T
6711-1-1	5	H	OGL	0	69	31	304	5	--	--	T	89	3	--	--			2	--
6711-1-2	50	H	OGL	0	58	42	316	20	1	1	3	64	4	--	--			7	--
6711-1-3	100	H	OGL	0	77	23	295	15	2	1	5	72	5	--	--			1	--
6711-1-4	150	H	OGL	0	59	41	290	10	1	--	2	82	4	--	--			T	--
6711-1-5	200	H	OGL	0	46	54	337	11	2	--	8	75	5	--	--			--	--
6711-1-6	252	H	OGL	0	71	29	274	7	3	--	6	80	5	--	--			--	--
6711-1-7	300	H	OGL	1	79	21	321	16	8	--	7	47	3	5	11			2	2
6711-1-8	350	H	OGL	0	54	46	350	13	4	--	4	34	3	36	4			--	1
6711-1-9	363	H	OGL	6	71	23	300	60	10	--	6	9	1	10	2			1	1
6711-1-10	378	H	OGL	1	81	18	250	18	2	--	1	13	3	60	1			2	1
6711-1-11	388	H	OGL	19	30	51	348	58	10	--	1	3	1	24	1			2	1
6711-1-12	392	H	OGL	1	60	39	286	7	1	--	T	4	--	87	--			T	--
6711-1-13	399	H	OGL	1	69	31	300	10	4	7	2	13	1	60	1			2	--
6711-1-14	405	H	OGL	1	34	65	458	32	7	8	3	16	2	27	2			2	--
6711-2-1phl	0	H	OGL	--	--	--	288	61	3	T	2	21	4	--	4			3	2
6711-2-1	5	H	OGL	18	34	49	412	68	3	2	3	22	4	--	4			4	2
6711-2-2	30	H	OGL	16	34	50	379	48	4	1	2	27	4	4	9			1	1
6711-2-3	55	H	OGL	6	47	47	333	69	4	--	1	5	2	14	5			1	1
6711-2-4	80	H	OGL	8	48	44	278	40	4	--	1	2	1	43	7			T	1
6711-2-5	108	H	OGL	7	50	43	258	42	2	--	--	1	--	14	3			1	35
6711-2-6	130	H	OGL	7	40	53	297	44	2	--	--	2	2	15	7			1	27

Sample number	Depth in core (cm)	Age	Sediment Type	% sand	% silt	% clay	Total grains counted	Percent of coarse fraction by number									
								Detrital grains	Mica	Volcanic glass	Plant fibers	Radiolarians	Diatoms	Planktonic foraminifera	Benthic foraminifera	Fecal pellets	Glauconite
6711-2-7	145	H	OGL	9	47	44	353	71	--	--	--	--	--	--	--	--	11
6711-2-8	185	H	OGL	4	39	57	343	56	4	9	1	20	1	--	--	1	6
6711-2-9	223	H	OGL	1	45	54	336	57	7	6	3	23	4	--	--	1	1
6711-2-10	265	H	OGL	0	52	48	295	49	9	--	1	35	5	--	--	1	1
6711-2-11	285	H	OGL	1	46	54	257	51	9	--	4	31	3	--	--	1	1
6711-2-12	313	H	OGL	1	44	55	278	57	7	--	5	25	1	--	--	3	2
6711-2-13	325	H	OGL	1	48	51	268	46	8	--	2	27	2	--	--	3	2
6711-2-14	348	H	OGL	1	51	48	293	66	9	--	2	17	3	--	--	2	1
6711-2-15	365	H	OGL	1	44	55	283	76	4	--	3	18	4	--	--	2	1
6711-2-16	393	H	OGL	2	43	56	305	61	6	--	4	25	2	--	--	1	1
6711-2-17	420	H	OGL	2	46	52	297	46	3	--	5	23	7	--	--	5	11
6711-2-18	430	H	OGL	1	38	62	261	60	5	--	7	16	5	--	--	3	5
6711-5-1-phl	0	H	OGL	1	51	48	357	51	8	--	1	31	5	--	1	2	1
6711-5-2	40	H	OGL	0	42	58	310	28	5	--	2	9	1	--	21	4	29
6711-5-3	75	H	OGL	1	52	48	321	88	--	--	--	--	2	--	10	--	--
6711-5-4	110	H	OGL	1	39	61	314	90	--	--	--	--	2	--	8	--	--
6711-5-5	145	H	OGL	0	46	54	293	85	--	--	--	--	3	--	12	--	--
6711-5-6	180	H	OGL	0	42	58	289	90	--	--	--	--	2	--	8	--	--
6711-5-7	200	H	OGL	0	48	51	301	90	--	--	--	--	2	--	8	--	--
6711-5-8	215	H	OGL	1	50	50	311	87	--	--	--	--	3	--	10	--	--
6711-5-9	255	H	OGL	0	43	57	341	80	--	--	--	--	6	--	14	--	--
6711-5-10	285	H	OGL	0	43	56	317	84	--	--	--	--	3	--	13	--	--
6711-5-12	320	H	OGL	0	45	55	281	81	--	--	--	--	7	--	12	--	--

APPENDIX 3. (Continued)

Sample number	Depth in core (cm)	Age	Sediment Type	Percent of coarse fraction by number										Total grains counted	Detrital grains	Mica	Volcanic glass	Plant fibers	Radiolarians	Diatoms	Planktonic foraminifera	Benthic foraminifera	Fecal pellets	Clauconite
				% sand	% silt	% clay																		
6711-5-13	355	H	OGL	0	44	56	312	85	--	--	--	--	--	9	--	6	--	--	--	--	--	--	--	
6711-5-14	380	H	OGL	0	41	59	331	86	--	--	--	--	--	12	--	2	--	--	--	--	--	--	--	
6711-5-15	415	H	OGL	0	40	60	317	70	4	4	--	4	11	1	--	4	1	4	4	4	1	5		
6711-5-16	450	H	OGL	4	45	51	291	69	4	4	--	5	12	2	--	4	4	4	4	4	4	10		
6711-5-17	480	H	OGL	1	46	53	300	100	--	--	--	--	--	--	--	--	--	--	--	--	--	--		
6711-5-19	516	H	OGL	2	47	51	321	100	--	--	--	--	--	--	--	--	--	--	--	--	--	--		
6711-5-20	516+	H	OGL	1	49	50	305	100	--	--	--	--	--	--	--	--	--	--	--	--	--	--		
6711-6-1 phl	0	H	OGL	--	--	--	279	73	8	8	--	3	8	T	--	3	5	5	3	5	5	T		
6711-6-1	10	H	OGL	4	29	67	290	70	9	9	--	4	7	1	1	5	2	2	2	2	2	--		
6711-6-2	55	H	OGL	0	22	78	231	76	3	3	--	2	8	1	--	6	3	1	3	1	3	1		
6711-6-3	105	H	OGL	1	17	82	182	78	5	5	--	2	7	1	--	4	2	1	2	1	2	1		
6711-6-4	155	H	OGL	2	15	83	229	73	6	6	--	4	7	3	--	5	1	1	1	1	1	1		
6711-6-5	205	H	OGL	1	19	80	283	70	9	9	--	4	7	1	1	5	2	2	2	2	2	--		
6711-6-6	260	H	OGL	16	19	64	270	76	3	3	--	2	8	1	T	6	3	3	3	3	1	1		
6711-6-7	340	H	OGL	2	28	71	334	64	5	5	--	2	9	3	4	5	2	2	2	2	4	4		
6711-6-8	340+	H	OGL	2	11	87	305	48	4	4	--	--	4	1	40	2	1	1	1	1	--	--		
6711-8-1 phl	0	H	OGL	--	--	--	308	34	8	8	--	10	19	24sp-	--	1	2	2	2	2	1	1		
6711-8-1	5	H	OGL	0	49	51	268	31	6	6	--	14	18	sp 27sp-	--	2	2	2	2	2	1	1		
6711-8-2	55	H	OGL	0	54	45	262	43	5	5	--	3	20	sp 15sp-	1	2	4	4	4	2	2	2		
6711-8-3	105	H	OGL	0	52	48	350	11	4	4	--	11	53	sp 19	--	1	1	1	1	1	1	1		

Sample number	Depth in core (cm)	Age	Sediment Type	% sand	% silt	% clay	Total grains counted	Percent of coarse fraction by number									
								Detrital grains	Mica	Volcanic glass	Plant fibers	Radiolarians	Diatoms	Planktonic foraminifera	Benthic foraminifera	Fecal pellets	Clauconite
6711-8-4	155	H	OGL	0	57	44	324	15	6	--	9	47	19sp-	--	3	2	1
6711-8-5	205	H	OGL	0	56	44	339	19	8	--	5	48	15	--	4	2	T
6711-8-6	250	H	OGL	0	60	40	277	18	8	--	8	44	14	--	6	2	T
6711-8-7	305	H	OGL	0	59	41	260	20	10	--	10	31	15	--	8	6	--
6711-8-8	355	H	OGL	1	54	46	218	27	9	--	6	30	19sp-	--	6	3	1
6711-8-9	405	H	OGL	1	54	45	223	30	10	--	6	27	17	--	5	5	1
6711-8-10	412	H	S-S	38	50	13	187	50	11	--	2	26	6	--	2	2	2
6711-8-11	416	H	OGL	17	43	40	180	61	9	--	T	21	3	--	2	3	1
6711-8-12	419	H	OGL	3	50	48	219	64	6	--	1	19	6	--	1	3	1
6711-8-13	431	H	OGL	2	15	82	174	60	5	--	3	17	5	1	3	4	2
6711-8-14	455	H	OGL	1	47	52	239	66	7	--	1	16	4	3	3	3	1
6711-8-15	505	H	OGL	2	57	41	190	59	3	--	1	21	7	4	1	4	--
6711-8-16	560	H	OGL	1	39	60	193	63	8	--	2	12	3	17	1	3	--
6711-8-17	560+	H	OGL	0	47	53	186	56	7	--	2	10	2	17	3	6	2

^a phl - indicates Phleger core sample from multiple corer trip weight.

^b Plus (+) sign indicates sample from piston core cutting head.

^c No textural data for even-numbered samples; see Appendix 4 for texture of odd-numbered samples.

^d includes sponge spicules; spicules are dominant in samples where "sp-sp" is indicated.

^e includes shell fragments; shell fragments are dominant where "sh frg" is indicated.

^f includes pyrite where "py" is indicated.

APPENDIX 4. TEXTURAL ANALYSES OF SEDIMENT SAMPLES

OSU ^a Sample Number	Depth Interval in cores (cm)	Sediment Type	M_{ϕ}^b	σ_{ϕ}^b	α_{ϕ}^b	Percent Sand	Percent Silt	Percent Clay	Textural Classification ^c
6706-1-1	0-5	OGL	6.51	2.17	-0.05	5.2	67.5	27.3	CLSL
6706-1-2	8-11	S-S	5.75	2.22	0.08	55.2	28.7	16.1	SLSN
6706-1-3	55-60	OGL	7.15	2.38	-0.08	8.6	50.9	40.5	CLSL
6706-1-4	100-105	OGL	7.40	2.10	-0.08	1.6	55.0	43.4	CLSL
6706-1-5	145-150	OGL	7.83	2.04	-0.04	3.0	47.6	49.4	SLCL
6706-1-6	200-205	OGL	10.58	5.41	-1.00	2.4	25.9	71.7	SLCL
6706-1-7	250-255	OGL	8.85	1.52	0.00	1.8	28.3	69.9	SLCL
6706-1-8	300-305	OGL	9.02	3.88	0.58	1.8	58.7	39.5	CLSL
6706-1-9	346-352	GL	8.71	4.99	0.23	30.2	22.2	47.6	SSC
6706-1-10	405-410	GL	10.08	5.92	-0.13	15.0	20.9	64.0	SLCL
6706-1-11	425-430	GL	10.00	6.00	1.00	2.0	98.0	0	SL
6706-1-12	430+	GL	10.83	5.17	-1.00	1.4	31.4	67.2	SLCL
6706-2-1	0-5	OGL	5.62	2.72	-0.61	29.3	42.8	27.9	SSC
6706-2-2	45-50	OGL	6.74	2.43	0.38	3.0	66.9	30.1	CLSL
6706-2-3	110-115	OGL	7.23	2.41	-0.17	5.9	49.4	44.7	CLSL
6706-2-4	150-155	OGL	8.43	2.20	0.02	4.3	39.4	56.3	SLCL
6706-2-5	185-190	OGL	9.70	3.66	0.10	3.5	35.0	61.5	SLCL
6706-2-6	196-198	OGL	No data						
6706-2-7	200-205	OGL	8.00	2.66	0.18	5.7	49.3	45.0	CLSL
6706-2-8	223-224	S-S	2.80	1.04	-0.10	100.0	0	0	SN
6706-2-9	245-250	OGL	6.36	2.58	-0.17	22.2	46.0	31.8	SSC
6706-2-10	253-254	OGL	6.84	2.94	-0.06	19.3	42.4	38.3	CLSL
6706-2-11	282-283	S-S	2.75	1.03	-0.09	100.0	0	0	SN
6706-2-12	295-302	OGL	6.90	2.51	-0.21	3.8	55.3	40.9	CLSL
6706-2-13	300-315	OGL	7.36	2.22	-0.08	6.1	50.9	43.0	CLSL
6706-2-14	320-321	OGL	7.22	2.32	-0.09	11.2	46.3	43.5	CLSL
6706-2-15	330-335	OGL	6.57	2.51	-0.20	15.8	49.4	34.8	CLSL
6706-2-16	355-360	OGL	8.22	3.28	0.20	4.3	49.3	46.4	CLSL
6706-2-17	370-375	GL	8.06	1.43	-0.06	3.1	42.6	54.4	SLCL

Appendix 4. (Continued)

OSU ^a Sample Number	Depth Interval in cores (cm)	Sediment Type	M ϕ	σ ϕ	α ϕ	Percent Sand	Percent Silt	Percent Clay	Textural Classification ^c
6706-2-18	385-390	GL	7.44	2.29	-0.04	5.3	51.4	43.3	CLSL
6706-2-19	390+	GL	7.36	2.62	-0.12	4.5	50.0	45.6	CLSL
6706-3-1	0-5	GL	6.95	2.73	-0.07	14.6	46.4	39.0	CLSL
6706-3-2	50-55	GL	7.11	2.27	0.01	7.0	56.0	37.0	CLSL
6706-3-3	100-105	GL	5.73	1.43	0.47	1.9	85.9	12.2	SL
6706-3-4	118		No data						
6706-3-5	150-155	GL	7.29	2.36	0.07	4.4	57.0	38.6	CLSL
6706-3-6	200-205	GL	7.80	2.54	0.06	5.0	49.1	45.9	CLSL
6706-3-7	250-255	GL	7.54	2.47	0.04	6.1	50.8	43.1	CLSL
6706-3-8	300-305	GL	8.39	3.74	0.47	6.1	56.3	37.6	CLSL
6706-3-9	350-355	GL	7.71	2.96	0.25	7.2	51.9	40.8	CLSL
6706-3-10	375-377	GL	7.02	2.56	0.00	11.0	51.4	37.5	CLSL
6706-3-11	377+	GL	8.49	4.85	0.62	21.0	44.9	34.0	SSC
6706-3-12	380+	GL	6.84	2.69	0.00	14.0	51.0	35.0	CLSL
6706-4-1 [*]	0-10	OGL	7.23	2.41	-0.08	4.3	49.9	46.8	CLSL
6706-4-2	60-65	OGL	7.61	2.01	0.03	5.1	41.3	54.6	SLCL
6706-4-3	92-97	OGL	7.53	2.62	-0.02	2.9	52.6	44.5	CLSL
6706-4-4	108-112	S-S	2.12	1.01	-0.03	99.7	0.3	0	SN
6706-4-5	145-150	GL	7.54	2.10	-0.04	3.2	41.5	56.3	SLCL
6706-4-6	150+	GL	7.67	2.41	-0.08	3.6	38.3	59.1	SLCL
6706-5-1 [*]	0-10	OGL	6.94	2.62	0.06	12.8	52.2	35.0	CLSL
6706-5-2 [*]	25-30	OGL	6.81	3.11	0.04	14.2	48.3	37.5	CLSL
6706-5-3	85-90	OGL	9.51	5.63	0.53	16.7	45.3	38.0	CLSL
6706-5-4	90-91	S-S	2.93	2.10	-0.01	96.3	2.1	1.6	SN
6706-5-5	93-95	S-S	2.71	1.00	0.04	94.7	1.7	3.6	SN
6706-5-6	96-97	S-S	2.62	1.21	0.03	100.0	0	0	SN
6706-5-7	107-110	OGL	7.11	2.15	-0.08	9.3	40.2	50.5	SLCL
6706-5-8	115-117	OGL	6.83	2.53	0.21	10.0	37.2	53.8	SLCL
6706-5-9	120-121	S-S	3.81	1.43	0.05	95.1	3.1	1.8	SN
6706-5-10	125-127	OGL	6.56	2.54	0.13	15.7	55.3	28.9	CLSL

Appendix 4. (Continued)

OSU ^a Sample Number	Depth Interval in cores (cm)	Sediment Type	M ϕ	σ ϕ	α ϕ	Percent Sand	Percent Silt	Percent Clay	Textural Classification ^c
6706-5-11	138-140	OGL	6.71	2.63	0.09	11.3	44.2	44.5	SLCL
6706-5-12	145-148	S-S	2.92	1.61	0.07	97.3	2.2	0.5	SN
6706-5-13	185-187	OGL	6.47	2.58	0.27	18.3	55.6	26.1	CLSL
6706-5-14	207-210	OGL	6.70	2.53	0.43	11.6	61.4	27.0	CLSL
6706-5-15	227-230	OGL	6.82	2.67	0.08	8.3	53.6	38.1	CLSL
6706-5-16	243-245	OGL	7.15	2.16	-0.03	7.4	41.3	51.3	SLCL
6706-5-17	270-273	OGL	6.93	2.61	0.05	11.6	40.8	47.6	SLCL
6706-5-18	273+	OGL	5.83	2.44	0.31	9.3	51.0	39.7	CLSL
6706-6-1	0-5	OGL	5.50	2.19	0.54	3.9	41.1	55.0	SLCL
6706-6-2	15-20	OGL	6.89	2.14	0.04	6.3	61.3	32.4	CLSL
6706-6-3	35-38	OGL	7.20	2.12	0.21	6.1	60.6	33.3	CLSL
6706-6-4	60-65	OGL	7.09	1.71	0.16	2.2	68.5	29.3	CLSL
6706-6-5	80-83	OGL	6.95	1.35	-0.17	2.6	71.4	25.9	CLSL
6706-6-6	100-103	OGL	6.45	2.34	-0.08	15.0	56.8	28.2	CLSL
6706-6-7	125-127	S-S	3.14	0.66	-0.41	100.0	0	0	SN
6706-6-8	150-155	OGL	8.01	3.39	0.40	4.8	58.0	37.4	CLSL
6706-6-9	190-193	OGL	7.20	1.86	-0.10	11.5	50.4	38.1	CLSL
6706-6-10	199-201	S-S	3.17	0.67	0.07	100.0	0	0	SN
6706-6-11	250-255	OGL	7.05	2.29	-0.02	7.4	55.8	36.8	CLSL
6706-6-12	285-288	OGL	6.56	2.09	0.12	7.7	67.7	24.6	CLSL
6706-6-13	320-323	OGL	7.50	3.24	0.18	13.58	46.1	40.4	CLSL
6706-6-14	350-355	OGL	6.93	2.48	0.04	10.4	54.3	35.2	CLSL
6706-6-15	335+	OGL	7.19	2.65	0.22	9.2	56.4	34.4	CLSL
6706-7-1	0-5	S-S	5.25	2.33	0.81	67.4	18.4	14.2	SLSN
6706-7-2	40-45	S-S	10.28	7.35	0.77	45.1	16.8	38.1	CLSN
6706-7-3	70-75	S-S	5.28	2.39	0.82	63.3	21.7	15.0	SLSN
6706-7-4	120-125	S-S	5.15	2.41	0.74	65.0	20.2	14.8	SLSN
6706-7-5	171	S-S	5.23	2.40	0.81	64.9	20.3	14.8	SLSN
6706-7-6	195-200	S-S	4.78	1.90	0.76	71.8	16.0	12.2	SLSN
6706-7-7	225-230	S-S	5.01	2.21	0.70	68.2	12.8	19.0	CLSN

Appendix 4. (Continued)

OSU ^a Sample Number	Depth Interval in cores (cm)	Sediment Type	M_{ϕ}	σ_{ϕ}	α_{ϕ}	Percent Sand	Percent Silt	Percent Clay	Textural Classification ^c
6706-7-8	253	S-S	5.53	2.53	0.78	64.6	18.9	16.5	SLSN
6706-7-9	275-280	S-S	5.18	2.20	0.80	65.7	10.2	24.1	CLSN
6706-7-10	285-290	S-S	4.83	1.92	0.77	63.9	25.4	10.7	SLSN
6706-7-11	315-320	S-S	5.11	2.21	0.80	64.5	23.0	12.5	SLSN
6706-7-12	345-350	S-S	5.61	1.88	0.84	63.4	12.8	23.8	CLSN
6706-7-13	385-390	S-S	5.09	2.21	0.79	66.9	20.1	13.0	SLSN
6706-7-14	410-415	S-S	4.75	1.86	0.83	66.1	25.3	8.5	SLSN
6706-7-15	445-450	S-S	4.96	2.09	0.77	67.8	22.0	10.2	SLSN
6706-7-16	465	S-S	5.32	2.41	0.74	56.2	28.3	15.5	SLSN
6706-8-1*	0-10	S-S	3.64	0.57	0.40	83.9	8.3	7.8	SN
6706-8-2*	35-40	S-S	6.68	3.75	0.81	63.2	16.8	20.1	CLSN
6706-8-3	95-100	S-S	3.40	0.54	0.04	89.7	7.8	2.4	SN
6706-8-4	250-255	OGL	6.23	2.41	-0.32	18.2	51.7	30.1	CLSL
6706-8-5	355-360	OGL	6.13	3.26	0.43	35.5	34.0	30.5	SSC
6706-8-6	375	OGL	6.55	2.60	-0.29	17.3	45.0	37.7	CLSL
6708-20-1	0-5	S-S	3.82	1.77	0.31	83.6	9.0	7.8	SN
6708-23-A	4-6	S-S	4.52	2.16	0.59	51.6	36.3	12.1	SLSN
6708-23-B	50-52	S-S	5.49	2.21	0.38	42.9	42.4	14.7	SLSN
6708-23-C	75-77	S-S	4.31	1.98	0.51	48.9	39.2	11.9	SLSN
6708-23-D	98-100	S-S	4.29	2.38	0.59	52.8	34.8	12.4	SLSN
6708-23-E	124-126	S-S	4.93	2.31	0.37	43.9	41.8	14.3	SLSN
6708-23-F	168-170	S-S	5.28	2.15	0.31	36.0	49.0	15.0	SNSL
6708-23-G	200-202	S-S	4.36	2.17	0.39	53.9	34.7	11.4	SLSN
6708-23-H	205-207	S-S	4.71	2.98	0.57	52.8	36.7	10.5	SLSN
6708-23-I	213-215	S-S	5.62	1.99	0.10	20.2	62.8	17.0	SNSL
6708-23-J	241-243	S-S	5.41	1.89	0.13	19.3	66.0	14.1	SNSL
6708-25-1	0-5	OGL	7.18	1.18	-0.07	1.7	70.0	28.2	CLSL
6708-25-2	75-80	OGL	6.70	1.95	-0.29	8.5	58.9	32.7	CLSL
6708-25-3	150-155	OGL	7.17	2.22	-0.13	3.5	55.4	41.1	CLSL
6708-25-4	225-230	OGL	6.62	2.01	0.09	6.0	68.7	25.3	CLSL

Appendix 4. (Continued)

OSU ^a Sample Number	Depth Interval in cores (cm)	Sediment Type	M ϕ	σ ϕ	α ϕ	Percent Sand	Percent Silt	Percent Clay	Classification ^c
6708-25-5	287	OGL	7.65	3.42	0.52	12.8	67.6	19.6	CLSL
6708-25-6	320-325	OGL	7.38	2.06	0.09	2.8	59.0	38.2	CLSL
6708-25-7	350-355	OGL	6.63	1.91	-0.33	3.6	64.9	31.4	CLSL
6708-25-8	395-400	OGL	6.13	1.62	-0.24	9.6	81.9	8.5	SL
6708-25-9	420-425	OGL	6.89	2.53	0.01	5.3	59.4	35.3	CLSL
6708-25-10	440-445	OGL	6.81	2.29	0.08	7.3	56.1	36.6	CLSL
6708-25-11	460-465	OGL	6.86	2.09	-0.41	9.0	48.3	42.7	CLSL
6708-25-12	480-485	OGL	6.41	2.48	-0.36	17.0	47.2	35.8	CLSL
6708-25-13	500-505	OGL	8.01	3.28	-0.21	10.9	29.5	59.5	SLCL
6708-25-14	520-525	OGL	7.95	3.98	0.64	16.2	46.8	37.0	CLSL
6708-25-15	540-545	OGL	7.22	3.29	-0.12	18.2	35.8	46.0	SLCL
6708-25-16	578-580	OGL	7.24	3.35	0.03	17.0	41.1	41.9	SLCL
6708-25-17	610	OGL	7.88	3.95	-0.17	17.5	26.5	56.0	SLCL
6708-33A	1-3	S-S	3.48	0.67	0.48	81.8	12.4	5.8	SN
6708-33B	21-23	S-S	4.03	1.26	0.73	77.9	2.1	7.0	SN
6708-33C	41-43	S-S	2.97	0.31	0.22	91.1	10.9	6.8	SN
6708-33D	61-63	S-S	3.47	0.70	0.54	82.4	27.3	6.7	SN
6708-37-1	10-15	OGL	7.41	2.08	0.15	2.1	60.1	37.7	CLSL
6708-37-2	100-105	OGL	7.68	2.33	0.31	2.5	58.8	38.7	CLSL
6708-37-3	200-205	OGL	7.14	2.21	0.12	4.0	61.6	34.5	CLSL
6708-37-4	300-305	OGL	7.42	3.12	0.46	2.5	61.7	35.9	CLSL
6708-37-5	400-405	GL	7.39	2.48	0.20	1.6	61.0	37.5	CLSL
6708-37-6	505-510	GL	7.41	2.30	0.17	3.2	58.7	38.1	CLSL
6708-37-7	570-575	GL	7.59	2.08	0.08	1.1	57.0	41.9	CLSL
6708-37-8	583	GL	7.54	2.45	0.22	1.0	59.9	39.1	CLSL
6708-38-1	0-5	OGL	8.44	2.32	0.06	0.5	44.8	54.7	SLCL
6708-38-3	55-60	OGL	8.33	2.80	0.17	1.1	50.1	48.9	CLSL
6708-38-5	100-105	OGL	7.41	2.28	0.26	2.3	61.9	35.7	CLSL
6708-38-7	150-155	OGL	7.96	2.33	0.11	1.1	52.4	46.5	CLSL
6708-38-9	200-205	OGL	7.56	2.70	0.08	4.6	52.5	42.8	CLSL

Appendix 4. (Continued)

OSU ^a Sample Number	Depth Interval in cores (cm)	Sediment Type	M ϕ	σ ϕ	α ϕ	Percent Sand	Percent Silt	Percent Clay	Textural Classification ^c
6708-38-11	250-255	OGL	8.52	2.97	0.39	1.2	53.8	45.0	CLSL
6708-38-13	300-305	OGL	8.23	2.93	0.42	1.5	56.5	42.0	CLSL
6708-38-15	350-355	OGL	7.40	2.45	0.04	1.3	57.6	41.1	CLSL
6708-38-17	400-405	OGL	10.63	5.37	0.60	1.8	50.4	47.8	CLSL
6708-38-19	450-455	OGL	7.53	2.31	0.18	1.2	59.4	39.4	CLSL
6708-38-21	469-472	OGL	9.93	4.84	0.51	0.7	51.6	47.7	CLSL
6708-38-22	472+	OGL	10.68	5.32	-1.0	1.3	40.2	58.5	SLCL
6708-39-1*	0-10	S-S	5.87	3.03	0.65	55.7	23.2	21.1	SLSN
6708-39-2*	25-30	S-S	6.57	3.17	0.21	30.9	39.2	29.9	SSC
6708-39-3	65-70	S-S	4.77	2.59	0.58	72.3	11.9	15.7	CLSN
6708-39-4	113-115	S-S	4.93	2.42	0.41	70.9	8.0	21.1	CLSN
6708-39-5	125-130	S-S	7.33	2.16	-0.04	4.6	54.6	40.8	CLSL
6708-39-6	130-135	S-S	3.62	0.37	0.05	84.5	6.2	9.3	SN
6708-39-7	180-185	S-S	8.48	5.11	0.76	35.8	39.8	24.4	SSC
6708-39-8	230-235	S-S	7.39	3.37	0.39	15.6	50.4	34.0	CLSN
6708-39-9	280-285	S-S	3.87	0.56	0.41	82.7	7.2	10.1	SN
6708-39-10	330-335	S-S	3.12	0.20	-0.18	73.8	6.0	20.2	CLSN
6708-39-11	380-385	S-S	4.85	1.52	0.74	68.4	17.3	14.3	SLSN
6708-39-12	412-417	S-S	9.85	6.15	0.73	22.4	43.1	34.5	SSC
6708-39-13	427	S-S	5.83	3.07	0.87	67.5	15.6	16.8	CLSN
6708-40-1	0-5	S-S	8.67	5.32	0.62	46.1	13.9	40.0	CLSN
6708-40-2	30-35	S-S	9.71	6.25	0.24	29.1	19.7	51.2	SNCL
6708-40-3	40-42	S-S	5.02	1.94	0.78	72.9	16.5	10.6	SLSN
6708-40-4	87-92	S-S	9.62	6.38	0.73	45.6	13.3	41.1	CLSN
6708-40-5	123-127	S-S	8.59	5.23	0.63	46.0	15.4	38.6	CLSN
6708-42-1	225-230	S-S	3.42	0.62	0.21	93.6	4.8	1.6	SN
6708-42-2	434-454	S-S	3.10	0.31	0.11	98.8	1.2	0	SN
6708-43A	0-10	S-S	3.15	0.36	0.45	89.7	7.8	2.5	SN
6708-43B	10-20	S-S	3.12	0.33	0.05	93.8	4.2	2.0	SN
6708-43C	20-30	S-S	3.26	0.38	0.17	89.4	7.7	2.9	SN

Appendix 4. (Continued)

OSU ^a Sample Number	Depth Interval in cores (cm)	Sediment Type	M ϕ	σ ϕ	α ϕ	Percent Sand	Percent Silt	Percent Clay	Textural Classification ^c
6708-43D	30-40	S-S	3.23	0.41	0.21	90.9	7.4	1.7	SN
6711-1-1	0-5	OGL	6.67	2.20	-0.08	0.2	68.6	31.2	CLSL
6711-1-2	45-50	OGL	7.19	2.44	-0.09	0.3	58.2	41.5	CLSL
6711-1-3	95-100	OGL	6.68	1.50	-0.30	0.3	76.7	23.1	SL
6711-1-4	145-150	OGL	7.63	1.78	-0.28	0.2	58.9	40.9	CLSL
6711-1-5	195-200	OGL	8.20	2.21	-0.01	0.1	45.9	54.1	SLCL
6711-1-6	248-252	OGL	6.66	1.98	-0.01	0.1	70.9	29.0	CLSL
6711-1-7	295-300	OGL	6.46	1.70	-0.03	0.5	78.9	20.6	SL
6711-1-8	345-350	OGL	8.32	2.89	0.27	0.3	53.7	46.0	CLSL
6711-1-9	363	OGL	6.43	2.06	0.04	5.6	71.0	23.4	CLSL
6711-1-10	375-378	OGL	6.31	1.84	0.37	0.8	81.0	18.2	SL
6711-1-11	385-388	OGL	8.30	4.46	0.05	18.9	30.1	51.0	SLCL
6711-1-12	390-392	OGL	7.34	1.75	-0.04	0.9	60.2	38.9	CLSL
6711-1-13	397-399	OGL	6.92	1.69	-0.13	0.7	68.5	30.8	CLSL
6711-1-14	404-408	OGL	9.36	3.42	-0.03	0.8	33.9	65.3	SLCL
6711-2-1	0-5	OGL	5.98	4.45	-0.42	17.6	33.6	48.8	SLCL
6711-2-2	25-30	OGL	9.77	6.23	0.32	16.3	34.0	49.7	SLCL
6711-2-3	50-55	OGL	7.78	2.64	0.01	6.3	46.6	47.1	SLCL
6711-2-4	72-80	OGL	7.28	2.19	0.04	8.1	47.6	44.3	CLSL
6711-2-5	103-108	OGL	8.01	2.42	0.21	7.3	50.0	42.7	CLSL
6711-2-6	125-130	OGL	8.22	1.99	0.30	6.8	40.2	53.0	SLCL
6711-2-7	135-145	OGL	7.24	2.02	-0.23	8.8	46.9	44.4	CLSL
6711-2-8	180-185	OGL	8.26	1.87	-0.05	4.1	38.6	57.2	SLCL
6711-2-9	217-223	OGL	8.31	2.30	0.03	0.9	45.2	53.9	SLCL
6711-2-10	260-265	OGL	8.60	3.68	0.24	0.4	51.6	48.1	CLSL
6711-2-11	280-285	OGL	8.81	3.09	0.14	0.5	45.6	53.9	SLCL
6711-2-12	305-313	OGL	8.74	3.48	0.06	0.7	44.2	55.1	SLCL
6711-2-13	320-324	OGL	8.00	2.48	-0.01	1.0	48.2	50.8	SLCL
6711-2-14	342-348	OGL	8.55	3.05	0.28	1.3	51.2	47.5	CLSL
6711-2-15	360-365	OGL	10.96	5.04	0.34	0.9	44.4	54.6	SLCL

Appendix 4. (Continued)

OSU ^a Sample Number	Depth Interval in cores (cm)	Sediment Type	M ϕ	σ ϕ	α ϕ	Percent Sand	Percent Silt	Percent Clay	Textural Classification ^c
6711-2-16	387-393	OGL	8.17	3.25	-0.10	1.6	42.5	56.0	SLCL
6711-2-17	415-420	OGL	8.50	2.45	0.14	2.2	45.6	52.3	SLCL
6711-2-18	430	OGL	9.07	2.74	0.05	0.9	37.5	61.6	SLCL
6711-5-1 [*]	0-5	OGL	7.84	1.61	-0.03	0.8	50.9	48.3	CLSL
6711-5-2 [*]	35-40	OGL	8.22	1.81	-0.08	0.4	41.6	58.0	SLCL
6711-5-3	70-75	OGL	8.37	2.55	0.24	0.5	51.9	47.7	CLSL
6711-5-4	105-110	OGL	8.45	1.80	-0.04	0.6	38.6	60.8	SLCL
6711-5-5	140-145	OGL	8.89	3.35	0.15	0.2	46.2	53.6	SLCL
6711-5-6	175-180	OGL	8.93	3.18	0.06	0.3	41.9	57.7	SLCL
6711-5-7	195-200	OGL	7.93	1.42	-0.07	0.3	48.3	51.4	SLCL
6711-5-8	210-215	OGL	8.15	1.93	0.10	0.5	49.8	49.7	CLSL
6711-5-9	250-255	OGL	9.43	3.22	0.22	0.1	43.2	56.6	SLCL
6711-5-10	280-285	OGL	10.22	4.66	0.25	0.2	43.4	56.3	SLCL
6711-5-11	315	OGL	No data						
6711-5-12	315-320	OGL	8.20	1.99	-0.03	0.1	44.6	55.3	SLCL
6711-5-13	350-355	OGL	8.80	2.94	0.10	0.1	44.1	55.8	SLCL
6711-5-14	375-380	OGL	8.40	1.99	-0.03	0.1	41.0	58.9	SLCL
6711-5-15	410-415	OGL	10.78	4.58	0.24	0.2	39.6	60.2	SLCL
6711-5-16	445-450	OGL	8.03	2.15	0.00	4.4	44.8	50.8	SLCL
6711-5-17	475-480	OGL	8.35	2.03	0.09	0.6	46.3	53.1	SLCL
6711-5-18	490	OGL	No data						
6711-5-19	500-516	OGL	8.36	2.43	0.14	2.4	46.9	50.7	SLCL
6711-5-20	516+	OGL	10.28	4.18	0.57	1.0	49.4	49.7	SLCL
6711-6-1	0-10	OGL	10.85	5.15	-0.02	3.7	29.0	67.3	SLCL
6711-6-2	50-55	OGL	11.16	4.84	-1.00	0.2	22.3	77.5	CL
6711-6-3	100-105	OGL	11.77	4.23	-0.66	0.8	17.3	81.9	CL
6711-6-4	150-155	OGL	11.93	4.07	-0.22	1.5	15.2	83.2	CL
6711-6-5	200-205	OGL	11.41	4.59	-1.00	0.5	19.3	80.1	CL
6711-6-6	255-260	S-S	7.63	3.79	-0.36	16.4	19.2	64.4	SLCL
6711-6-7	335-340	OGL	10.34	4.25	-0.03	1.5	27.7	70.8	SLCL

Appendix 4. (Continued)

OSU ^a Sample Number	Depth Interval in cores (cm)	Sediment Type	M_ϕ	σ_ϕ	α_ϕ	Percent Sand	Percent Silt	Percent Clay	Textural Classification ^c
6711-6-8	340+	OGL	12.35	3.65	-1.00	1.5	11.3	87.2	CL
6711-8-1	0-5	OGL	8.22	2.58	0.07	0.3	48.7	51.0	SLCL
6711-8-2	50-55	OGL	7.82	3.10	0.10	0.3	54.3	45.4	CLSL
6711-8-3	100-105	OGL	8.83	2.72	0.42	0.2	52.2	47.5	CLSL
6711-8-4	150-155	OGL	8.91	2.92	0.60	0.3	55.6	44.1	CLSL
6711-8-5	200-205	OGL	7.25	1.75	-0.27	0.2	56.3	43.5	CLSL
6711-8-6	245-250	OGL	7.45	1.92	0.03	0.3	59.6	40.1	CLSL
6711-8-7	300-305	OGL	7.02	2.36	-0.17	0.2	59.2	40.6	CLSL
6711-8-8	350-355	OGL	8.92	3.66	0.44	0.6	53.7	45.7	CLSL
6711-8-9	400-405	OGL	10.69	5.31	0.72	1.4	54.0	44.6	CLSL
6711-8-10	410-412	S-S	5.20	2.22	0.39	37.7	49.7	12.6	CLSL
6711-8-11	415-416	OGL	7.53	3.57	0.20	17.1	43.4	39.5	CLSL
6711-8-12	417-419	OGL	9.05	4.26	0.35	3.0	49.5	47.5	CLSL
6711-8-13	430-431	OGL	11.84	4.16	-0.71	2.4	15.3	82.3	SLCL
6711-8-14	450-455	OGL	8.14	2.38	0.02	1.1	47.2	51.7	SLCL
6711-8-15	500-505	OGL	7.43	1.72	-0.06	1.8	57.3	40.9	CLSL
6711-8-16	555-560	OGL	10.95	5.05	-1.00	0.7	39.1	60.2	SLCL
6711-8-16	560+	OGL	9.73	4.02	0.33	0.4	46.9	52.8	SLCL

^a Asterisk after sample number indicates Phleger core sample from multiple corer trip weight; all other samples are from piston cores.

^b M_ϕ = Phi Mean Diameter; σ_ϕ = Phi Standard Deviation (Sorting); α_ϕ = Phi Skewness; computed from equations of Inman (1952).

^c SN = sand; SL = silt; CL = clay; SSC = sand-silt-clay; SNCL = sandy clay; SLCL = silty clay; SLSN = silty sand; CLSN = clayey sand; SNSL = sandy silt; CLSL = clayey silt; textural classification after Shepard (1954).

APPENDIX 5. LIGHT MINERAL COMPOSITION OF THE SAND FRACTION IN SELECTED SEDIMENT SAMPLES

Sample Number	Depth in core (cm)	% sand in sample	Physiographic province	Age	Total grains counted	Percent of light minerals by number						
						Quartz	K-Feldspar	Plagioclase Feldspar	Rock fragments	Volcanic Ash	Mica	Other ^a
6706-1-2	11	55	US	H	263	45	12	35	3	2	2	1
6706-2-8	224	100	MB	LP	304	29	41	21	7	0	0	3
6706-3-7	225	6	KP	LP	345	26	17	22	26	0	4	5
6706-6-1	5	4	URCW	H	317	19	14	42	5	13	4	4
6706-7-1	5	67	URC	LP	332	33	33	14	7	8	3	2
6708-25-5	287	13	SH	H	339	40	9	21	10	11	7	3
6708-39-1	10	56	CBB	LP	312	36	13	14	23	5	2	6
6708-40-1	5	46	CBB	LP	293	48	13	22	5	5	3	4
6708-42-2	454	99	SH	LP	302	14	16	50	10	1	2	7
6708-43A	10	90	SH	LP	331	38	19	18	9	5	6	5
6711-1-9	363	6	LS	H	365	23	8	55	6	2	4	12
6711-8-10	412	38	LS	H	258	19	23	37	13	2	4	2

^a Other--glauconite, diatoms, radiolarians and unidentified grains

APPENDIX 6. HEAVY MINERAL COMPOSITION OF THE SAND FRACTION IN SELECTED SEDIMENT SAMPLES^a

Mineral data	Sample number	6708-25-5	6708-25-15	6708-42-1	6708-42-2	6708-43A	6708-43B	6708-8-1	6708-8-3	6708-8-5	6708-39-1	6708-39-13	6708-40-1	6708-40-5	6708-3-1	6708-3-7	6708-3-10	6708-2-8
Depth in core (cm)		289	545	230	454	10	40	10	100	360	10	427	5	127	5	255	377	224
Age		H	H	H	LP	LP	LP	LP	LP	LP	LP	LP	LP	LP	LP	LP	LT	LP
Physiographic Province		SH	SH	SH	SH	SH	SH	CBB	CBB	CBB	CBB	CBB	CBB	CBB	KP	KP	KP	MB
% sand in sample		13	18	94	99	90	91	84	90	36	56	68	46	46	15	6	11	100
% heavies in sand fraction		9.0	12.0	18.8	12.7	33.4	39.2	7.6	6.1	10.2	7.1	13.8	6.3	6.4	13.3	8.0	3.3	11.8
Total grains counted		222	216	348	285	235	192	287	254	240	379	312	177	203	301	298	162	235
P/A (CP/H) Ratio ^b		2.00	1.10	4.3	5.2	5.1	5.1	3.3	1.1	2.2	4.3	6.6	2.1	6.3	4.1	4.1	6.3	1.1
Amphibole group		(38.8)	(43.1)	(34.5)	(24.9)	(33.0)	(35.0)	(20.5)	(27.6)	(21.3)	(28.8)	(26.6)	(22.5)	(18.8)	(21.0)	(23.2)	(6.8)	(32.4)
Actinolite + tremolite		3.7	4.6	4.6	1.4	4.5	3.6	2.1	4.7	2.1	4.7	6.4	1.7	2.0	3.0	2.0	--	4.7
Glaucophane		--	--	3.4	2.1	--	--	T	T	T	2.4	4.5	1.1	T	2.0	T	--	T
Hornblende		(35.1)	(38.5)	(26.5)	(21.4)	(28.5)	(31.4)	(18.1)	(22.1)	(18.4)	(21.7)	(15.7)	(19.7)	(16.3)	(16.0)	(20.5)	(6.8)	(26.8)
Blue-green		35.1	38.5	21.0	21.4	26.8	30.4	15.0	18.9	16.7	16.4	13.1	15.2	16.3	16.0	18.5	6.8	26.5
Basaltic + brown + green		--	--	5.5	--	1.7	1.0	3.1	3.2	1.7	5.3	2.6	4.3	--	--	2.0	--	--
Epidote group		11.7	14.4	9.5	7.7	26.0	25.1	9.8	12.6	15.0	6.3	12.2	5.6	21.2	10.3	4.4	6.8	18.7
(clinzoisite, epidote, zoisite)																		
Garnet group		3.2	1.4	2.9	2.5	3.0	--	2.4	2.8	1.6	5.8	5.8	5.6	8.4	5.0	2.7	1.9	2.6
(clear, pink, salmon)																		
Olivine group		1.8	4.1	2.0	1.4	8.9	--	2.1	2.7	3.3	T	T	1.7	3.5	1.0	1.3	3.7	3.0
Pyroxene group		(8.6)	(5.6)	(14.4)	(13.6)	(16.6)	(17.5)	(5.2)	(3.2)	(3.7)	(11.1)	(15.4)	(4.5)	(6.0)	(11.7)	(8.4)	(4.3)	(3.9)
Orthopyroxenes (enstatite + hypersthene)		8.6	5.6	6.3	9.4	14.9	15.4	4.2	2.4	2.9	3.7	5.8	3.4	3.0	6.4	5.7	2.5	2.6
Clinopyroxenes (augite + diopsidite)		--	--	8.1	4.2	1.7	2.1	1.0	T	7.4	9.6	1.1	3.0	5.3	2.7	1.9	1.3	(5.6)
Other minerals		(4.6)	(5.2)	(2.7)	(4.2)	(2.2)	(2.6)	(14.6)	(9.9)	(10.0)	(7.2)	(5.2)	(4.8)	(5.0)	(8.6)	(6.0)	(1.8)	(5.6)
Apite		--	--	--	--	--	--	4.5	3.2	4.6	2.1	T	1.1	T	5.3	2.0	--	--
Chlorite		--	--	--	--	--	--	--	--	T	T	--	T	1.5	T	1.3	1.2	2.1
Corundum		--	--	--	--	--	--	--	--	--	--	--	--	--	--	--	--	--
Kyanite		--	--	--	--	--	--	--	--	--	--	--	--	--	--	T	--	--
Mica		--	--	--	--	--	--	1.0	T	T	T	1.3	T	--	T	--	--	--
Monazite		--	--	--	--	--	--	--	--	--	--	--	--	--	--	--	--	--
Rutile		--	--	--	--	--	--	4.2	2.4	3.3	1.0	T	1.1	T	1.3	T	--	T
Serpentine		T	--	--	T	--	--	--	--	--	--	--	--	--	--	--	--	--
Sillimanite		--	--	--	--	--	--	--	--	--	--	--	--	--	--	--	--	--
Sphene		T	1.4	T	T	T	--	--	--	--	2.0	1.8	--	1.0	--	T	--	--
Spinel		--	--	--	--	--	--	--	--	--	--	--	--	--	--	--	--	--
Staurolite		--	--	--	--	--	--	--	--	--	T	--	--	--	--	--	--	--
Tourmaline		T	--	T	1.0	T	T	--	--	--	--	--	--	--	--	--	--	--
Volcanic glass		--	--	--	--	--	--	--	--	--	--	--	--	--	--	--	--	--
Zircon		2.3	2.8	1.2	2.1	T	2.1	4.9	3.5	1.3	T	T	1.1	1.5	1.0	T	T	2.6
Opaque minerals		(10.4)	(15.9)	(14.7)	(27.1)	(10.0)	(20.4)	(14.6)	(18.6)	(19.2)	(29.3)	(19.8)	(29.3)	(20.8)	(20.6)	(23.5)	(24.1)	(13.2)
Hematite + limonite		1.4	1.9	2.9	13.7	--	--	10.8	9.9	12.9	22.7	13.1	22.6	10.9	13.6	18.5	19.8	
Others ^d		9.0	17.0	11.8	13.4	10.0	20.4	3.8	8.7	6.3	6.6	6.7	6.7	9.9	7.0	5.0	4.3	
Miscellaneous		(21.3)	(7.5)	(19.0)	(18.6)	--	--	(30.7)	(22.8)	(25.8)	(10.8)	(14.1)	(26.0)	(16.8)	(22.0)	(30.6)	(49.6)	(20.5)
Rock fragments		1.4	--	T	T	--	--	--	--	--	--	1.3	--	--	--	--	17.3	2.6
Weathered grains ^e		9.5	7.5	18.4	17.9	--	--	30.7	22.8	25.8	10.8	11.7	26.0	16.8	22.0	30.6	32.3	17.9
Others + unknown		10.4	--	--	--	--	--	--	--	--	--	T	--	--	--	--	--	--

APPENDIX 6. (Continued)

[illegible]

Appendix 6. (Continued)

NOTES

- ^a Only 62μ - 125μ portion of the sand fraction counted; mineral quantities expressed as percents of total count.
- ^b Pyroxene/Amphibole (Clinopyroxene/Hornblende) ratio.
- ^c Numbers in parentheses refer to the percentage sub-total for that particular mineral group or sub-group.
- ^d Includes ilmenite, magnetite, chromite and pyrite.
- ^e Includes minerals that occur in minor amounts: chloritoid, dumorierite, serpentine, spodumene and all unidentified minerals.

APPENDIX 7. QUANTITATIVE ANALYSES OF THE MAJOR CLAY MINERALS FROM
X-RAY DIFFRACTION RECORDS OF SELECTED SAMPLES

Sample Number	Depth in core (cm)	Sediment type	Age	Physiographic province	% chlorite	% illite	% montmorillonite	Chlorite/illite (C/I) ratio	Other minerals present
6711-2-1	5	OGL	H	LS	62	30	8	2.1	
6711-2-12	313	OGL	H	LS	58	41	1	1.4	
6706-3-1	5	CL	P	KP	57	41	2	1.4	amphiboles
6706-3-10	377	GL	P	KP	59	39	2	1.5	amphiboles
6711-6-1	10	OGL	H	LRC(LS)	52	43	5	1.2	
6711-6-8	345	OGL	H	LRC(LS)	49	49	2	0.9	
6708-37-1	15	OGL	LP	URC	71	26	3	2.7	
6708-37-7	575	GL	LP	URC	56	43	1	1.3	
6708-25-4	230	OGL	H	SH	53	43	4	1.3	amphiboles
6708-25-16	580	OGL	H	SH	62	37	1.	1.7	amphiboles
6706-1-1	5	OGL	H	US	61	36	3	1.7	
6706-1-11	430	GL	LP	US	63	35	2	1.7	
6706-2-12	302	OGL	LP	MB	57	40	3	1.4	
6706-2-17	375	GL	LP	MB	56	42	2	1.3	
6708-38-1	5	OGL	H	LS	64	33	2	1.9	
6708-38-21	472	OGL	H	LS	58	40	2	1.5	
6706-6-8	155	OGL	H	URCW(US)	69	29	2	2.4	amphiboles
6706-6-15	355	OGL	H	URCW(US)	68	32	1	2.1	amphiboles
6802-D3-1	a	c	LT ^d	LS	67	31	2	2.1	amphiboles
6802-D2	a	c	H	CBB	64	32	4	2.0	amphiboles
6706-3-11-2	377+ ^b	c	LT ^e	KP	78	20	2	3.9	amphiboles

^a Sample from dredge haul.

^b Rock fragment from piston core cutting head.

^c 6802-D3-1 = Mudstone; 6802-D2 = Mud; 6706-3-11-2 = Mudstone.

^d Early Pliocene.

^e Mid-Pliocene.

APPENDIX 8. MINERALOGY OF THE MAJOR ROCK TYPES FROM DREDGE HAULS

Sample number	Percent of haul	Percent grains	Percent matrix	Grain Mineralogy (%)				Classification name ^b	Remarks
				Quartz	Feldspar (K+Plagioclase)	Rock fragments	Other ^a		
6708-22-1	75 ^c	50	50	40 ^d (57)	25 (36)	5 (7)	30	Arkose	Minor stratification present; grains angular to sub-rounded with some highly altered to argillaceous material; some grains exhibit calcite replacement rims.
6708-36-1	33	25	75	(35)	(20)	(45)	-	Lithic Wacke	Grains sub-angular to sub-rounded, most with minor alteration; calcite replacement rims and calcite rhombs (< 1%) present; foraminifers and other microfossils present.
6708-36-2	33	35	65	40 (50)	25 (31)	15 (19)	20	Arkosic Wacke	Grains splintery to angular; most exhibit alteration rims, basaltic fragments common.
6708-36-3	33	35	65	35 (50)	20 (29)	15 (21)	30	Arkosic Wacke	Grains angular to sub-angular; most have clayey alteration rims; glauconite present (5%).
6708-41-1	40	30	70	50 (59)	30 (35)	5 (6)	15	Arkose	Pebbly to conglomeratic texture; pebble-sized grains mostly highly altered sub-rounded to rounded feldspar and quartz, with minor amounts of glauconite (5%); large (3-4 cm) gastropod shells and fragments are present and foraminifers occur as sand-sized grains.
6708-41-2	25	60	40	50 (53)	30 (31)	15 (16)	5	Arkosic Wacke	Most grains sub-angular and highly altered; calcite (< 1%) and calcite cement (1%) present.
6708-41-3	25	30	70	70 (80)	8 (9)	10 (11)	12	Sub-feldspathic Lithic Wacke	Grains sub-angular to sub-rounded; most are moderately to highly altered; calcite and calcite cement present (2-3%).

APPENDIX 8. (Continued)

Sample number	Percent of haul	Percent grains	Percent matrix	Grain Mineralogy (%)				Rock fragments	Classification name ^b	Remarks
				Quartz	Feldspar (K+Plagioclase)		Others ^a			
6708-41-4	10	70	30	30 (55)	20 (36)		45	5 (9)	Arkosic Wacke	Grains sub-rounded and moderately altered to argillaceous material; mica (2-3%), calcite (15%), and calcite cement (10%) present.
6711-D1	100	25	75	45 (63)	20 (29)		35	5 (8)	Arkose-Arkosic Wacke	Grains sub-angular to sub-rounded, most with clayey alteration rims; calcite and calcitic cement (5%) present; foraminifers present (10%) as sand-sized grains.
6711-D2	100			e					Calcareous Mudstone	Nodular; possibly concretionary.
6711-D3	100			e					Calcareous Mudstone	Nodular; possibly concretionary.
6802-D1	100			e					Mud	Unconsolidated olive gray lutite.
6802-D2	100			e					Mud	Unconsolidated and semi-consolidated olive gray lutite.
6802-D3-1	80			e					Mudstone	Silty to pebbly texture.
6802-D3-2	20			e					Siltstone	Slightly micaceous siltstone.
6802-D4	100			e					Siltstone	
6706-3-11-1	50 ^f			e					Siltstone	
6706-3-11-2	50 ^f			e					Mudstone	Foraminiferal mudstone.

Appendix 8. (Continued)

NOTES

- ^aOther--includes: heavy minerals, authigenic minerals, opaque grains and all unidentified grains.
- ^bNomenclature assigned to all samples examined petrographically according to the classification of impure sandstones of Williams, Turner and Gilbert (1954).
- ^cShell fragments comprised 25% of haul.
- ^dNumber in parentheses indicates a re-computed percentage, wherein only quartz, feldspar and rock fragments are assumed to constitute 100% of the sample.
- ^eAll samples of this rock type contain < 10% grains, and are too fine-grained for petrographic examination; identification based on megascopic and binocular-microscopic examination.
- ^fSamples are from rock fragments in basal portion and cutting head of piston core 6706-3; 50% of fragments are siltstone and 50% are mudstone.

AN ABSTRACT OF THE THESIS OF

JOSEPH JOHN SPIGAI for the DOCTOR OF PHILOSOPHY
(Name) (Degree)

in OCEANOGRAPHY presented on _____
(Major) (Date)

Title: MARINE GEOLOGY OF THE CONTINENTAL MARGIN OFF
SOUTHERN OREGON

Abstract approved: _____
L. D. Kulm

The continental margin off southern Oregon, which includes the shelf and slope from Cape Blanco to the Oregon-California border, exhibits a distinctive marginal-plateau structural pattern which divides the margin into the continental shelf, the upper continental slope and its associated benches, and the lower continental slope. Lutum transport and deposition have dominated the sedimentary processes on the margin since the start of Holocene time.

The structure of the southern Oregon margin is characterized by north-south trending compressional folds, and near-vertical faults which have been down-dropped to the west. Large-scale folds on the upper slope have ponded sediments behind them resulting in the formation of the Klamath Plateau, Cape Blanco Bench, and other bench-like features. Development of the structural pattern is most likely a result of the compressive underthrusting of the oceanic lithospheric plate beneath the southernmost Oregon-northern California margin and the

crustal extension which exists throughout the nearby continent and ocean basin.

Useful stratigraphic horizons within the late Pleistocene and Holocene margin deposits include Mazama Ash (6600 years B.P.) and several recognizable shifts in the abundance of Radiolaria and planktonic Foraminifera, particularly one dating from 5000-4000 years B.P. Holocene sedimentation rates vary from an average of 10 cm/1000 years on the upper slope to an average of 50 cm/1000 years on the lower slope, indicating that the lower slope is out-building and up-building more rapidly than the upper slope. The paleo-depth range of Pliocene fauna in sedimentary rocks from the margin suggests that subsequent to their deposition both uplift and subsidence occurred on the southern Oregon margin.

Sediments from the southern Oregon margin consist primarily of olive gray lutite, gray lutite, and sand-silt layers. Olive gray lutite is Holocene in age and is ubiquitous on the margin, with the thickest accumulation (10 m average) found on the lower slope, while the distribution of Holocene lutite on the upper slope is thin and patchy (3-4 m or less). The gray lutite appears to be a late Pleistocene deposit, and the sand-silt layers reflect both ages. The surface sediment distribution pattern on the shelf consists of modern inner shelf sand, modern central shelf mud, and mixed deposits of both types. Relict deposits are present at the shelf edge. The lower slope consists entirely of modern mud, but the surface sediment on the upper slope

and benches consists of both modern and relict deposits, and mixtures of the two.

The mineralogy of the unconsolidated and consolidated sediments from the margin indicates that the Klamath Mountains have been the dominant source for these deposits since early Tertiary time. This is reflected in the abundance of blue-green hornblende and other heavy minerals indicative of the Mesozoic rocks of the Klamath Mountains; the same source is suggested for the abundant chlorite found in the clay fraction of margin sediments and rocks. There are indications in the mineralogy of lower slope sediments which suggest that the Tertiary strata of the southern Oregon Coast Ranges may be a secondary source for the deposits in this environment. When compared to the upper slope sediments, those from the lower slope have a higher feldspar content, a higher pyroxene-to-amphibole ratio, and an apparently higher illite content.

As a result of the Holocene rise in sea level, the deposition of coarse clastics on the southern Oregon margin has been restricted to the inner shelf. Consequently, only the fine-grained lutum discharged from rivers is deposited on the outer margin environments. Submarine topography, oceanographic conditions, and gravity are important factors which effect transport and deposition of lutum on the margin. A model of modern lutum transport by bottom turbid layers and fine-particle suspensate is proposed for the southern Oregon margin. Long-period swell is believed to be responsible for much of the

formation of bottom turbid layers on the shelf. Once formed, these turbid layers move north and west over the shelf under the influence of shelf currents, alternating tidal action, and gravity; upon reaching the slope they are funneled into submarine valleys and deposited on the lower slope and adjacent deep sea. Lutum deposited on the upper slope is eventually re-suspended and transported by southerly bottom currents into down-slope valleys; very little lutum remains behind on the upper slope. Deposition of the fine-particle suspensate as well as slumping and other gravitational processes contribute to the lower slope sediments. The end result of modern lutum transport is the continual up-building and out-building of the lower slope.

Gaylord

CASE BINDER

Syracuse, N. Y.

Stockton, Calif.

188971

18898

119908

Thesis
S66845

Spigai

Marine geology of the
continental margin off
southern Oregon.

NOV 70

188971

DISPLAY
18898

8

he
c

Thesis
S66845

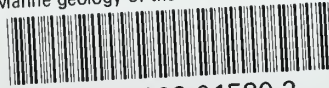
Spigai

Marine geology of the
continental margin off
southern Oregon.

119908

thesS66845

Marine geology of the continental margin



3 2768 002 01580 2

DUDLEY KNOX LIBRARY